ATZ live

Wolfgang Siebenpfeiffer *Hrsg.*

Heavy-Duty-, On- und Off-Highway-Motoren 2017

Effizienz und Emissionen

12. Internationale MTZ-Fachtagung

Proceedings

Springer Vieweg

Proceedings

Ein stetig steigender Fundus an Informationen ist heute notwendig, um die immer komplexer werdende Technik heutiger Kraftfahrzeuge zu verstehen. Funktionen, Arbeitsweise, Komponenten und Systeme entwickeln sich rasant. In immer schnelleren Zyklen verbreitet sich aktuelles Wissen gerade aus Konferenzen, Tagungen und Symposien in die Fachwelt. Den raschen Zugriff auf diese Informationen bietet diese Reihe Proceedings, die sich zur Aufgabe gestellt hat, das zum Verständnis topaktueller Technik rund um das Automobil erforderliche spezielle Wissen in der Systematik aus Konferenzen und Tagungen zusammen zu stellen und als Buch in Springer.com wie auch elektronisch in SpringerLink und Springer Professional bereit zu stellen.

Die Reihe wendet sich an Fahrzeug- und Motoreningenieure sowie Studierende, die aktuelles Fachwissen im Zusammenhang mit Fragestellungen ihres Arbeitsfeldes suchen. Professoren und Dozenten an Universitäten und Hochschulen mit Schwerpunkt Kraftfahrzeug- und Motorentechnik finden hier die Zusammenstellung von Veranstaltungen, die sie selber nicht besuchen konnten. Gutachtern, Forschern und Entwicklungsingenieuren in der Automobil- und Zulieferindustrie sowie Dienstleistern können die Proceedings wertvolle Antworten auf topaktuelle Fragen geben.

Today, a steadily growing store of information is called for in order to understand the increasingly complex technologies used in modern automobiles. Functions, modes of operation, components and systems are rapidly evolving, while at the same time the latest expertise is disseminated directly from conferences, congresses and symposia to the professional world in ever-faster cycles. This series of proceedings offers rapid access to this information, gathering the specific knowledge needed to keep up with cutting-edge advances in automotive technologies, employing the same systematic approach used at conferences and congresses and presenting it in print (available at Springer.com) and electronic (at SpringerLink and Springer Professional) formats.

The series addresses the needs of automotive engineers, motor design engineers and students looking for the latest expertise in connection with key questions in their field, while professors and instructors working in the areas of automotive and motor design engineering will also find summaries of industry events they weren't able to attend. The proceedings also offer valuable answers to the topical questions that concern assessors, researchers and developmental engineers in the automotive and supplier industry, as well as service providers.

Weitere Bände in der Reihe http://www.springer.com/series/13360

Wolfgang Siebenpfeiffer
(Hrsg.)

Heavy-Duty-, On- und Off-Highway-Motoren 2017

Effizienz und Emissionen

12. Internationale MTZ-Fachtagung

Springer Vieweg

Herausgeber
Wolfgang Siebenpfeiffer
Stuttgart, Deutschland

ISSN 2198-7432 ISSN 2198-7440 (electronic)
Proceedings
ISBN 978-3-658-21028-1 ISBN 978-3-658-21029-8 (eBook)
https://doi.org/10.1007/978-3-658-21029-8

Die Deutsche Nationalbibliothek verzeichnet diese Publikation in der Deutschen Nationalbibliografie; detaillierte bibliografische Daten sind im Internet über http://dnb.d-nb.de abrufbar.

Springer Vieweg

Verantwortlich im Verlag: Markus Braun

Gedruckt auf säurefreiem und chlorfrei gebleichtem Papier

Springer Vieweg ist ein Imprint der eingetragenen Gesellschaft Springer Fachmedien Wiesbaden GmbH und ist ein Teil von Springer Nature
Die Anschrift der Gesellschaft ist: Abraham-Lincoln-Str. 46, 65189 Wiesbaden, Germany

Vorwort

Effizienz und Emissionen – das Motto der diesjährigen internationalen MTZ-Fachtagung „Heavy-Duty-, On- und Off-Highway-Motoren“ beschreibt zutreffend die Situation, in der sich die Hersteller von Großmotoren für mobile, stationäre und maritime Anwendungen befinden. Sie müssen einerseits immer höhere Leistungsanforderungen erfüllen und andererseits Kraftstoffverbrauch und Schadstoffe reduzieren.

Die jährlich stattfindende Fachtagung hat sich in den letzten Jahren als das Forum des Informations- und Erfahrungsaustauschs zwischen den Entwicklern und Konstrukteuren großer Motoren etabliert. Aus den zahlreichen Einreichungen hat der Wissenschaftliche Beirat ein spannendes Programm zusammengestellt. Die Schwerpunkte sind neue Motorkonzepte und -komponenten, nachhaltige Mobilität durch den Einsatz von alternativen Kraftstoffen, Schadstoffreduzierung, Ventiltrieb- und Zylinderabschaltung sowie Motor- und Systemoptimierung. Am Ende des ersten Tages lädt MAN Diesel & Turbo SE zu einem Besuch des Motorenwerks Augsburg ein. Eine begleitende Fachausstellung rundet das Programm ab.

„Heavy-Duty, On- und Off-Highway-Motoren“ ist für Sie die ideale Plattform um sich über die aktuellen technischen Entwicklungen ausführlich zu informieren und diese im Expertenkreis zu diskutieren. Nutzen Sie die Gelegenheit, Ihr Netzwerk zu erweitern und wertvolle Kontakte zu knüpfen. Ich freue mich auf Ihre Teilnahme an der Tagung.

Für den Wissenschaftlichen Beirat
Wolfgang Siebenpfeiffer
Herausgeber ATZ | MTZ | ATZelektronik

Inhalt

Autorenverzeichnis

Dr. Christian Poensgen MAN Diesel & Turbo SE, Augsburg, Deutschland

Dr. Udo Schlemmer-Kelling FEV Europe GmbH, Aachen, Deutschland

Falko Arnold MAN Truck & Bus AG, Nürnberg, Deutschland

Thomas Stamm MAN Truck & Bus AG, Nürnberg, Deutschland

Andrew Auld Ricardo UK Ltd, Shoreham-by-Sea, UK

Andre Barroso Ricardo UK Ltd, Shoreham-by-Sea, UK

Dr. Matthew Keenan Ricardo UK Ltd, Shoreham-by-Sea, UK

Panagiotis Katranitsas Ricardo UK Ltd, Shoreham-by-Sea, UK

Rhys Pickett Ricardo UK Ltd, Shoreham-by-Sea, UK

Tiago Carvalho Ricardo UK Ltd, Shoreham-by-Sea, UK

Garrett Anderson Southwest Research Institute, San Antonio, USA

Dr. Jan Zelenka LEC GmbH - Large Engines Competence Center, Graz, Österreich

Dr. Martin Kirsten LEC GmbH - Large Engines Competence Center, Graz, Österreich

Dr. Eduard Schneßl LEC GmbH - Large Engines Competence Center, Graz, Österreich

Gernot Kammel LEC GmbH - Large Engines Competence Center, Graz, Österreich

Prof. Dr. Andreas Wimmer LEC GmbH - Large Engines Competence Center, Graz, Österreich

Björn Henke Universität Rostock, Rostock, Deutschland

Sascha Andree Universität Rostock, Rostock, Deutschland

Karsten Schleef Universität Rostock, Rostock, Deutschland

Prof. Dr. Bert Buchholz Universität Rostock, Rostock, Deutschland

Prof. Dr. Egon Hassel Universität Rostock, Rostock, Deutschland

Marius Hoff Caterpillar Motoren GmbH & Co. KG, Rostock, Deutschland

Robert Graumüller Caterpillar Motoren GmbH & Co. KG, Rostock, Deutschland

Dr. Carsten Baumgarten MTU Friedrichshafen GmbH, Friedrichshafen, Deutschland

Tobias Weiß MTU Friedrichshafen GmbH, Friedrichshafen, Deutschland

Dr. Günter Zitzler MTU Friedrichshafen GmbH, Friedrichshafen, Deutschland

Christian Herkommer MTU Friedrichshafen GmbH, Friedrichshafen, Deutschland

Dr. Boban Maletic MTU Friedrichshafen GmbH, Friedrichshafen, Deutschland

Christian Braun MAN Diesel & Turbo SE, Augsburg, Deutschland

Dr. Alexander Rieß MAN Diesel & Turbo SE, Augsburg, Deutschland

Peter Böhm MAN Diesel & Turbo SE, Augsburg, Deutschland

Hauke Lund MAN Diesel & Turbo SE, Augsburg, Deutschland

Dr. Klaus Eder MAN Diesel & Turbo SE, Augsburg, Deutschland

Katsuyuki Toda Niigata Power Systems Co.,Ltd, Ohta-City, Japan

Dr. Satoru Goto Niigata Power Systems Co.,Ltd, Ohta-City, Japan

Shigeki Ogura Niigata Power Systems Co.,Ltd, Ohta-City, Japan

Daichi Kawai Niigata Power Systems Co.,Ltd, Ohta-City, Japan

Jochen Heizmann Hirschvogel Automotive Group, Denklingen, Deutschland

Dr. Hans-Willi Raedt Hirschvogel Automotive Group, Denklingen, Deutschland

Patrice Lasne Transvalor S.A., Mougins, Frankreich

Helmut Dannbauer Steyr GmbH & Co. KG, St. Valentin, Österreich

Tobias Winter Motorenfabrik Hatz GmbH, Ruhrstorf a.d. Rott, Deutschland

Andreas Heitmann MAGMA GmbH, Aachen, Deutschland

Andreas Eichenberg Porsche Engineering Services GmbH, Bietigheim-Bissingen, Deutschland

Johannes Konrad TU Wien, Wien, Österreich

Prof. Dr. Thomas Lauer TU Wien, Wien, Österreich

Dr. Mathias Moser MAN Diesel & Turbo SE, Augsburg, Deutschland

Enrico Lockner MAN Diesel & Turbo SE, Augsburg, Deutschland

Dr. Jianguo Zhu MAN Diesel & Turbo SE, Augsburg, Deutschland

Dominik Lamotte HJS Emission Technology, Menden, Deutschland

Klaus Schrewe HJS Emission Technology, Menden, Deutschland

Ingo Zirkwa HJS Emission Technology, Menden, Deutschland

Dr. Simon Schneider MAHLE International GmbH, Stuttgart, Deutschland

Holger Conrad MAHLE Filtersysteme GmbH, Stuttgart, Deutschland

Geno Marinov MAHLE Powertrain GmbH, Stuttgart, Deutschland

Thibault Fouquet Faurecia Clean Mobility, Nanterre, Frankreich

J. Roussilhe Faurecia Clean Mobility, Nanterre, Frankreich

Andreas Fuchs Springer Fachmedien Wiesbaden GmbH, Wiesbaden, Deutschland

Development of the MAN Diesel & Turbo engine portfolio and future challenges

(Entwicklung des MAN Diesel und Turbo Motorenportfolios und zukünftige Herausforderungen)

Dr. Christian Poensgen

W. Siebenpfeiffer (Hrsg.), *Heavy-Duty-, On- und Off-Highway-Motoren 2017*,
Proceedings, https://doi.org/10.1007/978-3-658-21029-8_1

Die letzten Jahre in der Motorenentwicklung waren geprägt von der Umstellung und Neuentwicklung von Motoren auf Gas und Dual Fuel Fähigkeiten. Das Produkt Portfolio wurde am unteren Rand (1-4 MW Klasse) um einen 5l High Speed Motor erweitert. Gleichzeitig erfolgte die Umstellung aller Motoren auf die neuen NOx Vorgaben der IMO von Tier II auf Tier III. Dies hat zu einer Entwicklung von SCR- Lösungen geführt, welche sowohl hinter dem Motor als auch zwischen den Turbinen bei einer 2-stufigen Aufladung oder vor der Turbine der Turbolader bei 2 -Takt Motoren eingesetzt werden können. Die parallele Umstellung von PLD Einspritzsystemen zu CR Systemen erlaubte es, Motoren wesentlich effizienter zu gestalten, die Regeneration der Abgasnachbehandlung zu unterstützen und durch Systemintegration des konventionellen Antriebsstranges wesentliche Kraftstoffverbrauchsvorteile zu erzielen. Im Anschluss werden die zukünftigen Herausforderungen der Hybridisierung der Antriebstränge, des „unmanned shippings“ sowie der Kraftstoffumstellungen im Rahmen der IMO Schwefelgrenzwerte ab 2020 und Infrastrukturthemen der Häfen dargestellt.

Die MAN Motorenentwicklung in diesem Jahrzehnt unterlag einer Zeit des starken Strukturwandels bei unseren Kunden und in den Regularien.

In der Marine war, ist und bleibt Schweröl der dominierende Kraftstoff. Das damalige Produktportfolio der MAN (Abb.: 1) trug dem Rechnung. Gas und Dual Fuel Anwendungen waren auf wenige Spezialanwendungen z.B. für LNG Gastanker beschränkt. Gas als Kraftstoff für die Handelsschifffahrt, war jedoch aufgrund der lückenhaften Infrastruktur nicht umsetzbar. Obwohl die Dichte der LNG Bunkeranlagen zur Versorgung der Schiffe zugenommen hat, hat sich LNG als Kraftstoff aufgrund der höheren Anschaffungskosten bzw. Umrüstkosten nur in Nischen durchsetzen können.

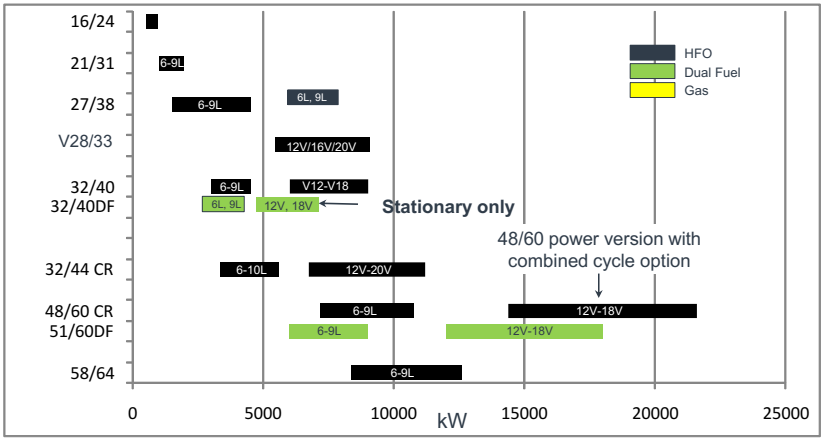

Abb.1: MDT 4-Takt Engine Portfolio 2010

Motoren für Kraftstoffe wie LPG, Methanol, Ethanol und LNG werden meist nur eingesetzt, wenn es kommerziell vertretbar ist, dass ein Teil der Ladung für den Schiffsantrieb verwendet werden kann. Der Gesamtmarkt für LNG Transport wird weiter zunehmen. Während Ende 2016 ca. 270 IMO registrierte LNG angetriebene Schiffe im Markt waren, ist die Prognose (1) für 2020 bei 400-600 LNG angetriebenen und registrierten Schiffen. Diese Zahl ist in Relation zu setzen mit der Gesamtanzahl an IMO registrierten Schiffsneubauten, die allein für 2020 mit ca. 2200 Neubauten prognostiziert wird. Damit würde der Anteil an LNG angetrieben Schiffsneubauten auch 2020 noch deutlich unter 10% verbleiben. Von den Neubauten werden daher nur ca. 120 LNG Tanker sein (2).

Im Gegensatz zum Marinemarkt hat sich der Marktanteil von Erdgas in der stationären Power Generation nahezu verdoppelt. 2010 war der Verbrauch von Schweröl und Erdgas pari. Während die Anzahl an Kraftwerksneubauten für Schweröl stagniert, hält das Wachstum von Erdgas angetriebenen Kraftwerken weiter an.

In den letzten Jahren hat die MAN eine Produktoffensive durchgeführt (Abb. 2). Das heutige Produktportfolio trägt den veränderten und sich weiter verändernden Anforderungen des Marktes Rechnung. Für die Marine wurden Dual Fuel Motoren 35/44 DF und 51/60 DF weiterentwickelt. Im 2-Takt Geschäft wurden Applikationen für Methanol, LPG und Ethanol entwickelt. Im Viertakt-Markt ist bis heute die Attraktivität für eine Entwicklung solcher Motorvarianten nach wie vor beschränkt. Man sieht im Markt als auch bei Wettbewerbern nur verhaltene Aktivitäten. Wichtig für den Marine Markt sind

1. die Erfüllung der durch die IMO Zug um Zug eingeführten neuen Grenzen für die Stickoxyde als auch für die Schwefelemissionen durch die Verwendung von Schweröl.
2. Die kontinuierliche Effizienzsteigerung des Antriebssystems im Rahmen der IMO EEDI Vorgaben

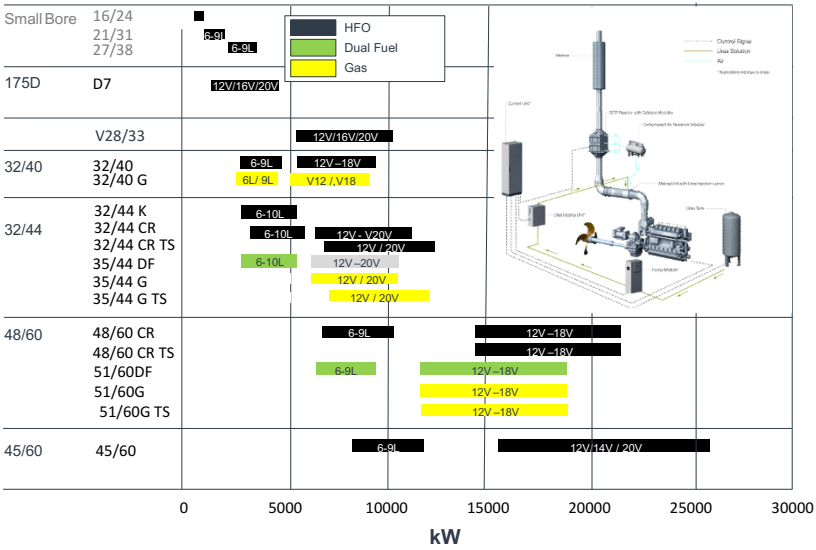

Abb.2: MDT Engine Portfolio 2017

Um beides optimal darstellen zu können hat MAN bereits vor über einem Jahrzehnt auf schweröltaugliche Common Rail Systeme gesetzt. Durch die Entkopplung von Einspritzdruck und Einspritzzeitpunkt können Optimierungen im Motorkennfeld deutlich besser und einfacher dargestellt werden als mit herkömmlichen Systemen.

In der Power Generation ändern sich die Anforderungen, die sich aus der zunehmenden Verbreitung der regenerativen Energieerzeugung als auch der partiellen Rückführung der Kernkraftwerke ergeben. Motordynamik, hohe Anzahl an Start/Stopps pro Zeiteinheit und Verfügbarkeiten über 95% sind charakteristische Merkmale. Herausfordernde Anwendungen sind u.a. die Notstrombereitstellung für Rechenzentren für Cloud Operations (3). In der Zukunft werden Kraftwerksausrüster wie die MAN daher neben den Kraftwerken auch Speichertechnologien, regenerative Erzeugerquellen und Netzwerktechnik bereitstellen müssen (4).

Der hohe Ölpreis in der ersten Hälfte des Jahrzehnts war Treiber für Steigerungen der Motor-wirkungsgrade. Die Einführung der IMO Tier II führte zu einer Umstellung der Motoren und mit der Einführung der IMO Tier III wurden SCR und AGR Lösungen entwickelt. Die Reduzierung der Schwefelgrenzwerte durch die IMO in den Küstengewässern von 1.5% auf 0.1% führte im Wesentlichen dazu, dass Destillat- und low sulphur HFO Kraftstoffe verwendet werden müssen. Der Einsatz von SO2 Wäschern ist bis heute

überschaubar. Mit der Umstellung der Schwefelgrenzwerte auf der hohen See auf 0.5% im Jahr 2020 werden weitere Änderungen der Kraftstoffe erwartet. Schiffsneubauten werden mit SO2 Wäschern ausgerüstet werden, was dazu führen kann, das der HFO Kraftstoff höhere Schwefelanteile als 3.5% aufweist, was die Kraftstoffqualität in der Regel verschlechtert. Schweröle mit Schwefelgehalten unter 1.5% werden u.U. mit Destillatkraftstoffen als Blend vermischt, wobei durchaus Anteile von Biokraftstoffen FAME (Fettsäuremethylester) mit eingemischt werden. Letztere sind nur begrenzt lagerbar. Schiffe werden, wenn sie von der Hochsee in die ECA Küstengewässer einfahren, den Kraftstoff von Schweröl auf Destillat umstellen. Die Reduktionsraten der Wäscher reicht derzeit nicht aus, um in den Küstengewässern die dort gültigen Schwefelgrenzwerte bei Verwendung von Schweröl sicher einzuhalten. Es ist davon auszugehen, dass beim Umschalten von Schweröl auf Destillatkraftstoffe mit FAME Zusätzen Unverträglichkeiten entstehen, so dass eine Verstopfung der Kraftstofffilter wahrscheinlicher wird, was in der Regel einen Schaden im Einspritzsystem zur Folge hat.

Abb. 3 zeigt die Innovationsschwerpunkte der MAN 4-Takt Motoren Entwicklung der letzten Jahre. Alle Entwicklungen wurden gleichzeitig durchgeführt. Zündkerzen Gasmotoren für die Power Generation wurden mit einstufigen und zweistufigen Ladesystemen entwickelt. Die Markteinführung des CR 1.6 Systems hat von anfänglicher Skepsis der Marktteilnehmer nach einigen Jahren zu einer vollständigen Akzeptanz geführt. Anfänglich traf diese Technologie das Betreiberpersonal an Bord der Schiffe praktisch unvorbereitet. Intensive Schulungs- und Trainingsprogramme wurden durchgeführt, ebenso wie eine rigorose Behebung aller Fehler im Rahmen eines Service Readiness Programmes. Die Laufzeiten der CR Systeme entsprechen heute denen der konventionellen Systeme.

Abb.3: Schwerpunkte der Entwicklung der letzten Jahre

Die Motorregelung kann die unterschiedlichen Kraftstoffarten selbstständig erkennen. Je nachdem wo das Schweröl produziert wurde sind die Stickstoffkonzentrationen als auch die Zündeigenschaften unterschiedlich. Dies hat Konsequenzen auf die NOx Emissionen der Motoren. Die MAN Motorkennfelder sind daher so parametriert, dass die NOx Emissionen konstant gehalten werden können. Durch Kennfeldoptimierungen, die durch das CR System möglich wurden, hat sich eine signifikante Verbrauchsverbesserung eingestellt. Inzwischen arbeitet die MAN an der Entwicklung eines Nachfolgesystems mit 2200 bar Einspritzdruck mit Druck bis an die Düse. Dieses System befindet sich derzeit im Außenversuch.

Die Motorsteuerung SaCos One wird derzeit durch die Motorsteuerung SaCos 5000 abgelöst. Der Hintergrund ist die Umstellung der Software- und Hardware Architektur von einer zentral organisierten Motorsteuerung auf eine dezentral strukturierte Motorsteuerung. Eine dezentrale Architektur ist Voraussetzung für

– die Einbindung der Motorsteuerung in zukünftige digitale Systeme, welche im Rahmen der Initiativen zum „Unmanned Shipping“ (6) erforderlich werden.
– Anpassung des Umfanges der Sensorik und S/W Funktionen entsprechend dem geforderten Ausrüstungsstandes der Antriebsanlage.

Zeitgleich mit der Änderung der Philosophie der S/W Architektur wurde in der Motorentwicklung der mechatronische Ansatz eingeführt. Die klassische Trennung der mechanischen Konstruktion und der Steuerungs- und Regelungstechnik wurde damit aufgehoben.

Im Rahmen der IMO Tier III Anforderungen wurde die Entwicklung von SCRs im Schwerölbetrieb erforderlich. Der Schwefel im Kraftstoff oxidiert in der Verbrennung zu SO_2 und SO_3, welches im Abgastrakt in Verbindung mit Ammoniak bei Temperaturen unter 310° Ammoniumbisulfat bildet. Dies wird im SCR abgelagert und eine Verblockung der Reaktivität des SCR zur Folge. Ein sicherer SCR Betrieb erfordert Abgastemperaturen von 320°C sowie eine Überschussreaktivität, so dass der Ammoniak vollständig abgebaut wird.Ansonsten würde Restammoniak an den nachgelagerten Wärmetauschern (Boileren) ebenfalls zu Ablagerungen von Ammoniumbisulfat führen. Bei Motoren mit einer 2-stufigen Aufladung sind die Abgastemperaturen deutlich unter 320°, so dass andere Konzepte erforderlich werden. Darüber hinaus können die Waben durch langkettige Asphalten versotten, so dass eine Regeneration bis zu einer Temperatur von 360°C bis 400°C erfolgen muss. Um dies zu erfüllen wurden alle Motoren mit Waste Gates ausgerüstet. Die Abb. 4 zeigt schematisch den Verlauf der Regenerationszyklen als auch der damit verbundenen Kosteneinsparungen.

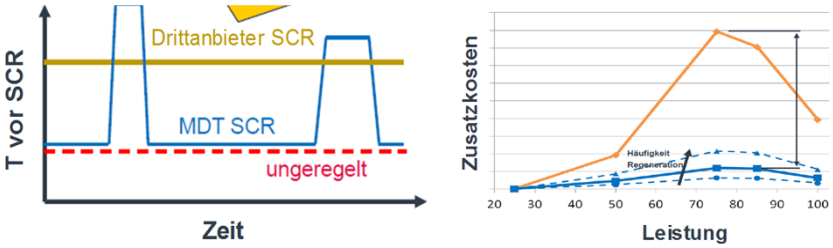

Abb.4: SCR Regenerationzyklen und resultierende Kosten

Für zweistufige Dieselmotoren als auch bei 2-Takt Motoren ist die Abgastemperatur in weiten Betriebsbereichen unter 320°C so dass mit Ammoniabisulphat -Versottung zu rechnen ist. In der Konsequenz hat die MAN einem kompakten Hochdruck SCR entwickelt. Die Kompaktheit und geringe Leitungslängen ermöglichen eine sehr effiziente Isolierung, so dass reaktorbedingte thermische Trägheiten die Dynamik der Motoren nicht beeinträchtigen.

Die Einführung eines durch NOx Sensoren geregelten gegenüber einem gesteuerten System hat sowohl Vorteile im Bereich der Betriebsführung der SCRs als auch um Motoren gemäß Schema B zu qualifizieren. Die Arbeiten zur Einstellung der SCRs bei der Inbetriebnahme der Schiffe, um die geforderte Abscheiderate zu erfüllen, sind wesentlich effizienter und prozesssicherer geworden.

Das Vorgehen der MAN sichert, dass die vorgegebenen Abscheideraten bei jedem Kraftstoff zu jeder Zeit erfüllt werden können. Eine Abschaltung des SCR Systems, wie es im Automotive Bereich unter den Randbedingungen des Motorschutzes durchgeführt wird, ist nicht erforderlich.

Die Einführung einer geregelten SCR Betriebsführung ermöglicht es, die Rohemissionen des Motors variabel zu halten (Abb. 5). Die SCR Regelung stellt zudem sicher, dass die geforderten NOx Grenzwerte nicht überschritten werden. Dadurch kann ein Kostenoptimum von Kraftstoff- und Urea-Kosten erzielt werden. Wenn der SCR in Tier II Zonen abgestellt wird, schaltet die Motorsteuerung automatisch auf Tier II Betrieb um.

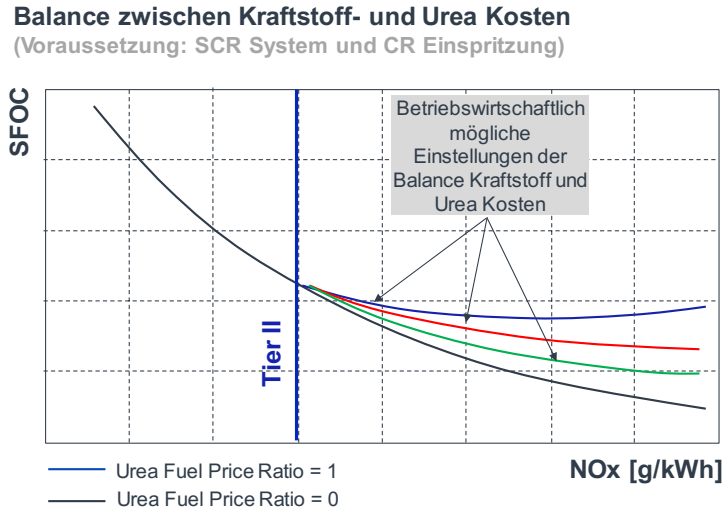

Abb. 5

Der derzeitige technologische Trend der innermotorischen Wirkungsgradsteigerung von Dieselmotoren der letzten 20 Jahre (Abb. 6) zeigt einen linearen Trend von 0.25% jährlicher Verbesserung des Wirkungsgrades. Dem gegenüber sind die Potentiale der Verbesserung des Antriebsstranges überproportional größer und lassen sich zudem kurzfristig realisieren. Dies gilt für elektrische Propulsionsanlagen als auch für den direkten Propellerantrieb.

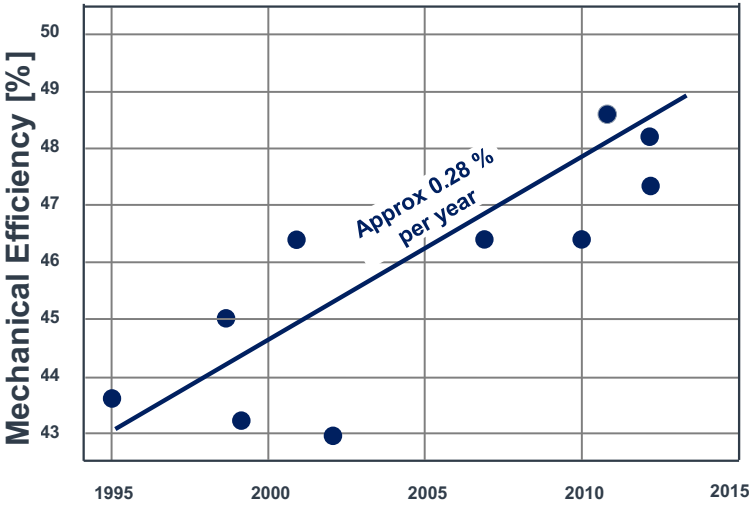

Jährliche Wirkungsgradsteigerung

Gasmotoren	**0,30%**
Dieselmotoren	**0,25%**

Potential in 10 Jahren Motorenentwicklung

Gasmotoren	**3%**
Dieselmotoren	**2.5%**

Abb. 6: Wirkungsgrad Trends durch innermotorische Maßnahmen

Die Kombination von CR Systemen, variabler Propeller als auch Frequenz-Umrichter-Technik erlaubt eine weitest gehende Optimierung des gesamten Antriebstranges. Die klassische Betriebskurve für den Antrieb eines Festpropellers (Abb.:7 gelb dargestellt)

verläuft durch den 85% Leistungspunkt bei 100% Drehzahl, um dann bei niedrigeren Leistungen bei ca 95 % zu verharren. Damit kann die Hauptmaschine die Bordstromversorgung mit einer Gleitfrequenz sicherstellen. Erst bei einer Leistungsabnahme von unter 30% werden die Hilfsmotoren für die Bordstromversorgung eingeleitet. Mit Hilfe von Frequenzumrichtern kann die Propellerkurve neu ausgelegt werden (Abb.:7 blau dargestellt). Dies hat den Vorteil, dass die Propellerkurve im Motorkennfeld in den Bereichen der höchsten Motoreffizienz durchläuft. Mit Reduzierung der Drehzahl nimmt der Propellerwirkungsgrad überproportional zu, was der dominierende Hebel zur Effizienzsteigerung ist. Zusammen ergeben die Maßnahmen Frequenzrichtertechnik, Propelleroptimierung sowie Propellerbetrieb im Kennfeldoptimum eine Kraftstoffeinsparung von ca. 10%. Der Einsatz von Hilfsmotoren zur Bordstromerzeugung erübrigt sich.

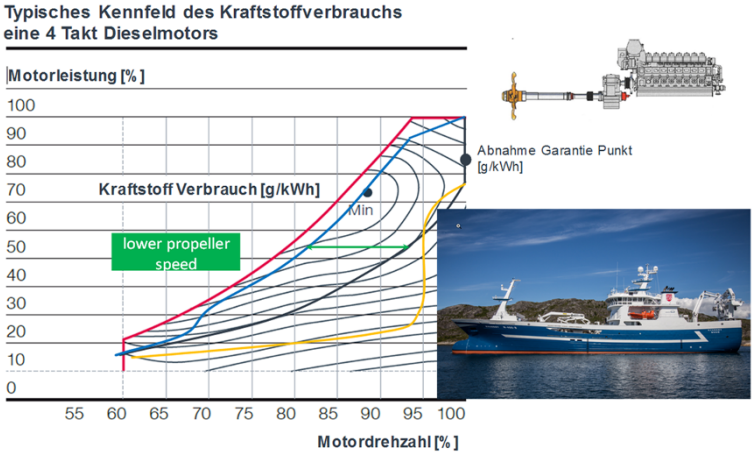

Abb.7: Optimierte Abstimmung Motor-Propeller

Bei herkömmlichen dieselelektrischen Antrieben summieren sich die Verluste im elektrischen Teil des Antriebsstranges um ca. 9%-10%. Diese Verluste haben unter anderem dazu geführt, dass bei LNG Tankern die MAN 2-Takt ME-GI Motoren mit einem direkten Propellerantrieb die 4-Takt Dual Fuel Motoren mit dem in der in Abb.8 skizzierten dieselelektrischen Antrieb verdrängen konnten.

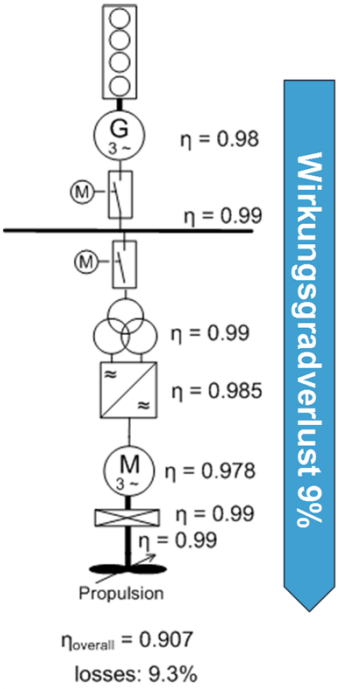

Abb.8: konventionelles Diesel – elektrisches Antriebssystem

Abb.: 9 zeigt Anlagenstudien, um die Wirkungsgradverluste eines herkömmlichen dieselelektrischen Antriebsystems weitestgehend zu kompensieren. Darüber hinaus werden bei kleineren Anlagen derzeit Gleichstromschienen diskutiert und eingesetzt. Derzeit ist die maximale Leistung für Gleichstromnetze auf Schiffen bei 15-20 MW begrenzt. Die verfügbaren Trennschalter für ein solches Gleichspannungsnetz sind derzeit auf 1kV begrenzt. Obwohl in der Hochspannungsgleichstrom-technik Trennschalter für 380 kV entwickelt wurden, stehen aufgrund des geringen Marktvolumens derzeit keine Trennschalter im Bereich um 3kV zur Verfügung, was Voraussetzung für Einheits-leistungen von 50 MW entspricht. Die Wirkungsgradgewinne, die durch Gleichspannungsnetzwerke entstehen. betragen zwischen 5%-8%. Für Leistungen über 20MW können alternativ zum klassischen dieselelektrischen System mit Festfrequenz Systeme mit Gleitfrequenzen eingesetzt werden. Die Motoren werden mit Drehzahlen von 80% – 100% betrieben. Dies ermöglicht einen Motorbetrieb im optimalen Wirkungsgradbereich des Motorkennfeldes. Mit einer reduzierten Motordrehzahl sinkt die Drehzahl des Propellers, was

weitere Vorteile in der Effizienz erzeugt. Insgesamt können je nach Betriebsweise des Schiffes Wirkungsgradgewinne von 3% – 6 % erzielt werden. Der Einsatz von Batterien zeichnet sich derzeit bei kleineren Schiffsleistungen und im Kurzstreckenverkehr ab. Projekte für kleine und mittlere Fähren mit 100% elektrischen Betrieb mit Batteriespeichern sind in der Projektierung. Bei Hafenschleppern bieten sich batteriegetriebene Elektroantriebe an, bei denen die Dieselmotoren nur noch für die Spitzenleistung zugeschaltet werden. Leistungsglättungen durch Batterien zur Positionsstabilisierung von Plattformen unserer Supply Schiffe ist ein weiterer Anwendungsfall. Die Stromversorgung in den Häfen ist derzeit noch ein Engpass für den Einsatz von batteriegetriebenen Schiffen. Einerseits haben viele kleine Häfen auf Inseln z.B. in der Ägäis, Adria oder Färöer keine ausreichende Anschlussleistung verfügbar, um z.B. größere Fähren mit genügend Strom zu versorgen und anderseits sind die Strompreise lokal unterschiedlich (Abb. 10). Bei den heutigen Kraftstoffpreisen rechnet sich eine Batterieaufladung durch die im Schiff befindlichen Motoren ab 7 – 9 c/kWh. Zum Vergleich: der Industriestrom in Deutschland beträgt ca. 14 c/kWh und in Malta ca. 25 c /kWh. Reine batteriebetriebe Schiffe sind daher auf Routen angewiesen, entlang derer die Stromversorgung langfristig zu günstigen Preisen dargestellt werden kann.

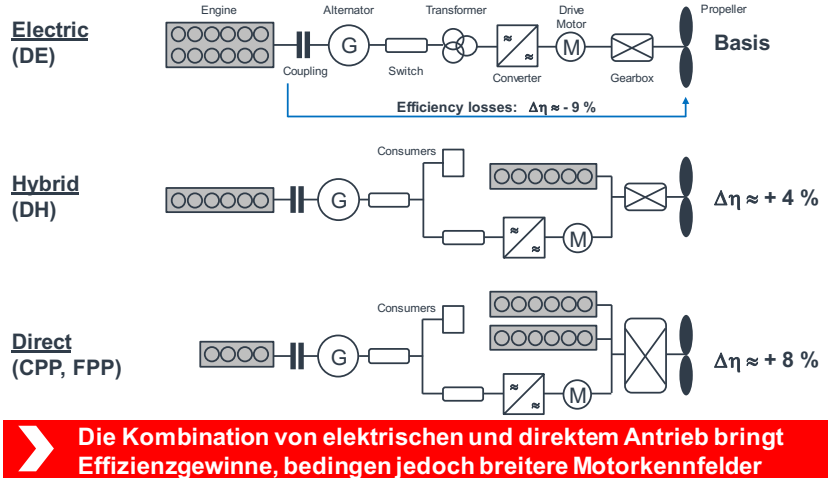

Abb.9: Optimierung des Antriebsstranges

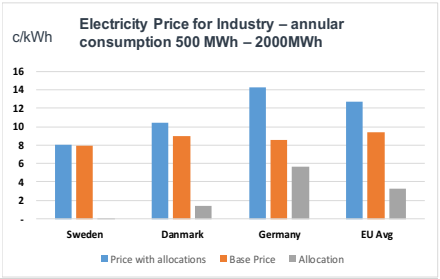

cent/kWhr	Sweden	Danmark	Germany	EU Avg
Price with allocations	8,04	10,45	14,28	12,70
Base Price	7,99	9,00	8,60	9,43
Allocations	**0,05**	**1,45**	**5,68**	**3,27**

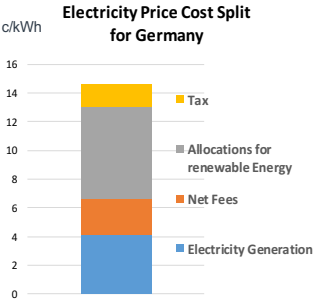

On Board Generation Break Even (Price Bunkerindex 29.3.2016)					
MDO	396	$/to	el. Prod. Cost	7,3	c/kWh
MGO	518	c/kWh	el. Prod. Cost	9,6	c/kWh

"Bunkering" of electric energy is highly dependent on local electricity prices and local achievable contracts

Abb.10: Industriestrompreise im Vergleich

Eine der wesentlichen Herausforderungen für die Schiffausrüsterindustrie wird in den nächsten Jahren die Digitalisierungsoffensive sein, die der Branche bevorsteht. Diese wird noch verstärkt durch die Initiativen zum „remote control shipping" und der unbemannten Schiffsführung. Die Abb.: 11 zeigt exemplarisch die heutige Überwachung eines Container Schiffes. Die Reederei hat ein zentrales Operationscenter, in dem jedes Schiff überwacht wird. Während die Masse der Sensoren der Überwachung der Schweißnähte und der Verformung des Schiffsrumpfes durch den Wellengang dienen, ist der Maschinenraum mit 200 Sensoren extra überwacht. Die Hersteller der Motoren und der Ausrüstung des Maschinenraums entwickeln Modelle, wie sie diese Überwachungsfunktion durch das eigene Haus darstellen können. Gerade im Fall des remote control shippings oder des unmanned shippings kann die Expertise für ein „on condition maintenance" nur durch den Ausrüster des Maschinenraums sicher erfolgen, es sei denn, er gibt seine Expertise an den Betreiber des Schiffes oder den Betreiber des Remote Control Centers weiter. Letzteres würde erhebliche Verwerfungen gegenüber dem heute üblichen Servicekonzepten der Ausrüstungsindustrie zur Folge haben.

Abb. 11: Überwachung eines Containerschiffes

Für den zukünftigen Service werden die Motorenhersteller neben den traditionellen Service Konzepten auch ein „on condition maintenance“ Konzept anbieten müssen. Die Lebensdauer von Einspritzkomponenten hängt entscheidend vom Mix der Qualität des verbrauchten Kraftstoffes ab und von der exakten Regelung der Kraftstoffaufbereitung. Die korrekte Wartung von Filtern, die genaue vorgegebene Einstellung der Niederdruck-Kraftstofftemperaturen zur Einstellung der richtigen Viskosität aber auch zur Vermeidung von Verlackungen haben entscheidenden Einfluss auf die Lebensdauer der Einspritzungskomponenten-. Eine Vorhersage eines Ausfalls derartiger Komponenten wird in Zukunft 500 oder 1000 Stunden vor dem Ausfall erwartet (7)

Die Abb.: 12 zeigt die heutige Praxis der Überwachung der Daten des MAN Online Monitoring Systems. Die Erfassung der Rohdaten erfolgt über die Motorsteuerung und einen Datalogger, der über einen VPN Client an das MAN Data Backbone angeschlossen ist. Die Analyse der Daten erfolgt in einem MAN Maintenance Operations Center.

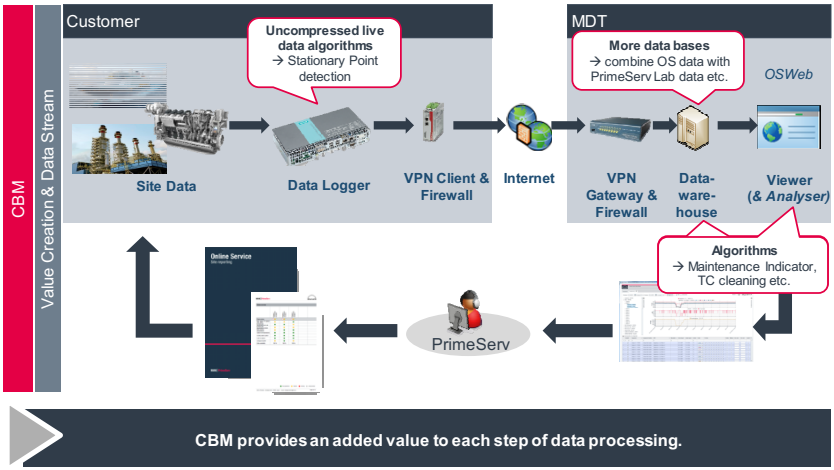

Abb. 12: Schematischer Datenfluss im Online Monitoring und bei CBM Systemen

Die Vorteile einer ferngesteuerten Schiffsführung sind eine Steigerung der Effizienz des Schiffsbetriebs (6). Schiffe haben mehr Platz für die Ladung und benötigen weniger Energieaufwand für die Hotellasten. Der Betrieb von Schiffen kann in engen Gewässern durch Platooning, analog zu dem, was derzeit beim LKW im Test ist, erfolgen. Ein wesentlicher Anteil der Effizienzsteigerung wird durch die Integration von Routendaten, Wetterdaten, aktueller Terminplanung der Häfen und dem sich erforderlichen optimalen Einsatz der Antriebssysteme ergeben. Die Personalkosten werden aufgrund der geringeren Mannschaftsstärke an Bord sinken oder entfallen ganz. Zukünftige Betreiber von remote control centers für die Schiffssteuerung geben an, dass ein Operator bis zu 6 Schiffe auf freier See gleichzeitig navigieren kann. Weitere Kosteneinsparungen werden über die Wartungskonzepte entstehen. Mit der Einführung von fernüberwachten Maschinenräumen werden CBM Systeme zur Plicht. Ein Ausfall von kritischen Bauteilen muss auf 500 – 1000 Std (7) im Voraus erkannt werden, so dass eine planbare Wartung ermöglicht werden kann. Die ersten Ausrüster für Maschinenräume haben mit der Einführung von Power by the Hour Wartungsverträgen begonnen. Die Abb.:13 zeigt einen wahrscheinlichen Zeitplan der Roadmap zur autonomen Schiffsführung (8).

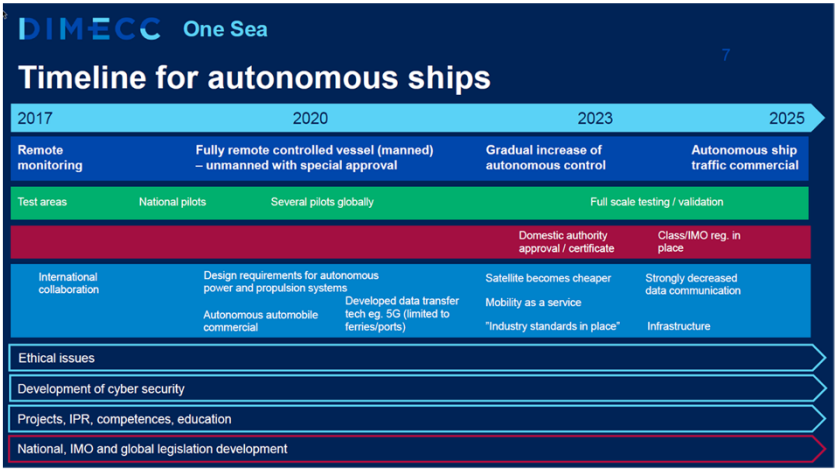

Abb.13: DIMECC Roadmap for Autonomous Ship

Quellenverzeichnis

(1) DNV-GL Gas Carrier Update 2017

(2) URI 2017 World LNG Report

(3) Data Centers – Opportunity to Cooperatives?
Matti Rautkivi (Wärtsilä) Annual AREGC Conference – June 26th-29th 2016

(4) Auftrag für weltgrößtes Wind-Diesel Hybridkraftwerk Bonaire
MAN Corporate Communication Juni 2009
www.man.eu/man/media/de/content...1/.../090623_md_wind_diesel_hybrid.pdf

(5) Dynamic AC Concept for variable speed power generation
Sami Kanerva, Pasio Pohjanheimo, Mikko Kajava, ABB Marine and Ports
Helsinki, Finnland 2016

(6) Munin – Maritime Unmanned Navigation through Intelligence in Networks
MESA Workshop on "The Connected Ship and Shipping"
Marinteck – Ornulf Jan Rodseth – June 29th 2016

(7) Munin D8.7: Final Report: Autonomous Engine Room 18.08.2015

(8) The Roadmap for Autonomous Ships
Päivi Haikkola, DIMECC, Electric & Hybrid Marine World Expo 6-8 June 2017 Amsterdam

Agenda 2030 – mega trends in the large-bore marine engine business

(Agenda 2030 – Mega-Trends im Bereich der maritimen Großmotoren)

Dr. Udo Schlemmer-Kelling, FEV Europe GmbH, Aachen

W. Siebenpfeiffer (Hrsg.), *Heavy-Duty-, On- und Off-Highway-Motoren 2017*,
Proceedings, https://doi.org/10.1007/978-3-658-21029-8_2

1 Einleitung

Betrachte man die Zeit bis zum Jahre 2000 im Marinegeschäft, so standen folgende Schwerpunkte bei der Entwicklung von Großmotoren im Vordergrund:

- Zuverlässigkeit der Anlage
- Anschaffungskosten
- Betriebskosten
- Wartungsfreundlichkeit

In der darauf folgenden Zeit kam als ein weiterer Schwerpunkt die Emissionsminderung hinzu. Die IMO (International Maritime Organisation) kümmert sich in dieser Hinsicht um die Belange der weltweiten Schifffahrt und damit auch um die Begrenzung der Emissionen [1]. Es wurden folgende Gesetze (Fig. 1) verabschiedet:

- Ab dem 1.1.2000 wurde die NO_X Emission begrenzt. Ab dem 1.1.2016 gilt die die Stufe Tier II mit Grenzwerten von etwa 2 g/kWh.
- Die SO_X Emission wird durch die Begrenzung des Schwefelgehalts reduziert. Ab 2020 gilt ein weltweiter Maximalwert von 5000 ppm.
- Für die CO_2 wird ein EEDI Index für die Gesamtanlage aus dem Kraftstoffverbrauch berechnet. Er ist für die verschiedenen Schiffstypen unterschiedlich und wird alle 5 Jahre um 10 % gesenkt.
- Die Ruß bzw. Partikel Emission wird zurzeit noch nicht begrenzt. Die Diskussionen bei der IMO dauern dazu noch an. Mit eine kurzfristigen Entscheidung ist nicht zu rechnen.

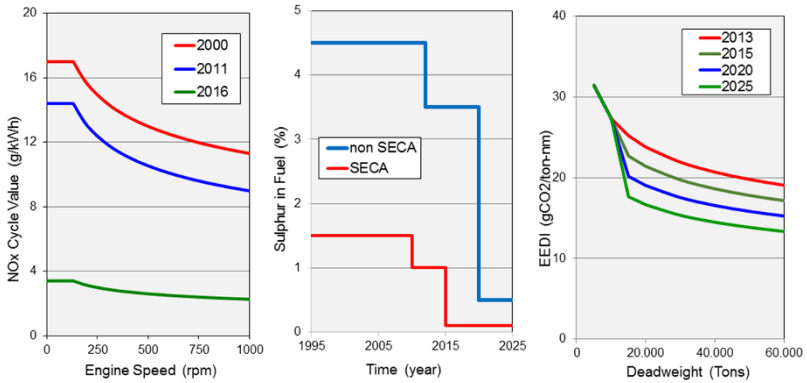

Fig. 1 Emission Gesetzgebung der IMO für NO_X, SO_X und CO_2

Seit 2015 sind die Grenzwerte für einige Komponenten so niedrig, dass sie motorintern nicht mehr erfüllbar sind und für Dieselmotoren ein Abgasnachbehandlungssystem notwendig wurde.

2 Entwicklungsschwerpunkte

Um einen besseren Überblick über die zukünftig notwendigen Entwicklungsarbeiten zu bekommen, wurde von der FEV eine Road Map erstellt. Sie zeigt für 8 verschiedene Kerntechnologien die Technikmodule, die zeitlich abgestuft von der Mehrheit der Motorbetreiber mit großer Wahrscheinlichkeit eingesetzt werden (Fig. 2).

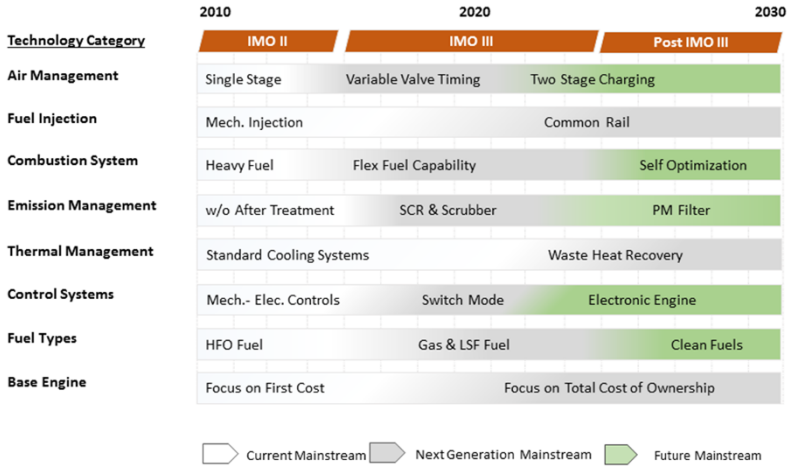

Fig. 2 Road Map für notwendige Entwicklungsschwerpunkte

Zusammengefasst lässt sich sagen, dass Auflade- und Einspritzdrücke steigen, eine Abgasnachbehandlung unumgänglich und eine erhöhte Flexibilität in der der Motorsteuerung erfordert wird. Grundsätzlich werden die Kraftstoffe sauberer werden müssen. In dieser Hinsicht hat auch der gasförmige Kraftstoff LNG einige Bedeutung.

Über die Jahre ist es gelungen, den Wirkungsgrad der Motoren immer weiter zu steigern Dabei sind die Potentiale in der Verbrennungsführung, dem Ladungswechsel und dem mechanischen Wirkungsgrad für den Hochlastbereich weitgehend ausgeschöpft. Als einzige übriggebliebene Maßnahmen sind die Erhöhung der Zünddruckes bei gegebener Motorleitung und der Übergang auf eine 2- stufige Aufladung mit Zwischenkühlung

anzusehen. Im Bereich der Teillast sind durch variable Konzepte, die die Einspritzung und die Luftversorgung des Motors betreffen, noch größere Potentiale vorhanden.

Natürlich sind die Maßnahmen mit zusätzlichen Kosten verbunden. Deshalb wurde in einer TCO (Total Cost of Owbership) Betrachtung die Bedeutung für Kunden und Umwelt untersucht. Wie aus Fig. 3 zu entnehmen kann der nach Betriebshäufigkeit gemittelte Kraftstoffverbrauch eines durchschnittlichen Basismotors durch verschiedene additive Maßnahmen um ca. 7 % gesenkt werden.

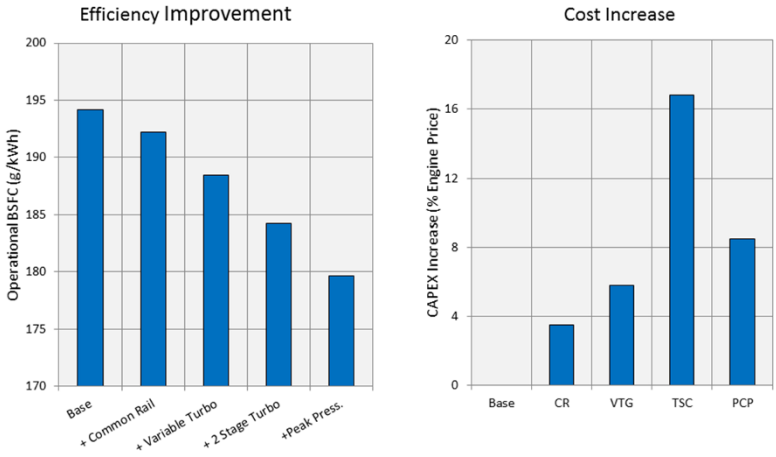

Fig. 3 Änderung der Betriebs- und Anschaffungskosten

Natürlich beeinflussen die Technologiepakete auch die Anschaffungspreise des Motors. Bei Addition aller Optionen sind Zusatzkosten in Höhe von ca. 35 % des Motors zu erwarten. Da sich in dieser Darstellungsform eine Amortisation der Anschaffung nicht klar erkennen lässt, wurde unter den Randbedingungen einer 10 MW Hauptmaschine mit 6000 Betriebsstunden pro Jahr, einem typischen Betriebsprofil und einem Kraftstoffpreis von 300 €/Tonne eine Vollkostenrechnung (TCO) durchgeführt. Wie Fig. 4 zeigt, rentieren sich die Anschaffung aller Einzelmaßnahmen schon nach einer Zeit von ca. 2 Jahren. In der Summe werden innerhalb von 5 Jahre 0,5 Mio. € eingespart. Das entspricht einer Kostenminderung von etwa 3,5 %.

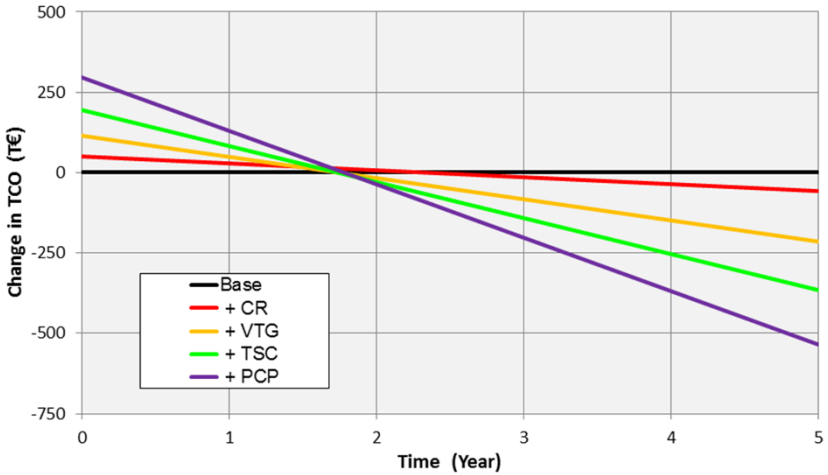

Fig. 4 TCO Berechnung für eine 10 MW Hauptmaschine

Bei der eben betrachteten Erhöhung des Zünddruckes von 10 % stellt sich unweigerlich die Frage, wie weit man hier sinnvoll gehen kann. Historisch gab es zwar eine kontinuierliche Erhöhung in den letzten Jahren von 140 bar (~ 1980) bis auf 270 bar (~2016), die allerding mit einer ebenso starken Leistungserhöhung gekoppelt war. Das für den Wirkungsgrad bedeutende Verhältnis von Zünddruck zu Mitteldruck stieg lediglich von damals ~8 auf heute ~9. Offen bleibt die Frage, bis zu welchem Verhältnis eine Zünddrucksteigerung sinnvoll ist. Mit dem Zünddruck steigt die Belastung der Mechanik, die zu größeren Abmessungen (Kosten) des Motors führt. Bei unveränderter Motorleistung sinkt der mechanische Wirkungsgrad entsprechend. Eine TCO Berechnung zeigt, dass eine weitere Erhöhung des Zünddruckes zwar die Kosten steigen lässt, aber den Wirkungsgrad nicht mehr wesentlich erhöht (Fig. 5). Oberhalb eines Verhältnisses von 10 sind keine Vorteile mehr zu erwarten.

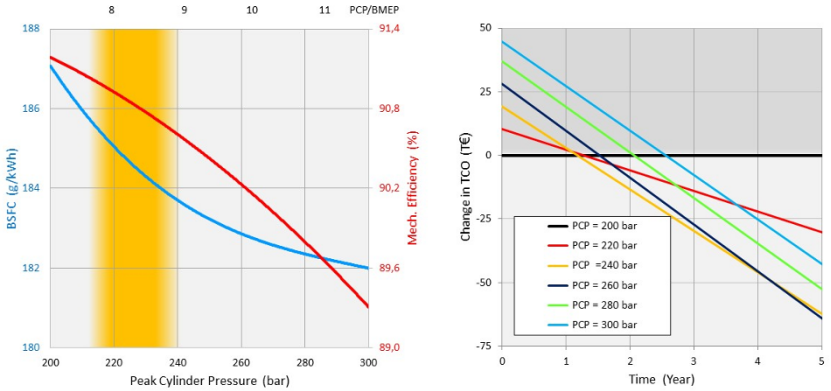

Fig. 5 Potential einer Zünddruckerhöhung

Um die Leistung eines Motors zu erhöhen, gibt es den Weg einer Mitteldruck- oder einer Drehzahlerhöhung. Im Vergleich zu einem Basismotor sinken in beiden Fällen die Anschaffungskosten. Bei einer Mitteldruckerhöhung ist die Minderung nicht ganz so stark, da die Zünddruckerhöhung einen Mehraufwand in der Aufladegruppe und im Kurbeltrieb erfordert. In der Gesamtschau der Kosten ist eine Drehzahlerhöhung auf Grund der Prozessnachteile in der Verbrennung, dem Ladungswechsel und dem mechanischen Wirkungsgrad für den Betreiber deutlich ungünstiger als eine Mitteldruckerhöhung (Fig. 6).

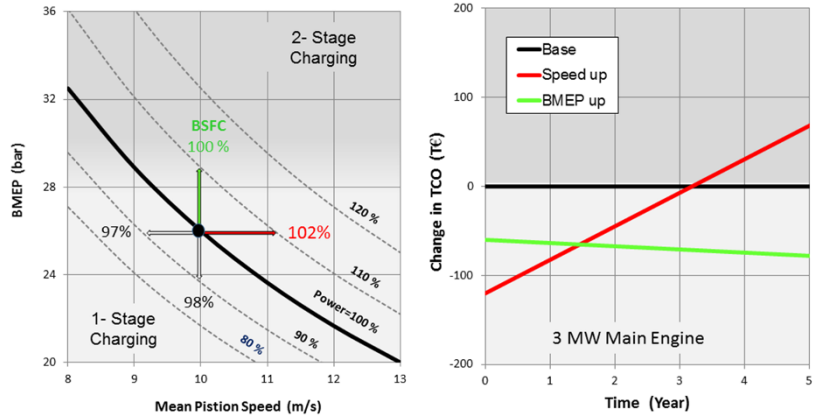

Fig. 6 Wege zur Leistungserhöhung und Wirkungsgradsteigerung

3 Schweröl als Kraftstoff

Um aus Rohöl die hochwertigen Kraftstoffe für Fahrzeuge herzustellen, nutzt man in den Raffinerien üblicherweise Destillationsprozesse. Da nicht alle Komponenten destilliert werden können, bleibt als Rückstand das sogenannte Schweröl über. Im Laufe der Zeit wurden diese Prozesse immer weiter verfeinert, so dass der Anteil des Schweröls kontinuierlich verringert dafür aber in der Handhabung problematischer wurde. Der hohe Schwefelgehalt und die chemischen Komponenten aus den Crack- Prozessen (Cat Fines) sind hierbei besonders zu nennen (Fig.7).

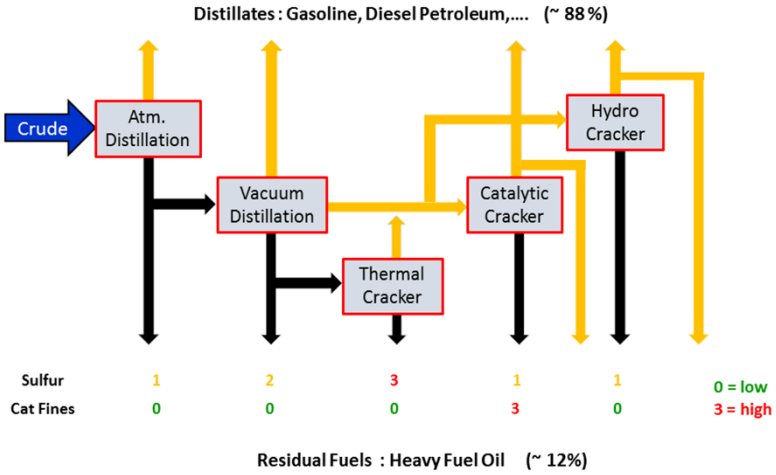

Fig. 7: Raffinerie- Prozess zur Herstellung von Kraftstoffen

Nachdem das Schweröl zuerst in Kesselanlagen verfeuert wurde, führten die Ölkrisen in den 1970'er Jahren mit stark steigenden Kraftstoffpreisen zur Suche nach kostengünstigen Alternativkraftstoffen. Das Schweröl war in den letzten Jahren im Durchschnitt 200 $/Tonne billiger als der bis dahin übliche Destillationskraftstoff MDO.

Während man im ersten Schritt den Motor und seine Peripherie noch unverändert ließ, stellte sich im Laufe der Zeit schnell heraus, dass Anpassungen an den Kraftstoff notwendig waren. Der Kraftstoff Schweröl musste aufwendig aufbereitet werden (Fig. 8). Dazu zählten:

- Setztanks, in denen sich Schwebstoffe absetzen konnten
- Separatoren, die Wasser und Schlamm abschieden
- Viskositätsregeleinrichtungen, die den Kraftstoff dünnflüssig hielten.

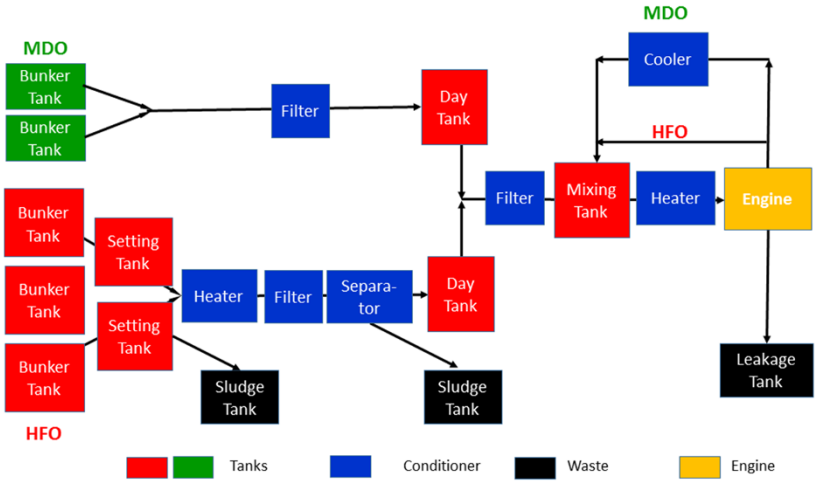

Fig. 8: Kraftstoffversorgungssystem für Schiffe im HFO Betrieb

Beim Betrieb fallen erhebliche Mengen abgeschiedener Schlämmen, die entsorgt werden müssen, an. Lange Zeit wurden sei einfach ins Meer gepumpt. Heute werden meist die Annahmestellen in den Häfen genutzt.

Auch die Motoren mussten an den Kraftstoff angepasst werden. Die Thermik des Motors war neu abzustimmen:

- Die Bauteiltemperaturen des Brennraums mussten in einem engen Fenster zwischen Kalt- und Heißkorrosion liegen. Die Kühlung der Bauteile (Laufbuchse, Ventile) sowie die Luftversorgung (Luftverhältnis, Luftdurchsatz) waren zu intensivieren.
- Um die bei der Verbrennung entstehende Schwefelsäure zu binden, waren kalziumhaltige Additive im Schmieröl notwendig.
- Es wurden Reinigungseinrichtungen (Turbolader) nötig.

Der Betrieb mit Schweröl erfordert also einige Zusatzmaßnahmen, die die Kostenbilanz (TCO) der Antriebsanlage erheblich beeinflussen. Sowohl die Anschaffung der Module für Kraft- und Schmierölpflege als auch die Kosten für den Betrieb (~ 5 % der Motorleistung) müssen sich durch den geringeren Kraftstoffpreis amortisieren. Dies gelingt auch mit zunehmender Betriebszeit und Motorauslastung nach kurzer Zeit. Da beides bei den Bordaggregaten für die elektrische Versorgung deutlich geringer ist, werden sie häufig auch mit MDO betrieben. Fig. 9 basiert auf den heutigen Kraftstoffpreisen, die verhältnismäßig niedrig sind. Höhere Preise reduzieren die TCO Zeit deutlich.

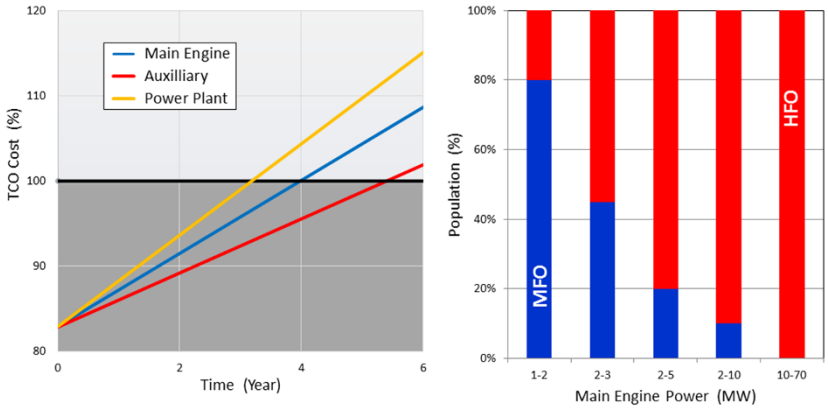

Fig. 9: TCO Kalkulation für den Betrieb mit HFO

4 Emissionen im HFO Betrieb

Der Betrieb mit Rückstandsölen ist aus Umweltgesichtspunkten nicht unproblematisch. Sowohl die NO_X als auch die Ruß und CO_2 Emission sind zwar nur geringfügig höher als beim Betrieb mit Destillatkraftstoffen, dafür sind SO_X und PM Emissionswerte aber extrem hoch. Ursache hierfür ist der hohe Schwefelgehalt von durchschnittlich 25000 ppm.

Mitte der 90-iger Jahre begann die Diskussion um die Begrenzung der Emissionen von Schiffsmotoren. Als erste Maßnahme wurde die NO_X Minderung eingeführt. Mit der Einführung der IMO III Grenzwerte für ECA- Gebiete im Jahre 2016 wurde der SCR Katalysator erforderlich. Für die Abgasrückführung enthält der Kraftstoff Schweröl zu viel Schwefel und Aschebestandteile, so dass diese Maßnahme ohne zusätzliche Reinigungseinrichtung nicht geeignet ist.

Die SO_X Emission wurde von der IMO über den Schwefelgehalt im Kraftstoff in mehreren Schritten reduziert. Der aktuelle Wert für die ECA Gebiete liegt zurzeit bei 1000 ppm und ab dem 1.1.2020 bei 5000 ppm für nonECA Gebiete. Da die PM Emission bei HFO- Betrieb im Wesentlichen vom Schwefelgehalt geprägt wird, stellt sich auch hier eine deutliche Verbesserung ein (Fig. 10). Die typischen PM Emissionen im HFO Betrieb liegen bei etwa 1,4 g/kWh. Über eine Reduktion des Schwefelgehalts auf 0,5 % sinkt der PM Wert auf etwa 0,6 g/kWh ab. Der Übergang auf Destillate und der Einsatz von Schmierölen mit weniger Säurebindern (Calcium zur Neutralisation) kann den PM Wert auf 0,2 g/kWh reduzieren. Das ist allerdings immer noch ein um den Faktor 10 höherer Wert als derjenige, der von LKW Motoren als Roh- Emission erreicht wird. Hier spielt der hohe Schmierölverbrauch der Großmotoren noch eine entscheidende Rolle.

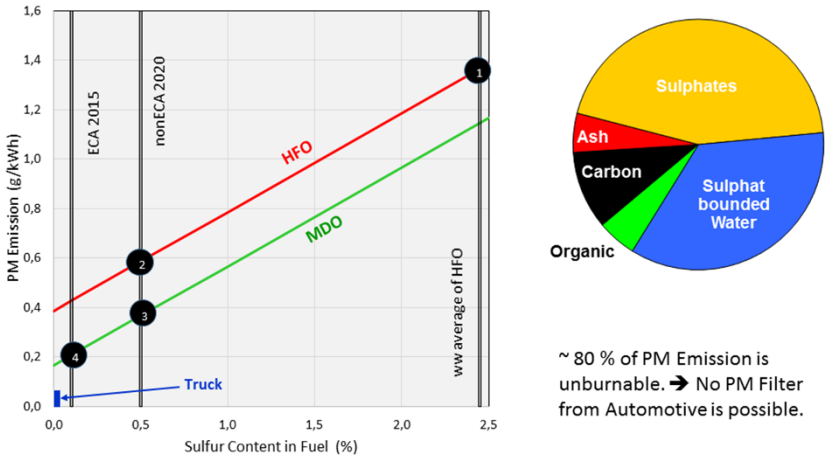

Fig. 10: Partikel- Emission und deren Zusammensetzung im HFO Betrieb

Die SO_X Emission kann durch den Motor selbst nicht beeinflusst werden. Hier sind schwefelarme Kraftstoffe wie Diesel (z.B. EN 590) oder Gas (LNG) erforderlich. Eine außermotorische Maßnahme ist der Abgaswäscher (Scrubber), bei dem sich der Nasswäscher gegenüber dem Trockenwäscher durchgesetzt hat.

Da die Weltmeere nicht einheitlich reglementiert und in ECA und nonECA Zonen mit unterschiedlichen Grenzwerten eingeteilt sind, muss sich der Betreiber über die Fahrtgebiete seines Schiffes im Klaren sein. Das Verhältnis von ECA- zu nonECA Betriebszeit beeinflusst seine Kostenbilanz und damit die sinnvoll einzusetzende Technologie erheblich.

5 Mögliche Konzepte

Der Dieselmotor ist heute die Hauptantriebsquelle bei Schiffen. Die Gasmotoren sind erst mit dem in der letzten Zeit zunehmendem Umweltbewusstsein hinzugekommen. Beide Motorenarten genügen der heutigen Emissionsgesetzgebung [2,3]. Der Dieselmotor benötigt dazu ein umfangreiches Abgasnachbehandlungssystem. Der Gasmotor ist dagegen von sich aus gesetzgebungskonform.

5.1 Der Dieselmotor

Die Architektur des Motors wird hier wenig beeinflusst. Die Maßnahmen beziehen sich auf den außermotorischen Bereich. Zur NO_X Reduktion wird ein SCR Katalysator eingesetzt, zur SO_X Reduktion ein Abgaswäscher (Fig. 11).

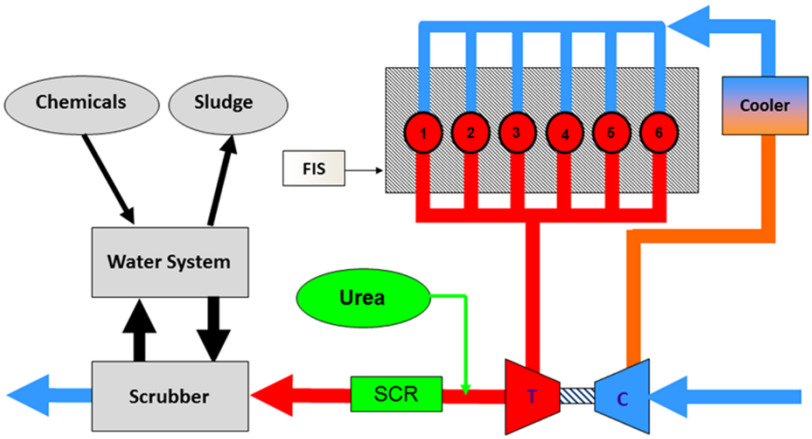

Fig. 11: Schwerölmotor für den IMO III Betrieb

Der Vorteil dieses Konzepts ist die klare Aufgabentrennung der Maßnahmen. Es gibt die Module Motor, Scrubber und SCR. Sollte ein Nachbehandlungssystem störungsbedingt ausfallen, ist die Anlage immer noch betriebsbereit. Des Weiteren ist die Infrastruktur für die Kraftstoffversorgung etabliert und die Kraftstoffkosten schwanken weltweit verhältnismäßig wenig.

5.2 Der Gasmotor

Im Prinzip würde der reine Otto- Gasmotor die gestellten Aufgaben hinreichend gut erfüllen. Da er aber im Marinebereich noch nicht weit verbreitet ist, wird der Dual Fuel Motor zurzeit favorisiert (Fig. 12).

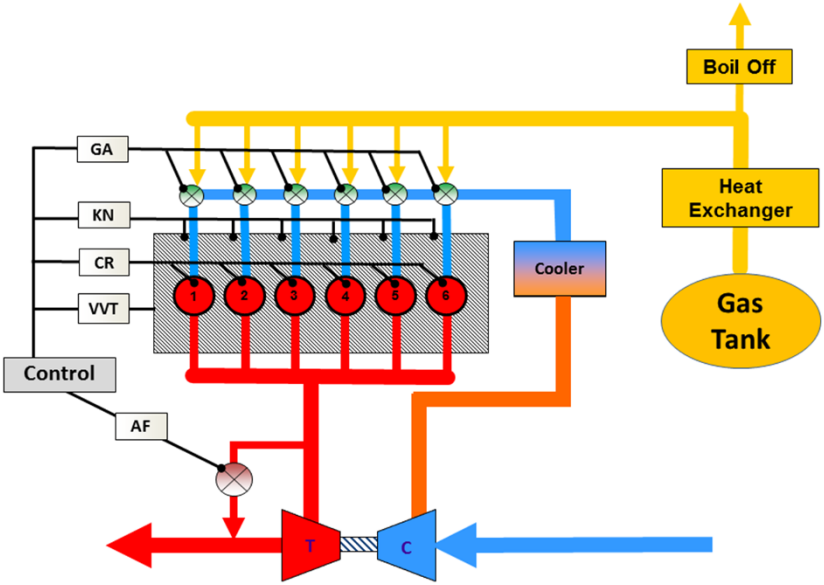

Fig. 12: Gasmotor für den IMO III Betrieb

Dieses Konzept kann sowohl mit Diesel als auch mit gasförmigen Kraftstoffen bis zur vollen Motorleistung betrieben werden. Die Betriebssicherheit ist durch zwei mögliche Kraftstoffe erhöht und die Kraftstoffart kann je nach Kostensituation angepasst werden.

Zur Emissionsminderung sind keine weiteren Module notwendig. Die Rohemissionen des Motors erfüllen alle heutigen und zukünftigen Grenzwerte der IMO. Die Komplexität des Motors ist bedingt durch den niedrigen Flammpunkt von Methan sowie durch das kleinere Betriebsfensters des Motors zwischen Klopfen und Zündaussetzer erheblich größer als beim Dieselmotor.

6 Kostenaspekte

Um sich für ein Konzept zu entscheiden, gelten je nach Konstellation verschiede Kriterien. Sollte bei einem Schiffsneubau der Eigner die Entscheidungshoheit haben, so dominieren folgende Kriterien:

1. Nachgewiesene Zuverlässigkeit, Referenzen
2. Erprobte Technik , keine ungeplanten Ausfallzeiten
3. Niedrige TCO
4. Wartungsfreundliches Motorkonzept
5. Möglichst wenig Komponenten / Module

Sollte die Werft einen Gesamtauftrag vom Eigner bekommen, so hat sie die Entscheidungshoheit und achtet verstärkt auf:

1. Niedrige Anschaffungskosten
2. Einfache Installation
3. Unterstützung durch den OEM bis zum Ende der Garantiezeit

Auch die Frage, ob das Schiff vom Eigner selbst betrieben oder verchartert werden soll, ist von Bedeutung. Im ersten Falle muss der Eigner die Betriebskosten selbst bezahlen, im zweiten ist der Charterer dafür verantwortlich. Der Eigner ist hier nur für die Fixkosten des Schiffes zuständig.

Die durchschnittliche Lebensdauer eines Schiffes beträgt ca. 25 Jahre. Für diesen Zeitraum muss der Eigner die Ausrichtung seiner Investition (Schiff) vornehmen. Die emissionsmindernden Maßnahmen, die zur Einhaltung der IMO III Gesetzgebung notwendig sind, verteuern die Anschaffungskosten erheblich (Fig. 13). Der Preis für den Motor, die notwendigen Module (HFO Anlage, SCR Katalysator und Scrubber) sowie der Einbau der Komponenten durch die Werft in das Schiff erhöhen den Preis einer HFO Anlage um ca. 50 %. Bei einem LNG Antrieb ist die Speicherung des Methans bei -163 °C sehr aufwendig und kostenintensiv. Wird der Motor nicht betrieben, so ist eine Rückverflüssigung des Boil Off Gases oder ein Modul zum Abfackeln nötig. Insgesamt steigt der Preis der Gesamtanlage um ca. 150 %.

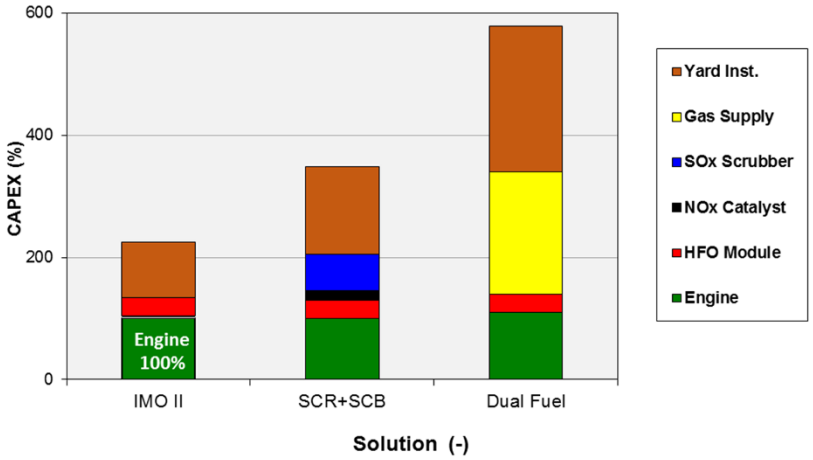

Fig. 13: Relative Anschaffungskosten für verschiedene Antriebskonzepte

Für die Betriebskosten spielt der Kraftstoffpreis eine entscheidende Rolle. Eine längerfristige Abschätzung in die Zukunft ist dabei extrem schwierig. Während die Mineralölpreise weltweit verhältnismäßig identisch sind, schwanken die Gaspreise dagegen erheblich. Fig. 14 zeigt die Schwankungen an der US Rohstoffbörse in den letzten Jahren.

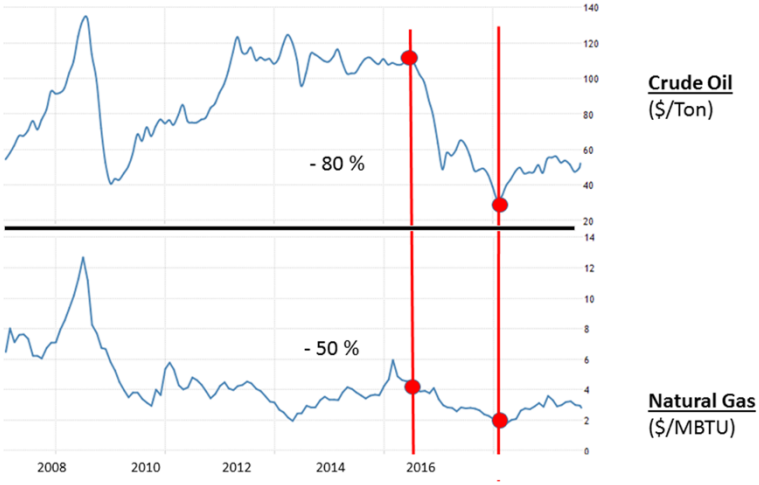

Fig. 14: Preise verschiedener Kraftstoffe an der US Börse

Während sich im Jahre 2014 deutliche Kostenvorteile mit einem ROI von ca. 3 Jahren beim Gasbetrieb ergaben, kehrte sich das Ergebnis im Jahre 2016 , getrieben durch die extrem niedrigen Mineralölpreise, um. Ein Betrieb mit Gas wurde zum Verlustgeschäft. Auch die Finanzierungs-kosten der sehr teuren Gasspeicherung bei -163 °C schlagen sich nicht unerheblich auf die Betriebskosten nieder. Die Kostenanalyse ist in Fig. 15 dargestellt.

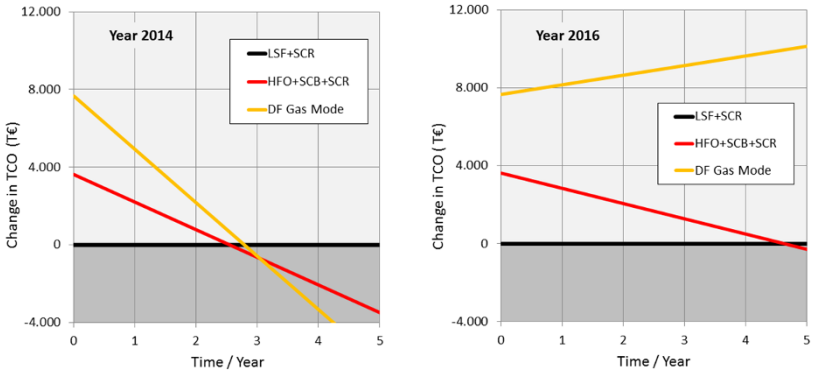

Fig. 15: TCO Analyse für einen 10 MW Antriebsmotor (ECA/nonECA = 50/50)

Da die SO_X Reglementierung nicht nur die Neubauten sondern alle Schiffe betrifft, müssen die Eigner der bestehenden Flotte die Frage der Nachrüstung von Technologien prüfen. Im Grundkonzept des Schiffes ist der nachträgliche Einbau voluminöser und schwerer Module meist nicht vorgesehen, so dass Frachtraumverluste zu beachten sind (Fig. 16). Der Einbau eines schweren Scrubbers in großer Höhe kann die Stabilität des Schiffes negativ beeinflussen.

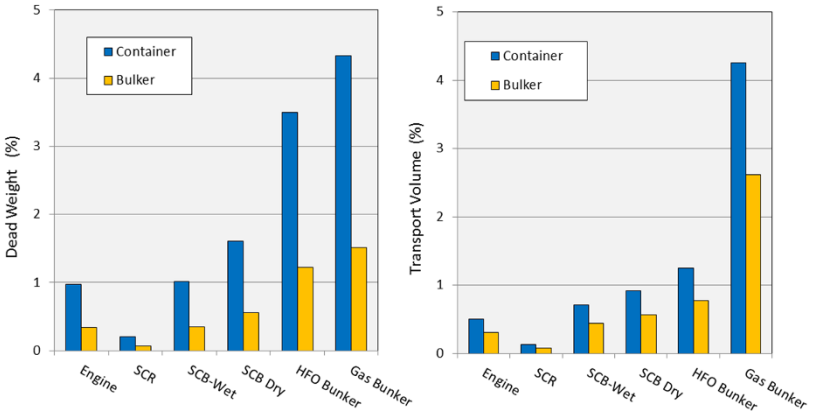

Fig. 16: Schiffbauliche Aspekte wichtiger Komponenten

Während die kleinen Schiffe ihre größten Betriebsanteile in ECA Zonen haben, operieren die großen Schiffe im weltweiten Linendienst fast ausschließlich in den nonECA Zonen. Bei den mittelgroßen Schiffen bedingt der häufige Wechsel zwischen den Zonen einen schaltbaren Betrieb, der optimal an die Vorgaben des jeweiligen Fahrgebietes angepasst ist.

7 Bewertung der Optionen

Will man eine Prognose zu zukünftigen Entwicklungen abgeben, so kommt man recht schnell zu der Frage: " Welcher Kraftstoff wird sich in Zukunft durchsetzen?" Die Kriterien, die zu einer Entscheidung führen, lauten wie folgt:

- Ist der Kraftstoff in meinem Fahrtgebiet uneingeschränkt verfügbar?
- Wie hoch ist der Kraftstoffpreis und wie wird er sich zukünftig entwickeln?
- Ist die Technologie der gesamten Antriebsanlage dafür zuverlässig?
- Kann meine Crew die Anlage sicher bedienen und warten?
- Auf welche zukünftigen Emissionsbeschränkungen muss ich vorbereitet sein?

Aus rein ökologischer Sicht haben Bio-Kraftstoffe hinsichtlich ihres Emissions-verhaltens deutliche Vorteile. Als ein Beispiel sei der Vergleich der Well-to-Propeller CO_2 Emission [6,7] angeführt. Das Minderungspotential von LNG ist mit 5 bis 10 % gegenüber dem Mineralöl nicht sehr groß. Bio-Kraftstoffe werden in näherer Zukunft nicht in ausreichender Menge zu Verfügung stehen. Die Benutzung von Alkoholen in Fuel Cells besitzt ein enormes Potential. Allerding sind sie sehr teuer und in der Leistungsklasse für Schiffe nicht verfügbar. Während die Infrastruktur für LNG zurzeit im Aufbau ist, sind die Bio-

Kraftstoffe deutlich weiter von der weltweiten Einführung in der Seeschifffahrt entfernt. Dies gilt insbesondere für die Nuklear- sowie die Wasserstofftechnik.

Legt man die heutige Situation zu Grunde, so spricht vieles dafür, dass Mineralöl Kraftstoff der Zukunft bleibt. Er ist in allen Fällen die einfachere und planbarere Lösung. Die Investition für eine Gasversorgung an Bord entspricht einem Vielfachen des Motorpreises. Für die Umrüstung der etwa 50.000 Handelsschiffe weltweit auf Scrubber oder LNG Lösungen wäre ein Finanzbedarf von mindestens 50 bis 200 Milliarden Euro notwendig. Den dafür benötigten Finanzbedarf muss der Schiffseigner meist als Darlehen von den Banken aufnehmen, was in der heutigen Situation mit sehr restriktiven Vergabekriterien sehr problematisch ist. Hinzu kommt, dass die Frachtraten auf sehr niedrigem Niveau liegen und somit ein ausreichendes Eigenkapital der Betreiber nicht vorhanden ist.

Aus diesem Grunde wird die Mehrheit der Schiffseigner bis zum Jahre 2020 vermutlich keine Nachrüstungsmaßnahme einleiten und sich auf das Versprechen der Mineralölindustrie verlassen, dass ein regelkonformer Kraftstoff zur Verfügungen stehen wird. In den darauf folgenden Jahren wird man sich an den gesammelten Erfahrungen der Vorreiter orientieren und eine Entscheidung fällen. Viele der betroffenen Schiffe werden dann schon so alt sein, dass sie durch Neubauten mit adäquater Technik ersetzt werden können.

Will man die Fragestellung zukunftsgerichtet beantworten, ist man auf Studien angewiesen. Dafür gibt es mehrere Veröffentlichungen von namhaften Organisationen [8, 9, 10,11, 12]. Die meisten von ihnen kommen zu dem Ergebnis, dass Mineralöl noch lange eine dominierende Rolle spielen wird. Als Beispiel, das dieses Scenario nachvollziehbar erklärt, sei hier Fig. 17 angeführt.

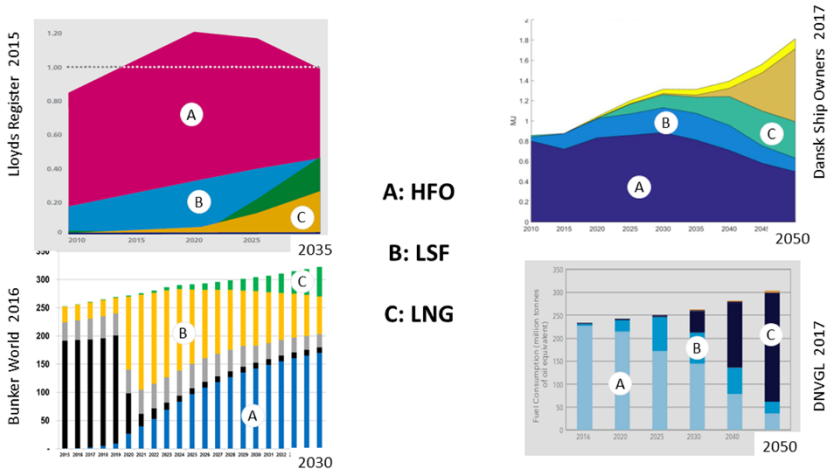

Fig. 17: Prognose über den zukünftigen Einsatz maritimer Kraftstoffe [7]

Die Quelle [7] geht davon aus, dass die Mineralölgesellschaften den benötigten schwefelarmen Kraftstoff (S < 0,5%) für die nonECA Gebiete zur Verfügung stellen wird. Dies wird nicht ein entschwefeltes Schweröl sein. Die Nachrüstung der bestehenden Raffinerien wäre zu teuer. Da damit zu rechnen ist, dass die mittelfristige Zukunft dem Scrubber gehört, ist dieser Kraftstoff nur eine Übergangslösung. Mit der zunehmenden Aus- und Nachrüstung der Schiffe wird der Bedarf von Standardschweröl mit S ~ 2,5 % nach 2020 langsam aber kontinuierlich ansteigen. Der Einsatz von LNG auf Schiffen wird nur einen kleinen Anteil ausmachen. Bis heute sind etwa 0,1 % der weltweiten Handelsflotte mit LNG Antrieben ausgerüstet. Die Prognose, bis 2020 mindesten 1000 Schiffe mit Gasbetrieb ausgerüstet zu haben, wurde in der letzten Zeit schon nach unten korrigiert.

Natürlich gibt es Anwendungen, die für einen Gasbetrieb prädestiniert sind. Dazu gehören in erster Linie die LNG Tanker, die keine zusätzliche Bunkereinrichtung benötigen. Als nächstens wären Kreuzfahrtschiffe zu nennen, die immer unter besonderer Beobachtung der Umweltorganisationen stehen. Auch für Fähren und RoRo Schiffe, die immer auf festen Routen verkehren und somit eine vereinfachte Logistik in der Gasversorgung haben, könnte LNG ein interessanter Kraftstoff werden.

8 Zusammenfassung

Für die Zukunft der Schiffsantriebe zeichnet sich ein ähnlicher Weg ab, wie ihn die Fahrzeugindustrie in den letzten Jahren beschritten hat. Durch immer stärkere gesetzliche Maßnahmen zur Emissionsminderung wird die Antriebsanlage immer umfangreicher und komplexer. Als Folge steigen Anschaffungs- und Betriebskosten.

Auf Grund des immensen Kostendrucks werden die meisten Betreiber immer die kostengünstigste Lösung, die die momentan gültigen Gesetze gerade eben erfüllen, bevorzugen. Das scheint aus heutiger Sicht ein Kraftstoff auf Mineralölbasis zu sein. Es gibt zwar einige Bereiche, in denen gasförmige Kraftstoffe eine sinnvolle Alternative darstellen. Sie werden aber vermutlich nicht zum Mainstream werden.

9 Abkürzungen

DF Dual Fuel

ECA Emission Control Area

HFO Heavy Fuel Oil

IMO International Maritime Organization

LSF Low Sulfur Fuel

MDO Marine Diesel Oil

nonECA Open Sea Outside ECA

SCB SO_X Scrubber

SCR NO_X Catalyst

TCO Total Cost of Ownership

10 Literatur

[1] MAPOL ANNEX VI, and NTC 2008, Edition 2013

[2] How legislation and customer needs drive innovation, S. Pischinger et al, 3. Großmotorentagung Rostock, 2016

[3] Operating Cost Optimized Engine and After-treatment Concepts for Marine Applications, U. Schlemmer-Kelling, CIMAC Congress 2016

[4] Alternative Fuels for Shipping, C, Chryssakis, DNVGK Position Paper 1-2014

[5] Well to Wake Greenhouse Gas Emissions from LNG in Marine Applications, M. Kofod et al., MTZ Industrial Sep. 2015

[6] Can we get to 2020 by 2025, what might happen? R. Meech, The Danish Ecological council, Copenhagen 2017

[7] The road loading to the 0,5 % sulfur limit and IMO's role moving forward, E. Hughes, The Danish Ecological council, Copenhagen 2017

[8] Global Marine Technology Trends 2030, Lloyd's Register et al 2015

[9] Green Ship of the Future Concept Study, B. Oendrup, Odense Ship Yard, 2009

[10] Outlook for Energy, A view to 2030, Exxon Mobil, 2009

Off-road engine based on a present-day 15.3 l truck engine

Dipl.-Ing. (FH) Falko ARNOLD
Lead-Engineer Design Industrial Applications
MAN Truck & Bus AG

Dipl.-Ing. (FH) Thomas STAMM
Development engineer Industrial engines
MAN Truck & Bus AG

W. Siebenpfeiffer (Hrsg.), *Heavy-Duty-, On- und Off-Highway-Motoren 2017*,
Proceedings, https://doi.org/10.1007/978-3-658-21029-8_3

Summary

Especially in the off-road segment with its small number of machines, a cost-efficient development is imperative. For this reason, solutions from the on-road sector are often transferred to mobile machines. With the D3876, MAN has developed an in-line six-cylinder engine for heavy commercial vehicles, agricultural applications and construction machines. While the basic power train and the injection equipment are identical for both application areas, the on-road and off-road versions differ in their concepts for turbocharging, combustion and electronics as well as the attachments and the exhaust gas aftertreatment.

With power ranging from 415 kW to 485 kW (564 to 660 PS) and torque of up to 3,100 Nm, the D3876 is available in the EU Stage IV and US Tier 4 final emissions categories.

1 DIFFERENCES BETWEEN ON- AND OFF-ROAD

The D3876 was presented as a completely new and standalone engine series from MAN in 2014. This 15.26 l in-line six-cylinder engine has replaced the previous D2868 16.2 l V8 engine in the commercial vehicles sector and will also gradually replace the V8 engine in off-road applications with the introduction of the new emissions categories. Key features of the D3876 are its excellent power-to-weight ratio, the high ignition pressure strength and the common rail injection system with injection pressures of up to 2500 bar. The basic engine is therefore predestined for a variety of different applications, whereby a distinction can be made between on-road and off-road applications. On-road applications include heavy trucks with a wide range of uses, from operation on construction sites and off-road traction transport to long-haul transport and heavy-duty transport. Off-road use focuses on applications requiring high power levels in agricultural engineering (self-propelled harvesters) and construction machinery (wheel loaders, earth movers, etc.).

While the basic power train and the injection equipment are identical for both application areas, the on-road and off-road versions differ in their concepts for turbocharging, combustion and electronics as well as the attachments and the exhaust gas aftertreatment. The 6-cylinder D3876 was revised in time for the IAA Commercial Vehicles 2016 and is thus available in commercial vehicles with power ratings from 397 to 471 kW (540 to 640 PS) for powerful trucks and heavy-duty semitrailer tractors. With power ranging from 415 kW to 485 kW (564 to 660 PS) and torque of up to 3,100 Nm, the D3876 is available for heavy, medium and light off-road applications in the EU Stage IV and US Tier 4 final emissions categories. Fundamental differences between the on-road and off-road applications can be found particularly in emissions legislation, the requirements regarding power characteristics and dynamics, the packaging and system integration of the engine and exhaust gas aftertreatment, as well as the environmental conditions and the on- and off-road load profiles. The requirements set by customers from both application areas overlap for the most part in regards to the total cost of ownership (TCO), power density and engine weight, as well as reliability, **FIGURE 1**.

FIGURE 1: The off-road engine (left) and the on-road Engine (right)

2 DEVELOPMENT OBJECTIVES

Typical requirements for commercial vehicles are high torque values at low engine speed ranges, low fuel and urea fluid consumption with relatively uniform driving cycles, dynamic power development, high brake output and low engine and system weight [1]. The production volumes are high and distributed across comparatively few variants. In contrast, off-road applications have a large variety of different driveline configurations, installation spaces and load profiles. These profiles range from light-duty, often semi-static operations, for example combine harvesters, up to heavy-duty dynamic operations, such as wheel loaders. It is therefore necessary for a wide range of torque values and dynamics to be available at up to 3000 m above sea level and in a range of different climate conditions. A simple interface design and flexible configurations are intended to simplify the engine and system integration for the different machines in complex installation conditions. In addition to the already demanding environmental conditions for commercial vehicles, off-road engines are often exposed to extreme vibrations and very dusty and hot conditions. Many applications also require inclinations of up to 45° in all directions. Thanks to modular components and standard interfaces, the lower production volumes which are typical in this sector can be handled using a manageable variety of options.

3 ROBUST LIGHT AND COMPACT BUILD

A robust basic engine is the foundation for all applications. The D3876 engine reaches this high strength and rigidity at a comparatively low weight. At MAN the basic engine consists of the crankcase, crankshaft, connecting rods, pistons, cylinder head including valve gear, camshaft and gear train, **FIGURE 2**. Just as for the smaller D20 and D26 engines, the crankcase of the D3876 is made exclusively from high-strength GJV-450 (vermicular graphite cast iron). The D3876 is designed for ignition pressures of 250 bar to meet the requirements of modern combustion processes and provide adequate potential for the future [1]. Moreover, the cylinder-liner concept selected for the D3876 enables a particularly filigree bulkhead design, as can be seen in the large ventilation openings above the main bearing, which enabled the weight of the component to be further optimised. As such, the engine is one of the lightest engines in its performance class. Despite having only four forged counterweights, the crankshaft has an adequately high degree of compensation. This means that even at engine overspeeds, the loads exerted on the bearings do not exceed permissible levels.

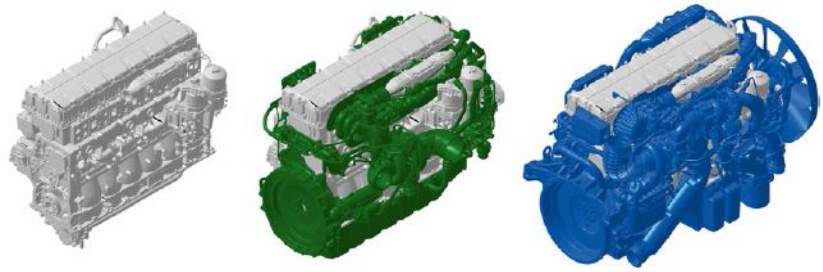

FIGURE 2: On-road and off-road versions of the D3876 are based on the same basic engine (grey) but vary in the application-specific parts (off-road: green; on-road: blue)

The cylinder unit (PCU – Piston Cylinder Unit) also originates from the on-road application. The robust PCU has been reliably undergone in extensive function and endurance tests to ensure the requirements for load spectrum and running time operations are met in both on- and off-road applications. The engine is fitted with steel pistons because of its high peak pressure. Their high strength and rigidity allow a low piston height with a low compression height. The favourable push-rod ratio made it possible to reduce the piston side force. This enables a reduction of the friction torque in the engine compared with types that are fitted with conventional aluminium pistons and contributes to economical fuel consumption. The connecting rod with its FEM-optimised design and weight is made out of heat-treated 70MnVS4 steel. This permits easy cracking at room

temperature. The engine has a single-piece cylinder head. This design has established itself as the standard for modern commercial-vehicle engines. The valve arrangement has been rotated through 45° to realise optimal charge cycles in conjunction with better protection against cracks developing in the valve links [1].

The engineering design of the cylinder head was also consistently optimised for the use of casting material GJV-450. In order to optimise the flow to the intake ports and thus the gas exchange and the tolerance of swirl, a slight amount of added weight resulting from the integration of the air distributor pipe into the cylinder head was accepted. One of the positive effects of this engineering design is the omission of the sealing between the cylinder head and the air manifold. Being able to omit this sealing, which is highly stressed by thermal cycling, contributes to increased reliability.

The valve gear is implemented with an overhead camshaft. Actuation of the valves is controlled by roller rocker arms and flying valve crossheads, resulting in a highly compact form. The high rocker-arm ratios for intake (1.3) and exhaust (1.5) are able to achieve high valve lifts with comparatively small cam lifts. This enables rapid opening of the valve to its maximum. A second overhead camshaft has been omitted for the sake of compact installation dimensions and for reasons of cost. What are known as domed valves are used in the D3876 series. Thanks to the dome-shaped reinforcement to the combustion-chamber side of the valve plate, optimised by means of FEM, there is as good as no deformation and relative movement of the valve in the area of the valve seat ring. This minimises seat wear, making it possible to extend the intervals between valve-clearance checks [1]. The engine has a dual timing gear train with high, straight-toothed gears. Due to the type of toothing, axial bearings for the intermediate gears can be dispensed with, so that the minimum engine length is achieved. For optimising the weight and the manufacturing costs, nitrided or case-hardened gears are employed, depending on the application. The basic engine is also fitted with the latest-generation common-rail system from Bosch, which achieves a maximum rail pressure of 2500 bar and is used for all applications.

For commercial vehicle applications, low weight is prioritised to attain the highest possible payload. The basic engine is a good starting point for achieving this. Components made from aluminium, such as the flywheel housing, and plastic, such as the oil sump and cylinder head cover, contribute to the low weight of the complete engine. The priority for off-road applications is compactness, robustness and ease of servicing, which is attained by lowering the complexity, amongst other things. It must also be easy to make adjustments for different installation conditions. The more stringent requirements for robustness and rigidity are met by using a flywheel housing made of the material GJS-500. Different oil sump types for differing installation spaces and for operational inclinations up to 45° are available.

4 RELIABILITY AND SERVICE LIFE

So-called ‘top-down cooling’ is used for the cylinder head, with the upper cooling jacket functioning as coolant distributor. The coolant is distributed longitudinally to the engine by the upper cooling jacket of the cylinder head. This saves an additional coolant-distribution manifold with consequent sealing points, increasing the robustness and reducing costs. Coolant for each cylinder flows from the upper cooling jacket along the injector sleeve to the points subjected to high thermal loads, such as the injector nozzles, valve seat rings and valve links on the floor of the combustion chamber. Using cross-sections which have been specially harmonised using CFD simulation, the coolant is then used for cooling the cylinder liners of each cylinder in the crankcase. With this flow configuration, the full amount of coolant is available to the cylinder head, considerably reducing the total volumetric flow rate required by the engine. Top-down cooling ensures a robust and uniformly high cooling performance for all cylinders [1]. As a result, by preventing local overheating with its consequent peak stresses it was possible to design a cylinder head that is thermomechanically very robust.

5 SERVICE COSTS AND COMMON PARTS

The engine uses proven components from the modern D20/D26 engine series such as the fan drive unit, PTOs, fuel filters and air filters [1]. This increases ease of servicing and repairs and optimises parts logistics across all MAN series. Long service intervals further reduce the total cost of ownership. For example, it is possible for trucks to have an oil-change interval of 100,000 km and the valve clearance must only be checked at every second oil change. For off-road applications, the service intervals are every 500 operating hours.

6 PERFORMANCE AND EMISSIONS

The requirements placed on a modern turbocharging system in a commercial vehicle engine in the top power segment are multi-faceted. A high torque output which is already available at just above idling speed, a high specific power output at nominal (engine) speed, as well as low fuel consumption in the main operating range with only a minimal increase in fuel consumption when moving to full-load operation all require efficient turbocharging. As the two-stage exhaust-gas turbocharging with intercooling fulfils these requirements very well, all D3876 on-road engines are equipped with this type of turbocharging. The air system is made up of a low-pressure compressor with a downstream low-temperature water-cooled intercooler as well as a high-pressure compressor and a downstream low-temperature water-cooled intercooler [1].

The two differently sized turbo chargers are connected in series on the exhaust side and charge air side. The smaller, high-pressure charger responds well at low engine speeds. As the engine power increases it receives an increasing amount of assistance from the larger, low-pressure charger. In the upper characteristic map area, the charging pressure governing system of the engine control system opens the pneumatically operated wastegate of the smaller high-pressure charger. The larger low-pressure charger, which is better suited to these engine operating points, takes over the majority of the compression work. With this system, the engine air requirements (which depend on the operating point) are fulfilled by whichever charger size offers optimal efficiency. The advantages of a two-stage turbocharging concept are a particularly high total compression efficiency which is attained by using intercooling to reduce energy losses, as well as by a very wide working range.

The exhaust gas recirculation (EGR) is a key technology in the D3876 thermodynamics concept which helps reach both emissions and fuel consumption targets. The cooled exhaust gas recirculation is known to have a large influence on the engine's NOx emissions. The most important parameters here are the EGR rate and the EGR temperature downstream of the exhaust gas cooler. A two-stage cooling concept with a high-temperature (HT) and a low-temperature (LT) EGR cooler was implemented for on-road applications to reduce the exhaust gas outlet temperature as much as possible. The on-road engine has a high-pressure exhaust gas recirculation system which extracts exhaust gases upstream of the turbine, cools them in the two exhaust gas coolers and returns them to the engine mixed with charge air. An electric EGR shut-off flap on the hot side upstream of the EGR cooler controls the amount of the returned exhaust gases and allows fast actuating and exact positioning of the shut-off flap [1].

One of the most important development objectives for the D3876 off-road engine was compliance with the legal limit values for US EPA/CARB Tier 4 final and EU Stage IV, while also providing the best possible fuel efficiency at nominal (engine) speed as well as high torque values at low engine speeds. These development objectives are crucial for off-road applications for serving a broad driveline and application spectrum in contrast to trucks. A comparison of torque and power characteristics of the engines, as well as other characteristics, is shown in **TABLE 1** as well as **FIGURE 3**. Built on the solid foundations of the on-road engine, the off-road engine employs one-stage variable turbine geometry (VTG) charging and a one-stage high-temperature (HT) EGR cooling system. The omission of the intercooler, as well as the simpler piping of the charge-air system and EGR system, combined with the compact VTG turbo charger, cover all requirements for a robust, smaller unit for off-road applications. Due to the required EGR rate being lower for the off-road engine, a more powerful one-stage, high-temperature EGR cooler is used and the second cooling stage is omitted. The omission of the second cooling stage also considerably simplifies the system integration.

TABLE 1: Technical data

Eengine designation	**D3876 LFxx**	**D3876 LExx**
Configuration	Inline six-cylinder engine	
Displacement [l]	15.26	
Bore [mm]	138	
Stroke [mm]	166	
Valves per cylinder	4	
Application	On-road	Off-road
Emission level	Euro 6 c	EC Stage IIIA, EC Stage IV, EPA Tier 4 final/CARB
Charging	Two-stage with intercooling	One-stage with VTG
Peak pressure capacity [bar]	250	
Power [kW/PS] / maximum torque Md max [Nm]	D3876 LF09: P = 471 kW (640 PS) / Md = 3000 Nm D3876 LF07: P = 427 kW (580 PS) / Md = 2900 Nm D3876 LF08: P = 397 kW (540 PS) / Md = 2700 Nm	D3876 LE1xx: P = 485 kW (660 PS) / Md = 3100 Nm D3876 LE1xx: P = 450 kW (612 PS) / Md = 2900 Nm D3876 LE1xx: P = 415 kW (564 PS) / Md = 2700 Nm
Emission concept	EGR, DOC, DPF, SCR	EGR, SCR

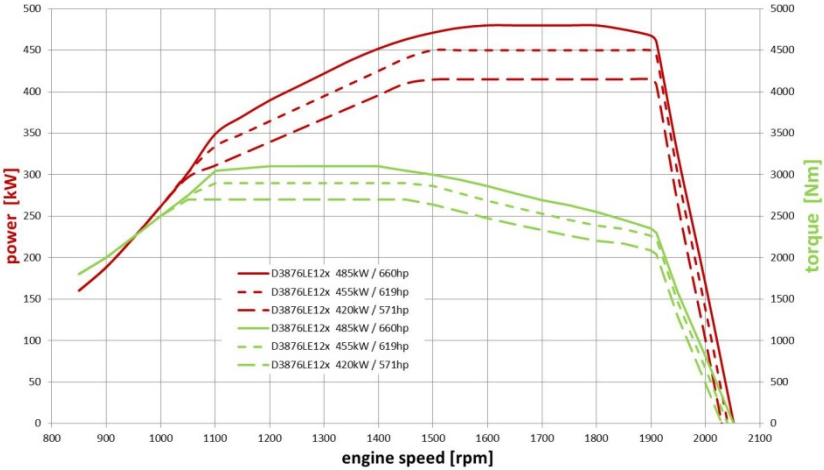

FIGURE 3: Torque and power characteristics

All D3876 engines are equipped with a common rail injection system that works at an injection pressure of 2500 bar for optimal fuel atomisation quality, which in turn helps to achieve a considerable reduction in particle emissions. Due to low particle masses in the exhaust gas, the off-road engine does not require a Diesel particulate filter (DPF), while the on-road engine benefits from improved fuel consumption, for example. At 2500 bar, the common rail injection system offers one of the highest pressures on the market.

The dynamic response in off-road-specific engine speed ranges was optimised using the VTG technology. Especially for off-road use, a fast and dynamic response is vital to ideally cover the wide range of requirements placed on the application-specific engine characteristics. The fuel consumption map of the off-road engine has been adjusted, so that the best fuel consumption as well as another area of low fuel consumption occur at medium engine speeds during partial load operation. Field trials further confirm the leading position of the unit regarding fuel consumption in its branch. The fuel consumption map of the on-road engine shows two features which improve efficiency: In a wide map area, the specific fuel consumption is below 200 g/kWh. At the same time, the best fuel consumption, as well as a second area of low fuel consumption, occur at the typical load spectrum for long-haul applications [1].

The EDC control unit of the off-road engine is an EDC17 by Bosch. It brings together the CAN customer interface which is based on the protocol SAE-J1939. This includes the connection of sensors and actuators on the vehicle, as well as all control unit functions necessary for engine operation and diagnostics. This also includes the completely integrated recording, triggering and monitoring of exhaust gas aftertreatment components. Additional control units are therefore not required [2]. **FIGURE 4** provides an overview of the entire system.

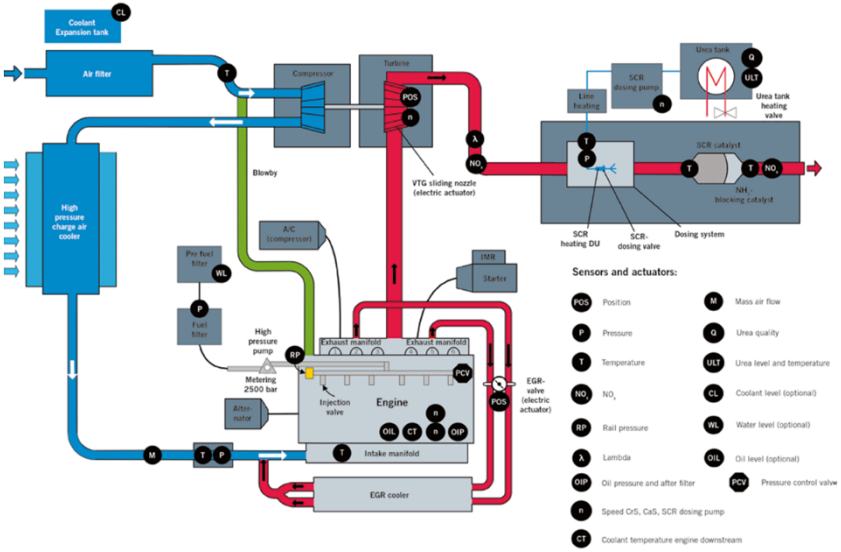

FIGURE 4: Sensors and actuators

As is usually the case for Euro 6, the truck's permanent exhaust gas aftertreatment system is made up of an oxidation catalytic converter (DOC), a closed Diesel particulate filter (DPF), a urea hydrolysis section and an SCR catalytic converter with an ammonia slip catalytic converter (AMOX-SCRT) [3], all connected in series. All components are contained in a silencer box to be installed in the truck frame. Despite the higher exhaust gas volumetric flow, the silencer of the D3876 on-road engine requires the same installation space and is the same design as the one in the D20/D26 engines [4], making it one of the most compact systems in its performance class.

The well-known and proven MAN modular exhaust gas aftertreatment system from the D2676 Tier 4 final and D2862 Tier 4 final off-road applications, which consists of an SCR catalytic converter and slip catalytic converter, has been adjusted to fulfil the requirements of the D3876 off-road engine. The modular exhaust gas aftertreatment system provides maximum flexibility to adjust to different installation spaces as the components can be installed flexibly. Customers can thus make better use of the limited installation space and complex installation situations than with a bulky integrated individual solution, **FIGURE 5**. The emissions regulations EU Stage IV and EPA Tier 4 final are met without using a DOC and a DPF. The modular exhaust gas aftertreatment system can easily be expanded to include additional components, such as a DPF, enabling the system to already fulfil the upcoming EU Stage V emissions requirements.

FIGURE 5: The modular exhaust gas aftertreatment system provides maximum flexibility for many different off-road applications

7 SUMMARY AND OUTLOOK

With the D3876, MAN has released an engine that can be specifically equipped for a wide range of applications thanks to its basic concept. The use of the same basic engine concept for on- and off-road applications reduces costs in development, production and after sales. Application-typical special features and requirements are optimally fulfilled by specifically chosen technology concepts which build on the basic engine. This enables maximum flexibility. The state-of-the-art design of the engine provides the best foundation for additional stages of emissions regulations regarding on- and off-road use, as well as more stringent future requirements regarding power and dynamics. Particularly the upcoming emissions category EU Stage V for off-road, which is currently being developed, is set to benefit significantly from the current experience gained with commercial vehicle engines at similar emissions levels in Euro VI. The engine has the long-term potential to be fully included in the product portfolio for all application areas covered by MAN.

REFERENCES

[1] Schatz, N.; Wiebicke, U.; Klinger, H.: Highly Efficient Commercial Vehicle Engine – the New 15.2 l MAN. 36th International Vienna Motor Symposium, Vienna, 2015

[2] Arnold, F.; Gail, K.; Haberland, J.; Rauth, S.: Adaptation of the MAN D2862 Off-Road Engine to Tier 4 final. In: ATZoffhighway, October 2015, pp. 68–78

[3] Kamm, S.: Particle and NOx Reduction in Euro 6 Commercial Vehicles, Clean Air Planning – Measures against Particulates and Nitrogen Oxides, Augsburg, 2012

[4] Döbereiner, R.; Kamm, S.; Neumayr, K.; Weiskirch, C.: The Next Generation of Construction Vehicles for the Euro 6 Emissions Standard. In: ATZoffhighway, March 2013, pp. 40–49

Authors

Dipl.-Ing. (FH) Falko ARNOLD
Lead-Engineer Design Industrial Applications
MAN Truck & Bus AG, Vogelweiherstraße 33, D-90441 Nürnberg
Tel.: +49 (911) 420-6230
E-Mail: falko.arnold@man.eu

Dipl.-Ing. (FH) Thomas STAMM
Development engineer Industrial engines
MAN Truck & Bus AG, Vogelweiherstraße 33, D-90441 Nürnberg
Tel.: +49 (911) 420-6738
E-Mail: thomas.stamm@man.eu

A high-efficiency lean-burn mono-fuel heavy-duty natural gas engine for achieving Euro VI emissions legislation and beyond

Andrew Auld

Andre Barroso

Matthew Keenan

Panagiotis Katranitsas

Rhys Pickett

Tiago Carvalho

W. Siebenpfeiffer (Hrsg.), *Heavy-Duty-, On- und Off-Highway-Motoren 2017*,
Proceedings, https://doi.org/10.1007/978-3-658-21029-8_4

1 Introduction

Within the EU, Heavy-DutyVehicles (HDVs) are a major contributor to on-road CO_2 emissions, accounting for 30% thereof [1]. Heavy-Duty Diesel engines currently dominate the HDV sector due to their relatively high thermal efficiency and proven durability. In recent years, advances in engine thermal efficiency within the HDV sector have reduced the per vehicle CO_2 emissions. However, given the relative increases seen in on-road freight traffic across the EU, CO_2 emissions are still rising. Contribution of heavy-duty diesel engines to local pollution, particularly NO_2, is also a concern. As such, methods to reduce fuel consumption, CO_2 and other emissions within the HDV market are of primary concern to legislative bodies, Original Equipment Manufacturers and operators alike. Effective and practical CO_2 reduction technologies within the Heavy-Duty (HD) haulage sector are limited. Strategies now being introduced in the Light-Duty Vehicle sector, such as electrification and hybridisation are ineffective in many HDV applications due to prohibitive on-cost, high associated mass and compromised range and load carrying capacity. Without a sector-specific carbon reduction technology, the relative contribution and importance of HDV carbon emissions will inevitably rise as other sectors adopt effective low carbon propulsion solutions.

To address the significant CO_2 production within the sector, the advancement of Direct Injection (DI) Gas technology, which is considered to be a viable alternative to diesel powered HDVs, could facilitate this market's need. At present, the European market for both Natural Gas (NG) and Dual Fuel Vehicles is modest in absolute vehicle numbers. However, a major opportunity exists to expand the deployment of Heavy-Duty Natural Gas vehicles within inter-city haulage applications and beyond. The main aim of the Heavy-Duty Gas Engines integrated into Vehicles project, referred to as HDGAS herein, is to accelerate targeted development within the HDV sector. HDGAS aims to increase technology know-how, with a specific Ricardo focus on lean burn NG engine operation, and drive increased operator uptake of NG powered HDVs, ultimately leading to reduced vehicle CO_2 emissions for inter-city haulage applications.

HDGAS is a three-year Horizon 2020 (H2020) project to develop knowledge and know-how in several areas surrounding Natural Gas powertrains, including: engine design, fuel storage, supply systems, aftertreatment system specification, development and calibration. Within this project, Ricardo are developing a lean burn variant capable of achieving the project performance targets whilst also achieving emissions compliance. For the lean burn positive ignition direct injection NG engine, the targets are detailed below:

– 10% improvement in fuel economy compared to state-of-the-art stoichiometric 2013 natural gas engine
– 10% reduction in CO_2 emissions compared to state-of-the-art stoichiometric 2013 natural gas engine
– 10% improvement in peak torque and rated power compared to the baseline engine

This paper focuses on the specification, control and subsequent environmental impact of a lean burn NG engine. The calibration and evaluation of which, will be subject to a further publication in due course.

2 Well-to-wheel Emissions

Well-to-Wheel (WtW) analysis is part of the broader life-cycle analysis (LCA), which in itself, is a technique to measure and evaluate the impact that a product has on the environment from raw material extraction, manufacture and use, and through to disposal. WtW is a subset that only considers the fuel emissions impact, as a function of CO_2, from extraction and processing through to use within the transport sector. To evaluate WtW emissions, an understanding of the 'fuel pathway' is required. The term 'fuel pathway' is used to describe the processing and transport steps necessary to deliver a fuel to an application from the source. This typically includes fuel production (e.g. drilling) or conversion (e.g. bio-methane), fuel upgrading, transport of the fuel and dispensing of the fuel. The fuel pathway of bio-methane is shown below in Figure 1.

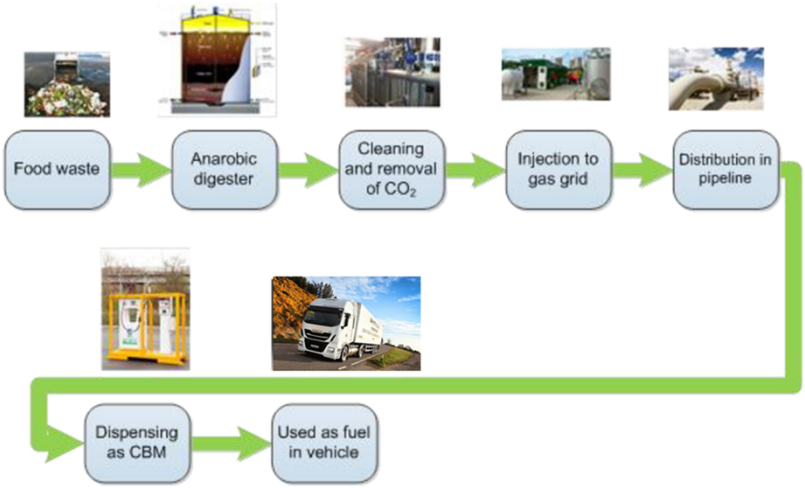

Figure 1: Example fuel pathway of bio-methane [2]

The Well-to-Wheel (WtW) emissions of an application depend on the fuel type and source, as well as the powertrain efficiency, drive cycle and the tailpipe emissions. The emissions derived from the application are referred to as Tank-to-Wheel (TtW). WtW are typically stated in CO_2 equivalent values (CO_2e) with greenhouse gases (GHG), methane (CH_4) and nitrous oxide (N_2O) emissions, assigned weightings based on the global warming potential, in comparison to CO_2, for a given time horizon.

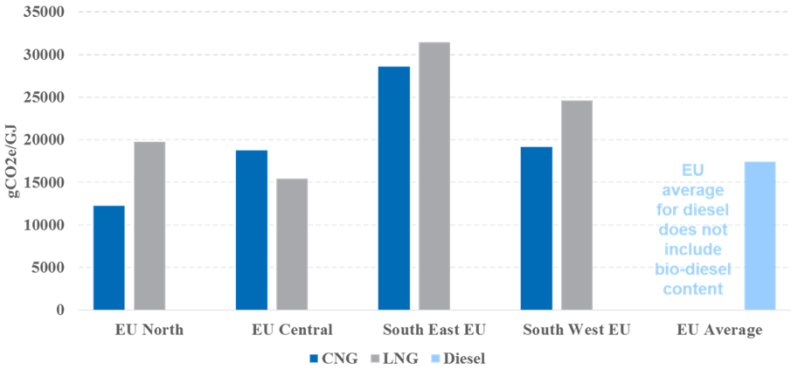

Figure 2: European well-to-tank emissions for 2015 [3]

Natural gas, as stated previously, has an inherent benefit over diesel fuel owing to the lower carbon to hydrogen ratio and therefore lower CO_2 emissions for a given energy release. However, when the 'fuel pathway' is considered for natural gas, in comparison to diesel fuel, the TtW benefit can in some cases be overshadowed by the Well-to-Tank (WtT) impact. This, in itself for natural gas, varies heavily across Europe, as detailed in Figure 2, and is a function of not only location of the acquisition of the fuel but also the original fuel source. There have been a number of recent studies (JEC [4], NGVA [5], DBI [6], and EXERGIA [3]) on WtW emissions. For the work reported here, the analysis performed by EXERGIA and NGVA has been used to derive fuel pathway values. In all cases the trends published by the various studies, listed earlier, are similar but the absolute emissions levels are different owing to methodology, changes in fuel source composition and infrastructure changes between the different time periods reviewed.

The WtW emissions have been evaluated for three powertrain options within the long haul transport sector in Europe in 2014; diesel, CNG operated under stoichiometric conditions and dual fuel. The dual fuel variant considers pre-mixed CNG ignited by a small diesel pilot injection. Figure 3 shows the WtW emissions incorporating European average WtT dataset from NGVA and EXERGIA. It is evident that although the in-use emissions of both of the predominately natural gas fueled powertrains is lower than that

of the diesel (6.4% and 4.0% for the mono fuel and dual fuel applications respectively), the larger variability (indicated by the minimum and maximum bars) in upstream emissions reported by both EXERGIA and NGVA can lead to a worse environmental impact compared to the diesel fuelled application. It should be noted that, when using the European average WtT value for both datasets, the NG applications both have a lower WtW emissions impact compared to diesel.

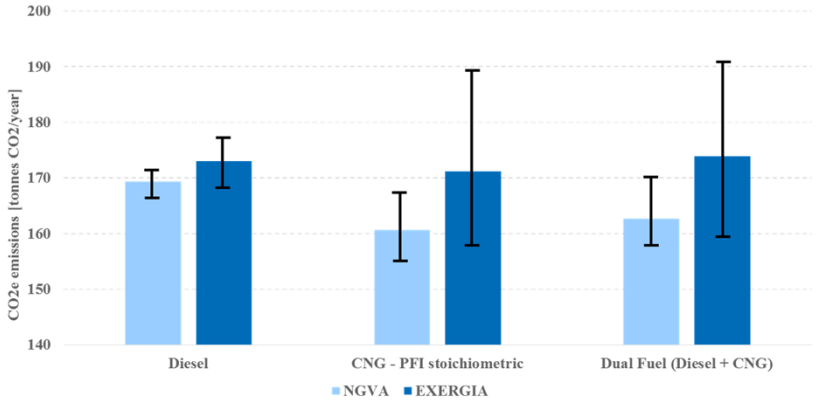

Figure 3: WtW emissions for three long haul powertrains with NGVA and EXERGIA European average WtT data

3 Lean burn powertrain specification

It has been shown that the upstream emissions (WtT) for long haul transport applications can vary depending on a number of factors, and as a result can mitigate any downstream (TtW) benefit of natural gas as a fuel. It is clear that focus should be made on improving natural gas infrastructure from the extraction through to delivery but also there is scope to improve the powertrain efficiency as a mitigating factor to the variability in WtT emissions. The following section details the specification of a lean burn powertrain targeting improved efficiency compared to current state-of-the-art NG fuelled transport applications.

3.1 Approach

The approach chosen was to use a sub-set of the Ricardo Integrated Model Based Development (IMBD) environment and simplified tools to provide a faster than real time evaluation, therefore enabling system optimisation over the large matrix of input

conditions. The block diagram of the IMBD environment for the simulations is shown below in Figure 4.

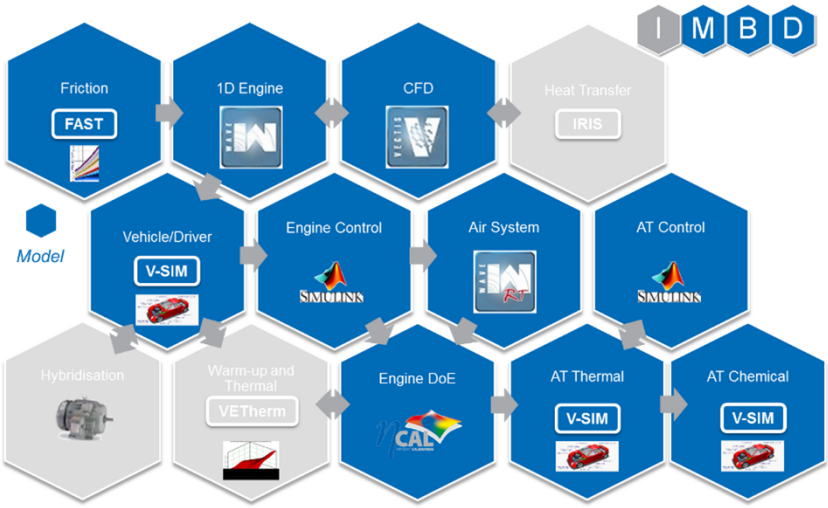

Figure 4: Models adopted with the IMBD environment

With this method, the likely success or failure of a specific technical solution can be reviewed before committing to a costly development activity. This approach, frequently ultilised by Ricardo, has been shown to enable fast adaptation to varying inputs and system properties.

To specify the lean burn engine variant and aftertreatment system, the baseline engine was simulated within 1D and 3D environments and the results validated against test data. Then additional technologies were evaluated with regard to CO_2 reduction and emissions control capability over the World Harmonised Transient Cycle (WHTC). Considerations were also made to real world performance and hardware design limitations. The technologies or strategies considered were:

– Lean and stoichiometric operation
– Direct injection of fuel gas and high energy ignition system
– Variable valve timing and optimised turbocharging system
– Highly turbulent port development and updated combustion system geometry
– Advanced catalysts for emissions control
– Mean value engine model and Kalman filter

Simulations were performed with the relevant system information and then, where appropriate, an optimisation process was completed for the calibration or design of the additional technology or strategy. This was conducted to achieve the lowest fuel consumption within emissions and design constraints.

3.2 Engine Technologies

One of the main benefits of lean burn operation compared to stoichiometric operation is the ability to vary the lambda according to the speed, load and engine conditions. At low load throttled conditions, allowing higher excess air reduces the pumping losses incurred from throttling, although there is a trade-off with longer combustion burn duration. At higher loads, where boosting is required, the increased excess air reduces the peak combustion temperature thereby reducing heat transfer – again this is offset against the increase in combustion burn duration.

3.2.1 Lean burn operation

For the lean burn engine, the full load lambda target is controlled by the boosting capability of the turbocharging system and the structure and temperature limits of the intake and exhaust valves. At part load, when throttled, temperature and pressure limits are not a concern and, therefore, the main limitation on lambda is combustion stability, which is a function of combustion system design, charge mixture homogeneity and fuel gas composition.

For appropriate simulation of the lean burn engine, an understanding of the combustion speed is required. Although the simulation model was validated to test data, the change in engine specification and intake conditions will affect the combustion ([7], [8]). To fully capture these effects, a combustion model was used that defines the duration as a function of geometry, charge (fuel and air) conditions and fuel composition. The effect of increased lambda operation on the burn duration is shown below, in Figure 5; the higher level of excess air results in a longer combustion burn duration.

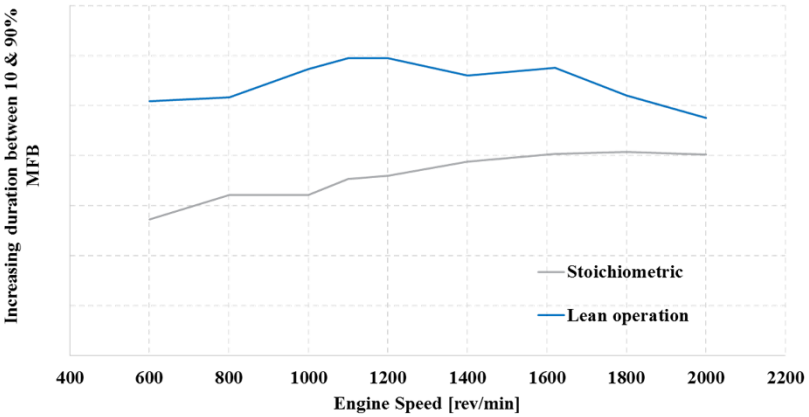

Figure 5: Impact of lean operation on combustion duration at full load – target lambda optimised for minimum fuel consumption

As expected, the main benefit of lean burn operation is apparent at part load, where the pumping losses are greatly reduced at throttled keypoints; this is shown below in Figure 6. The higher compression and, as a result, higher expansion ratio of the lean operation result in a higher peak cylinder pressure. However, this is well within structural limitations of the engine.

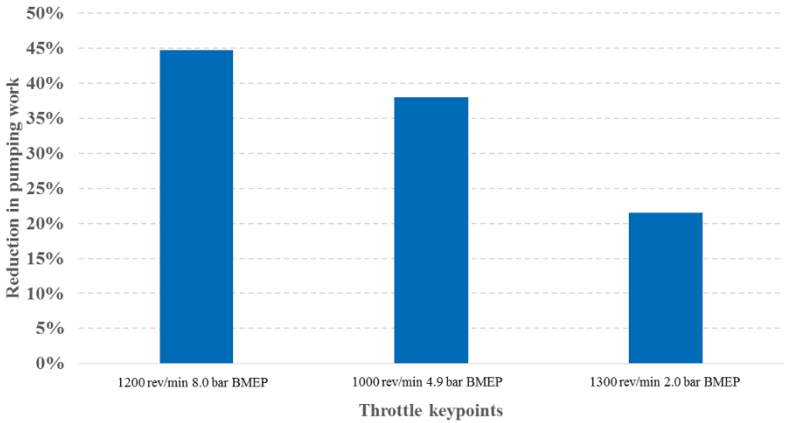

Figure 6: Reduction in pumping work at three part load keypoints from lean operation

This reduction in fuel consumption does lead to a corresponding reduction in exhaust gas temperature, for the three throttled keypoints. However, the increase in mass flow, owing to the higher excess air, leads to a similar exhaust enthalpy between stoichiometric and lean burn operation.

3.2.2 Charge mixture preparation

Key to successful operation of a direct injection NG engine is the charge mixture preparation. Typically, port or manifold fuelled engines will have sufficient mixing length and time to ensure mixture homogeneity at the point of ignition, whereas a direct injection approach, although beneficial, carries risk, especially for long injection duration periods and highly transient operation.

Previous experience [9] and literature [10], [11] & [12] has shown the importance of the charge conditions preceding ignition of the charge. These relate to mixture velocity and kinetic energy within the cylinder, globally and locally around the point of ignition. The aim of port development was to increase the desired air motion whilst maintaining a suitable flow coefficient (Cf). The development centred on removing air flow restrictions (to improve Cf) within the ports whilst directing airflow to target tumble motion within the cylinder. A summary of the results of the iterative process are shown below, in Figure 7. Literature and previous experience has shown that tumble ratio is key for in-cylinder turbulence development and mixture homogeneity.

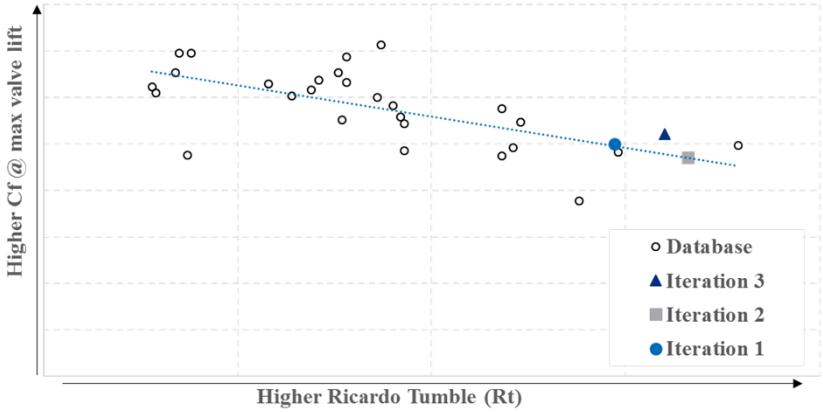

Figure 7: Port design iteration impact on CF and Tumble

3.2.3 Air management

Air system and charge mixture preparation are key to the successful operation of a lean burn direct injection engine [13]. To define the specification of the air system hardware, 1D simulation was used to assess the boost and air delivery systems, exhaust gas recirculation assessment and valve profile and timing optimisation. The aim of the air system is to ensure delivery and preparation of the correct excess air, whilst minimising system losses and maintaining transient performance.

Variable valve timing (VVT) has been shown to be an effective enabler of CO_2 reduction on gasoline engines by improving scavenging at low speed high load and reducing pumping losses within throttled regions. The plots below (Figure 8) show the Brake Specific Fuel Consumption (BSFC) at various keypoints for a full range of intake and exhaust phasing within the structural limitation of the engine. The zero on each axis is the baseline phasing. At the throttled part load keypoint, it can be seen that an increased overlap, leading to higher residual content within the cylinder, lowers the pumping work, thereby improving fuel economy. Whereas at rated power, the optimum is for a slightly reduced overlap to improve engine breathing. At the low speed, full load point, a longer overlap period and positive engine pressure difference results in improved in-cylinder scavenging, hence BSFC.

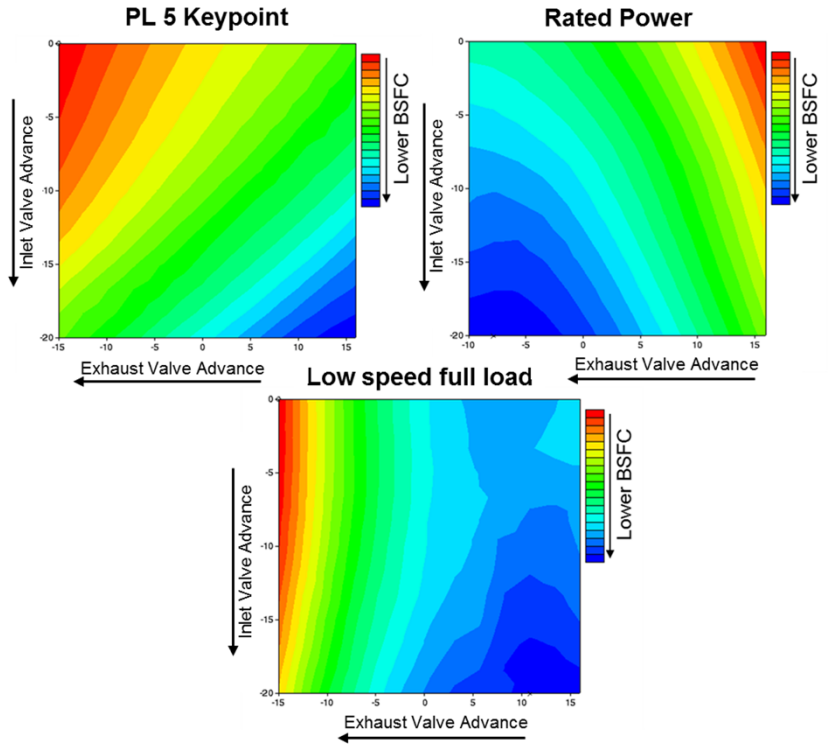

Figure 8: Change in fuel consumption from varying in valve event timing

In addition to the phasing of the valve events, the shape of the profiles themselves will affect the performance of the lean burn engine. To optimise the valve profiles, a design of experiments approach was used, which targeted lowest fuel consumption. The optimisation process resulted in an intake valve profile with an earlier closing event (EIVC). The main reason for the BSFC benefit compared to the baseline profile is the reduced pumping loss at throttled conditions. For the high load boosted conditions, the lower effective compression ratio (from the additional expansion during the intake stroke) reduces combustion temperature allowing combustion advance within knock constraints and a reduction in effective compression work.

3.3 Aftertreatment System Challenges

A lean engine operating on a mono fuel of natural gas has its own set of unique challenges. These consist of combined methane and NO_X exhaust emissions control as in a diesel application, however, there is an added challenge that methane is a very stable compound and does not oxidise to significantly greater than 400ºC. A lean operating engine spends significant amount of time below 400ºC and hence methane control becomes a significant challenge. The stability of methane requires thermal management to control tailpipe emissions and the challenge is to meet the legislative requirements whilst minimising the impact on engine efficiency and the associated CO_2 emissions.

Methane catalysts are known to be susceptible to sulphur poisoning. Sulphur from the fuel can stick to the catalyst surface and effectively mask the precious metal sites and hence impact efficiency. This is a significant challenge for long term durability of methane emission control systems.

NO_X control for Heavy Duty lean operating applications require urea based SCR systems. It is known that SCR systems can produce N_2O emissions during the NOx control process. As N_2O is a significant contributor to greenhouse gas emissions and is approximately 300 times that of CO_2 it is desirable to minimise its formation. Hence, developing an SCR with low N_2O emissions needs to be taken into account during the catalyst development process.

To evaluate the ability of the lean burn engine to meet to the emissions limits (Euro VI), an approach was chosen, to develop a Simulink based model of a developed aftertreatment system, within the IMBD architecture, using the Ricardo vehicle simulation framework (VSIM). The VSIM model uses the output of the 1D calculations and steady-state emissions maps to simulate the behaviour of the aftertreatment system. Additionally, the output of the 1D steady-state map for exhaust gas temperature was manipulated to create a more realistic transient exhaust gas temperature profile.

3.3.1 Thermal Management

Exhaust thermal management is an effective process to enable catalysts to operate in their optimum efficiency window. There are a range of techniques that can be used to control exhaust temperatures and the approaches used during this simulation exercise were; reduced engine target lambda and electrical heating of the first catalyst in the exhaust system. Reducing the target lambda makes the engine operate in an inefficient manner and rejects more heat to the exhaust. Electric heating of the catalyst uses direct electrical energy to heat a filament which is physically connected to the front face of the first catalyst in the exhaust.

Figure 9 shows the simulated impact of the two heating strategies on the first 600 seconds of the cold WHTC. Both the electric heating and reduced lambda approaches reached 400ºC after approximately 180 seconds in the cold start cycle with the base application not reaching 400ºC until 400 seconds into the cycle. Electric heating maintains temperature greater than 400ºC between 200 and 400 seconds whereas the reduced lambda dropped below 400ºC during the same time period.

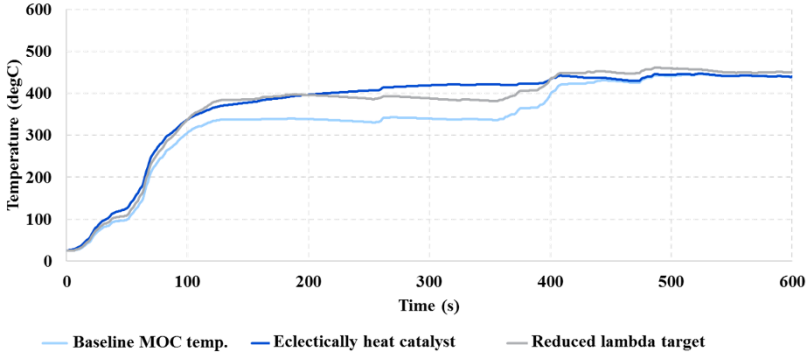

Figure 9: Impact of thermal management techniques on MOC brick temperature

The fuel penalty associated with both heating strategies for the combined hot and cold WHTC cycles was between 0.5-1% with the reduced lambda strategy giving marginally higher fuel penalty over the combined hot and cold WHTC compared to electric heating.

3.3.2 Methane Results

In the simulation, the engine out methane over the WHTC was approximately 5 g/kWh. The simulated tailpipe emissions results show that the legislative limit of 0.5 g/kWh can be met including engineering margin with the assistance of exhaust thermal management. This required methane conversion efficiencies greater that 95%, which is a significant achievement for a lean burn application. Figure 10 shows the weighted tailpipe methane results. All strategies meet the limit, but the two thermal management strategies have a significant engineering margin compared to the baseline. Having a significant engineering margin is key due to the long term durability requirements on Euro VI applications.

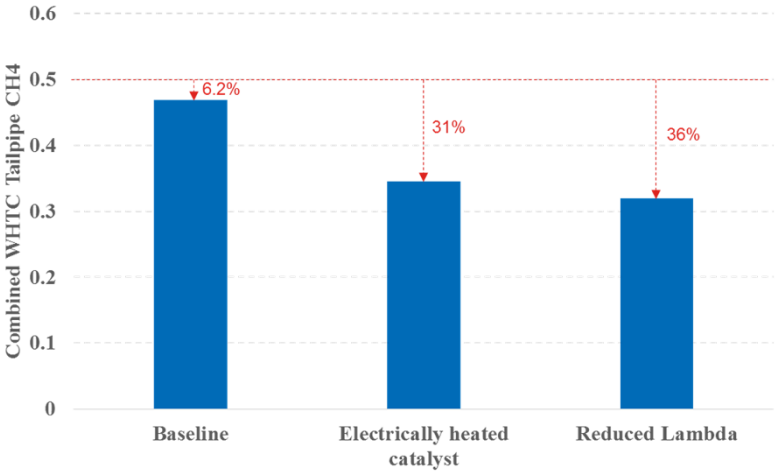

Figure 10: WHTC tailpipe CH4 for varying thermal management techniques – engineering margin in % stated

In addition to rapid thermal management, the methane catalyst needs to be kept free of sulphur. Therefore, a sulphur removal strategy has been developed in order to maintain the catalyst in its high efficiency state and minimise the sulphur poisoning effect. The strategy will use engine mode switching to remove stored sulphur. The mode switching will use temperature and lambda variations to purge the total exhaust system of sulphur. There will be a fuel penalty associated with the strategy, but using parasitic opportunities for sulphur removal and optimisation of the frequency requirement will minimise the impact [14].

3.3.3 SCR catalyst Selection

The NO_X control SCR system has to operate in tandem with the upstream methane control requirements. Due to the lean combustion process of the NG engine, the exhaust temperatures are higher than a diesel application, but lower than a stoichiometric gasoline application.

The SCR temperature histogram (Figure 11) shows that for a significant amount of time over the cycle the SCR catalyst will see temperatures greater than 400°C. At these temperatures, the NO_X control efficiency is high. However, NH_3 oxidation can occur especially over copper based SCR catalysts at temperatures greater that 400°C. Iron based SCR catalysts have a lower NH_3 oxidation rate at higher temperatures compared to copper and hence can utilise the injected urea more efficiently.

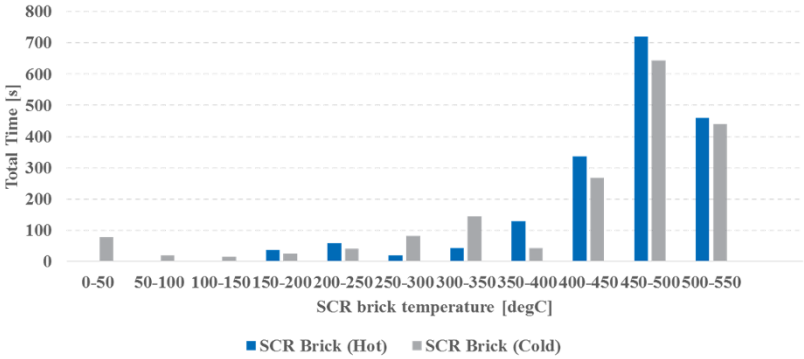

Figure 11: SCR brick temperature over cold and hot WHTC

Minimising N_2O emissions formation over the SCR is key in reducing the greenhouse gas potential of the application. Copper based SCR catalyst can produce more N_2O compared to iron based systems [15]. Therefore, the use of an Iron based SCR system for this specific lean burn natural gas application has advantages compared to a copper only system.

3.3.4 System Selection

Due to the unique challenges of a lean operating mono fuel NG application, the after-treatment system contains multiple elements for the tandem control of methane and NOx emissions.

The selected concept, which will be calibrated on a testbed, utilises an electrically heated catalyst which is used to rapidly warm up the methane control catalyst system (MCCS). The MCCS comprises of two catalysts with different functionalities and precious metal content for methane control. The order of the two catalysts is significant, which leads to an increase in durability of the MCCS maintaining the desired light off characteristics required to meet the Euro VI emissions legislation after ageing.

The Hybrid NO_X control catalyst system, comprises of two SCR catalysts and an ammonia slip catalyst. The SCR catalysts are an iron based zeolite followed by a copper based zeolite. The order of the catalyst is fundamental in minimising the formation of N_2O emissions whilst maintaining high efficiency over the exhaust temperature regime that the application undergoes.

Figure 12 shows a schematic of the layout of the selected aftertreatment system to meet Euro VI emissions legislation for a lean burn NG application. It has added complexity

compared to a diesel fuelled Euro VI exhaust system due to the methane control requirements, but doesn't require a particulate filter owing to the combustion nature of methane producing low particulate matter and particle number.

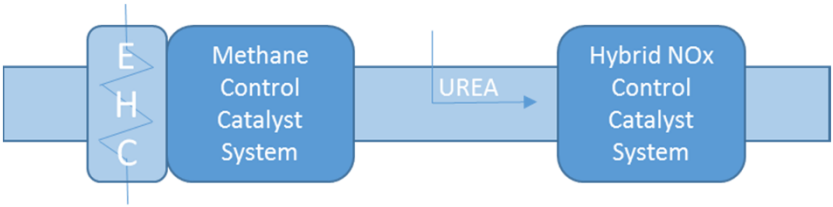

Figure 12: Schematic of aftertreatment system

3.4 Control Approach

In order to realise the benefits of the various technologies incorporated into the lean burn specification, a control system is required that would enable the calibration optimum to be reached. For this reason, a clean sheet approach that utilises past Ricardo experience on the topic, was decided for the engine control strategy.

Since the engine for this application is a new concept and a mule engine was not available, model based development was imperative. The 1D WAVE simulation model of the engine was first of all configured. A WAVE-RT version of this was then exported and tuned to assist in the development of the control strategy. This is a fast (crank-angle resolved) engine simulation tool enabling accurate prediction of engine behaviour, capable of running in real-time on Hardware-in-the-Loop or ECU hardware. The model was optimised to work in a Simulink environment enabling Software-in-the-Loop (SiL) testing. Therefore, the WAVE-RT engine model serves as a plant model, as shown in Figure 13, where the control strategy can be exercised and provide an initial calibration ahead of real engine application. The synergy of using a model-based approach for both the powertrain specification and controls development is highlighted by the fast and accurate assessment of various engine hardware options considering system constraints, emissions impact and control requirements. A further benefit of utilising WAVE-RT is that it can also operate on Hardware-in-the-Loop environments and rapid prototyping control units thereby enabling hardware control evaluation and streamlining the concept testing process.

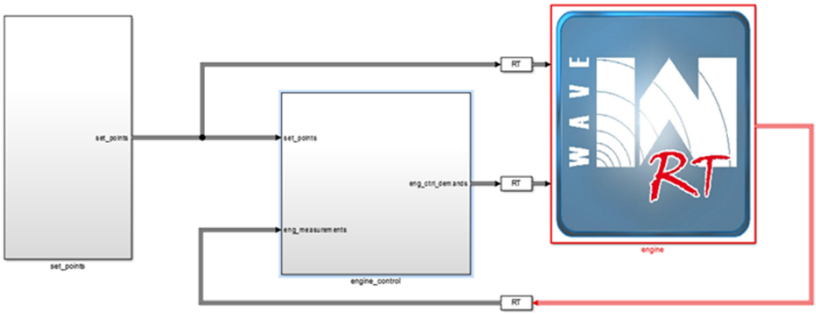

Figure 13: Schematic of WAVE-RT as software-in-the-loop

3.4.1 MVEM and Kalman Filter

To achieve accurate control, a non-linear Mean Value Engine Model (MVEM) has been developed. This enables access to information about the in-cylinder conditions without having the usual transport delays and measurement noise of the sensors. The observer model, based on mean value lumped physical parameters, was developed using standard equations that are widely available in the literature [16], [17]. It is intended to have the MVEM running in the Engine Control Unit (ECU) so the control strategy can have access to accurate mean in-cylinder air mass estimates without sensor noise or phase lag.

Moreover, an MVEM can enable engine diagnostics ([18], [19]), or sensor-less control strategy [20]. In Figure 14, the full state model is presented. There are 16 states in total where the numbers in the figure show the number of states in various parts of the model. Pressure measurements are shown with the notation p, the letter ρ is used for density, z for burned gas fraction and n for rotational speed. To reduce the computational requirement of the MVEM and improve the stability of the model, the states are reduced to 12 by eliminating the 4 states immediately before and after compressor. This is achieved by combining the effect of the two volumes and dump valve into the compressor flow map and compressor pressure ratio map.

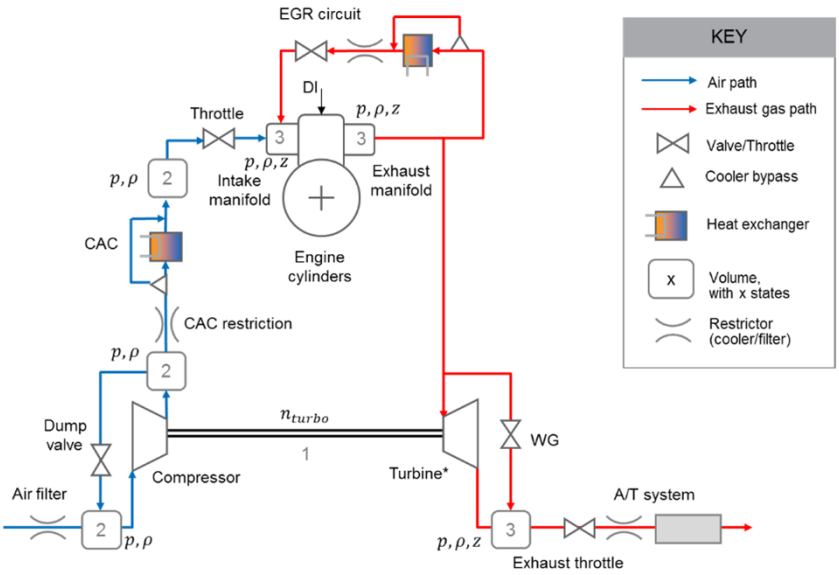

Figure 14: MVEM bock diagram

In order to enhance the accuracy of the MVEM, a linear Kalman Filter [21] (KF) was deployed to work in parallel. It is based on a pre-processed approach in which Kalman gains applied to correct each model state are mapped against engine conditions. Intake manifold pressure and exhaust manifold oxygen concentration are the sensor measurements that are utilised by this KF design. The performance of the MVEM, KF and control strategy has been tested in various conditions within the model-based environment. As it is shown in Figure 15, the outputs of the MVEM match well the outputs of WAVE-RT at specific keypoints, and the closed loop controllers (intake throttle & wastegate position) meet the demands.

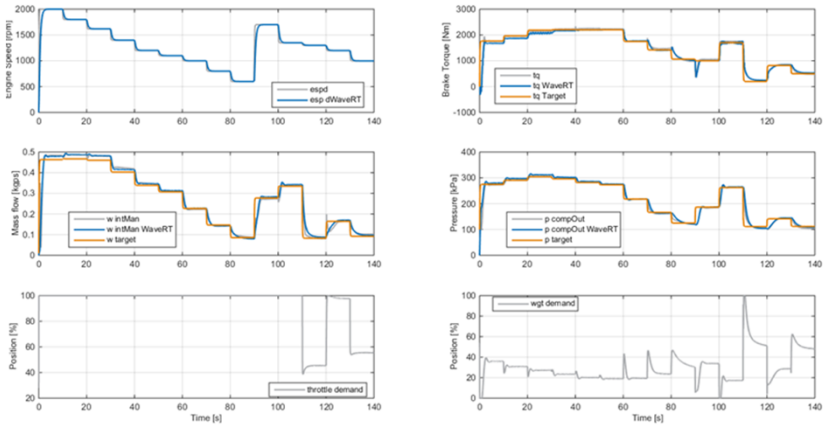

Figure 15: Control system response simulation results

4 Discussion

Heavy-duty natural gas engines that operate under lean conditions are not currently in production at Euro VI. However, if the right combustion characteristics can be achieved, a lean burn application could be viable within Euro VI emissions legislation when used in conjunction with a state of the art aftertreatment system.

The relative CO_2 benefit of the specified lean burn engine is shown below as a technology route, in Figure 16. It can be seen that the 10% target improvement over a baseline 2013 NG engine is realised with the various additional technologies. A further 2% CO_2 improvement is achieved over a comparable diesel fuelled engine. The majority of CO_2 improvement is from lean operation and direct injection of the gaseous fuel – this highlights the relatively high pumping and increased heat transfer penalty from stoichiometric operation. Further incremental benefits are seen from incorporating EIVC intake valve profile to further lower part load pumping losses; the CO_2 benefit from optimised variable valve timing is also included within this step. The simulation indicated an additional benefit of the EIVC intake valve profile was to reduce the charge temperature and, thereby, lower the knocking propensity of the engine. This enabled a compression ratio increase for further efficiency gains. The reduced fuel consumption from the various technologies and lower combustion temperatures from lean operation combine to delay oxidation catalyst light-off and subsequent hydrocarbon control during warm-up. Consequently there is a fuel penalty due to exhaust thermal management penalty in order to meet the emissions targets, however this is carefully managed to minimise the CO_2 increase.

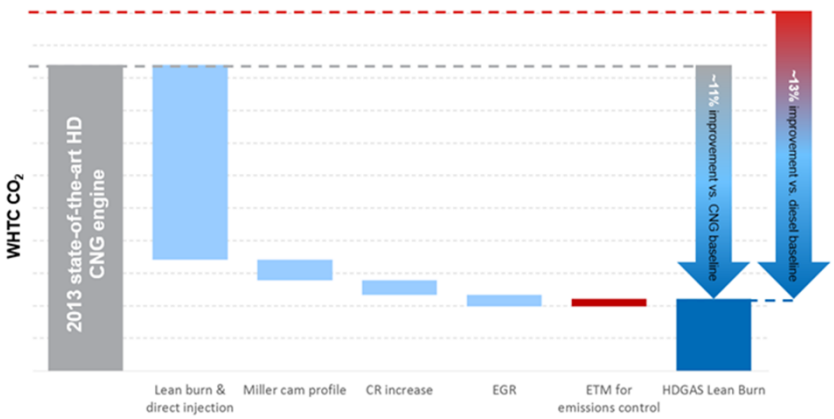

Figure 16: Simulated CO_2 improvement of the lean burn

Previously it has been shown that the inherent benefit of natural gas powertrains can be impacted and negated by upstream emissions caused by the extraction, refining, delivery and storage processes of the fuel before it reaches the vehicle. These can vary depending on location and it some cases are severe enough to negate any TtW benefit of NG over diesel fuel. Incorporating the simulated HDGAS powertrain into this analysis, an understanding of the full environmental impact a high efficiency lean burn NG engine and aftertreatment can be achieved. Figure 17 below shows the WtW emissions for the HDGAS engine compared to the baseline diesel engine. It can be seen that for both the EXERGIA and NGVA fuel pathway analysis, the WtW emissions of the HDGAS engine are lower than that of the diesel engine: 9.9% and 14.7% for the EXERGIA and NGVA data respectively. Further analysis using liquid natural gas (LNG) as a fuel source indicates a worse WtW impact than for CNG. This is caused by the increased processing 'cost' of LNG. Upstream emissions (WtT) are likely to change over time (for both gas and diesel), and as the differential between the NG and diesel WtW emissions is small, it is important that this is kept under review.

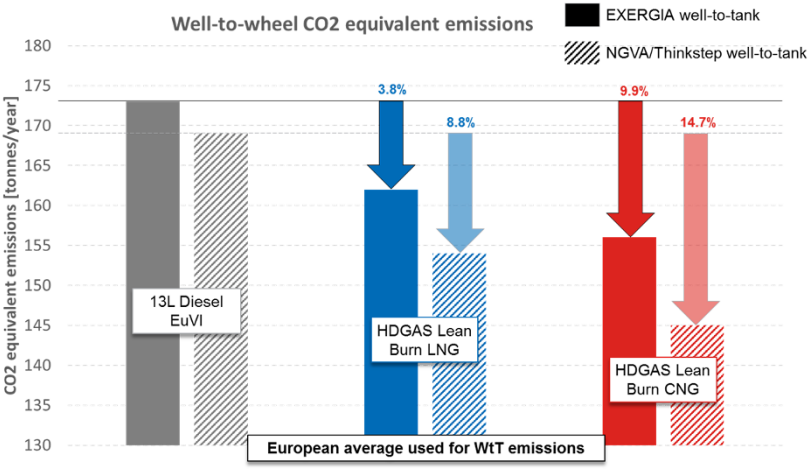

Figure 17: Simulated WtW emissions of HDGAS versus a representative diesel fuelled powertrain

5 Conclusions

The Ricardo IMBD process has aided the specification of a lean operating natural gas HD engine and aftertreatment system to meet the Euro VI emissions legislation, with exhaust thermal management, whilst delivering 13% CO_2 benefit over a diesel fuelled baseline.

– Simulation has shown that efficiency gains, compared to diesel fuel and stoichiometric NG operation, of a lean burn NG engine for the transport sector can be realised. The appropriate combustion characteristics for lean operation have been achieved through the development of a unique combustion system incorporating a tumble port architecture and direct gas injection, and the careful management of the air system from an optimised turbocharger, variable valve timing with early intake valve closing and selected use of EGR
– A complex and novel aftertreatment system has been developed to simultaneously control methane and NO_X emissions whilst minimising the exhaust thermal management fuel penalty and nitrous oxide slip
– The clean-sheet control system, utilising a mean value engine model corrected by a Kalman filter, has been shown through software-in-the-loop validation, with a WAVE-RT engine model as the plant model, to provide accurate management of the engine hardware and estimation of the in-cylinder conditions

The efficiency benefit of the lean burn NG engine compared to the 2013 state-of-the-art 2013 NG baseline improves the environmental impact of NG as a transport fuel compared to diesel, when considering both in-use (TtW) and upstream (WtT) emissions.

The calibration of the engine and aftertreatment system will be subject to a further publication in due course.

6 Acknowledgements

The authors would like to thank the Ricardo team members Joshua Dalby, Andy Noble, Waheedullah Safi, Mahesh Jeshani and colleagues in Ricardo Energy and Environment for their contributions to the work reported here. Thanks also go to the partners within the HDGAS project consortium for their assistance and permission to publish this paper.

The work reported here received funding from the European Union's Horizon 2020 research and innovation programme, under grant agreement No 653391.

7 References

[1] "Overview of the heavy-duty vehicle market and CO2 emissions in the European Union", Muncrief, R. and Sharpe, B., ICCT Working Paper 2015-16

[2] "The role of natural gas and biomethane in the transport sector", Sujith Kollamthodi, John Norris, Craig Dun, Charlotte Brannigan, Fiona Twisse, Marius Biedka, Judith Bates, 16 February 2016

[3] "Study on actual GHG data for Diesel, Petrol, Kerosene and Natural Gas", EX-ERGIA, EM Lab and COWI, 2015

[4] "Well-to-wheels Analysis Of Future Automotive Fuels And Powertrains In The European Context", Robert Edwards (JRC), Jean-François Larivé (CONCAWE), David Rickeard (CONCAWE), Werner Weindorf (LBST), 2014

[5] "Greenhouse Gas Intensity of Natural Gas", Dr Oliver Schuller, Dr Benjamin Reuter, Jasmin Hengstler, Simon Whitehouse, Lena Zeitzen, 5 May 2017, Think-step AG on behalf of NGVA Europe

[6] "Critical Evaluation of default Values for the GHG Emissions of the Natural Gas Supply Chain", DBI Gas- und Umwelttechnik, prepared for Zukunft Erdgas e.V., Leipzig, Germany, 2016.

[7] "Lean SI Engines: the Role of Combustion Variability in Defining Lean Limits", Ayala, F. and Heywood, J., SAE Technical Paper 2007-24-0030, 2007

[8] "Effects of Combustion Phasing, Relative Air-fuel Ratio, Compression Ratio, and Load on SI Engine Efficiency", Ayala, F. et al, SAE Technical Paper 2006-01-0229, 2006

[9] "A study of the correlation between in-cylinder air motion and combustion in gasoline engines", Kyriakides, S. and Glover, A., I.Mech.E C55/88, 1988

[10] "Impact of Tumble on Combustion in SI Engines: Correlation between Flow and Engine Experiments", He et al., SAE Technical Paper 2007-01-4003, 2007

[11] "Effects of Different Geometries of the Cylinder Head on the Combustion Characteristics of a VVA Gasoline Engine", Millo et al., SAE Technical Paper 2013-24-0057, 2013

[12] "Combustion Chambers for Natural Gas SI Engines Part 2: Combustion and Emissions", Johansson et al., SAE Technical Paper 950517

[13] "A Lean Burn Turbocharged, Natural Gas Engine for the US Medium Duty Automotive Market", Clarke, D., Such, C., Overington, M. and Das, P., SAE Technical Paper 921552, 1992, doi:10.4271/921552.

[14] “Case study of a modern lean-burn methane combustion catalyst for automotive applications: What are the deactivation and regeneration mechanisms?”, Kinnunen, N. et al, Applied Catalysis B: Environmental 207 (2017) 114-119

[15] “The effect of CH4 on NH3-SCR over metal-promoted zeolite catalysts for lean-burn natural gas vehicles”, Tronconi, E. et al, Submitted to Applied Catalysis B: Environmental September 2017

[16] “High-frequency Ignition System Based on Corona Discharge,” S. Bohne, G. Rixecker, V. Brichzin and M. Becker, MTZ Worldwide, pp. 30-34, Jan 2014.

[17] “The Internal Combustion Engine in Theory and Practice”, C. F. Taylor, vol. 1, Cambridge MA: The M.I.T. Press, 1977.

[18] “Mean Value Observer For A Turbocharged SI Engine,” P. Andersson and L. Eriksson, in 4th IFAC symposium on Advances in Automotive Control, Fisciano, 2004.

[19] “Model Based Diagnosis of the Air Path of an Automotive Diesel Engine,” M. Nyberg, T. Stutte and V. Wilhelmi, in 3rd IFAC Workshop – Advances in Automotive Control, Karlsruhe, Karlsruhe, 2001.

[20] “Simulation of Gas Path Faults in a VGT Diesel Engine for the Development of Diagnosis Algorithms,” A. Truscott, A. Noble, A. Cotta and T. Stutte, in What Challenges for the Diesel Engine of the Year 2000 and Beyond?”, Ecully, 2000.

[19] “Sensorless Control Strategy Enabled by a Sophisticated Tool Chain,” A. Kouba, J. Navratil and B. Hnilicka, in SAE Technical Paper, 2015.

8 Definitions and Abbreviations

BSFC – Brake Specific Fuel Consumption
Cf – Flow Coefficient
CH_4 – Methane
CO – Carbon Monoxide
CO_2 – Carbon Dioxide
CBM – Compressed Biomethane
degCA – degrees crank angle
DI – Direct Injection
EGR – Exhaust Gas Recirculation
EHC – Electrically Heated Catalyst
EIVC – Early Intake Valve Closing
Euro VI – Euro 6 HD Emissions Legislation
HD – Heavy-Duty
HDGAS – Heavy-Duty Gas Engines integrated into Vehicles
HDV – Heavy-Duty Vehicle
IMBD – Integrated Model Based Development
KF – Kalman Filter
MOC – Methane Oxidation Catalyst
MVEM – Mean Value Engine Model
NG – Natural Gas
NH_3 – Ammonia
NO_X – Nitrogen Oxides
SCR – Selective Catalytic Reduction
TtW – Tank to Wheel
VVT – Variable Valve Timing
WHTC – World Harmonised Transient Cycle
WtT – Well to Tank
WtW – Well to Wheel

Characterization of abnormal dual-fuel combustion

Garrett Anderson

W. Siebenpfeiffer (Hrsg.), *Heavy-Duty-, On- und Off-Highway-Motoren 2017*,
Proceedings, https://doi.org/10.1007/978-3-658-21029-8_5

Introduction

The boom in natural gas within the last decade from shale formations reduced the price of natural gas dramatically. This shift in price generated a great deal of interest in dual-fuel conversion for many high-horsepower engines. These conversions are designed to replace a portion of the diesel fuel with natural gas. While low oil prices have eroded the cost savings for natural gas in recent years, there is still interest in using this concept as a means to achieve reduced emissions [1].

The dual-fuel combustion process is complex and relies on diesel fuel to ignite the natural gas and air mixture. The ratio of diesel replaced by natural gas is referred to as the substitution ratio. The substitution of natural gas for diesel in high-horsepower applications can be significant and depends on the tolerable substitution ratio over the operating cycle of the engine.

Emissions of unburned natural gas and severe combustion phenomena can limit the substitution ratio. Severe combustion phenomena include pre-ignition, end gas knock and high rates of pressure rise during the initial portion of the combustion event. The substitution ratio, the ratio of natural gas to air, the ignition delay period, and the entrainment of the natural gas-air mixture in the diesel spray can all impact the type and severity of these combustion events.

These different combustion modes create a requirement for a well-calibrated knock detection and mitigation system which can correctly identify knock at all operating conditions. Many dual fuel conversions systems use accelerometer-based systems to detect knock. This detection strategy monitors combustion noise to infer the presence of knock. Inconsistencies in the noise caused by the diesel combustion can make reliable knock detection difficult [2], [3].

Some fundamental research has been conducted into the root cause of abnormal combustion, but it has focused mainly on observing the behaviour to determine the root cause of the problem rather than classifying various types of combustion [4]–[7]. The resulting nomenclature has yielded classifications that specify lube oil as the only root cause.

Lube oil has been investigated as a potential contributor to abnormal, dual fuel combustion through visualization in a rapid combustion machine. These visualizations show combustion initiated by lube oil droplets and the pilot diesel injection [4]. The nature of this research led to names such as lube oil auto-ignition, lube oil high rate of combustion, and lube oil pre-ignition combustion. These names imply lube oil is the only cause of abnormal combustion [5]. While this research shows a link between lube oil and abnormal combustion, this may not be the only cause.

Other research has focused upon fuel composition and air fuel ratio. These two parameters can impact abnormal combustion. Methane number can quantify the fuel quality of natural gas and is based upon its composition. However, multiple compositions can result in the same methane number with dissimilar combustion tendencies [7].

Other researchers converted passenger car, diesel engines for dual fuel operation. These studies compared abnormal, dual fuel combustion with Low Speed Pre-Ignition (LSPI) in similarly sized engines. LSPI is an abnormal combustion behaviour found in highly boosted SI gasoline engines at low speed and high load[6].

The low speed coupled with the high load generate conditions which can result in random pre-ignition. The pre-ignition can severely advance the combustion phasing which results in excessive peak cylinder pressure and severe knock. This combustion can produce catastrophic engine failure[8].

A large amount of work has been done to reduce or eliminate the occurrence of LSPI, including engine dyno testing and on road testing. These tests evaluated the impacts of oil formulation, fuel composition, fuel delivery, and EGR. This testing shows engine design, oil additives, and fuel composition all have an impact in LSPI occurrence [8]–[11]. Specific LSPI tests to gain ILSAC GF-6 and DEXOS lubricant certifications exist because the impact of lubricant oil is large [12], [13].

The framework presented in this paper attempts to classify each type of combustion based upon heat release data. A methodology is then described that can be applied to large data sets to identify each type of abnormal cycle. The resulting classification can then be used to fully calibrate a knock detection and mitigation algorithm to enable safe engine operation at elevated substitution ratios.

Test Setup

A Navistar MaxxForce 13 engine was used as the base engine for this work. The stock engine has a high pressure common rail diesel injection system. This provides flexibility in controlling the injection timing and the injection pressure. Natural gas was introduced through a single admission point in the intake to provide a premixed charge. The specifications for this engine are shown in Table 1.

Table 1. Engine specifications

•MY2012 Navistar Maxxforce13	
•**Displacement**	•12.4L
•**Bore x Stroke**	•126 mm x 166 mm
•**Compression Ratio**	•18:1
•**Configuration**	•Inline 6 cylinder
•**Injection system**	•DI diesel: Common-rail 2200 bar max •Premixed: Single-point CNG

Data for this study was taken at a steady state operating condition specified in Table 2. This condition was selected because it exhibited a tendency for abnormal combustion without causing severe engine damage. The data presented for end gas knock is advanced by 1 CA° on a single cylinder to increase the frequency of its occurrence.

Table 2. Steady state test conditions

Parameter	Value
Engine Speed (RPM)	1000
BMEP (bar)	15.8
SOI (°BTDC)	5°
Substitution Ratio (% mass)	87%
Pipeline Natural Gas	~84 MN

Classification

Three types of abnormal combustion exist within this framework. Each type exhibits higher than normal peak cylinder pressure and elevated heat release rates. However, the shape of the heat release rate and frequency of occurrence all differ. These variations can identify each combustion mode and allow for different mitigation strategies driven by different root causes.

End Gas Knock

The first type of abnormal combustion is end gas knock and is shown in Figure 1. The upper plot in this figure illustrates the cylinder pressure and heat release for each cylinder as a function of crank angle. The cylinder of interest is highlighted in blue and red respectively. The black line is the injection current. The lower plot contains the peak cylinder pressure for the cylinder of interest as a function of cycle number.

This combustion mode can be very consistent from cycle to cycle unlike SI engines. A rapid acceleration in heat release rate late in the combustion process characterize this mode of combustion. However, the first half of combustion is unchanged. It can exhibit ringing similar to knock in SI engines, but it may not always produce this behaviour.

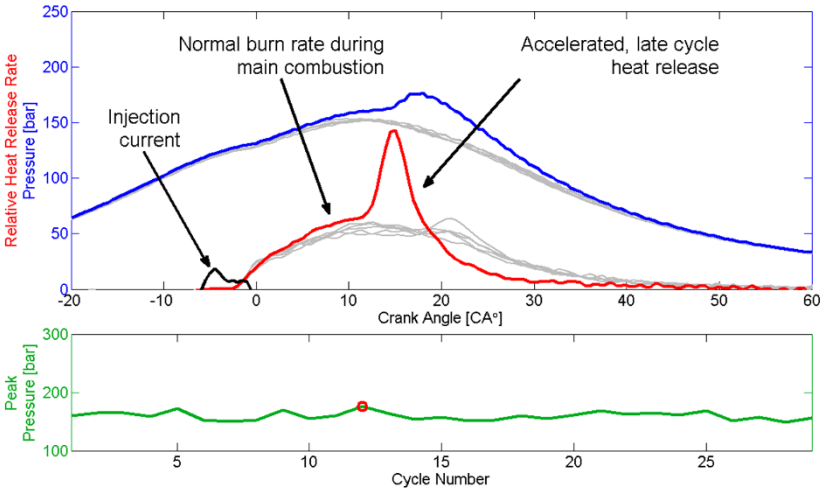

Figure 1. Cylinder pressure, relative heat release rate, and peak cylinder pressure from a cycle exhibiting incipient end gas knock.

A small retard in combustion phasing or a reduction in substitution ratio can mitigate this form of abnormal combustion. The required amount of mitigation action may increase as the combustion become more severe.

Two subcategories of end gas knock exist: heavy end gas knock and insipient end gas knock. The presence or lack of ringing caused by the accelerated heat release determines these two classifications. Two reasons justify the classification of all cycles that exhibit accelerated, late cycle heat release as end gas knock.

The same mechanism causes both classifications. The more severe case produces an impulse large enough to excite the combustion gases and engine structure. The lack of this impulse for incipient knock may greatly reduce or eliminate its potential for engine damage.

The ringing in dual fuel combustion is not always caused by the end gas knock. The diesel pilot can initiate the ringing during the initial phase of combustion. Differentiation between these two sources of noise can be difficult. They both excite the same modes of the combustion chamber and engine structure.

The cycle in Figure 2 exhibits ringing from the diesel pilot. It also contains end gas knock that may contribute to the ringing present in this cycle, but distinguishing this difference is difficult. This methodology intentionally avoids the use of frequency to overcome this difficulty. A frequency agnostic perspective can allow for experiments to optimize the complete engine calibration and increase the sensitivity of a frequency based knock detection system.

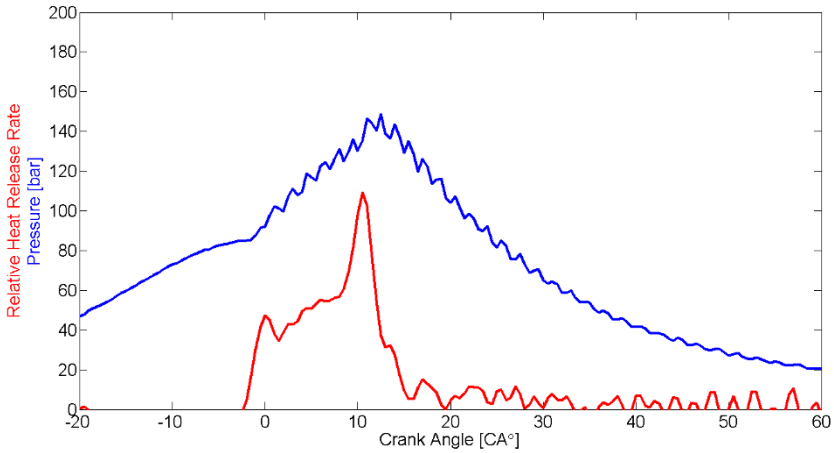

Figure 2. Cylinder pressure and relative heat release for a cycle exhibiting ringing that is initiated by diesel pilot and end gas knock behavior

Rapid Combustion

The next type of abnormal combustion is rapid combustion (RC). Figure 3 provides an example of this combustion mode. The presence of increased heat release rate throughout the entire engine cycle characterizes this type of combustion, but it initiates at the same crank angle as normal combustion. This type of combustion can also exhibit end gas knock behaviour as a result of advanced combustion phasing.

Rapid combustion can occur as a single cycle or in a group. The lower plot in Figure 3 depicts its multicycle cycle behaviour. This mode of combustion is difficult to proactively mitigate because of its stochastic nature. It will typically initiate and terminate without any changes in engine conditions.

However, the severe nature of it does warrant severe action to prevent subsequent cycles within a multicycle event. Large reductions in substitution ratio or a load reduction can be effective actions.

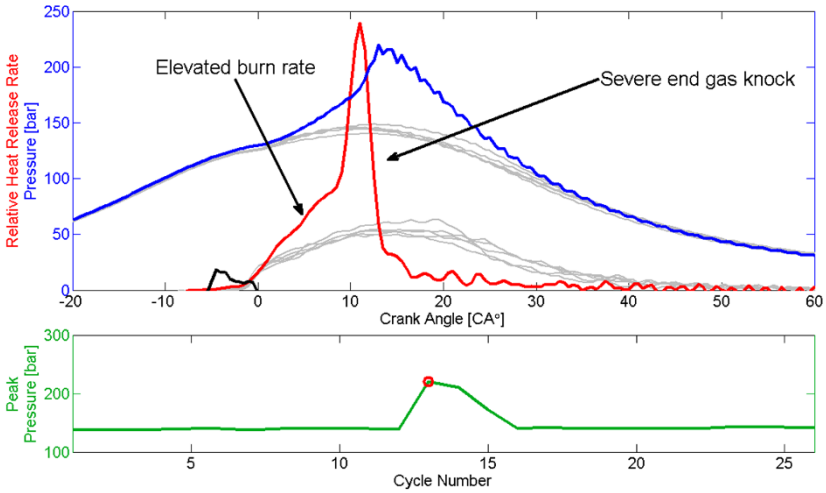

Figure 3. Cylinder pressure, relative heat release rate, and peak cylinder pressure from a cycle exhibiting rapid combustion.

Pre-ignition

Figure 3 depicts the third type of abnormal combustion known as pre-ignition (PI). Pre-ignition and rapid combustion contain many similarities, but pre-ignition exhibits heat release prior to the start of injection. Simultaneous dual ignition from the pilot injection and alternate ignition source during rapid combustion may cause this similarity.

This combustion type can occur in groups or as a single event like rapid combustion. However, the advanced combustion phasing can increase its severity. The pre-ignition observed under these conditions differs from hot-spot pre-ignition because it does not sustain itself.

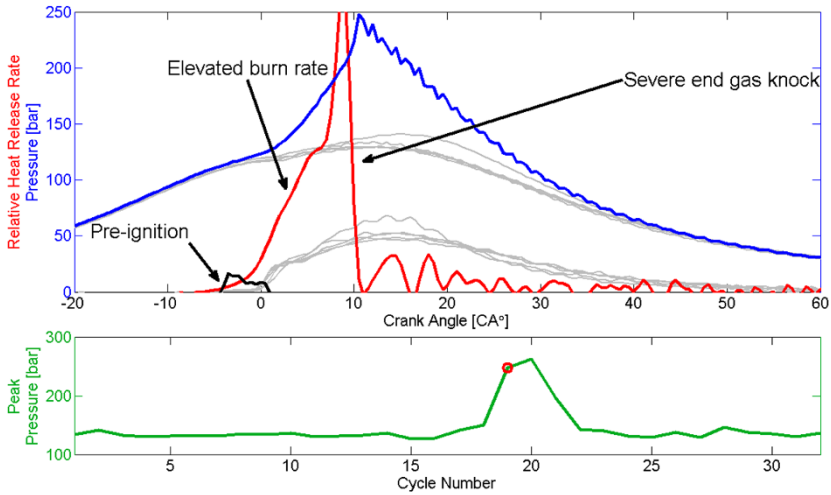

Figure 4. Cylinder pressure, relative heat release rate, and peak cylinder pressure from a cycle exhibiting pre-ignition.

Cycle Analysis

Analysis of single cycles can aid in the identification of the various combustion modes, but analysis of a large population can also give insight into the present types of observed abnormal combustion. The histograms in Figure 5 depict the different modes of abnormal combustion relative to normal combustion.

End gas knock exhibits a bimodal distribution (top right plot). Rapid combustion and pre-ignition appear as outliers when viewed on a histogram (top right and lower plots). This example shows peak cylinder pressure is higher for the pre-ignition case, but this trend may not always be true.

The lack of differentiation limits the use of peak cylinder pressure to recognize differences between these two modes. A histogram is a simple method of identifying abnormal combustion in large sets of data at steady state. It does not replace a visual analysis of individual cycles, but it does complement it.

Visual analysis of heat release rate can provide a great amount of information. It is a very important step in any data analysis, but it is difficult to visually compare large numbers of cycles. Visual comparison also suffers because it can be somewhat subjective. However, algorithms can analytically approximate a visual analysis to quantitatively identify various phases of the combustion process.

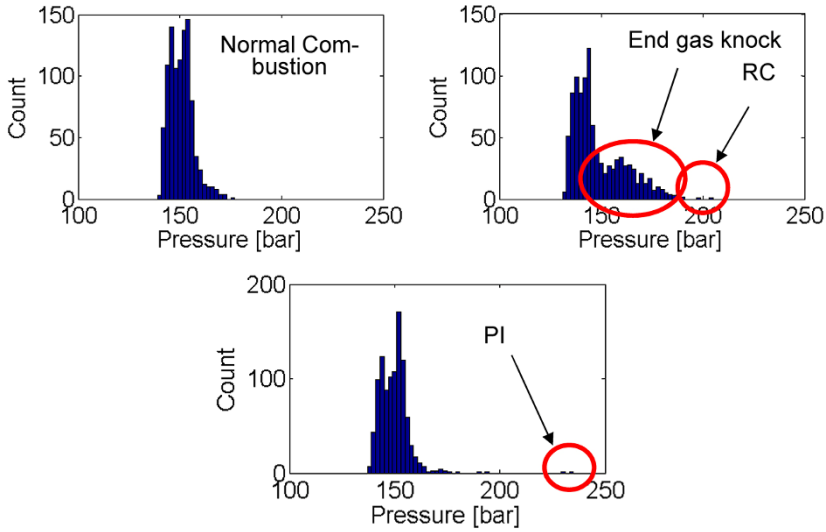

Figure 5. Histograms of peak cylinder pressure that demonstrate normal combustion, end gas knock, rapid combustion, and pre-ignition behavior.

A single Wiebe function is used to fit combustion data in SI engines [14]. More complex models such as a double Wiebe can estimate spark assisted HCCI combustion and diesel combustion. Each Wiebe function models a combustion phase. The application of the double Wiebe model applied to the diesel cycle captures the premixed and main combustion phases [15]. The spark assisted HCCI case quantifies the contribution of SI and HCCI combustion modes [16].

Dual fuel combustion and traditional diesel combustion contain two phases. In dual fuel combustion there is a pilot ignition phase that is dominated by diffusion combustion of the diesel pilot, and the second phase is dominated by a premixed, propagating flame through the natural gas [7]. This similarity allows for a double Wiebe function to fit normal, dual fuel combustion. However, this model breaks down when end gas knock is present because knock adds a third combustion mode. The addition of a third Wiebe function can address this problem.

The implementation of multiple Wiebe functions must allow each Wiebe function to model a specific phase of combustion throughout the cycle. Parameter constraints force each term to properly model the combustion. This ensures the first Wiebe function will fit the pilot ignition combustion, the second will fit the main combustion phase, and the third will capture knocking combustion if present.

$$x_i = b_i\left(1 - \exp\left[-a_i\left(\frac{\theta-\theta_{0i}}{\Delta\theta}\right)^{m_i+1}\right]\right) \quad (1)$$

$$x_{tot} = x_1 + x_2 + x_3 \quad (2)$$

$$Error = \left(\frac{HRR}{Cum.HR} - (\dot{x}_1 + \dot{x}_2 + \dot{x}_3)\right)^2 + (1 - (b_1 + b_2 + b_3))^2 \quad (3)$$

The triple Wiebe function uses the form shown in Equation 1. A summation of the three Wiebe functions calculates a total normalized heat release as shown in Equation 2. A least squares approach fits the data with Equation 3.

The error calculation uses the derivative of the combined Wiebe functions and the normalized heat release rate. This method more accurately fits the data near the start and end of combustion where the pilot ignition and knocking combustion occur. A second error term implements a summation of the b terms to prevent total normalized heat release from diverging from 100%.

Figure 6 depicts the components of the triple Wiebe methodology. The "knocking Wiebe" term quantities the accelerated heat release rate late in the cycle. The various coefficients from each Wiebe term can give some insight into the combustion behaviour and imitate a subjective visual analysis. For instance, the b term from the knocking combustion Wiebe can indicate how much combustion occurred during this phase.

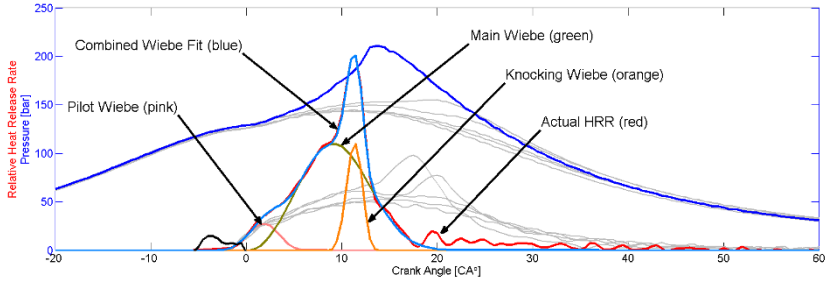

Figure 6. "End Gas Knock" type cycle fit using the triple Wiebe methodology.

Fitting the Wiebe model to each individual cycle allows for a quantitative analysis to approximate a visual analysis of many cycles. This level of automation solves many of the limitations associated with the visual analysis.

The scatter plots in Figure 7 represent at least 150 cycles and depict several trends to classify knocking cycles. The trends are based upon traditional cycle statistics and coefficients from the proposed methodology. In these graphs, the maximum rate of heat

release was chosen for the x-axis since the maximum rate of heat release often occurs during the knocking phase of combustion.

End Gas Knock

Peak cylinder pressure can identify knocking cycles, but it can fail to identify incipient knocking cycles where the peak cylinder pressure is not severe. This is evident in the bottom left plot in Figure 7. Several of the knocking cycles (blue points) have similar peak pressures to non-knocking cycles (gray points) despite the 1 CA° advance applied to the knocking cylinder.

The MFB 50-90 can identify knock and seems to classify the knocking cycles well in this case[7]. A shorter late cycle burn duration (MFB 50-90) indicates an increased level of knock, and the top left plot in Figure 7 demonstrates this condition.

Figure 7 contains three plots of parameter from the proposed model. The top right plot shows the b3 parameter which is the weight of the Wiebe term representing knocking combustion. An increase in this parameter indicates an increased level of knock. It can be used much like MFB 50-90 to identify knocking combustion.

The plot with main burn duration shows minor differences in the duration of the main combustion event. The increase in end gas knock can shorten this duration. More severe end gas knock can transfer heat release from the main combustion phase to the end gas knock phase. The knock anchor angle provides further confirmation because it will advance as the knock becomes more severe.

The MFB05 location shows negligible differences for end gas knock cycles but can be used for classification of other types of cycles. However, it demonstrates the lack of pre-ignition in these cycles.

The analysis of the scatter plots do not show the full capability of the model. The scatter plots demonstrate the general trend of the b3 term, but it does not show the full performance of the model for cycles exhibiting very slight knock.

Figure 1 shows this type of cycle in the adjacent cylinders. Those cycles exhibited an increased heat release rate very late in the cycle. The delayed phasing resulted in end gas knock that did not greatly exceed the peak pressure or maximum heat release rate observed during main combustion. This results in a piecewise function rather than a straight line for the scatter plot of b3.

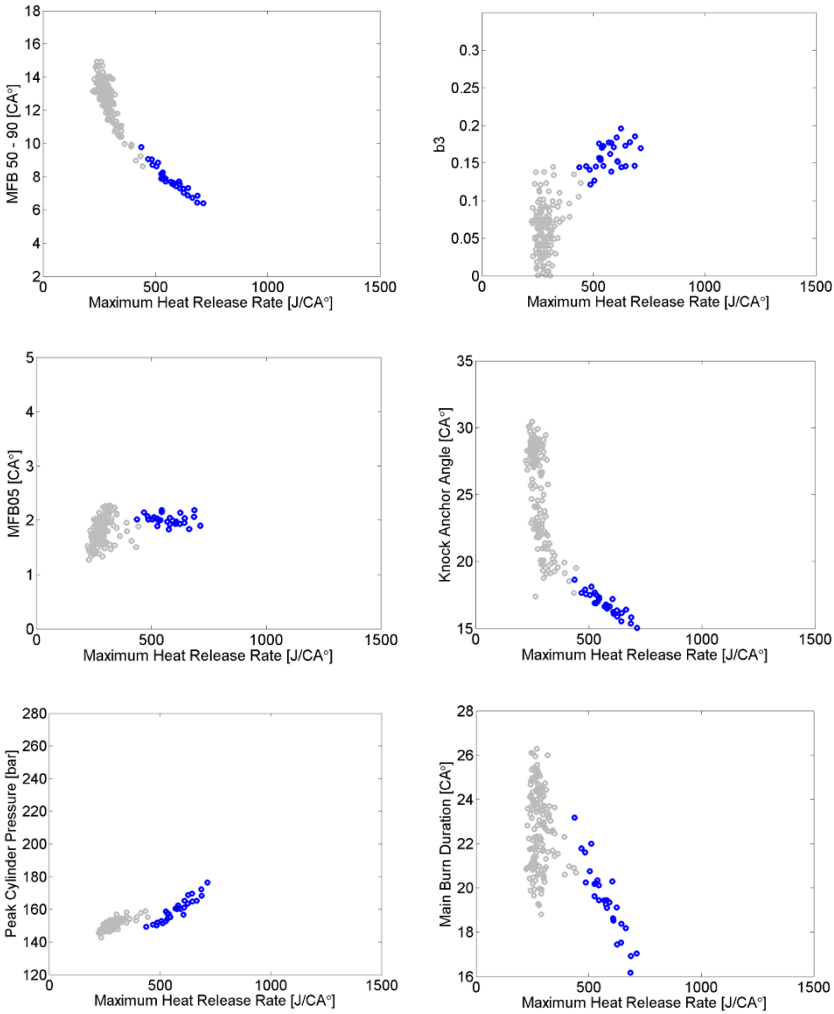

Figure 7. Scatter plots of peak pressure, MFB 50-90, and MFB05, b3, knock anchor angle, and main burn duration that are used to aid in the classification of end gas knock type cycles;

Rapid Combustion

Peak cylinder pressure and MFB 50-90 both identify rapid combustion type cycles as abnormal in Figure 8, but they do not indicate anything other than severe, end gas knock. This instance demonstrates how the additional steps to fit the data can provide greater insight.

The plot of b3 versus maximum heat release rate in Figure 8 shows a similar trend to the plots for peak pressure and MFB 50-90. The first two cycles contained in Figure 9 exhibited high levels of end gas knock behaviour. The third cycle did exhibit this type of behaviour but not as severe.

The coupling of the rapid combustion and moderate levels of knock generate a higher than normal peak cylinder pressure and shortened MFB 50-90. The use of b3 and the main burn duration help to differentiate these types of combustion from end gas knock, but these parameters cannot identify rapid combustion individually.

The b3 parameter works well to indicate knocking combustion, and the main combustion burn duration will indicate the rate at which combustion occurred during the initial portion of the cycle. However, the weight for the main combustion Weibe (b_2) can provide further insight into the shape and size of the main combustion phase, but it is not a requirement for proper cycle classification.

The plot of main combustion duration in Figure 8 shows the shortened main combustion duration. This differs from the plot shown in Figure 7 where the combustion duration remains almost unchanged.

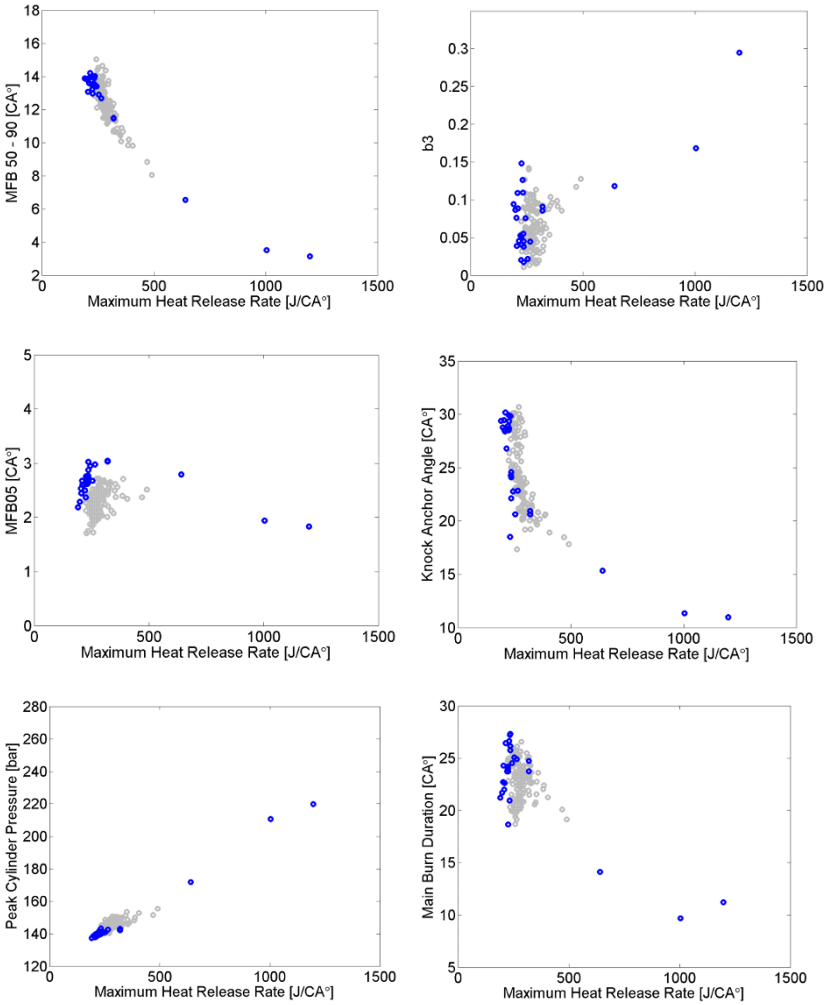

Figure 8. Scatter plots of peak pressure, MFB 50-90, MFB05, b3, knock anchor angle, and main burn duration that are used to aid in the classification of rapid combustion type cycles.

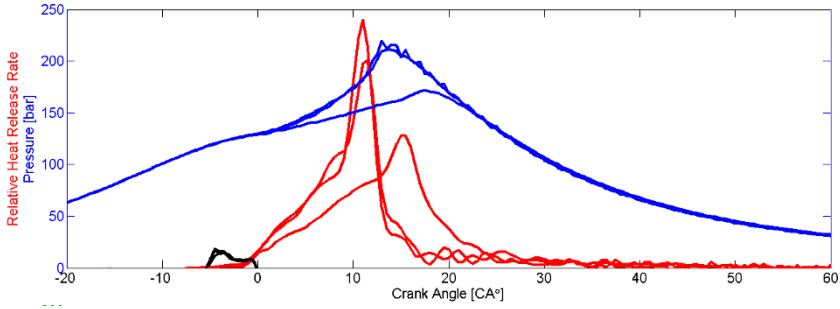

Figure 9. Cylinder pressure and relative heat release rate for three consecutive cycles exhibiting rapid combustion.

Pre-ignition

The b3 and main combustion duration parameters have proven useful for identifying knock and rapid combustion, but they cannot identify pre-ignition because they have a weak relationship with the initial portion of combustion. Peak cylinder pressure and MFB 50-90 can suffer from the same trends observed with rapid combustion. Peak pressure and MFB 50-90 do flag these cycles as abnormal in Figure 10, but these metrics do not indicate a difference from knocking or rapid combustion cycles.

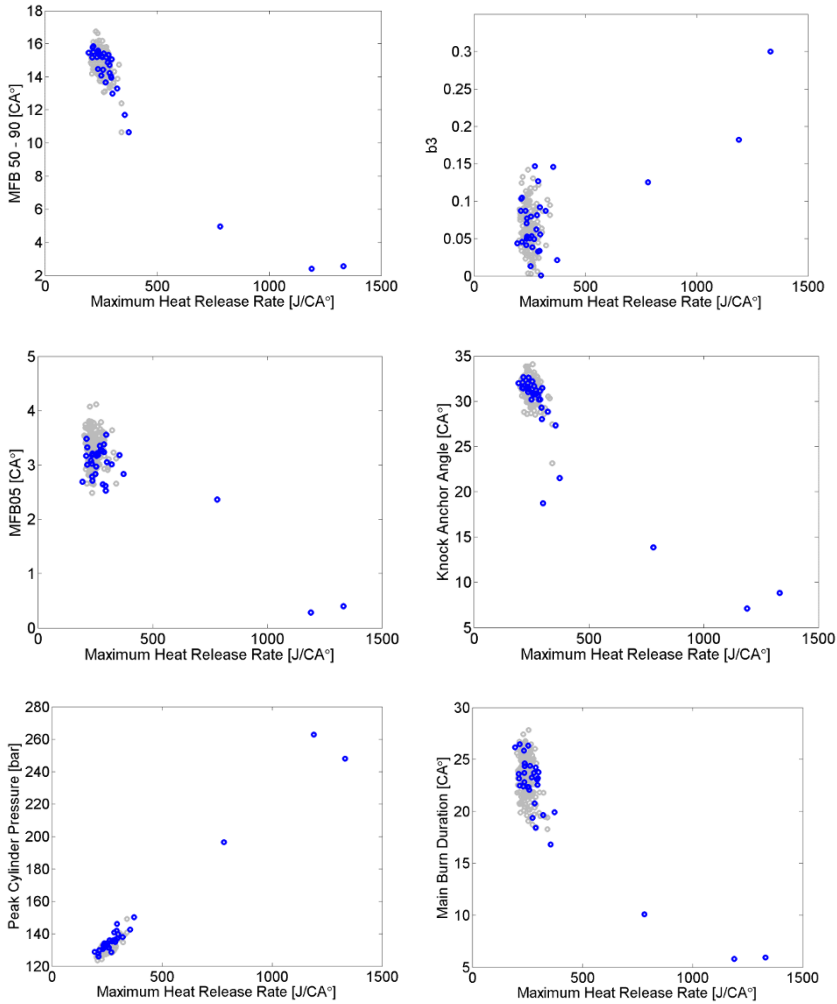

Figure 10. Scatter plots of peak pressure, MFB 50-90, MFB05, b3, knock anchor angle, and main burn duration that are used to aid in the classification of pre-ignition type cycles.

The MFB05 is used to identify the start of combustion. MFB05 was chosen rather than MFB02 because MFB02 is susceptible to noise, and the MFB05 performs much better when applied to single cycles. The anchor angle for the premixed combustion Wiebe

term should identify early combustion, but it does not always fit the data well because the shape of the heat release rate can be much different for pre-ignition type cycles.

Conclusions

The proposed classification scheme can identify various types of dual fuel abnormal combustion. The three types of combustion are end gas knock, rapid combustion, and pre-ignition. Each individual cycle can exhibit all three types of combustion, but they can occur independently depending upon operating conditions, fuel composition, and engine design.

Peak cylinder pressure or MFB 50-90 can identify each combustion type as abnormal, but these metrics cannot differentiate between each combustion type. Potential engine damage from abnormal combustion requires the proper identification of each type. The lack of information about type can reduce the ability to successfully mitigate and understand the problem.

The proposed framework can differentiate between these three types of combustion. Knowledge of different combustion types help to better frame the problem and aid in many aspects of the engine development process.

The calibration of the knock detection and mitigation system is one of the most critical aspects of engine development in regard to abnormal combustion. Calibration of both accelerometer and cylinder pressure based systems can take advantage of the more detailed analysis. This methodology can detect the onset of knock at much lower levels than traditional metrics, and the increased detection will help to intelligently set various detection thresholds and understand the limitations of the detection system.

The calibration of the mitigation algorithm can benefit from the better classification of abnormal cycles. Some of these behaviours may occur and reach damaging levels sporadically, which makes mitigation difficult. In cases of preignition, typical actions, such as retarding ignition timing, may not be optimal.

Some light duty gasoline control systems can differentiate between end gas knock and low speed pre-ignition. These systems will use this information to take appropriate actions to suppress a multi-cycle event. These actions can include an immediate reduction in engine load or greatly enriching the cylinder exhibiting the pre-ignition. Continued occurrences of this phenomenon can even cause the control system to limit engine load until the condition is cleared [17]. Each engine will exhibit its own tendencies, but the ability to classify these cycles will ease the development of the appropriate mitigation actions.

Given the difficult nature of mitigating some of these combustion events, it may be necessary to investigate other aspects of the engine design to minimize their occurrence. This could include but is not limited to crankcase lubricant, fuel composition, and combustion chamber design. Improved combustion analysis can aid in these many different aspects of the engine development process for the complete engine system.

Nomenclature

θ_o: Wiebe anchor angle

$\Delta\theta$: Wiebe burn duration

a: Wiebe parameter

b: Wiebe weight factor

Cum. HR: Cumulative heat release

HRR: Heat release rate

m: Wiebe exponent

x: Wiebe result

References

[1] Ryan D. Johnson, Timothy J. Callahan, David P. Branyon, and David P. Meyers, “Dual-fuel Engines — An Elegant Alternative for... – Google Scholar,” *MTZ Ind.*, vol. 7, no. 2, pp. 56–60, Sep. 2017.

[2] Suraj Nair, PhD, Jeff Carlson, Jason Barta, and Gregory J. Hampson, PhD, “Performance Comparison of Vibration Knock Sensors and In-Cylinder Pressure for Protection of Gas and Dual Fuel Engines,” presented at the 10th Dessau Gas Engine Conference, Dessau-Roßlau, Saxony-Anhalt Germany, 2017, pp. 217–230.

[3] M. Kirsten, G. Pirker, C. Redtenbacher, A. Wimmer, and F. Chmela, “Advanced Knock Detection for Diesel/Natural Gas Engine Operation,” *SAE Int. J. Engines*, vol. 9, no. 3, Apr. 2016.

[4] S. Yasueda, K. Takasaki, and H. Tajima, “The Abnormal Combustion Affected by Lubricating Oil Ignition in Premixed Gas Engine,” in *ASME 2012 Internal Combustion Engine Division Spring Technical Conference*, 2012, pp. 29–36.

[5] S. Yasueda, S. Zhu, and L. Tozzi, “The investigation of the abnormal combustion by lubricating oil with the advanced CFD simulation,” presented at the The Working Process of the Internal Combustion Engine, Graz, Austria, 2015, pp. 429–442.

[6] J.-M. Zaccardi and D. Serrano, “A Comparative Low Speed Pre-Ignition (LSPI) Study in Downsized SI Gasoline and CI Diesel-Methane Dual Fuel Engines,” *SAE Int. J. Engines*, vol. 7, no. 2014-01-2688, pp. 1931–1944, 2014.

[7] D. G. Van Alstine, D. T. Montgomery, T. J. Callahan, and R. C. Florea, “Ability of the Methane Number Index of a Fuel to Predict Rapid Combustion in Heavy Duty Dual Fuel Engines for North American Locomotives,” in *ASME 2015 Internal Combustion Engine Division Fall Technical Conference*, 2015, p. V001T02A010–V001T02A010.

[8] M. Amann, D. Mehta, and T. Alger, “Engine operating condition and gasoline fuel composition effects on low-speed pre-ignition in high-performance spark ignited gasoline engines,” *SAE Int. J. Engines*, vol. 4, no. 2011-1–342, pp. 274–285, 2011.

[9] M. Amann, T. Alger, B. Westmoreland, and A. Rothmaier, “The Effects of Piston Crevices and Injection Strategy on Low-Speed Pre-Ignition in Boosted SI Engines,” *SAE Int. J. Engines*, vol. 5, no. 2012-01-1148, pp. 1216–1228, 2012.

[10] K. Takeuchi, K. Fujimoto, S. Hirano, and M. Yamashita, “Investigation of Engine Oil Effect on Abnormal Combustion in Turbocharged Direct Injection – Spark Ignition Engines,” *SAE Int. J. Fuels Lubr.*, vol. 5, no. 3, pp. 1017–1024, Nov. 2012.

[11] C. Dahnz, K.-M. Han, U. Spicher, M. Magar, R. Schiessl, and U. Maas, “Investigations on Pre-Ignition in Highly Supercharged SI Engines,” *SAE Int J Engines*, vol. 3, pp. 214–224, 2010.

[12] “ILSAC GF-6,” *Lubrizol Additives 360 – Passenger*, 02-Jul-2016. .

[13] “dexos™,” *Lubrizol Additives 360 – Passenger*, 02-Jul-2016. .

[14] J. Heywood, *Internal Combustion Engine Fundamentals*, 1 edition. Tata Mcgraw Hill Education, 2011.

[15] F. Maroteaux, C. Saad, F. Aubertin, and P. Canaud, “Analysis of Crank Angle Resolved In-Cylinder Combustion Modeling for Real Time Diesel Engine Simulations,” SAE Technical Paper, 2015.

[16] W. J. Glewen, R. M. Wagner, K. D. Edwards, and C. S. Daw, “Analysis of cyclic variability in spark-assisted HCCI combustion using a double Wiebe function,” *Proc. Combust. Inst.*, vol. 32, no. 2, pp. 2885–2892, 2009.

[17] “Method and system for pre-ignition control,” 21-Aug-2015.

LDM Compact – an efficient methodology for the development of combustion concepts for non-natural gas

Dr. Jan Zelenka,
Area Manager – NG & NNG Combustion
LEC GmbH

Dr. Martin Kirsten,
Senior Research Engineer – Engine Applications
LEC GmbH

Dr. Eduard Schneßl,
Area Manager – Engine Applications
LEC GmbH

Dipl.-Ing. Gernot Kammel,
Research Engineer – NG & NNG Combustion
LEC GmbH

Prof. Dr. Andreas Wimmer,
CEO / Scientific Director
LEC GmbH
Institute of Internal Combustion Engines and Thermodynamics,
TU Graz

W. Siebenpfeiffer (Hrsg.), *Heavy-Duty-, On- und Off-Highway-Motoren 2017*,
Proceedings, https://doi.org/10.1007/978-3-658-21029-8_6

Introduction

World energy demand is escalating as the global population and wealth in emerging markets continues to grow. At the time this publication is being written, the price of fossil fuels, especially oil and gas, is moderate. Nevertheless, incentives through new and proposed emission policies are pushing energy suppliers to invest into alternative fuels. These fuels might originate from biomass feedstock (e.g., biogas), power-to-gas technologies (hydrogen-rich gases) or industrial processes. To further reduce costs, previously neglected fuel sources are becoming more and more interesting. Large bore gas engines in combined heat and power applications are a valuable option that make it possible to exploit these non-natural gases (NNG) in an economically sound manner. Non-natural gases, especially waste gases from oil and gas production or industrial processes, vary in quality (composition) and quantity, from source to source on the one hand and over time on the other hand. This places high demands on the combustion concept as well as the control concept.

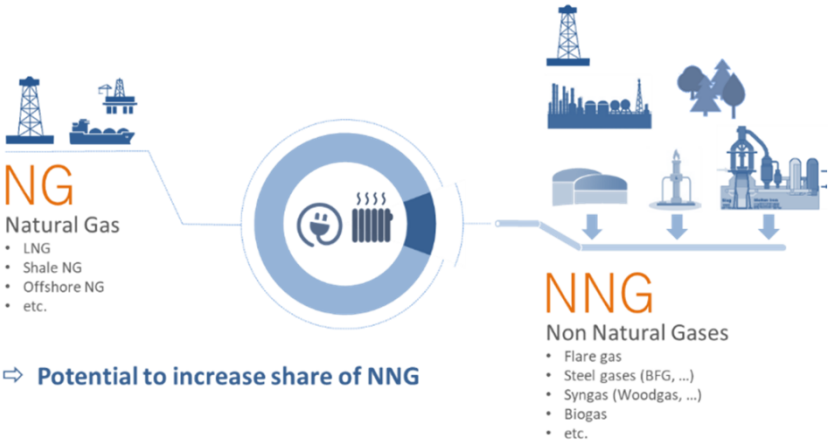

Figure 1: Shares of heat and power production from natural gas and non-natural gases

The development of combustion concepts for such applications is a difficult task for two main reasons. First, providing the very specific gas quality of a source in a quality sufficient for multicylinder engine (MCE) testing is expensive if not nearly impossible. Second, any potential volatility in gas quality has to be investigated beforehand, and the sensitivity of the combustion concept has to be determined. In order to overcome these economic and technological hurdles, the **L**EC **D**evelopment **M**ethodology **Compact** (LDM Compact) was developed to design a combustion concept for gas engines

that can be applied to a wide variety of NNG. This method does not require extensive testing on the MCE and relies solely upon results from simulation and single cylinder engine (SCE) testing.

Development Methodology

LEC **D**evelopment **M**ethodology (LDM) has arisen from decades of experience in developing combustion concepts for large bore engines. It consistently integrates various simulation techniques, measurements on a single cylinder research engine and measurements on a multicylinder engine [1][2]. As shown in Figure 1, the methodology makes use of 0D and 1D engine cycle simulation as well as 3D CFD simulation. 0D/1D engine cycle simulation is applied to preoptimize significant engine parameters such as compression ratio or valve timing, while 3D CFD simulation is mainly used to optimize details such as piston geometry or charge motion. Experimental investigations on the SCE allow validation of simulation results and provide input for a further loop that employs simulation tools. In addition to basic combustion concept development for steady-state operation, LDM facilitates the integrated treatment of durability, wear, ignition and fuel supply. Furthermore, the development of transient combustion concepts and controls is possible. After a combustion concept is validated on the SCE, it is ready for MCE testing and validation.

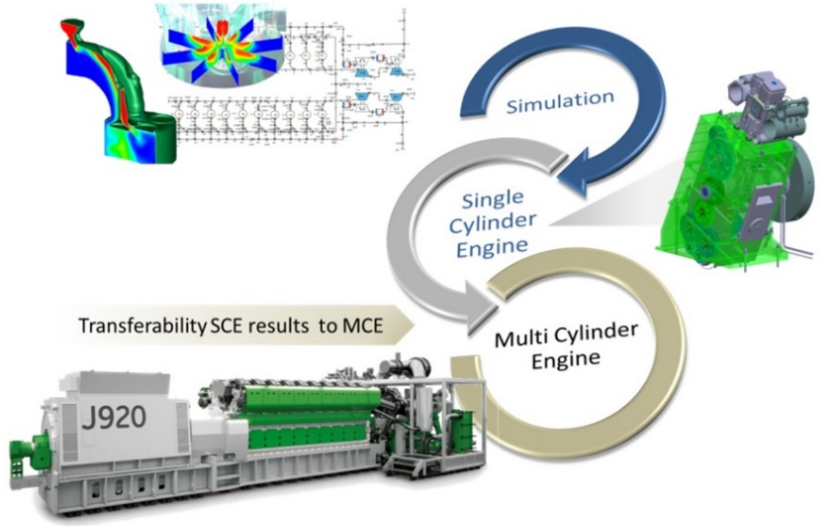

Figure 2 LEC Development Methodology – LDM

As mentioned above, MCE testing of niche NNG combustion concepts is not economically viable. Therefore, LDM has been modified in order comply with demands from the industry. LDM Compact completely relies on simulation tools and extensive measurements on the SCE; it can be directly transferred to the engine operator's facility (c.f. **Figure 3**).

Combustion concept pre-design

In the first step, the gas quality of each composition under investigation is assessed using characteristic values. These values include:

- Knock index excluding inert components
- Knock index including inert components
- Density
- Lower heating value
- Laminar flame speed

The selection of the appropriate knock index is dependent on the fuel gas composition. The various knock indices show major differences, especially for gas mixtures that contain hydrogen or higher hydrocarbons [3][4].

Once the knock index has been chosen, it is possible to pre-select the combustion concept and define basic engine parameters. Using 0D/1D engine cycle simulation, the operating parameters are described in detail. With gases with a very challenging composition, 3D-CFD simulation is preferable for pre-designing the combustion chamber geometry in order to avoid end-gas pockets where knocking might occur or for determining the necessary level of charge motion so that a high level of turbulence and subsequently high reaction rates are obtained. This is especially critical with gases that have a low calorific value.

A combustion concept that undergoes the pre-design process has fewer hardware variants that must be tested. Furthermore, 1D engine cycle simulation provides boundary conditions that emulate turbocharger behavior during SCE testing.

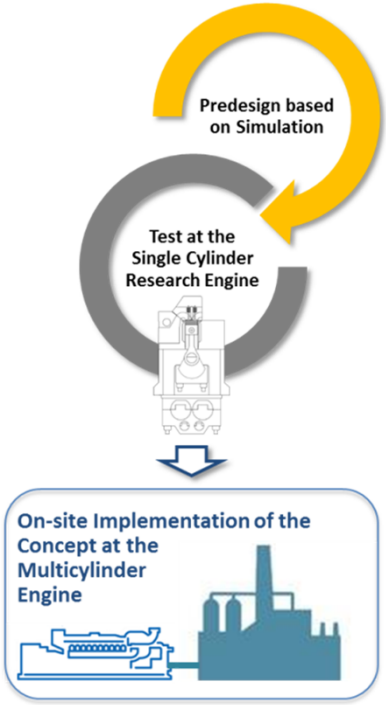

Figure 3: LDM Compact

Single cylinder test setup

The LEC single cylinder engine consists of a base frame that houses the engine's power unit and the single cylinder crankshaft. This engine also has first and second order mass balances, an oversized flywheel and a four-quadrant dynamometer to drive and brake the engine. The charge air is delivered by a screw-type compressor, which is cooled for dehydration and then heated to the desired level. The water content of the cylinder charge is adjusted via steam admixed to the charge air. The fuel gas is mixed with the charge air on the high pressure side using a Venturi mixer. To simulate the exhaust back pressure of the multi-cylinder engine, a throttle flap is placed in the exhaust duct. The engine back pressure is calculated using the turbocharger equilibrium equation (equation 1).

$$P_C = P_T \tag{1}$$

Where
P_C … compressor power
P_T … turbine power

By calculating the charging efficiency as the product of compressor efficiency and turbine efficiency, the influences of the different states in the turbocharging system can be outlined.

$$\eta_{TC} = \frac{\dot{m}_C \cdot c_{p,air} \cdot T_1}{\dot{m}_T \cdot c_{p,exh} \cdot T_3} \cdot \frac{\left(\frac{p_2}{p_1}\right)^{\frac{\kappa_{air}-1}{\kappa_{air}}} - 1}{1 - \left(\frac{p_4}{p_3}\right)^{\frac{\kappa_{exh}-1}{\kappa_{exh}}}} \tag{2}$$

Where…
η_{TC} … charging efficiency
$\dot{m}_C$ … mass flow compressor
$\dot{m}_T$ … mass flow turbine
T_1 … ambient temperature
T_3 … exhaust gas temperature (upstream of the turbine)
p_1 … ambient pressure
p_2 … intake manifold pressure
p_3 … exhaust gas back pressure (upstream of turbine)
p_4 … exhaust gas back pressure (downstream of turbine)
κ_{air} … isentropic coefficient of mixture on the intake side
κ_{exh} … isentropic coefficient of exhaust gas
$c_{p,air}$ … specific heat capacity of mixture on the intake side
$c_{p,exh}$ … specific heat capacity of the exhaust gas

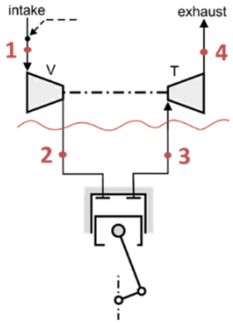

From equation 2, the scavenging gradient, i.e. the pressure difference between the intake side and the exhaust side, can be calculated (equation 3).

$$\Delta p_3 = p_2 - p_4 \cdot \left(1 - \frac{\dot{m}_C \cdot c_{p,air} \cdot T_1}{\dot{m}_T \cdot c_{p,exh} \cdot T_3} \cdot \frac{1}{\eta_{TC}} \cdot \left(\left(\frac{p_2}{p_1}\right)^{\frac{\kappa_{air}-1}{\kappa_{air}}} - 1\right)\right)^{-\frac{\kappa_{exh}}{\kappa_{exh}-1}} \tag{3}$$

The ratio of compressor mass flow to turbine mass flow can be expressed by the control margin either using compressor bypass control or waste gate control (equation 4).

$$\frac{\dot{m}_C}{\dot{m}_T} = (1 + bypass) \tag{4}$$

The calculation method can be simplified further by assuming constant values for the ambient conditions (T_1, p_1, p_4) and average values for the isentropic coefficients as well as the specific heat capacities of the fresh mixture and the exhaust gas. The only influences on the scavenging gradient are then the boost pressure, which is required to reach the desired BMEP, and the resulting exhaust gas temperature.

The SCE test bed is equipped with an exhaust gas analysis device that determines the concentrations of the most important components, namely CO_2, O_2, CO, THC, CH_4 and NO_x. The cylinder head of the engine houses fast pressure transducers that indicate the pressure trace in the main combustion chamber and pre-chamber as well as in the intake duct and exhaust duct.

In developing combustion concepts for non-natural gases, the most important infrastructure consists of the gas mixing device along with gas supply, storage and safety technology. Using the gas mixing device, virtually every gas composition consisting of

- Natural gas
- Propane
- Hydrogen
- Carbon dioxide
- Nitrogen
- Carbon monoxide

can be tested on a single cylinder engine. This is especially true given that the methane number of a specific gas composition can also be altered by admixing hydrogen or propane to the base gas.

Testing procedure

After the required engine components have been procured, the relevant engine operating range is determined in a screening phase. The screening measurements usually include load sweeps to determine the maximum achievable load and the determination of the engine operating range at nominal load (or maximum possible) in terms of ignition timing/air-excess ratio maps. Depending on the number of gases under investigation, the statistical design of experiments (DoE) method may be applied to further reduce testing time during the screening phase [5].

The sensitivity of the combustion concept to changes in boundary conditions is determined in detailed investigations with selected fuel gases that have more challenging compositions. These investigations are required since a multicylinder engine is normally subject to an imbalance between the individual cylinders in terms of charge temperature, mixture quality and (in the case of prechamber gas engines) fuel admission to the prechamber. The efficiency, load potential and emissions of the combustion concept are optimized.

The final step for single cylinder engine testing is to determine whether the combustion concept can also be run on natural gas. This step is necessary so that the multicylinder engine can pass a “roll-out” test after production and before delivery and commissioning at the customer’s site.

Application Example – Flare Gases

An enormous amount of valuable energy is lost from the flaring of waste gases. These gases arise from oil and gas production, industrial processes, steel production or agriculture. One of the major concerns of oil and gas companies is how to reduce flaring while using the energy content for their own operation or energy sales. Studies show that approximately 150 billion cubic meters of gas are flared globally each year, wasting natural resources and generating 400 million metric tons of CO2 equivalent global greenhouse gas emissions [6]. Flare gases originating from oil production contain a great share of nitrogen as well as carbon dioxide because wells are flooded with these gases to increase the output. In addition, these associated petroleum gases have high concentrations of not only methane but also ethane and propane as well as other higher hydrocarbons.

Characterization of the gases

A great number of potential gas compositions can be referred to as flare gas; however, it was necessary to limit the number of gas compositions in the investigations. The gas compositions feasible for power generation with large gas engines were selected based on certain gas properties, cf. **Table 1**. The important value in the selection is methane number excluding inerts. Since all gases were subdivided into groups of MN 60, 52 or 42, **Table 1** provides an example of one from each group. Calculated according to the AVL method, this methane number was set as the baseline to make these gases comparable to pure methane. The lower heating value of the selected gas compositions declines as the MN goes down. The laminar flame speed of all three flare gas compositions is much lower than that of pure CH4 because of the high inert proportion of CO2.

Table 1: Selected flare gas compositions and characteristic values

Gas		NG	GT1	GT2	GT3
CH_4	%Vol	100	39	28	20
C_3H_8	%Vol	0	6	6	7
H_2	%Vol	0	5	11	18
CO_2	%Vol	0	50	55	55
MN excl. Inerts	-	100	60	52	42
MN incl. Inerts	-	100	111	117	107
Density	kg/nm3	0.717	1.398	1.506	1.449
LHV	kJ/kg	50125	14529	7653	6346
Energy Density	kJ/nm3	35930	20304	11524	9195
Lam. Flame Speed	cm/s	37.8	24.5	23.1	24.9

Combustion concept pre-design using simulation

After the gas compositions were selected, it was possible to use 0D and 1D engine cycle simulation to pre-select the combustion concept and define basic engine parameters such as compression ratio and pre-chamber volume. The range of certain engine operating parameters and limits such as exhaust gas temperature were also simulated, allowing the selection of potential hardware variants in the process of combustion concept pre-design.

Experimental development on the SCE

Based on the pre-design process, a scavenged pre-chamber combustion concept was chosen for the experimental investigations. Three different power unit configurations were selected. Power unit 1 (PU1) has a moderate compression ratio. The compression ratio of power unit 2 (PU2) was increased by one point. Power unit 3 (PU3) has the same compression ratio as PU2 but its pre-chamber has a 25% higher volume. **Table 2** provides an overview of the baseline engine configuration.

Table 2: Engine configuration

Parameter	SCE
Swept volume [dm³]	~ 6
Nominal BMEP [bar]	22
Rated speed [rpm]	1500
Engine process	4-stroke spark ignited
Combustion concept	Scavenged pre-chamber with passive pre-chamber valve
Charging concept MCE	Single stage
Power control MCE	Compressor bypass and throttle valve

The first step in screening gas composition is to perform a load sweep in order to determine the maximum knock limited brake mean effective pressure (BMEP) at a certain NO_x level. To achieve good comparability, the center of gravity of combustion (MFB50%) was held constant with all investigated gas compositions. **Figure 4** illustrates the measurement procedure.

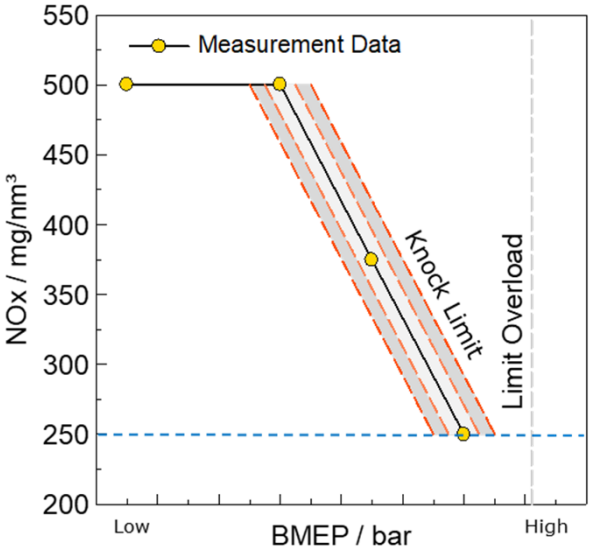

Figure 4: Procedure for determining maximum knock limited BMEP

Starting at approximately 50% of the nominal load, the load was successively increased. When the knock limit is reached and the NO_x emission level and MFB50% are constant, the engine load can be increased further only by leaning out the mixture and thus reducing NO_x emissions. The tests were aborted when either 10% overload operation was reached or a NO_x emission level of 250 mg/nm³ was achieved. Further restrictions are the misfire limit and the exhaust gas temperature limit.

Investigations of the gas compositions included in **Table 1** revealed that it was possible to achieve overload operation at the TA Luft NO_x emission level of 500 mg/nm³ with all gas compositions and that knock was not a limitation, meaning NO_x derating was not necessary.

Since full load operation has not been an issue with any of these gases, EAR/IT were varied. **Figure 5** shows the results. A sufficient operating range was obtained with state-of-the-art large gas engines combustion concepts operated with flare gas. NOx emissions at the misfire limit decrease as the H2 content increases and above all the exhaust gas temperature limit or knock limit is reached at higher NOx emissions. The abort criteria for misfire was a $COV_{IMEP} \geq 3$ %.

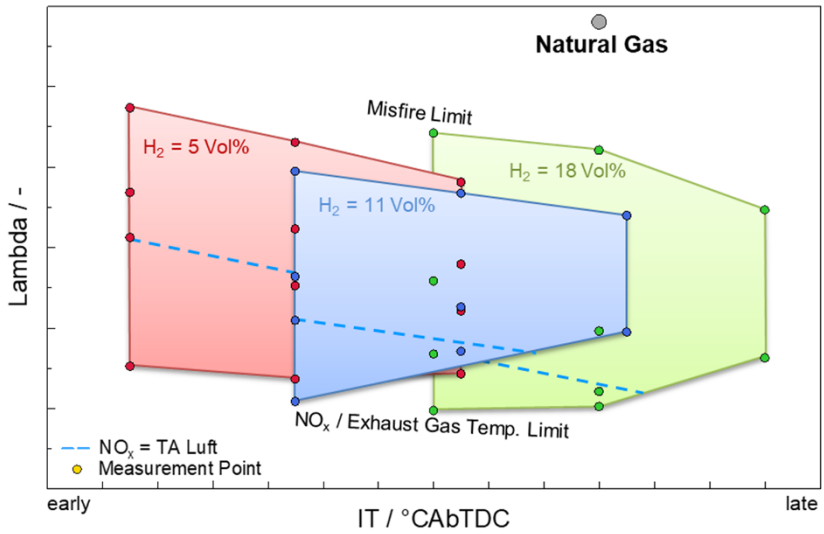

Figure 5: Operating range of selected gas compositions

The measurements revealed that overload operation was possible at the TA Luft emission level of 500 mg/nm³ of NO_x with every gas composition and power unit under investigation.

Since full load capability was a given with all the gas compositions investigated, the next step was to evaluate the knock margin in the manifold air temperature. Starting with an initial manifold air temperature at normal operating conditions, the temperature was increased by a total of 20 K in increments of 5 K as shown in **Figure 6**. Load (BMEP, **Figure 6**a) and NO_x emissions (**Figure 6**c) were held constant by adjusting the boost pressure and the EAR. In addition, the ignition timing (**Figure 6**b) was adjusted to reach the same center of combustion. As the amount of hydrogen increased, combustion had to be retarded since flame propagation differs because of the varied gas propositions the ignition timing.

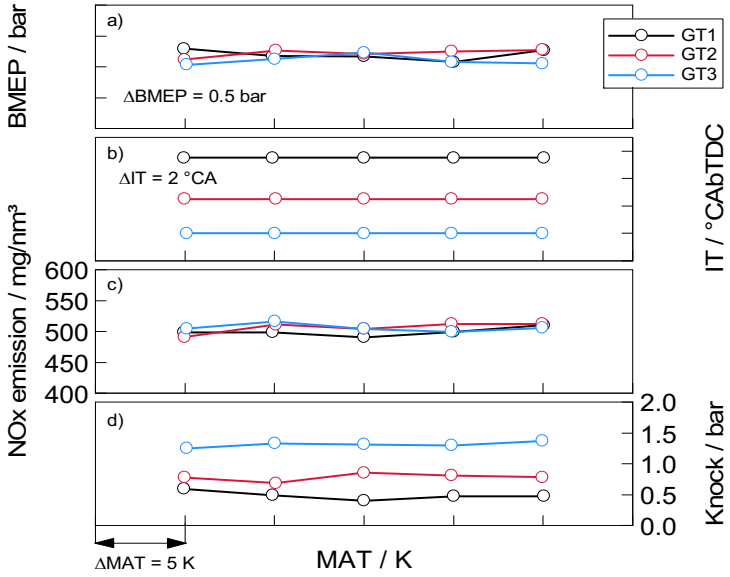

Figure 6: Manifold air temperature variation

Once again the main focus was on knock, which occurs when the remaining fresh charge is suddenly consumed as ignition conditions are reached. In lean burn gas engines, this combustion anomaly is recognizable from the in-cylinder pressure signal. Knock is identified with algorithms that focus on the sudden superposition of the in-cylinder pressure signal by high frequency pressure oscillations. [7][8][9]

The result of the algorithm used during the measurement campaign is shown in **Figure 6**d. The maximum amplitude from 100 consecutively measured combustion cycles is shown. The graph shows a clear trend in terms of hydrogen; increasing the hydrogen ratio causes noise to increase in the in-cylinder pressure signal. The term “noise” is used instead of knock because amplitude does not increase throughout the MAT range of 20 K, thereby leading to the conclusion that knock did not occur with any of the gas compositions.

The results from the SCE measurements can then be used in post-simulation. On the one hand, these results serve to validate and optimize 3D CFD simulation models, making it possible to develop a new piston shape or pre-chamber design. On the other hand, the 1D simulation model can also be matched with the measurement results, allowing simulation of data which cannot be measured such as the lambda in the pre-chamber, cf. ***Figure 7***. This figure illustrates the difference between the standard PC and the PC

with 125% volume. Lambda with the 125% PC is higher due to the flow of more of the lean mixture from the main chamber into the pre-chamber. Furthermore, the ignition timing is slightly retarded, which results in a longer mixing time.

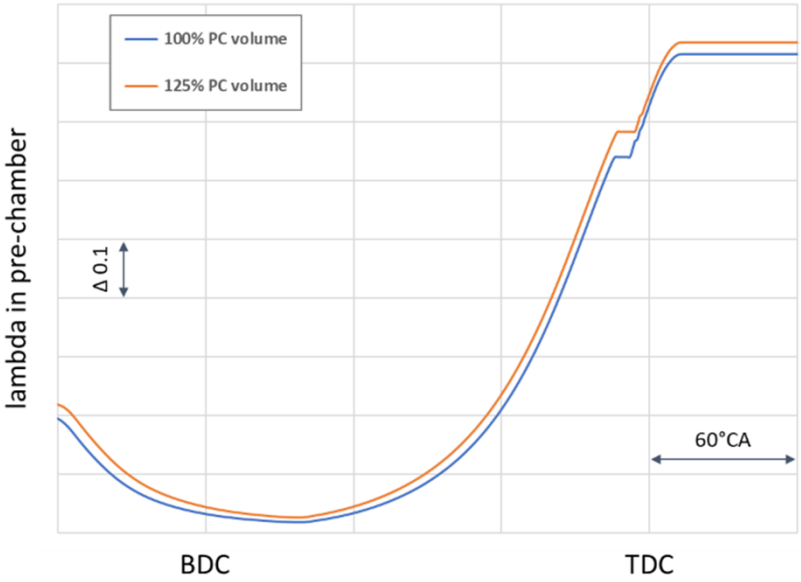

Figure 7: Simulated lambda in the pre-chamber

Summary

Large bore gas engines are operated not only with NG but increasingly with NNG from diverse sources such as biomass feedstock and industrial processes. However, the composition and therefore methane number of these gases differ widely. Maximum power output is restricted due to the occurrence of knock. Knock-free engine operation must be guaranteed in order to prevent engine failure.

Operation of gas engines with a variety of NG and NNG is contingent upon the adoption of a combustion concept that corresponds to the type of gas currently in use. The development of individual combustion concepts is a time-consuming process. LDM Compact uses state-of-the-art 0D/1D and 3D simulation tools to develop a combustion concept – in other words an engine configuration (e.g., compression ratio) – that is well-suited to the properties of the type of gas being used, thereby ensuring stable and reliable engine operation. The use of LDM Compact shortens the development process significantly.

The approach of LDM Compact was illustrated using the example of the development of a combustion concept for flare gas. Pre-design of the combustion concept using 0D/1D simulation yielded an engine configuration that was then verified by tests on a SCE.

The results of these tests indicated that this engine setup was capable of reaching the previously defined development targets for nominal load and knock margin.

The simulation models were then validated with data from the test phase. Judging from the SCE results, it will be possible to transfer the combustion concept to the MCE.

Acknowledgements

The authors would like to acknowledge the financial support of the "COMET – Competence Centres for Excellent Technologies Programme" of the Austrian Federal Ministry for Transport, Innovation and Technology (BMVIT), the Austrian Federal Ministry of Science, Research and Economy (BMWFW) and the Provinces of Styria, Tyrol and Vienna for the K1-Centre LEC EvoLET. The COMET Programme is managed by the Austrian Research Promotion Agency (FFG).

Nomenclature

APG	Associated Petroleum Gas
BFG	Blast Furnace Gas
BMEP	Brake Mean Effective Pressure
EAR	Excess Air Ratio
GT	Gas Type
LNG	Liquefied Natural Gas
MAT	Manifold Air Temperature
MCE	Multicylinder Engine
MFB50%	50% Mass Fraction Burned
NG	Natural Gas
NNG	Non-Natural Gas / Special Gas
SCE	Single Cylinder Research Engine
CO_2	Carbon Dioxide
CO	Carbon Monoxide
CH_4	Methane
H_2	Hydrogen
NO_x	Nitrogen Oxides ($NO+NO_2$)
O_2	Oxygen
THC	Total Hydrocarbons

References

[1] Wimmer, A., Winter, H., Schnessl, E., Pirker, G., Dimitrov, D., "Combustion Concept Development for the Next Generation of GE Jenbacher Gas Engines", 7th Dessau Gas Engine Conference, Dessau, Germany, March 24-25, 2011

[2] Wimmer, A., Pirker, G., Schnessl, E., Trapp, C., Schaumberger, H., Klinkner, M., "Assessment of Simulation Models for the Development of Combustion Concepts for the New Generation of Large Gas Engines" , 10th International Symposium on Combustion Diagnostics, Baden-Baden, Germany, May 22-23, 2012

[3] Zelenka, J., Kammel, G., Pichikala, K.C., Tritthart, W., "The Quality of Gaseous Fuels and Consequences for Gas Engines", 10. Internationale Energiewirtschaftstagung an der TU Wien IEWT 2017, Wien, Austria, February 15-17, 2017

[4] Wimmer, A, Chmela, F, Kirsten, M, Pirker, G, Christiner, P, Trapp, C & Schaumberger, H 2013, "LEC-GPN – a new index for assessing the knock behavior of gaseous fuels for large engines", in Knocking in Gasoline Engines, S. 239-254, Berlin, Germany, December 9-10, 2013

[5] Engelmayer, M., Zelenka, J., Wimmer, A., Salbrechter, S., Krenn, M., Pirker, G., Taucher, G., "Advantages of Statistical Methods in Development of Combustion Concepts for Large Engines", 28th CIMAC World Congress 2016, Helsinki, Finland, June 6-10, 2016

[6] Farina, M.F., "Flare Gas Reduction – Recent global trends and policy considerations", GE White Paper, 2010, http://www.ge-spark.com/spark/resources/whitepapers/Flare_Gas_Reduction.pdf

[7] Worret R., "Zylinderdruckbasierte Detektion und Simulation der Klopfgrenze mit einem verbesserten thermodynamischen Ansatz", Dissertation, Universität Karlsruhe, 2002.

[8] Dimitrov D., Chmela F., Wimmer A., „Eine Methode zur Vorausberechnung des Klopfverhaltens von Gasmotoren", 4. Dessauer Gasmotoren Konferenz, Dessau, 2005.

[9] Dimitrov D., Strasser Ch., Chmela F., Wimmer A., „Vorhersage des Klopfverhaltens für Groß-Gasmotoren mit Direktzündung oder Vorkammer", 2. Tagung Klopfregelung für Ot-tomotoren – Trends für Serienentwickler, Berlin, 2006.

Pilot injection strategies for medium-speed dual fuel engines

Björn Henke*[1], Karsten Schleef[1], Bert Buchholz[1]

Sascha Andree*[2], Egon Hassel[2]

Marius Hoff[3], Robert Graumüller[3]

1 Institute of Piston Machines and Internal Combustion Engines, University of Rostock
2 Institute of Technical Thermodynamics, University of Rostock
3 Caterpillar Motoren GmbH & Co. KG Kiel

W. Siebenpfeiffer (Hrsg.), *Heavy-Duty-, On- und Off-Highway-Motoren 2017*,
Proceedings, https://doi.org/10.1007/978-3-658-21029-8_7

Abstract

Against the background of the ongoing intensifying discussion about the emission legislation within the maritime sector the so called dual-fuel engine concept is one possible approach to minimize the air pollutants but to keep high efficiencies at the same time. For the optimal usage of such combustion processes a far reaching understanding of the fuel injection, mixture formation and the ignition behaviour is an essential needing. For this purpose, experimental investigations of these boundary conditions of the dual-fuel combustion process had been carried out at a medium speed single cylinder research engine as a part of the project "LEDF-concepts", which was realised at the University of Rostock.

Apart from a variation of the μ-Pilot injection timing these investigations included a multiple injection strategy combining an early μ-Pilot, placed during compression stroke, and a μ-Pilot injection positioned in the typical time-window before TDC. While best achievable values for indicated efficiency, coefficient of variation and NO_x-/CH_4-emissions do not differ remarkably between the tested single and multiple μ-Pilot strategy, it can be observed that these parameters behave much less sensitive against a change of the Pilot-timing for a multiple injection pattern when compared to a single injection mode. As part of the current project „LEDF-concepts 2", the findings shall be expanded to medium engine loads.

Thereby the test bed experiments are standing in close collaboration to simulative investigations, which should deliver the theoretical fundamentals for the understanding of the ongoing combustion phenomena.

The 0/1D simulation serves as a very efficient solution approach for the forecast of starting conditions of the 3D CFD models, while the 3D CFD simulation is focusing on the investigation of the complex chemical reaction paths of the multiple fuel combustion. Therefore, the laminar combustion velocity of the reacting natural gas-air mixture is investigated in the relevant temperature and pressure range. Furthermore, the ignition delay of the diesel pilot spray within the gas-air atmosphere and the subsequently reaction of the natural gas inside the cylinder are objectives of the investigations. A special adapted reaction mechanism is made available for the 3D CFD by a subsequent tabulation procedure.

All these measures are leading to a better understanding of the complex processes within the dual-fuel combustion and are providing the opportunity for the optimization and development of this combustion process.

This paper makes selected experimental results to the subject of discussion and gives an overview about the chosen simulation approach and the development status of the combustion model computation.

1 Introduction

The tightening of the international emission legislation as well as an increasing public interest in terms of environmental aspects are leading to the need of a consequent further development of efficient and low-emission marine propulsion systems. Regarding legal requirements, the limits for nitrous gases and sulphur oxides have to be confirmed, as they are mandatory by the IMO [1] for appointed maritime areas. Furthermore visible soot emissions are barely communicable any longer towards ship owners and the public. In addition, they are increasingly in the focus of possible future regulations. Due to the proven harmfulness of particulate emissions on organisms [2-5], it is to be expected that appropriate limits will be established within Europe before agreements on global levels are reached.

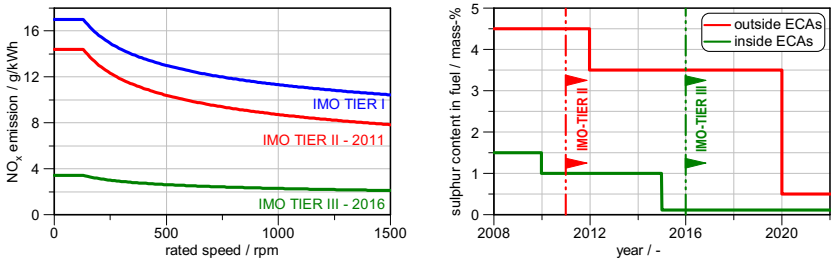

Figure 1: NO_X limits and permissible fuel sulphur content for marine propulsion machines

The achievement of the IMO-limits given in Figure 1 can be realised in general by different technology concepts [6]. Beside internal engine measures, post-engine technologies as SCR-catalysts (NO_x reduction) and sulphur scrubbers (SO_x reduction) are gaining in importance [7]. Unfortunately, these measures are requiring an immense installation space as well as the use of an additional fuel including the associating logistics. As measures for engine internal emission reduction concepts with exhaust recirculation (only usable with distillate fuel) or dual-fuel concepts (LNG – Liquefied Natural Gas, LPG – Liquefied Petroleum Gas) can be used. While exhaust gas recirculation concepts have not yet been introduced in series due to the high development effort, dual-fuel engines for LNG operation are already available as standard products from many ship diesel engine manufacturers [8-12, 14]. However, since this is a comparatively young technology, which is almost exclusively limited to medium-speed and slow-speed large engines, there is a high need for research and development within this area.

From own investigations as well as publications of other research institutes [13] it is known that the pilot injection has a decisive influence on the operating and emission behaviour of dual-fuel engines. Regarding the compliance and realization of minimal NO_x-

emissions, it is found that in particular a minimization of the pilot injection quantity (µ-pilot) is showing advantages. Unfortunately, these are typically accompanied by disadvantages in combustion stability, increased CH_4 emissions and efficiency losses. Therefore, it is important to achieve the best possible compromises in the target conflict of these parameters by applying optimal pilot injection strategies. The present work is intending to make a contribution to solve this trade of by presenting and discussing the effects of a varied single and multiple injection strategy on the operating and emission behaviour.

2 Research engine test bench

In order to carry out the experimental investigations, a representative medium-speed single cylinder research engine including associated auxiliary units required for operation had been built up at the University of Rostock. The first stage of the engine has a bore of 340 mm and a stroke of 460 mm. Possible variabilities and performance data of the basic engine are summarized in Table 1.

Table 1: Performance data of the single cylinder research engine

Parameter	Unit	First configuration	LEDF single cylinder research engine
Bore	mm	340	250 … 350
Stroke	mm	460	350 … 500
Power	kW	>500	850
Rated speed	min^{-1}	720	750
Speed limit	min^{-1}	900	900
Peak pressure	bar	>200	300
Gas system	Gas dosing over GAV into the intake manifold		
Injection system	Common rail system, max. rail pressure 2200 bar		

The following picture (Figure 2) presents the completed research engine at the test bench. With a 1.2 MW load unit, all load conditions can be displayed according to generator and propeller operation as well as motoring of the engine.

The supply of charge air with a mass flow up of to 5,400 kg/h and a maximum pressure of 8.5 bar_a is achieved by two electrically operated charge air compressors. The charge air pressure and exhaust gas pressure can be set independently of one another in accordance with the specifications. In addition, it is possible to thermally condition all operating media such as charge air, cooling water, lubricating oil and fuel in wide ranges.

In the load range from 0-100 %, diesel fuel, MDO and natural gas can be provided at the test bench. Due to the existing heavy oil infrastructure at the LKV, an extension to

heavy oil operation on the research engine is also possible. The exhaust emissions are analyzed by using a modern AVL SESAM i60 FT and a smoke meter. If needed, the particle number and particle size distribution can also be determined. An individual PLC- and LabView-based solution is used for the test bench control and measurement acquisition. The open and modular engine control unit was developed on the basis of a National Instruments hardware platform and LabView at the LKV.

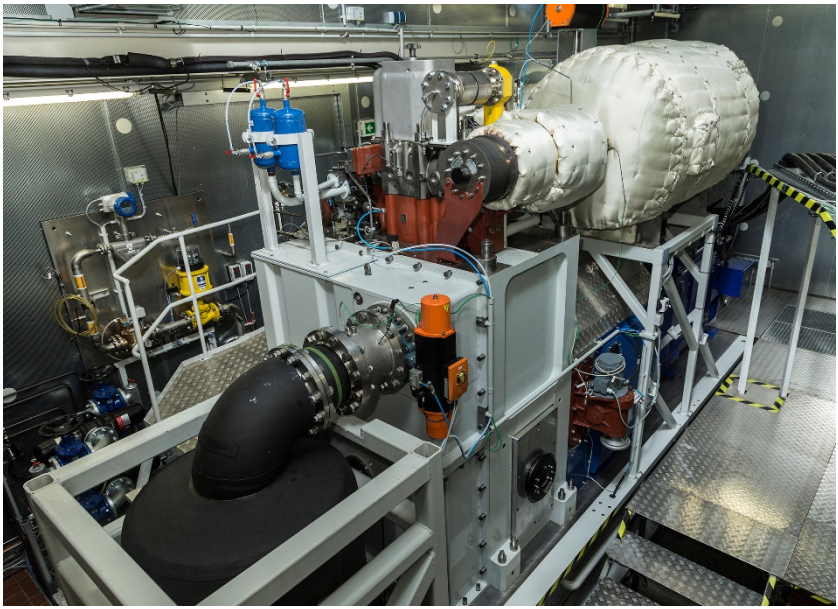

Figure 2: Test bench with the medium speed single cylinder research engine

3 Experimental investigations and results

The focus of the work presented here was the characterization of the operating behavior of the single cylinder research engine used in terms of combustion, emissions and efficiency at varying air ratios and pilot injection timings. In addition to a typical µ-pilot injection, a multiple injection was also applied and the observed results are discussed. The comparison of the different variations takes place in the part load point described in table below.

Table 2: Overview measuring points

Parameter	Unit	Value
Load	%	50
Indicated mean effective pressure	bar	10,8
Rated speed	min^{-1}	720
Rail pressure	bar	1400
Start of injection	DBTDC	constant/variable
Intake manifold air pressure	bar	variable/constant

3.1 Variation of SOI / IMAP

Variations of the injection timing had been carried out to characterize the testing configuration of the single cylinder engine. While doing that, charge air temperature, pilot injection pressure and pilot volume (1.8 % of the total energy amount) and the indicated mean pressure were kept constant. The following figure presents the results of the combustion process analysis as well as the energizing signal of the pilot injector.

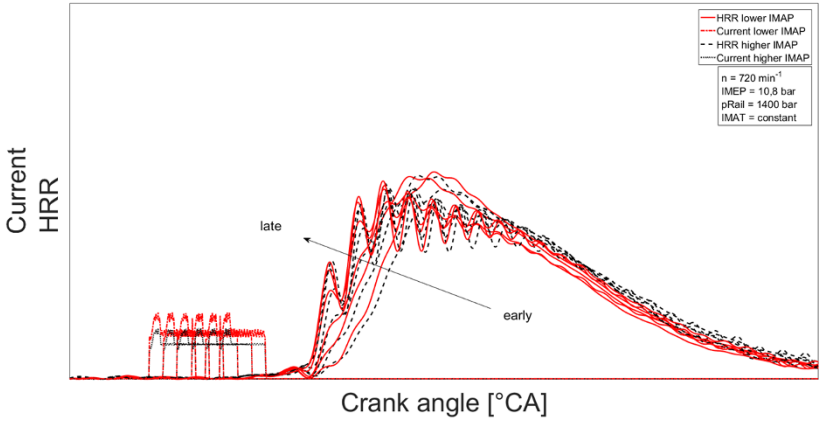

Figure 3: Heat release rate of the SOI variation

In direct comparison, two series of measurements of the start of injection variation with different charge air pressures were compared. The results of the tests with lower charge air pressure are shown in red. The ones with higher charge air pressure are in black. The current profile in red has been scaled up for a better illustration only. Therefore, it can be equated with the black one. When the start of injection is viewed separately, it can also be

seen from Figure 3 as well as from Figure 4 that an increase in the ignition delay is associated with an early-positioned pilot injection. An extension of the ignition delay provides more time for the distribution and mixing of the pilot injection quantity with the charge air. The thereby in each case changed starting conditions at the ignition point lead to appreciable deviating combustion processes. While early injection timings are causing comparatively late ignition times and short combustion durations, later injection timings are causing slightly earlier ignitions and longer combustion durations. In addition, an increase of the high-frequency components in the cylinder pressure signal is associated with a shortening of the ignition delays. The results presented for partial load tests here are correlating very well with the full load tests presented earlier this year [15].

In the comparison of the measurement series with different charge air pressures, there is initially no significant difference in ignition delay and intensity of the stimulation of the combustion chamber frequencies, as it can be seen in Figure 4. Both graphs are falling respectively rising in the same degree while moving the start of injection to a late position. The air-fuel ratio is, as expected, smaller at lower charge air pressures. Nevertheless, the lambda values for both measurement series are converging for late injection timings, due to the increased mass of combustion gas in order to keep the mean pressure constant.

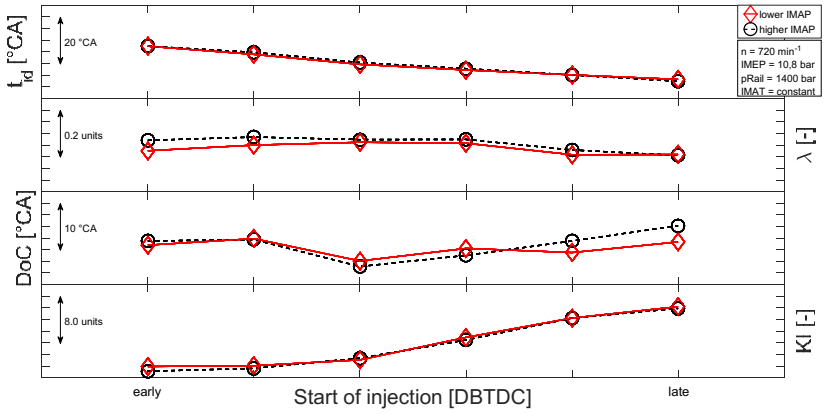

Figure 4: Ignition delay (t_{id}), Air-fuel ratio (λ), Duration of combustion (DoC) and Knock-Index (KI) depending on SOI

The results of the start of injection variation in relation to combustion stability, indicated efficiency and emissions are shown in Figure 5. The measurement series with higher charge air pressures and early injection timings are displaying significantly higher Coefficients of Variation of the indicated mean pressure in contrast to the

measurement series with lower charge air pressures, as it has been observed at full load operating conditions [15]. This means, that the stability of the combustion process decreases at the lean-burn limit rapidly. Nevertheless, it can be seen at part load conditions, that the COV_{IMEP} is fluctuating less at lower charge air pressures and remains at a similar level during the measurement series.

The indicated efficiency of the measurements series with lower charge air pressures lies in the range of the early and middle injection timings with more than 2% above the measurement series with higher charge air pressures. At lower charge air pressures, the indicated efficiency can be increased by using a leaner mixture. The indicated mean pressure stays unaffected by this procedure. On further consideration, it becomes apparent that positive characteristics of a stable and fast combustion (low CH_{4i} emissions) are associated with high NO_{xi} emissions in this combustion process. Out of this correlation the basic trade-offs for NO_{xi} emission, combustion stability and the efficiency are resulting.

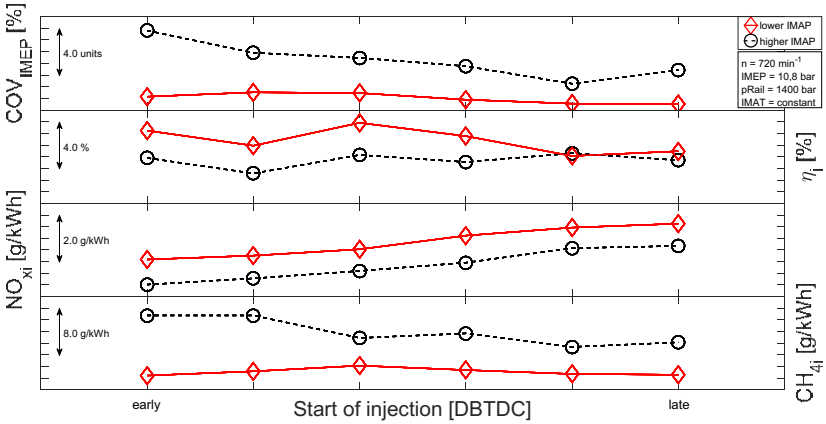

Figure 5: Coefficient of Variation of the indicated mean effective pressure (COV_{IMEP}), Indicated efficiency (η_i), NO_{Xi} and CH_{4i} emissions depending on SOI

These trade-offs are represented in Figure 6. It can be seen from the comparison of the two measurement series that the NO_{xi} emissions can be reduced by an increase of the combustion air ratio, and therefore all points of the test series with higher charge air pressures are within the permissible NO_{xi} limits.

Lowest NO_{xi} emissions are combined with low combustion stabilities but poor efficiencies. Consequently, an engine application, which wants to fit to the requirements for high efficiencies and a stable combustion, will be oriented close to the permissible limits.

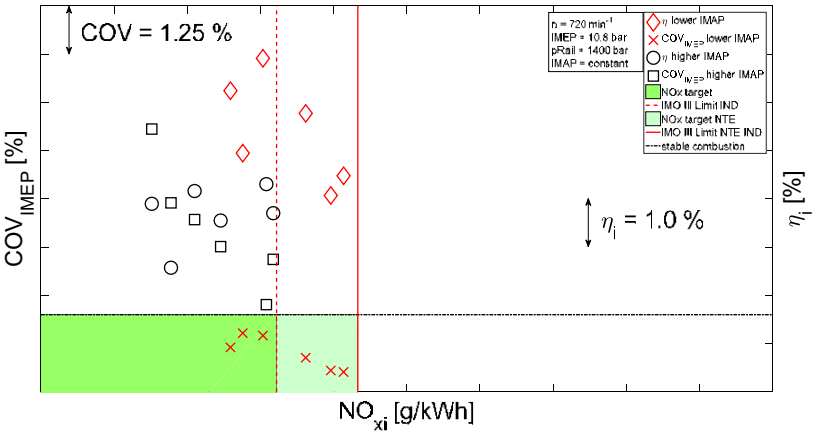

Figure 6: COV_{IMEP} and η_i over specifically indicated NO_{Xi} emissions depending on SOI

3.2 Multiple injection variation

With the aim of reaching a stable combustion as well as a NO_{xi} reduction at the same time, a further pilot injection (P1) was used in addition to a conventionally arranged pilot injection (P2). For the injections shown in red, the same injection amount was applied (1:1 split), for the ones in black a 2:1 split. Thereby the sum of the injected fuel mass equates in each case to 3.5 % of the total energy amount. While injection P2 was kept at a constant timing along the shown measurement series, the timing of the injection P1 was varied as visible in Figure 7. From the heat release rates, it can be seen that no prematurely self ignition of the injected fuel mass P1 takes place. Furthermore, a correlation between the ignition delay related to P2, the combustion duration and the injection mass of P2 can be noticed. Accordingly to this behaviour, a smaller injection mass of P2 results in a longer ignition delay and a longer combustion duration than a larger injection mass. These findings are differing from the full load results. In full load it was found, that by using a pre injection the ignition delay can be increased, but the combustion duration is shortened at the same time. This relationship needs to be further investigated.

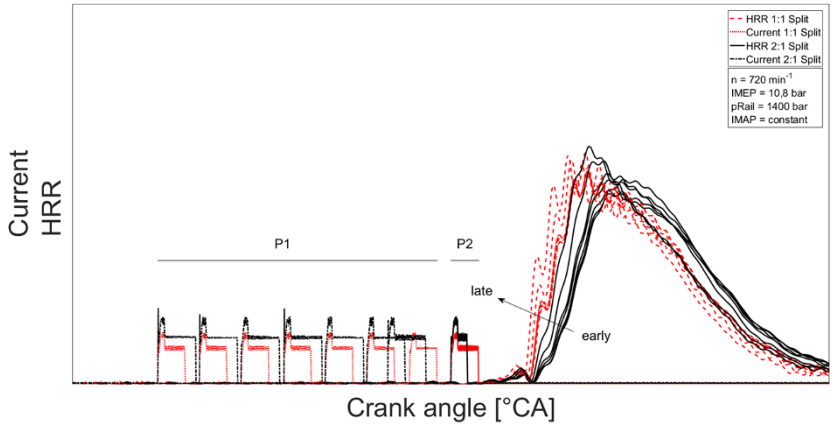

Figure 7: Heat release rate of the SOI P1 variation and different injection splits

In Figure 8 the ignition delay, lambda, combustion duration and knock intensity are compared for the multiple fuel injection variation 1:1 and 2:1 split. It can be seen that in the 2:1 split the ignition delay is about 5°CA longer than in the 1:1 split. The explanation for this phenomena is probably a lower injection mass (3.5 % of energy amount by pilot injections = 2/3 P1 plus 1/3 P2) in comparison to the 1:1 split (3.5 % of energy amount by pilot injections = 1/2 P1 plus 1/2 P2).

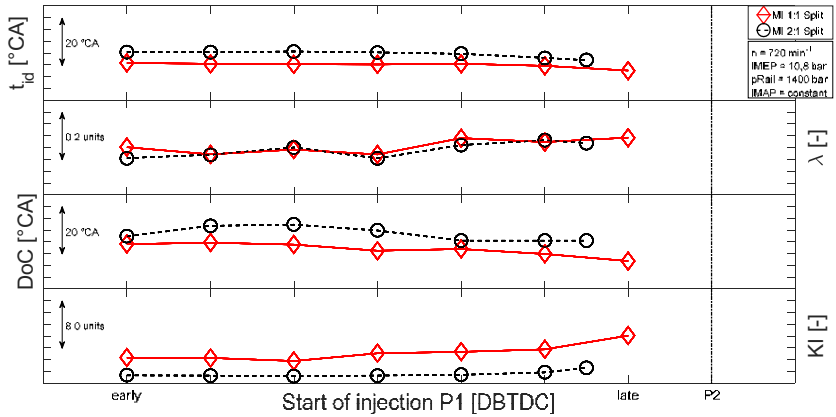

Figure 8: Ignition delay (t_{id}), Air-fuel ratio (λ), Duration of combustion (DoC) and Knock-Index (KI) depending on SOI P1 variation and different injection splits

In reference to the air-fuel ratio, the split variations are at a similar level. But yet a finding is that the combustion duration is along the whole series ≥ 5°CA longer as compared to the 1:1 split. It is assumed that this behaviour can be traced back to the smaller pilot fuel mass P2, which initializes the ignition within the cylinder. As a result, at the time of ignition, combustion conditions prevail, which are causing a slower late combustion phase of the air-fuel mixture. It needs to be investigated why the enrichment of the gas-air-mixture by the early injection of the pilot fuel is not causing an acceleration in combustion. In addition, significantly less high-frequency signal components can be observed in the cylinder pressure trace while operating with 2:1 split compared to the 1:1 split.

As illustrated in Figure 9, comparable values are obtained with respect to combustion stability. By using the 2:1 split the COV_{IMEP} is constantly at the same level over the entire range of variation, meanwhile the COV_{IMEP} is improving when the P1 fuel mass is moved to later injection timings. The comparison of the efficiencies shows that the 1:1 split as well as the 2:1 split are on the same level over the entire range of variation.

When comparing the NO_{xi} and CH_{4i} emissions clear advantages occur for the driven variations on the side of the 2:1 split while the same sensitivity of the single parameters to the injection timing can be observed. Along the entire injection range of P1 the NO_{xi} emissions are approximately 1 g/kWh below the 1:1 split. A similar tendency can be found in respect to the CH_{4i} emissions. In this comparison, the CH_{4i} emissions are almost 4 g/kWh below the level of the 1:1 split along the entire injection timing spread. In summary it can be stated that an improvement in emissions can be achieved by the usage of a 2:1 split without any reduction in efficiencies.

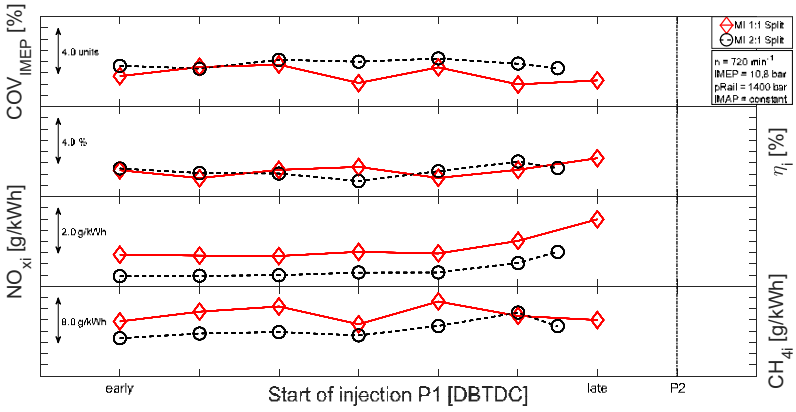

Figure 9: Coefficient of Variation of the indicated mean effective pressure (COV_{IMEP}), Indicated efficiency (η_i), NO_{Xi} and CH_{4i} emissions depending on SOI P1 variation and different injection splits

Figure 10 shows that, with exception of one operating point every other points with a very late injection timing of P1 are in compliance with the IMO Tier III limitations for NO_{xi}. When talking about the 2:1 split even five out of seven measuring points are on half of the IMO Tier III level. Although the P1 injection timing was varied over a comparatively wide range, the results for für COV_{pmi}, η_i und NO_{xi} are in a very small window. This fact suggests that the sensitivity of the combustion process is less pronounced against external influences, such as changing natural gas qualities and environmental conditions. In further works, it has to be investigated, which measures can be effecting the stabilization and acceleration of the combustion in a positive manner, in particular during part load operation. In addition, influences from changing boundary conditions have to be worked out and corresponding control concepts have to be derived.

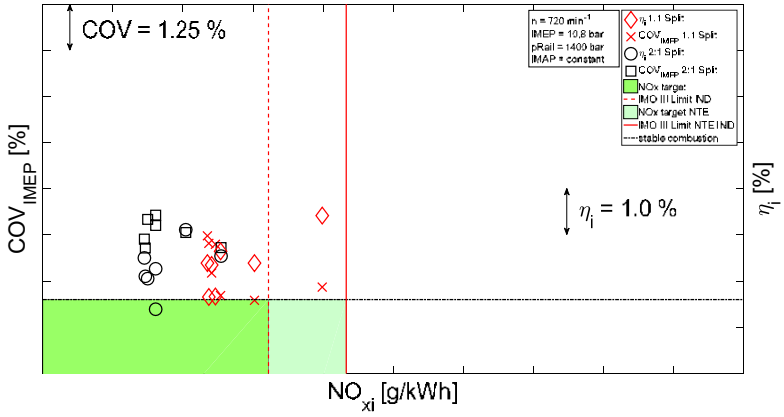

Figure 10: COV_{IMEP} and η_i over specifically indicated NO_{Xi} emissions depending on SOI P1 variation and different injection splits

4 Numerical investigations und results

In recent years, the numerical simulation of the dual-fuel combustion process shifted into focus of the combustion simulation community. There are several different approaches for dual-fuel combustion simulation. Some workgroups operate with modifications on established combustion models, other work with detailed chemical reaction mechanisms. The latter approach was chosen within the LEDF project for several reasons. First, the need of tuning of the reaction rate is strongly limited due to the fact, that multiple reaction paths are resolved. Secondly, the dependency of the combustion process towards varying compositions of natural gas can directly be reproduced if the species and reaction paths are included into the reaction mechanism.

4.1 Reaction mechanism for dual-fuel combustion

Basis for the chosen approach for dual-fuel combustion simulation is the chemical reaction mechanism. It describes the ignition of the air-fuel mixture and, in combination with a turbulence chemistry interaction model, the progress of the combustion. The dual-fuel combustion process is characterized by a lean natural gas mixture, which is ignited by a small diesel pilot spray. For this reason a mechanism with both reaction paths, the natural gas paths and the diesel paths is needed. Since diesel is a multicomponent mixture of several hydrocarbons a surrogate was chosen to model the influence of the diesel pilot spray. This surrogate should correctly reproduce the features of the pilot spray, the ignition delay and the influence on NO_x formation. N-heptane was chosen as surrogate for diesel, because it has similar ignition delays at engine relevant conditions [16].

First, a literature research was carried out to acquire an overview of existing reaction mechanisms for n-heptane and natural gas combustion. The following Table *3* provides an overview of some mechanisms that had been found. The most mechanisms are created for general combustion or gas turbines. That means that they are only validated in a low pressure range. In most cases only up to 10 or 20 bar. Therefore, it is necessary to investigate how these mechanisms behave at engine like conditions. Especially high pressures up to 200 bar are interesting. To examine the mechanism two parameters are chosen. The first parameter is the laminar flame speed, which describes the flame consumption and therefore the premixed or partial premixed combustion regime. The second parameter is the ignition delay. To investigate the laminar flame speed a one dimensional simulation with an adaptive grid is used. Fresh, well mixed and unburned gas is introduced on one side of the calculation domain and on the other side hot burned gas leaves the domain. In middle of the domain the flame front is defined by a temperature. This temperature has to be between fresh gas and burned gas temperature. During the calculation the fresh gas inlet speed will be adjusted in a way that the flame front stays at a fix point. In this case the laminar flame speed is equal to the inlet speed of fresh gas. The ignition delay is determined by zero dimensional homogenous reactor calculations. It is defined as the time span between the start of simulation until a predefined temperature rise is detected.

Table 3: Overview of available mechanisms from literature survey

Mechanism	Natural gas	n-heptane	Species/reactions	Usage
USC-Mech	Yes	No	111/784	General combustion
SanDiego	Yes	Yes	58/282	General combustion
Wisconsin	No	Yes	66/52	Combustion engine
LLNL	Yes	Yes	654/2827	Combustion engine
CTI-Mech	Yes	Yes	192/1156	General combustion
LawCG-Heptane	No	Yes	52/48	General combustion
LawCG-Methane	Yes	No	92/621	General combustion
Galway	Yes	No	118/665	Gas turbines
Grimech 3.0	Yes	No	53/325	Gas turbines
UBC-Mech	Yes	No	40/194	General combustion
CRECK	Yes	Yes	484/19341	General combustion
ERC-Mech	No	Yes	29/52	Combustion engine

The dual-fuel combustion process requires a mechanism, which contains the reaction paths for natural gas as well as for n-heptane. The literature research shows, that there are just a few mechanisms with both reaction paths. If they contain the necessary reaction paths, they are usually too large for a useful application within CFD. For this reason an own mechanism was created by combining mechanisms from literature.

4.2 Tabulation of reaction mechanism

The created mechanism consist of 114 species and 596 reactions. These mechanisms can be used for CFD calculations, but would lead to long computing times. Even by using HPC resources with several CPUs (>100 cores), calculation times for a combustion cycle can rise up to multiple weeks. This is caused by the need of a high resolution in time and space. Also the solver is less stable because of stiff differential equations of the reaction mechanism. This approach can be used for academic cases, but is not suitable for practical applications.

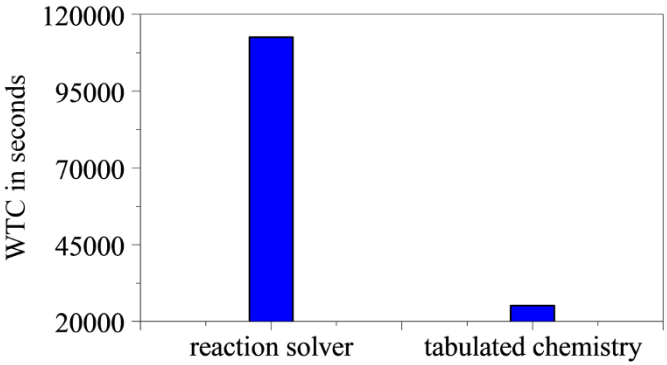

Figure 11: Wall time clock for an identical case calculated with detailed and tabulated chemistry

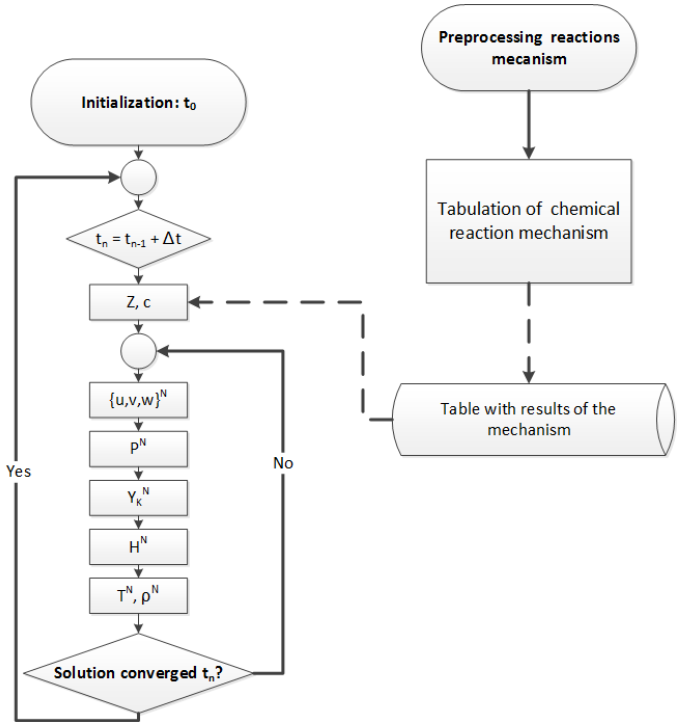

Figure 12: Flow chart of sequence of a CFD combustion simulation with tabulated chemistry

To undergo the mentioned disadvantages, the tabulation of the chemical reactions can be applied. The tabulation approach from AVL Dacolt is used. The mechanism is no longer solved directly during the CFD solution. But in a pre-processing step a multidimensional database will be created, which contains all necessary solutions of the reaction mechanism. The CFD solver uses a flamelet generated manifold model for combustion. This FGM model accesses the database to determine the combustion process. This method is illustrated in the flowchart in Figure 12. By using this procedure the computing times can be reduced enormously. The following figure shows a comparison between two identical cases simulated with detailed chemistry and tabulated chemistry based on the same mechanism. This shows the big advantage of the tabulation approach. This means that a dual-fuel simulation can be done on a well-equipped workstation in acceptable time and therefore it might be useful for industrial applications.

4.3 CFD simulation

According to current status, the implemented FGM model is able to handle with only one varying mixture fraction describing the fuel side. This mixture fraction describes the mixture of diesel and a homogenous natural gas-air mixture. For modelling the mixing process and the dual-fuel combustion process, the mixture fraction must contain two kind of fuels, which are mixed independently from each other. Therefore, now the combustion calculation can only be done in the high pressure phase of the engine with the assumption of a homogeneous natural gas-air mixture in the combustion chamber. At the current state, the gas injection into the intake manifold cannot be taken into account. Further developments to extend the model by a second mixture fraction are planned. With this new version full cycle processes with mixture formation and inhomogeneous natural gas contribution in the cylinder can be simulated. To take the influence of the port flow onto the in-cylinder flow into account, a cold flow simulation has to be done. Afterwards, the information of this flow field is mapped to the combustion simulation as initial conditions. So that only the natural gas is homogeneously distributed.

In Figure 13 the course of a dual-fuel combustion process based on progress variable and temperature is pictured. The progress variable displays how the gas-air mixture is ignited by the diesel pilot spray and burns afterwards with a flame front through the combustion chamber. Besides that, on temperature figures the advantage of the lean combustion is visible, which results in less NO_x emissions, due to less amount of created thermal NO_x. Well known is, that a high combustion temperature is the main reason for NO_x emissions. The figures are pointing out high combustion temperature around the spray area. By that the proven fact of the influence of diesel pilot as main source for NO_x emissions is affirmed.

5 Summary

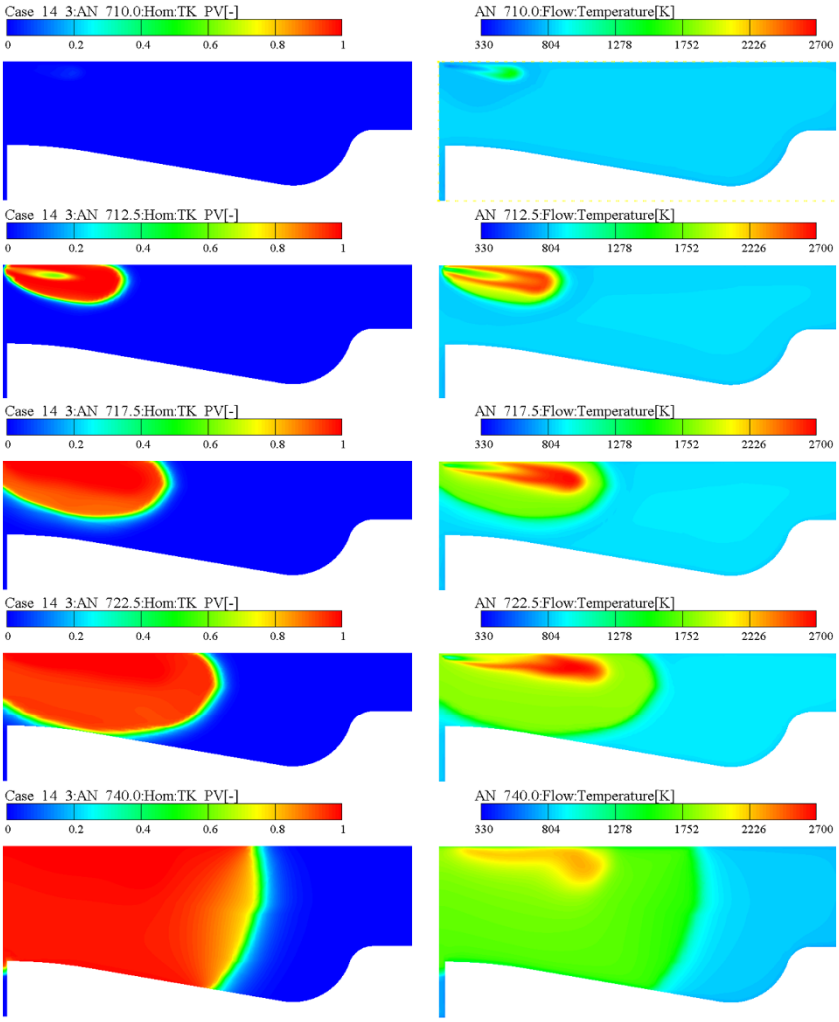

Figure 13: Progress variable (left) and temperature (right) during dual-fuel simulation using tabulated chemistry

At the Institutes for Piston Machines and Internal Combustion Engines and Technical Thermodynamics of the University of Rostock the investigation of two different pilot injection strategies were realised within the research project “LEDF-concepts 2”. It has been shown that there are also trade-offs existing for dual-fuel engines to comply with the existing emission legislation, which possibly require compromises on efficiency and combustion stability. As one option to alleviate these trade-offs a combustion process with a single pilot injection strategy as well as a combustion process with a double pilot injection was analysed. As a result, it can be proved that a separation of the injection amount can lead to a significant influence on the combustion duration, stability and emissions.

While the reached optimum values for the indicated efficiency, combustion stability and emissions as the main challenges of the engine development hardly differ between both injection strategies, it was observed that these parameters are reacting less sensitive to a change of the start of injection while using a split pilot injection compared to a single pilot injection. The dual-fuel combustion process allows a narrow target corridor, which had been achieved. Starting from this point further investigations will have to proof, if the robustness of the multi-pilot injection process can also be applied to changing gas qualities and fluctuating environmental conditions, which further fundamental optimization potentials are existing for this injection strategy and which process sequences are characterizing the observed behaviour in detail.

6 Acknowledgements

The authors would like to thank the Federal Ministry of Economics and Technology for the promotion of the "LEDF-concepts 2" project (project number: 03SX421A). In addition, we would like to thank the project partner FVTR GmbH for supporting the project. Furthermore, we would like to thank the associated project partners Caterpillar Motoren GmbH & Co. KG, KS Kolbenschmidt GmbH, Schaller Automation GmbH & Co. KG and Kompressorenbau Bannewitz GmbH.

Supported by:

on the basis of a decision
by the German Bundestag

7 Abbreviations and Symbols

COV_{IMEP}	Coefficient of variation
CH_{4i}	Methane indicated
DBTDC	Degrees before top dead center
DoC	Duration of combustion
FGM	Flamelet generated manifold
HRR	Heat release rate
IMAP	Intake manifold air pressure
IMAT	Intake manifold air temperature
IMEP	Indicated mean effective pressure
IND	Indicated
KI	Knock index
NO_{Xi}	Nitrogen oxide indicated
NTE	Not to exceed
P1	Pilot injection 1
P2	Pilot injection 2
p_{Rail}	Rail pressure
SOI	Start of injection
t_{id}	Time ignition delay
WTC	Wall time clock
°CA	Degrees crank angle
η_i	Indicated efficiency
λ	Air-fuel ratio

8 References

[1] International Maritime Organisation, MEPC 58/23/Add.1, ANNEX 13, “Amendments to the annex of the protocol of 1997 …”, 10/2008

[2] Streibel, T.: “Abgasuntersuchungen an Kraftstoffen/Biokraftstoffblends im Rahmen des Helmholtz Virtual Institute for Complex Molecular Systems in Environmental Health”, 6. Rostocker Bioenergieforum, 14.-15. Juni 2012

[3] Environmental Protection Agency (EPA): „Proposal of Emission Control Area Designation for Geographic Control of Emissions from Ships”, Office of Transportation and Air Quality, EPA-420-F-09-015, 2009

[4] Commission of the European Communities: „Impact assessment“, Annex to: The communication on thematic strategy on air pollution and the directive on „Ambient air quality and cleaner air for Europe”, Commission staff working paper, 2005, ec.europa.eu/environment/archives/café/pdf/ie_report_en_050921_final.pdf, aufgerufen am 15.02.2011

[5] Zimmermann, R.; Stengel, B.; Rabe, R.; Harndorf, H. und 24 weitere Autoren: "Feinstaub-Emissionen aus einem Schiffsmotor im Betrieb mit Schweröl oder Dieselkraftstoff: Chemische Zusammensetzung der Aerosole und deren biologische Wirkung auf menschliche Lungenzellen", 3. Rostocker Großmotorentagung, Rostock, 18.-19. September 2014

[6] Harndorf, H.; Rabe, R.; Wichmann, V.; Fink, C.; Buchholz, B.; "Strategien zur Erfüllung zukünftiger Emissionsvorgaben", 1. Rostocker Großmotorentagung – Zukunft der Großmotoren im Spannungsfeld von Emissionen, Kraftstoffen und Kosten, Rostock, 16.-17. September 2010, ISBN 978-3-8169-3032-7

[7] Buchholz, B.: “ Saubere Großmotoren für die Zukunft – Herausforderungen für die Forschung", 3. Rostocker Großmotorentagung, Rostock, 18.-19. September 2014

[8] Ott, M.; Hattar, C.; Weisser, G.: „Wärtsilä 2-Takt Dual-Fuel Motoren – Die technische Antwort auf veränderte Marktanforderungen“, 3. Rostocker Großmotorentagung, Rostock, 18.-19. September 2014

[9] Menage, A.; Gruand, A.; Berg, P.; Golloch, R.: „The New Dual Fuel Engine 35/44 DF from MAN Diesel & Turbo SE”, Paper no. 291, CIMAC Congress, Shanghai, China, May 13-16, 2013

[10] Ritscher, B.; Greve, M.: „CATERPILLAR M46 Dual fuel engine with new cylinder pressure based control strategies“, Paper no. 411, CIMAC Congress, Shanghai, China, May 13-16, 2013

[11] Troberg, M.; Portin, K.; Jarvi, A.: „Update on Wärtsilä 4-stroke Gas Product Development“, Paper no. 406, CIMAC Congress, Shanghai, China, May 13-16, 2013…

[12] Böckhoff, N.: „MAN L/V 51/60 DF: Der Dieselgasmotor für Marineanwendungen“ 1. Rostocker Großmotorentagung, 2010…

[13] Kiesling, C.; Redtenbacher, C.; Kirsten, M.; Wimmer, A.; Imhof, D.; Berger, I.; Garcia-Oliver, J.; “Detailled Assessment of an Advanced Wide Range Diesel Injector for Dual Fuel Operation of Large Engines”, Paper no. 078, CIMAC Congress, Helsinki, Finland, June 6-10, 2016

[14] Banck, A.; Sixel, E.; Rickert, C.: “Dual Fuel Engine optimized for marine applications”, Paper no. 047, CIMAC Congress, Helsinki, Finland, June 6-10, 2016

[15] Buchholz B.; Henke B.; Schleef K.; Wolfgramm M.; Graumüller R.; Andree S.; Fink C.: Pilot-Einspritzstrategien für mittelschnelllaufende Dual-Fuel Motoren, Dessauer Gasmotoren-Konferenz, Dessau, 06.-07. April 2017

[16] G. Stiesch, Modelling Engine Spray and Combustion Processes, Springer, 2003.

New MTU series 4000 rail engine fulfilling most ambitious emission regulation

Dr.-Ing. Carsten Baumgarten, Tobias Weiß, Dr.-Ing. Günter Zitzler, Christian Herkommer, Dr.-Ing. Boban Maletic

MTU Friedrichshafen GmbH

W. Siebenpfeiffer (Hrsg.), *Heavy-Duty-, On- und Off-Highway-Motoren 2017*,
Proceedings, https://doi.org/10.1007/978-3-658-21029-8_8

1. Motivation

For services on non-electrified lines diesel locomotives are proven for great many years. Besides reliability and high operational availability, convincing arguments for diesel engines are an attractive power-to-weight ratio, excellent transient response characteristics and long-range capability. Like many other means of transport, diesel-powered rolling stock has been notably affected by increasingly stringent emission standards over the last few years.

Stage III-B pursuant to EU directive 97/68/EC is in force since 2012, and stipulates the emission limits listed in Figure 1 for the ISO-F cycle.

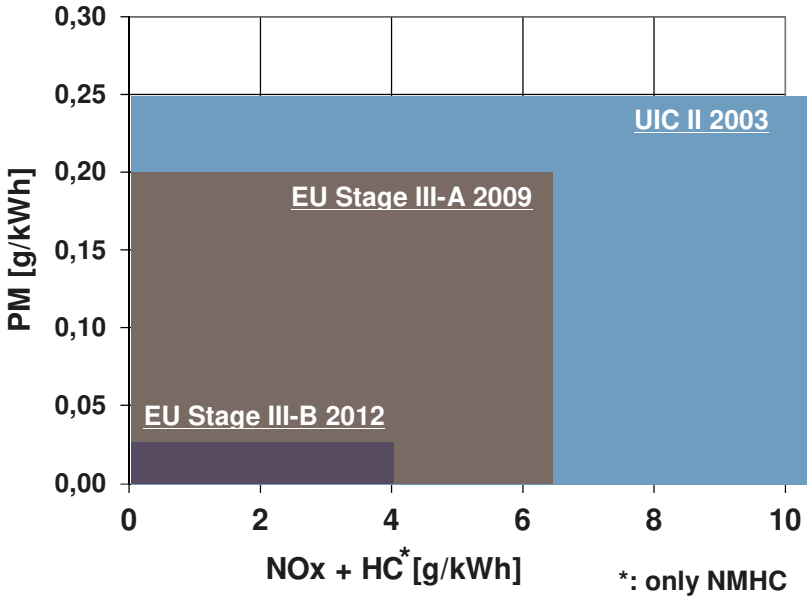

EU Stage III-B emission limits for locomotive engines > 130 kW	
NOx + HC	4,0 g/kWh
CO	3,5 g/kWh
Particulate	0,025 g/kWh

Figure 1: EU emission limits for diesel locomotive engines (>130 kW) since 2003

The latest Series 4000 models destined for use in rail applications meet these requirements by means of optimized engine-internal technology with exhaust gas recirculation and a diesel particulate filter, see Figure 2. The key characteristics of this engine are shown in Table 1:

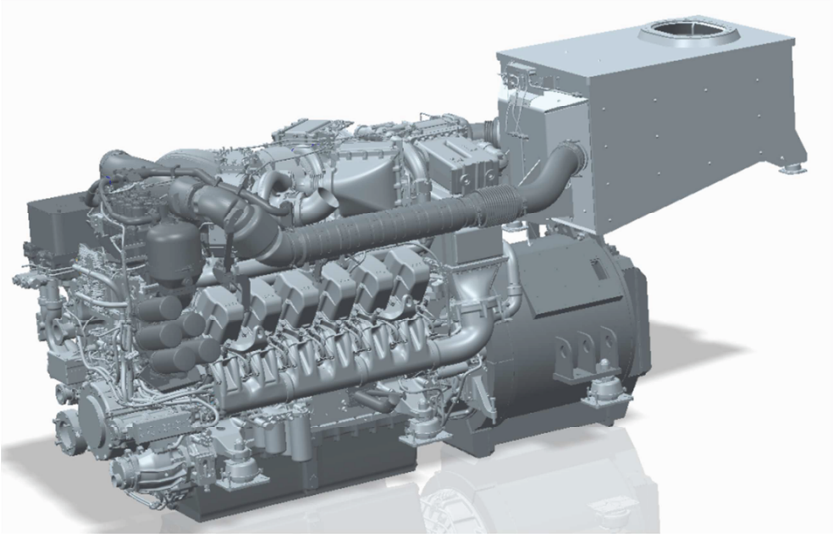

Figure 2: New MTU 12V4000R84 for diesel-electric / diesel-hydraulic locomotives

Table 1: Key technical characteristics

Bore	170 mm
Stroke	210 mm
Rated Power @ speed	1800 kW @ 1800 rpm
Air charging concept	2-stage controlled turbocharging
Emission concept	EGR, DOC+DPF
Certificates	EU Stage III-B

Even significantly tighter emission limits were imposed on a project for a new generation of heavy-duty multipurpose locomotives (Figure 3) intended for heavy shunting and medium freight service, as well as for use in construction.

Figure 3: Vossloh's new multipurpose diesel locomotive with MTU 12V4000R84 diesel engine

Whilst the fulfillment of EU Stage III-B requirements is necessary to certify an new diesel engine today, the new target for the development of the new MTU Rail engine was to cut the emissions by 50% for operation on construction sites – especially in tunnels – to avoid exposing the workforce to excessive levels of pollution in places where a steady exchange of air is not easily provided (see Figure 4).

Figure 4: Impressions of a rail tunnel construction site

2. Technical Concept

One of the biggest challenges in the development of diesel engines is the reduction of nitrogen oxides (NOx) and particulate matter (PM) while keeping excellent fuel consumption. NOx and PM are also the most important emissions concerning health risks. This is especially relevant for construction workers in tunnels, who do their work next to shunter locomotives.

To meet this challenge, engine internal and external emission reduction technologies are available. One concept is to reduce PM engine internally by optimizing the combustion process, and NOx externally with selective catalytic reduction (SCR catalyst), Figure 5. The big advantage by using this technology is that high conversion rates of NOx emissions (>80%) are possible. However, these conversion rates are only possible with exhaust gas temperatures above 250°C. Below approximately 200°C, and this is especially relevant for low-load operation in tunnels, there is no conversion of NOx emissions possible.

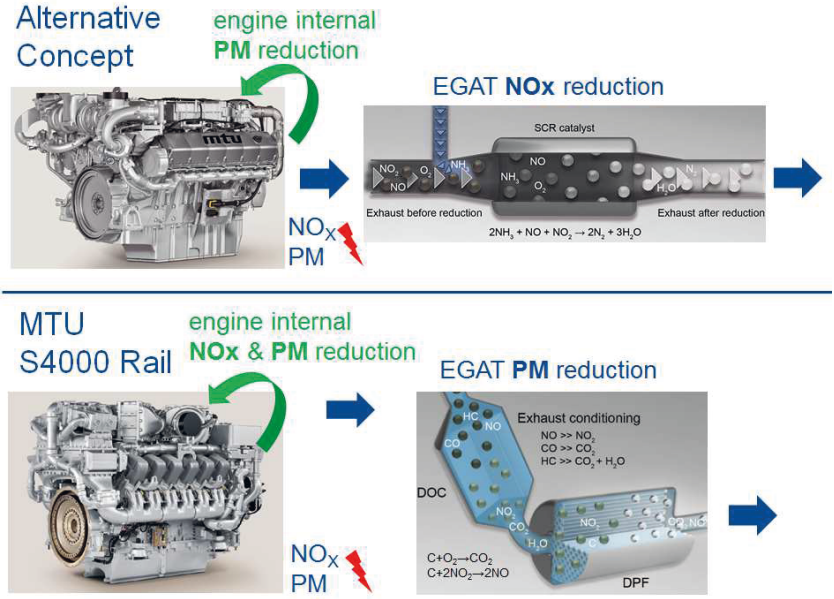

Figure 5: Technical concepts for exhaust gas emissions reduction

The alternative concept, which is used by MTU, is to reduce NOx and PM engine internally by optimizing the combustion process in combination with cooled exhaust gas recirculation (EGR), Figure 5. In addition we added a diesel particulate filtration system (DPF), especially for social responsibility and green image reasons. With this complete engine concept NOx reductions up to 50% are possible. The big advantage of this technology, compared to the SCR-concept, is that NOx reduction in low load and low temperature range is easily possible. The DPF reduces PM by more than 96%.

The customer specification was to halve the specific emissions in the ISO F-cycle. In relation to these specifications the SCR concept seemed to be in a much better starting position. By having a deep dive into actual customer needs behind the specification sheet and analyzing the strength of our technology, we figured out, how we could match the customer needs even better than by using SCR-technology.

The customer load profile for the tunnel operation is with a maximum power of approximately 700 kW almost exclusive in low load operation. As already mentioned, in this operating mode with low exhaust gas temperatures, it is not possible to reduce NOx emissions with an SCR-catalyst. With our technology we are able to reduce the real NOx mass flow that the shunter locomotive emits in the tunnel.

To realize this emission concept the following technologies shown in Figure 6 are necessary.

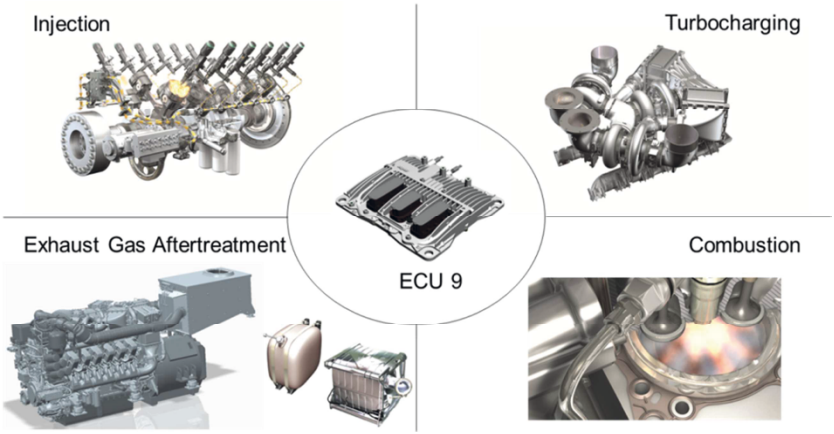

Figure 6: MTU Technology kit

Fuel injection and combustion

In order to achieve the necessary fuel spray quality and to contribute to a very intense air-fuel-mixing, which is crucial in case of high EGR combustion systems, the engines are equipped with a common rail injection system with maximum injection-pressure of 2.200 bar. The pressure is supplied by a high pressure fuel pump. The injector nozzle is equipped with 8 injection holes. Together with other relevant parameters of the combustion system like the shape of the piston bowl and the swirl inside the cylinder, this nozzle provides an excellent mixture formation with a maximum utilization of air and also results in a considerable reduction of particles. The increased NOx emissions are compensated by EGR.

Controlled two stage turbocharging

The turbocharger system consists of two low pressure turbochargers and one high pressure turbocharger. The exhaust gas first flows through the high pressure turbine followed by the low pressure turbines. Fresh intake air is compressed by the low pressure stage of the charging system and cooled by the intermediate air-to-water charge air coolers before entering the high pressure compressor. This intermediate cooling is well known in case of two-stage turbocharging and is necessary to minimize the energy needed to compress the air and to prevent the materials of the air system from overheating. The compressed air of both charging systems is cooled by the main air-to-water charge air cooler. Before entering the charge air manifold of each cylinder bank, the compressed air is feeded with cooled recirculated exhaust gas needed to fulfill the NOx emission limits. Intermediate as well as main charge air coolers are integrated into the low temperature cooling circuit of the engine. The low temperature cooling circuit is separated from the high temperature engine cooling circuit consisting of a separate coolant pump and temperature regulation with own thermostats.

Charge air pressure and thus the air mass flow supplied to the engine is regulated by an electronically controlled turbine bypass valve, integrated in a bypass line to the high pressure turbine, which is varying the exhaust flow to the high pressure turbocharger (Figure 7, flap (3)). Depending on the required charge air pressure, a part of the exhaust gas is bypassed around the high pressure turbine directly to the low pressure turbochargers. This feature is very effective and necessary in order to adjust the correct air-fuel ratio needed for combustion, to prevent the engine from damage due to excessive charge air pressures at full load, and to supply enough air to the cylinder during acceleration periods as well as operation in high altitude.

NOx controlling system

The fulfilment of NOx and PM emissions is guaranteed by a NOx-sensor and a lambda sensor, that are located after the turbochargers. The position after the turbochargers is necessary because these sensors do not withstand higher static pressures. The engine control unit (ECU) adjusts charge air pressure and lambda according to the demand values belonging to the respective operating points of the engine map. If the NOx-emission is too high, flap (1) is slightly opened and flap (2) is slightly closed. So lambda gets reduced by increasing the mass flow of recirculated exhaust gas and the NOx emission decreases. If the limit of lambda is reached, manifold pressure is adjusted.

In contrast to the charge air coolers, the EGR-cooler is integrated into the high temperature cooling circuit of the engine.

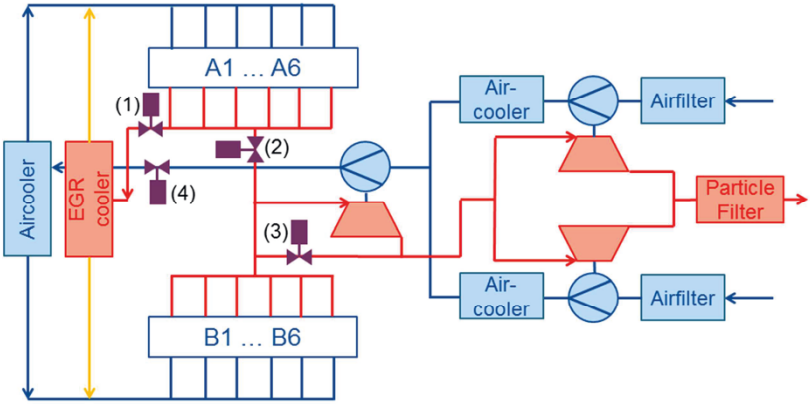

Figure 7: Schematic overview of air and exhaust gas system

3. Realization at MTU

Our engine for diesel electrical locomotives with rated power of 1800 kW is operated along a defined power curve as exemplarily shown in Figure 8. This engine is certified according to EU Stage III-B.

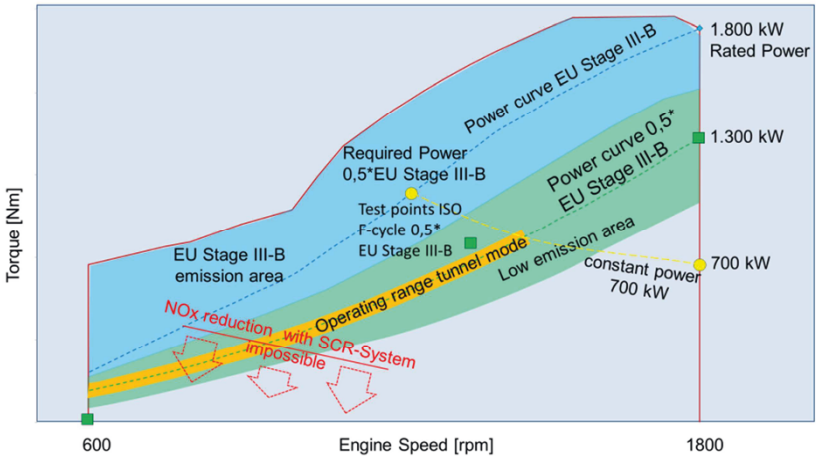

Figure 8: Engine operating map

As already mentioned the customer load profile for the tunnel operation is with a maximum power of approximately 700kW almost exclusive in low load operation.

To meet the required emissions we had to rise the EGR-rate, to adjust begin of injection, fuel pressure, manifold pressure and air to fuel ratio etc.

Another requirement was not to exceed the heat rejection of the standard EU Stage III-B engine. This is a special challenge, because increased EGR-rates result in an increase of coolant heat rejection. However, the existing cooling system of the locomotive was the limiting factor. So we had to find a compromise between maximum realizable power and allowed heat rejection. The analysis finally resulted in the fact, that we were able to create even more advantages for the customer than asked at the beginning: in the tunnel mode the presentable power is 1300 kW instead of the required 700 kW. The required 700 kW equates approximately 1400 rpm on the power curve 0,5*EU Stage III-B. With obtaining the required power at lower engine speed, we could operate the engine in areas with better fuel economy.

The next step was to implement a second power curve in the already existing engine map. With this it is possible to switch from the standard power curve with EU Stage III-B emissions to the tunnel mode power curve with EU Stage III-B halved emissions. This switchover is not done by the engine itself. It is done by the controller of the locomotive. So the customer has not just a limited number of locomotives that he can use for tunnel operation. The customer can use every locomotive for normal transportation and for construction works in tunnels. For normal operation he can use the standard power curve without any disadvantages in power supply and fuel consumption. For tunnel works he can choose the tunnel mode power curve with EU Stage III-B halved emissions.

The process from the customer demand to a validated product started with a concept based on proven and existing analytical models, Figure 9. The final development was performed on an engine on our test stand.

Therefore we did a two-step testing process on the test stand. In step one engine specific topics have been tested and calibrated. In step two the focus was on the Diesel Particulate Filter, transient engine behavior and the emission certification process.

Reducing the emissions means a change in engine calibration on wide areas of the engine operating map. This has to be done considering not to affect the standard operation of the engine, because the concept gives the operator the opportunity to switch between standard and tunnel mode. Furthermore, we had to take care that the load on the engine hardware is within the limits. As an example, the exhaust gas flaps of the engine work in a different way with the new tunnel mode calibration. This means that we checked for all situations and also for an aged system that the flaps should not reach their mechanical stops.

After qualifying the engine itself the calibration of the transient parameters was optimized. This meant that we had to find the optimum acceleration whilst fulfilling all emission limits. As particulate emissions are strongly reduced by the DPF system, black smoke during acceleration had to be quantified and limited, because it affects the resulting load in the filter whilst the real life operation and therefore the resulting maximum time in tunnel mode.

Before testing the new calibration in-field it had to be covered by emission certification according to EU Stage III-B. The official emission cycle was affected only in parts but the customer also asked us to qualify the tunnel operation area like it would be the official certification.

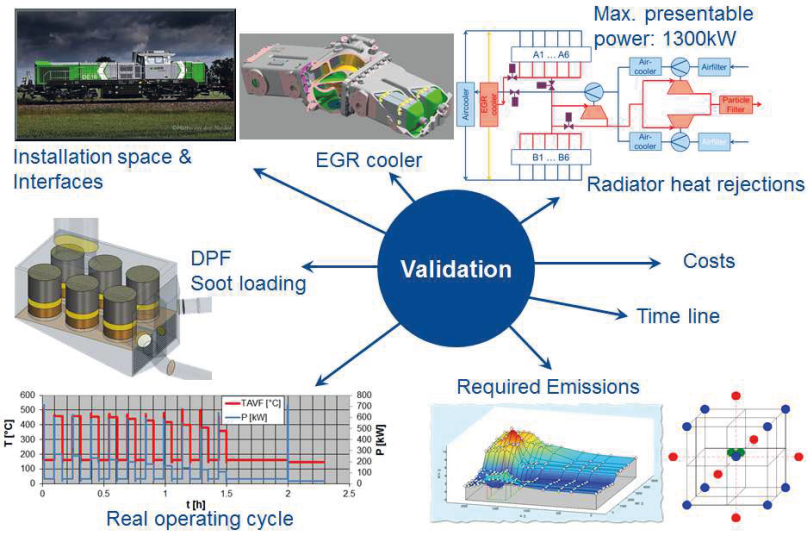

Figure 9: Development and validation process

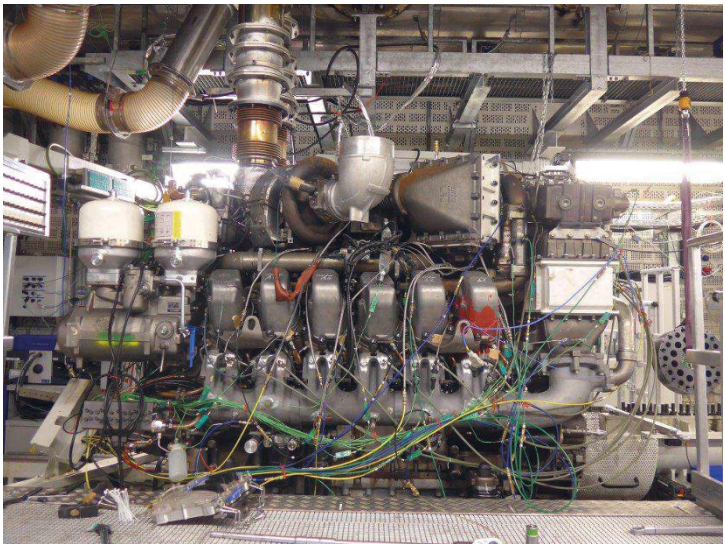

Figure 10: Engine calibration on a MTU test bench

Last but not least we had to ensure that no DPF regeneration is needed during the real operation in the tunnel. For that purpose an exhaust aftertreatment model consisting of a DOC and a DPF model was used, Figure 11. The DOC (Diesel Oxidation Catalyst) model takes into account the thermal inertia together with CO, CxHy and NO oxidations depending mainly on temperature and space velocity. As an intermediate product of the NO oxidation, NO2 is built. The reaction kinetic parameters are fitted using synthetic test bench measuring data and validated on the real engine test bench experiments. A correlation was used to predict the DOC activity at thermally and chemically aged stage. The DPF model takes into account the soot balance and DPF thermal inertia, which plays an important role at transient operating profiles. The soot coming from the engine is collected in the inlet channels but simultaneously burned using NO2 and O2 as oxidants. The soot burning reaction rate parameters are determined experimentally taking into account the soot income, NO2 consumption, CO production and soot weighing results at different regeneration temperatures. This exhaust aftertreatment model was fed with the exhaust gas flow rate, its temperature along with soot and gaseous raw emissions, based on a real operating profile during the tunnel mode. In that way, the time before the DPF soot limit is reached, could be simulated. Thanks to low soot concentration of the raw exhaust gas and the thermal inertia of the exhaust system, enough NO2 is produced during the tunnel mode, so that the soot limit causing a DPF regeneration is never reached during one working shift.

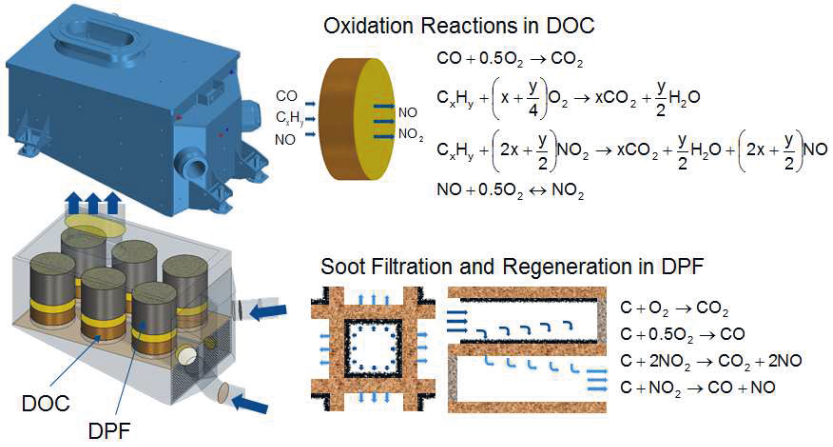

Figure 11: Exhaust gas aftertreatment system consisting of diesel oxidation catalyst and diesel particulate filter

4. Results and Summary

For this project the NOx and PM reduction by 50% according to EU Stage III-B without a complete redesign of the engine and the subsystems of the locomotive was the biggest challenge. Additionally, the target was not only to fulfil the requirements of the customer to halve the emissions in the ISO F-cycle. Furthermore, it has been necessary to reduce the most important health risks for construction workers in tunnels, who work next to shunter locomotives, in real operating profiles.

The new MTU 12V4000R84 engine with two stage turbocharging an cooled exhaust gas recirculation for rail applications with new low-NOx calibration and closed coupled DPF fulfils these requirements best and realizes furthermore additional advantages for our customer:

Low emissions even under low load operation. Compared to the SCR-concept, NOx-reduction in low load and low temperature range is easily possible.

Full fleet flexibility: All locomotives can be used as multipurpose locomotives with high power of 1800 kW under normal operating conditions and as special tunnel construction sides locomotives with low emissions.

No DEF (urea) logistics and infrastructure necessary

Since autumn 2017 first certification and commissioning measurements have been started.

The new MAN 175D high-speed engine – synthesis of commercial and medium-speed engine development

Christian Braun, Dr. Alexander Rieß, Peter Böhm, Hauke Lund, Dr. Klaus Eder

W. Siebenpfeiffer (Hrsg.), *Heavy-Duty-, On- und Off-Highway-Motoren 2017*, Proceedings, https://doi.org/10.1007/978-3-658-21029-8_9

Abstract

Packing the latest state-of-the-art technology into a minimum volume, the MAN 175D is characterized by clear-cut design: easy to commission, easy to operate, and easy to service. With 12, 16, and 20 cylinders and a power of up to 238 kW per cylinder, this high-performance marine engine is compact and modular with all auxiliaries attached.

Inheriting its genes from both our successful commercial and medium speed engine tradition, the MAN 175D is robust and reliable by nature. Through innovation, it is designed to be a very efficient engine family. It is firstly used for yacht, fast patrol vessel and commercial marine applications.

This work concerns the cutting edge development of this engine. It is focused on the synthesis of design, simulation and validation concepts from commercial and medium speed engines. Applications of this synthesis are discussed for major cranktrain parts including crankshaft and connecting rod.

Finally, the latest experiences from testbed and field are presented.

1 Introduction

For the new high speed engine MAN 175D our engineers used their very long and excellent experience and knowledge in the development of commercial and medium speed engines. Figure 1 shows the new MAN 175D in a 12V application, [1].

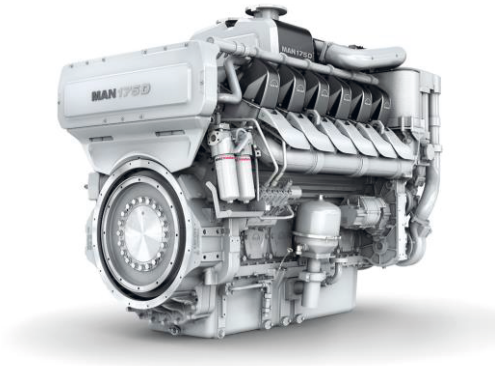

Figure 1: Engine MAN 175D with 12V cylinders.

One of its very early predecessors is the WV 17.5/22 which has been engineered in the early 1940s. This engine has been continuously developed until the 1970s. A comparison of main engine parameters and design features in Table 1 shows at a glance the development history and increasing demands for high speed engines.

MAIN ENGINE PARAMETERS AND DESIGN FEATURES		MAN 175D 	WV 17.5/22A 1940-1970 
Bore/Stroke	**mm**	175/215	175/220
Displacement	**l/cyl.**	5,2	5,3
Rated Speed	**rpm**	1200-2000	750-1200
Mean Piston Speed	**m/s**	max.14,3	max. 8,8
Rating	**kW/cyl.**	135-238	16-50
Mean eff. pressure	**bar**	27,6	max. 10,75
Cylinder versions		V-engine: 12, 16, 20	Inline: 3 to 8
Direction of rotation		ccw	cw & ccw
Combustion		Direct injection	Prechamber
Charging		With	Without or with
Piston		Steel (forged)	Al (casted)
Piston crown cooling		Cooled via oil-jet	No active cooling
Injection		Common rail	Single injection pumps
Gear drive		Coupling and counter coupling side	Coupling side
Crankshaft		Hardened pins and fillets	Hardened running surface

Table 1: Comparison of the MAN 175D with one of its very early predecessors with a same bore of 175 mm.

The wide range of applications combined with a fast ramp-up of engine population in the field requires a well-adjusted and proper development approach.

2 Development of the high speed engine MAN 175D

2.1 General engine development process

Medium speed (MAN Augsburg) and commercial engine (MAN Nuremberg) development is organized by product evolution process (PEP). Figure 2 shows this process for Augsburg. Depending on the engine class different work packages are required in each step of the PEP.

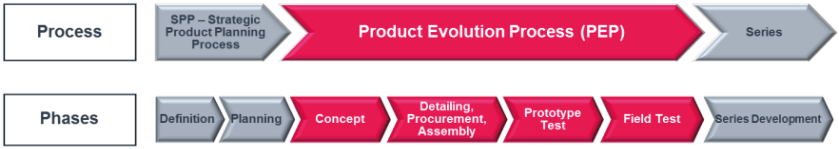

Figure 2: Production evolution process (PEP) for medium speed engine development.

2.2 Synthesis of the development process

As already stated, each engine class has its own design concepts and development methods. They are influenced by engine size, number of engines and their application.

The definition of the working packages for high speed engines are based on a synthesis of commercial and medium speed engine development. Table 2 presents an excerpt of the outcome of this analysis with a focus on the mechanical assessment for crankshaft and connecting rod. For an optimal market entry a prioritization of function, quality and production costs as main targets is basic requirement.

KEY ASPECTS (Selection)	COMMERCIAL ENGINE 	MEDIUM SPEED ENGINE 	HIGH SPEED ENGINE 
Market entry	Very strict installation spaces High reliability Small scope of service	Installation space Highest reliability Service orientated	Keep installation spaces (replace) Highest reliability Only minor serviceability
Range of Application	Wide speed range/High dynamics Application of engine unknown High population	Defined range of application Application and position known Small population	Focus on speed range/dynamics Application unknown High population
Components technologies	Established and highly automated production technologies	Limited scope of technologies due to component size Limited numbers of suppliers	Transfer automotive/ commercial engine technologies/components Follow second supplier strategy
Grade of Serialization	High batch numbers High process capability Focused in serial production	Low batch numbers Make to order production Single assembly	Common parts - avoid variants Establish serial process from start for component and assembly
Costs – R&D	Front-loading Components testing Several test engines	Strong front-loading Component measurement Very few test engines	Simulate only with experience Combine test approaches Some test engines

Table 2: Comparison of key aspects of commercial, medium speed, and high speed engines.

2.3 High speed development process

The previous section showed that the cooperative development consists of four phases according PEP: concept, detailing, and validation by prototype and field test.

In the beginning of the concept phase both Augsburg and Nuremberg separately designed a basic engine layout. Afterwards, both designs have been merged to one common engine concept. Here, the implementation of focused and experienced project teams has been very helpful. Furthermore, an open minded attitude of the development team and the willingness to learn from each other has been enablers for the successful and cutting-edge engine development.

Table 3 provides an overview about selected design features. Here, the different views of commercial and medium speed engine are clearly apparent.

SELECTED DESIGN FEATURE	COMMERCIAL ENGINE	MEDIUM SPEED ENGINE
Screw connection	Head screws	Tie-rods
Hardened crankshaft	Standard	Not applied
Cylinder cooling water	Within crankcase – wet liner	Separate cooling component (water jacket)
Cylinder liner	Hanging liner	Mid-stop liner
Piston cooling	Via nozzles	Via conrod
Fully machined conrod	No	Yes
Conrod split line	Cracked	Machined
Cylinder head	One cylinder block single cylinder heads	Single cylinder heads
Crankcase windows	No	Yes
Gear drive	Only CS	CS and CCS
Support bearing	Not common	Yes
Crankshaft flanges	No	Yes
Power take out @ CCS	Yes for Marine	Yes – up to 100%

Table 3: Design features of commercial and medium speed engines.

After concept approval the detail phase begins. The lead in this phase was under the responsibility of medium speed engine development. Major reasons were:

- clear responsibility,
- availability of test facilities,

- product portfolio fits better to medium speed,
- experience with cylinder numbers higher than 12,
- a well-established simulation driven development approach by use of virtual cranktrain modelling for optimization has a long tradition in Augsburg, [2], [3],
- the knowledge from the compact, high speed diesel engine MAN VP185, [4].

The detail phase was accompanied by commercial engine development with focus on common components, support in serial production issues, technology transfer and validation aspects.

The third phase is the validation process. This includes testing of the engine and its parts. For the application of this process, a validation plan was set-up already in concept phase. It was derived from established commercial and medium speed validation philosophies and approaches. This standard plan was extended by further aspects. This includes field experience, design rules, FMEA and simulation results, experience and feedback from suppliers, components technologies, audit results, requests from production and so forth. Finally, the validation plan consists of several maturity levels starting from components' testing, to test-bed runs over field test application to a serial release. A technical risk number (TRN) helped to identify critical engine components. It was used for prioritization of development work and testing. During validation on test-beds and in field-tests the maturity level increases. As a consequence, the TRN drops. Finally, the engine is ready for series.

The next chapter illustrates the different steps in the PEP for selected components.

3 Examples

3.1 Crankshaft

The crankshaft converts the reciprocating movement of the piston into a rotary motion. The resulting dynamic loads from the crank drive that act on the crankpin induce torsional, axial and bending loads in the crankshaft. There is a long history at MDT in the use of advanced simulation methods for crankshafts and its use for assessment and optimization within an efficient simulation workflow, [5], [6]. Due to the wide operating speed range of high speed engines, compared to medium speed engines, possible resonances have to be analysed carefully.

The working packages for simulation were mainly derived from the medium speed engine development. During concept phase the base layout is designed using time-efficient calculation methods like 1-D Torsional Vibration Calculation and analytical

in-house tools, [7]. The fatigue assessment is carried out in accordance with UR M53, [8]. During the concept phase so-called K-Factors (fatigue strength increase compared to nominal material) for induction hardening were taken from literature and manufacturers' experience. This design is validated taking FEM based stress concentration factors for bending and torsion into account as shown in Figure 3.

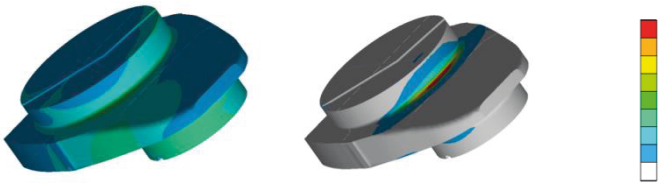

Figure 3: Stress concentration factors (SCF) of a single crank for torsion (left) and bending (right).

In order to identify critical engine speeds, a modal analysis of the cranktrain was carried out and analysed by the use of Campbell diagrams.

On conclusion of the concept phase, more detailed and advanced methods like multibody simulation are required. This method is well established for the design of crankshaft. Here, the crankshaft is modelled as a flexible body and connected to the main bearings in the crankcase by non-linear hydrodynamic bearings as shown in Figure 4.

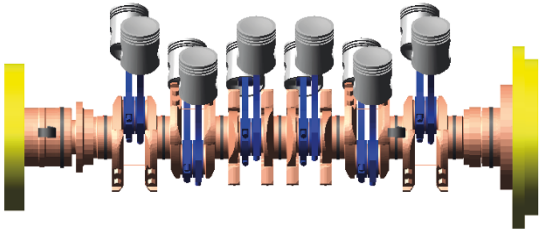

Figure 4: Multibody system of the 12V175D with flywheel (right: coupling side) and torsional vibration damper (left: counter coupling side).

Among other data the radial displacement of flywheel and damper and the bearing performance are analysed. The resulting stresses are used for a fatigue assessment as presented in Figure 5. Here, the highest loaded zones fillets and crankpin's oil bores are clearly apparent.

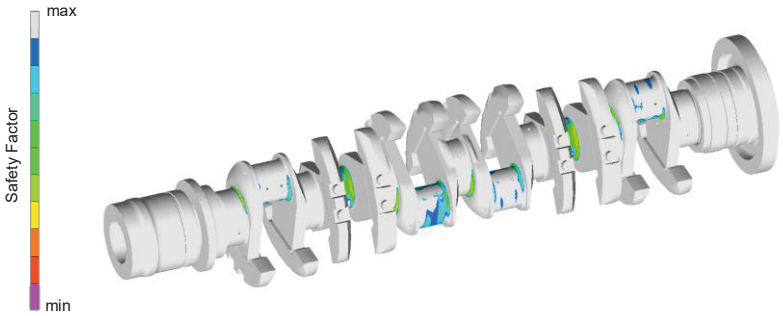

Figure 5: Safety factor of 12V175D crankshaft seen from counter coupling to coupling side.

Afterwards, it is mandatory to correlate simulated results with the real world behaviour of an engine. For this purpose strain measurements of the highest loaded locations of the crankshaft, based on simulation results, is a well-known approach for medium speed engines at MDT. The application of the strain gauges and acceleration sensors on the crankshaft is shown in Figure 6.

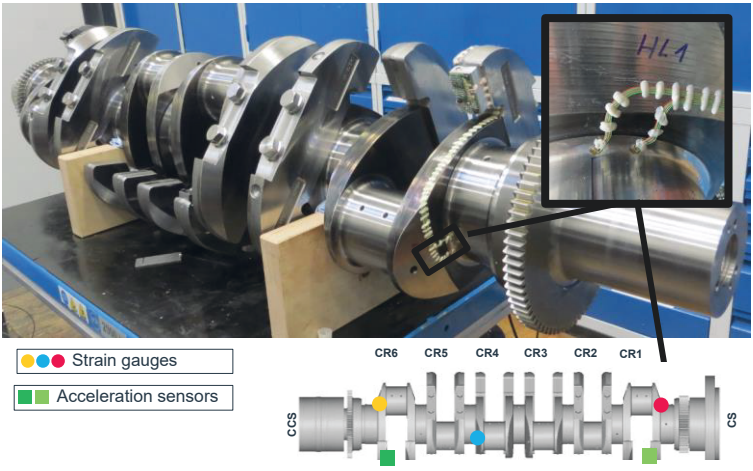

Figure 6: Strain gauge on crankshaft seen from coupling (CS) to counter coupling side (CCS).

Figure 7 compares simulated and measured stresses for a crankshaft fillet in the middle of the crankshaft at crank 4. The firing of the adjacent cylinders around 630° crankangle is clearly apparent within this data. The excellent correlation between simulation and measurement proves the reliability of the used simulation methods.

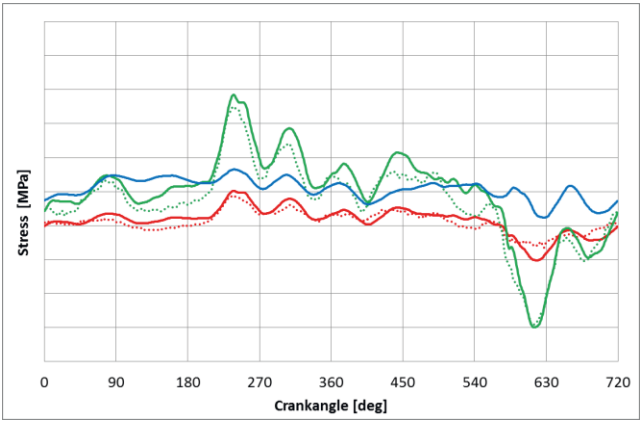

Figure 7: Correlation of computed (solid) and measured (dotted) 2d stresses (green: $\boldsymbol{\sigma_{xx}}$, red: $\boldsymbol{\sigma_{yy}}$, blue: $\boldsymbol{\tau_{xy}}$) for a crankshaft fillet of crank 5 for nominal speed.

As a further example, as depicted in Figure 8, temperature measurement of the viscous vibration damper was carried out. This data is used to correlate the friction loss of the damper between simulation and measurement.

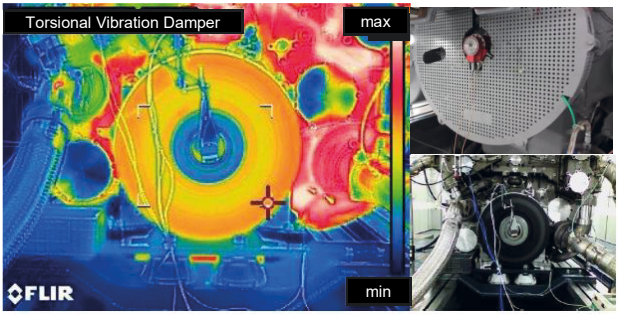

Figure 8: Temperature measurement at the viscous vibration damper.

For crank drive components of commercial engines it is quite common to investigate its fatigue strength by the use of full component tests. For medium speed engines such component tests are rarely used due to cost aspect and the availability of test machines of required size. It has been decided that real crankshaft's fatigue strength should be determined. For this purpose torsion and bending tests rigs have been set-up and test series have been conducted for single cranks. The corresponding test rigs are shown in Figure 9.

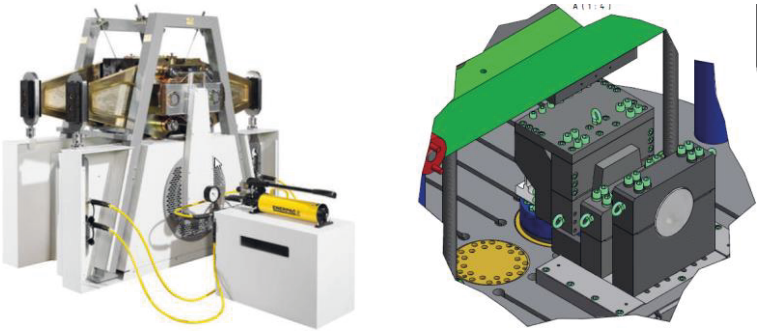

Figure 9: Test rig for torsion (left) and bending (right).

The investigations were carried out in accordance with the test procedure of the CIMAC IACS UR M 53, Appendix 4, [9]. This method allows component fatigue tests with a relatively low number of specimens. Furthermore, it allows the use of the specimen for several times. This saved time and costs. The component fatigue test results are subsequently used to determine the real safety factors. Afterwards, a correlation of the real determined K-factors with the pre-assumed K-factors from concept phase has been conducted. This analysis clearly showed that such component tests are mandatory for hardened crankshafts to ensure a safe and reliable operation.

3.2 Connecting rod

The simulation working packages for simulation were derived from the well-established medium speed engine development of connecting rods as presented in [10]. This includes a concept calculation of the connecting rod with the mass and gas forces. Afterwards, during detail phase an advanced bearing assessment has been carried out as presented in Figure 10.

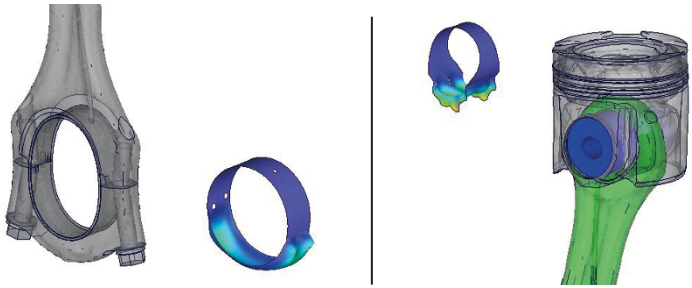

Figure 10: Elastohydrodynamic analysis of the connecting rod for big eye (left) and small eye (right).

The resulting pressure build-up and acceleration are subsequently used for contact and fatigue analysis of the connecting rod. The outcome of the fatigue assessment is shown in Figure 11. Based on this assessment the measurement positions have been selected. These positions were located in the highest loaded areas of the component. Furthermore, the fatigue assessment of the bolt connection indicated that the bolt lay-out should be changed from 2 to 4 bolts.

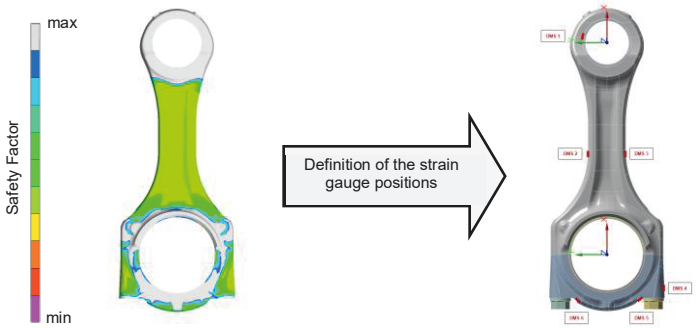

Figure 11: Fatigue assessment and definition of strain gauge positions.

Taking the methods from commercial engine into account this design has been validated by component tests. For the fatigue tests of the connecting rod the test rig was modified with a lube oil supply to test the connecting rod with its bearing shells as depicted in Figure 12. The established boundary conditions ensure a comparable load-

ing as in engine operation. The defined load steps represent the nominal load as well as overload points.

For the updated design a new tightening procedure for the bolts was defined and validated by strain measurements at all four bolts. These measurements were carried out not only to verify the tightening forces at the bolts, but also to ensure an uniform pressure for the bearing shells as well as the roundness of the connecting rod bearing after tightening. With the focus on the connecting rod bolts the measurement program was carried out as a dynamic tensile test to simulate the influence of the mass forces on the connecting rod.

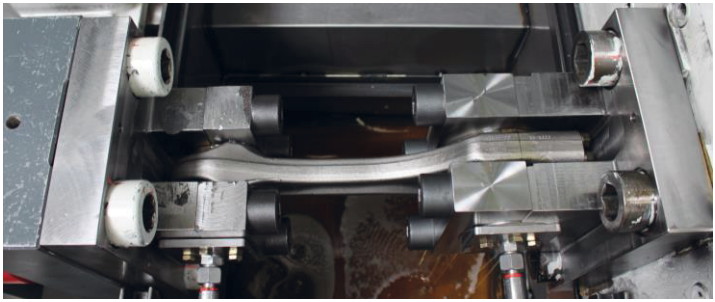

Figure 12: Component fatigue tests of the connecting rod.

For component and simulation validation of the connecting rod strain measurements during engine operation have been carried out. The strain measurements were carried out using a data logger as presented in Figure 13.

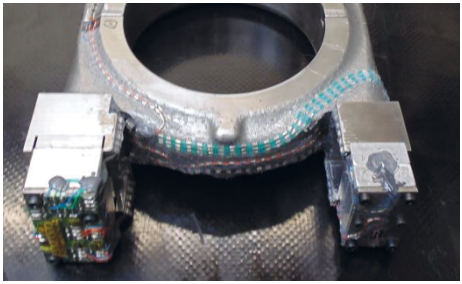

Figure 13: Application of the data logger for the strain measurement during engine operation.

Figure 14 shows the very good correlation of computed and measured stresses for selected positions.

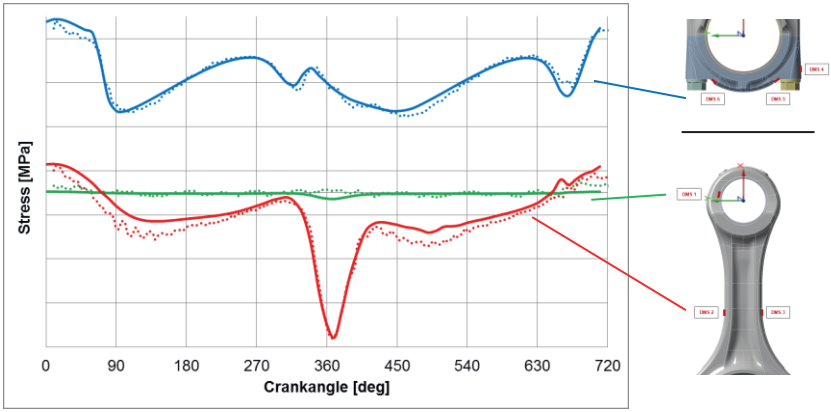

Figure 14: Comparison of the computed (solid) and measured stresses (dotted) for the positions DMS 1 at small eye (green), DMS 2 at shaft (red) and DMS 6 at connecting rod cap (blue) of Figure 11.

4 Conclusion and Outlook

This contribution presented the successful development of the high speed engine MAN 175D. Beside well-established product evolution processes the key for a reliable and fit for market engine was the cooperation of commercial and medium speed engine development departments. This includes a synthesis of design concepts and development methods from both worlds and is illustrated for two major components – crankshaft and connecting rod.

All engine components successfully passed the full set of relevant maturity levels. Over 20'000 running hours on test bed and in field prove the excellent robustness and highest reliability of the engine. The successful type approval in May 2017 and first customer deliveries clearly confirm the reliable design of the MAN 175D high speed engine. The next steps are the release of 16V and 20V cylinder configurations.

5 Bibliography

[1] M. Eder, “MAN175D The new High Speed engine familiy from MAN Diesel & Turbo,” in *ATZ - Heavy Duty Conference*, 2015.

[2] A. Rieß, P. Steffe, H. Große-Löscher, R. Krivachy, D. Pinkernell and A. Linke, “Reibungsreduzierung im Triebwerk mittelschnell laufender Großdieselmotoren durch Einsatz von Optimierungsmethoden in der Grundmotorauslegung,” *VPC - Virtual Powertrain Creation, 13. MTZ-Fachtagung,* 2011.

[3] P. Böhm, R. Krivachy, P. Steffe and D. Pinkernell, “Virtual cranktrain modelling of medium-speed large-bore engines – a key to optimizing mechanical efficiency and fatigue strength,” *Virtual Powertrain Creation 2010, 12. Internationale MTZ-Fachtagung,* 2010.

[4] MAN Diesel & Turbo SE, “MAN VP185,” [Online]. Available: http://marine.man.eu/docs/default-source/shopwaredocumentsarchive/man-vp185.pdf. [Accessed 10 2017].

[5] A. Rieß, Model Order Reduction Based Simulation and Optimization of Large Bore Internal Combustion Engines, Shaker, 2015.

[6] R. Krivachy, A. Linke and D. Pinkernell, “Numerical fatigue strength assessment for crankshafts,” *MTZ worldwide,* pp. 4-10, Volume 71, June 2010.

[7] M. Taubert and P. Böhm, “Transient and Steady State Torsional Vibration Analysis of Large Bore Diesel Engines,” *MTZ Industrial,* pp. 48-55, Ausgabe 2/2017, September 2017.

[8] CIMAC IACS Req. 1986, M53, Calculations for I.C. Engine Crankshafts, Rev.3 2017.

[9] CIMAC IACS Req. 1986, M53, Calculations for I.C. Engine Crankshafts, Appendix IV: Guidance for Evaluation of Fatigue Tests, Rev.3 2017.

[10] E. Eisenbeil, E. Pfab, A. Linke and D. Pinkernell, “Berechnungsverfahren zur Beurteilung von Pleuel für Großdieselmotoren bezüglich Festigkeit, Lauf- und Kontaktverhalten,” *CADFEM USERS MEETING 2011,* October 2011.

Non-visible smoke technology for extremely high-speed 4MW class 20FX diesel engine during ship transient operation

Katsuyuki Toda

Dr. Satoru Goto

Shigeki Ogura

Daichi Kawai

from Niigata Power Systems Co., Ltd.

W. Siebenpfeiffer (Hrsg.), *Heavy-Duty-, On- und Off-Highway-Motoren 2017*,
Proceedings, https://doi.org/10.1007/978-3-658-21029-8_10

1 Overview of Niigata

Since developing an original diesel engine for marine propulsion in 1919, Niigata Power Systems has developed and manufactured many diesel engines, gas engines, gas turbines, and Z-PELLER propulsion system. These products have contributed to society as the key hardware of power generation and cogeneration, and engines for marine propulsion. In recent years, a high efficiency hybrid propulsion system for tugboats and a low-pollution, high efficiency dual-fuel engine for marine propulsion have been developed to protect the sea environment, which are being launched into the market.

Fig.1-Hybrid Propulsion Tugboat

Fig.2-Tugboat Applied Dual Fuel Engine

In the context that the way of freight transport has been shifted from land transport to seaway in order to prevent air pollution and the speed up of ship is advanced in the world. Niigata has developed and delivered high-speed diesel engines adapted to high-speed passenger boats, Ferries, patrol boats, etc. independently with accumulated technology and experience since 1980's**.** Since 2000, Niigata has developed the 4,000 kW class 16V20FX as high output power high-speed diesel engines, and after repeated manufacturing and sales, more than 150 units have been delivered. Niigata is contributing to society as the only domestic manufacturer of original large high-speed diesel engines at now.

Table 1-Principal Particulars of 16V20FX

Number of cylinder	16
Cylinder Bore	205 mm
Stroke	220 mm
Rated Power	4000 kW
Engine Speed	1650 min^{-1}
B.M.E.P.	2.5 MPa
Peak Firing Pressure	18 MPa

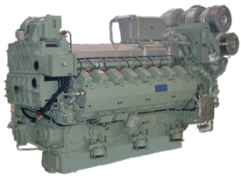

Fig.3-Overview of 16V20FX

2 Exhaust gas regulations for marine in Asia

The current exhaust gas regulations for marine in Japan and neighboring Asian countries are shown in Table 2 and Table 3. Regulations in Asian countries conform to IMO regulations, and there are currently no areas designated as ECA or SECA. Only China is discussing of its own regulations and enforcement into inland water vessels.

Table 2-IMO Regulation

IMO – Seagoing Ships / in the Annexes of MARPOL				
NOx	Tire Ⅱ, beginning from 2011		Tire Ⅲ, beginning from 2016 in ECA*	
	Engine Speed :n[min^{-1}]	NOx [g/kWh]	Engine Speed :n [min^{-1}]	NOx [g/kWh]
	n < 130	14.4	n < 130	3.4
	130 ≤ n < 2000	44.0・$n^{(-0.23)}$	130 ≤ n < 2000	9.0・$n^{(-0.20)}$
	≥ 2000	7.7	≥ 2000	2.0
	*There is no ECA in Asian region at the present time.			
SOx Sulphur Content in the Fuel	Global		in SOx Emission Control Area**	
	3.50 % , beginning from 2012		1.00 % , beginning from 7.2010	
	0.50 % , beginning from 2020		0.10 % , beginning from 2015	
	**There is no SECA in Asian region at the present time.			

Table 3-Exhaust Gas Regulation in China

China - Seagoing Ships						
SOx Sulphur Content in the Fuel	Ports			Territorial Waters		
	Voluntary application of a limiting value of 0.5 % in ships at berth , beginning from 2016			-		
	The formerly voluntary application becomes mandatory , beginning from 2017			-		
	-			Seagoing ships may use no fuel with a sulphur content of 0.5% or more , beginning from 2019		
	In 2019 a decision is expected, if Chinese authorities lower the limiting value for sulphur in fuel to 0.1%.					
China – Inland waterway vessels Tier Ⅰ , beginning from 7.2019						
Category	Cyl. disp. [L]	Output Power [kW]	CO [g/kWh]	HC + NOx [g/kWh]	CH_4 for GE [g/kWh]	Particle [g/kWh]
Category 1	$V_{h,z} < 0.9$	$P_n \geq 37$	5.0	7.5	1.5	0.40
	$0.9 \leq V_{h,z} < 1.2$			7.2	1.5	0.30
	$1.2 \leq V_{h,z} < 5$			7.2	1.5	0.20
Category 2	$5 \leq V_{h,z} < 15$			7.8	1.5	0.27
	$15 \leq V_{h,z} < 20$	$P_n < 3300$	5.0	8.7	1.6	0.50
		$P_n \geq 3300$	5.0	9.8	1.8	0.50
	$20 \leq V_{h,z} < 25$			9.8	1.8	0.50
	$25 \leq V_{h,z} < 30$			11.0	2.0	0.50

There are no regulations in Japan concerning black carbon and particulate matter in marine engines now, but the enforcement of their emission reduction is expected because they are worried about effect to the body such as respiratory and circulatory organs. Therefore, from the perspective of keeping ship crews working on deck healthy, and also from the perspective of preventing sea environmental pollution, authors consider that eliminating of black smoke emissions is an important future issue. Moreover, eliminating of black smoke leads to a reduction in fuel consumption, bringing economic benefits and contributing to the reduction of CO_2, one of the greenhouse gas.

Authors decided to focus on the eliminating of black smoke emission during quick ship operation in the high-speed diesel engine 16V20FX. This engine has a sequential turbocharging system to secure adequate air quantity in the entire low load to high load range, but black smoke tends to be emitted at the switching point of its working turbocharger's number. The eliminating of this black smoke to non-visible level was held up as technical goal. This paper reports on the practical technology being adapted to reduction of black smoke emitting, as well as successful examples.

3 Mechanisms design and issues of 16V20FX engine

3.1 Turbocharging system and its operating mechanism

The configuration of the turbocharging system, and its control diagram are shown in Fig.4 and Fig.5.

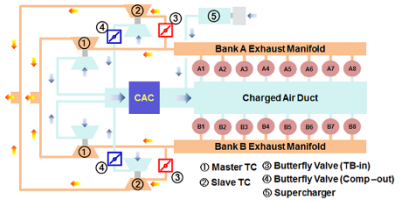

Fig.4-Turbocharging System

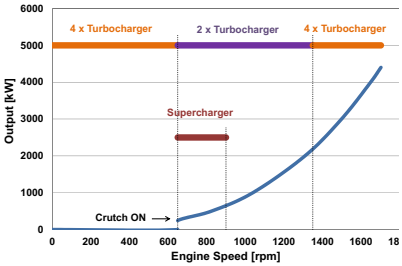

Fig.5-Control Diagram
for Sequential turbocharging System

This engine is equipped with four turbochargers per unit. A sequential turbocharging system is applied in which two turbochargers work from the low load to the medium load range, and four turbochargers work from the medium load to the high load range.

An independent exhaust manifold and two turbochargers are arranged in both A bank and B bank. Two of the four turbochargers are continuously working master turbochargers and the remaining two turbochargers are slave turbochargers that work when necessary. A butterfly valve is installed at the compressor outlet and turbine inlet of the slave turbocharger, and the activation and inactivation of the slave turbocharger is controlled by these butterfly valves. In addition, this engine has one mechanical driven supercharger, and secures the supply of adequate air quantity from the idling to the extremely low load range.

Visible black smoke is emitted at the switching point of sequential turbocharging system when the working turbochargers increases from two units to four units during engine load transient conditions in this system, and its occurrence mechanism is considered to be as follows.

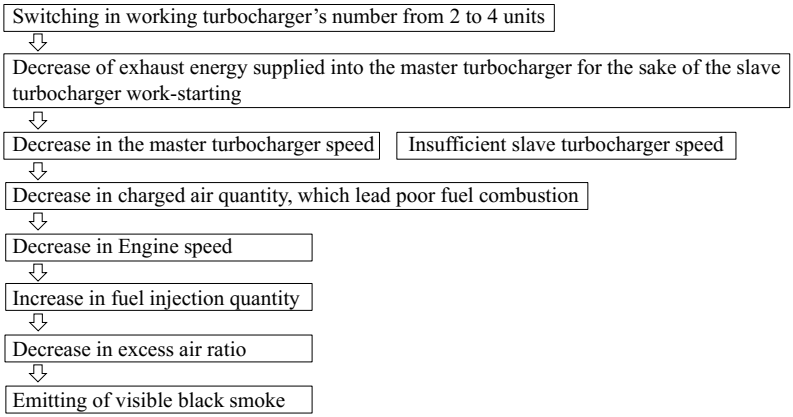

How to control the turbocharger speed drop down at the switching point is key point in solving this issue from the turbocharging system side.

3.2 Fuel injection system

The conventional fuel injection system of this engine uses a jerk fuel injection pump equipped in each cylinder and a mechanical fuel injector, and its injection pressure is approximately 145 MPa at the rated power. The nozzle hole diameter must not be reduced too much at this injection pressure level because lower injection pressure and smaller nozzle hole diameter lead to long injection duration. Furthermore, since the injection pressure depends on engine speed, the injection pressure decreases in the low and medium load range. In case of the jerk fuel injection pump, the injection pressure during injection is lower at the start of injection and the end of injection since it depends on the plunger speed driven by fuel cam, as shown in Fig.6.

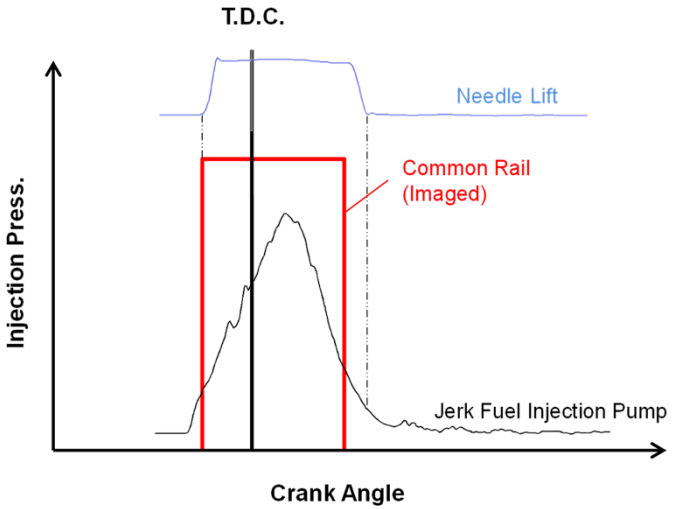

Fig.6-Injection Pressure Curve

Therefore, the atomization of fuel particle size by high pressure injection and smaller nozzle hole diameter is key point in solving this issue from the fuel injection side.

4 Required technologies for black smoke reduction

The mixture of fuel spray and adequate air is essential for eliminating black smoke. Turbocharging system and fuel injection system are focused as key devices, and the technologies and target values that it is necessary to solve this issue were considered from both aspects.

4.1 Excess air ratio

In order to eliminate black smoke emitted at the switching point of sequential turbocharging system, the control of the turbocharger speed drop down was focused. Three turbochargers working range was added as its countermeasure and it were examined. This is aimed at reducing the turbocharger speed drop down by increasing the working turbocharger's number gradually; from two to three and four units. This modified control system leads to reduction of the exhaust energy dispersion when the working turbocharger's number is increased, and reduction of the turbocharger speed drop down is expected. The structure of exhaust manifold was changed for three turbocharger

working range. The independent exhaust manifold in banks A and B were connected in order to maintain the performance balance of banks A and B. The configuration of the turbocharging system and its control diagram are shown in Fig.7 and Fig.8.

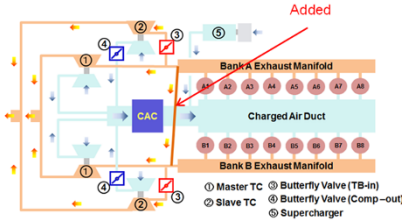

Fig.7-Modified Turbocharging System

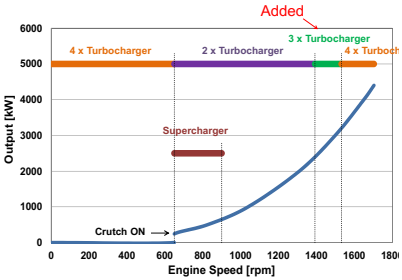

Fig.8-Modified Control Diagram for Sequential turbocharging System

The excess air ratio was selected as the performance index of improvement effect because the purpose of improving the turbocharging system is to secure the adequate air quantity. Especially during engine load transient conditions, the charged air quantity is insufficiency due to delayed turbocharger's response and a larger quantity of fuel is injected than at steady state condition to compensate speed down of engine. For these reasons, the excess air ratio is low and black smoke is emitted at transient condition. The adequate excess air ratio for bring the exhaust gas from the engine to non-visible level is not considered strictly constant due to various conditions such as fuel spray characteristics, but a target value of at least 1.75 was set for the excess air ratio of λ_{trap}, defined by trapped air in the cylinder based on our past experiences and many insights. Fig.9 shows the relationship between λ_{trap} and black smoke level according to experiences with our engines. It shows that exhaust gas can be brought to be considered as non-visible level if a λ_{trap} is 1.75 or more, and the target value of λ_{trap} in transient conditions was set to 1.75 or more.

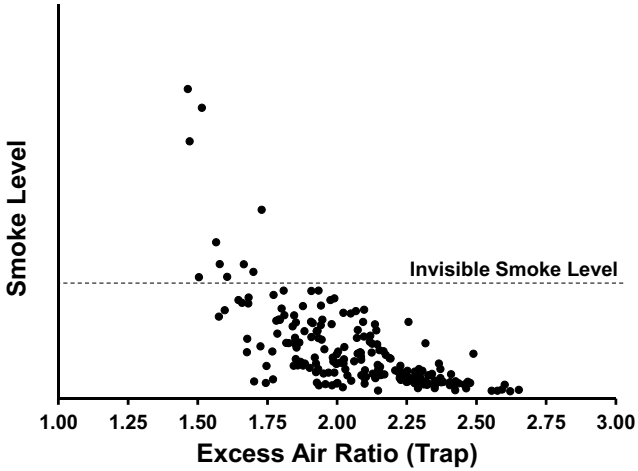

Fig.9-Relationship between excess air ratio and black smoke

4.2 Fuel spray characteristics

Said the excess air ratio is an important factor for solving this issue, on the other hand fuel spray characteristics are also important factors affecting combustion efficiency and emission characteristics. The optimal atomized diesel fuel particle size and its optimal distribution in the combustion chamber are necessary in order to facilitate mixing of fuel spray and air. Higher injection pressure and smaller nozzle hole diameter are necessary for atomization of the fuel spray, and from the perspective of the degree of freedom for injection timing and injection pressure control, a common rail system is required for the fuel injection system. Based on a system designed for 200 MPa or greater rail pressure, the engine secures adequate capacity with high pressure pumps. The high pressure pipes have no function as an accumulator by adopting a built-in accumulator for the injector, and high-pressure pipe with jumper line structure was adopted instead. The nozzle hole diameter of the injector could be reduced by approximately 10% compared with the case of jerk fuel injection pump by securing this high pressure injection. Fig.10 shows the overview of a conventional engine and Fig.11 shows the overview of an engine equipped with the newly adopted common rail system.

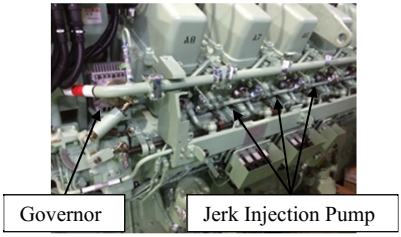

Fig.10-Conventional Engine

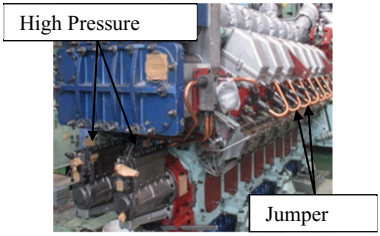

Fig.11-Test Engine with Common Rail System

Sauter Mean Diameter SMD is generally known as the performance index of spray atomization. Various empirical formulas have been proposed for finding SMD, where SMD is cited by Knight's formula and use it as the performance index.

Knight's formula (1)

$$SMD\ (X_{32}) = 207.6\ de^{0.418}(\triangle P)^{-0.351}$$

(SMD: (Sauter Mean Diameter), X_{32} : volume-surface mean diameter [μm]
de: nozzle hole diameter [mm], ΔP: injection differential pressure [MPa]) (1)

SMD for bringing exhaust gas from the engine to non-visible level is also not considered a constant due to various conditions such as charged air conditions, but SMD ≤ 30 μm was set as the target value based on our past experience. Fig.12 shows the relationship between SMD and smoke level in our engine.

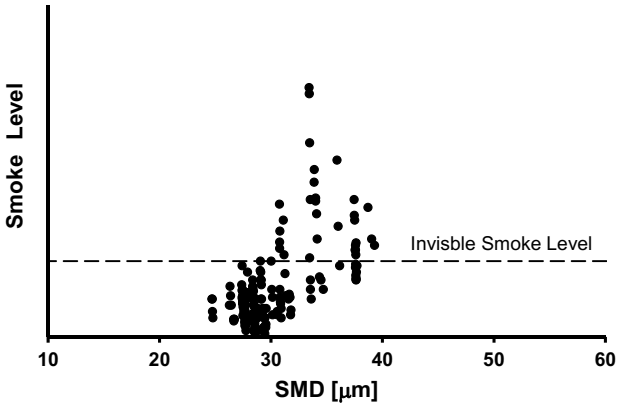

Fig.12-Relationship between SMD and black smoke

5 Verification result

First, various parameters such as working load range of each turbocharger's number including optimization of turbocharger matching parts, Rail pressure and Start of injection timing were adjusted in steady state conditions. As a result, both the excess air ratio and SMD could meet the target value at each load in steady state conditions. The target value for excess air ratio was a λ_{trap} of 1.75 or more, but λ_{trap} cannot be measured directly. Therefore λ_{all} including the scavenge air quantity at the timing of valve overlap is used as the performance index. The target value of λ_{all} is set on 2.14 or more from the consideration based on 1D cycle simulation. Fig.13 shows λ_{all} in steady state condition, Fig14 shows SMD in steady state condition.

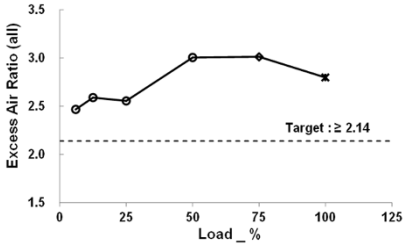

Fig.13-Excess Air Ratio in Steady State condition

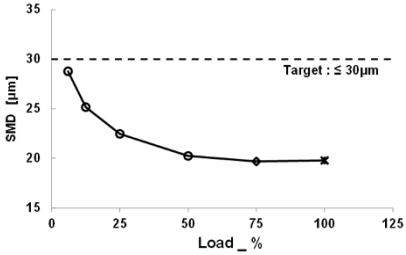

Fig.14-SMD in Steady State Condition

After setting various parameters in steady state conditions, examination was shift to the transient condition. From the idle speed to the rated speed, the load was increased by the hydraulic braking according to the propeller law, and the engine behavior was measured. Smoke level was measured and evaluated using an opacimeter.

(1) Step 1: The transient performance test was conducted at the sequential turbocharging switching point determined by the steady state conditions test. Switching from two to three working turbochargers was carried out at 60% load, and switching from three to four was carried out at 80% load. The test results are shown in Fig.15.

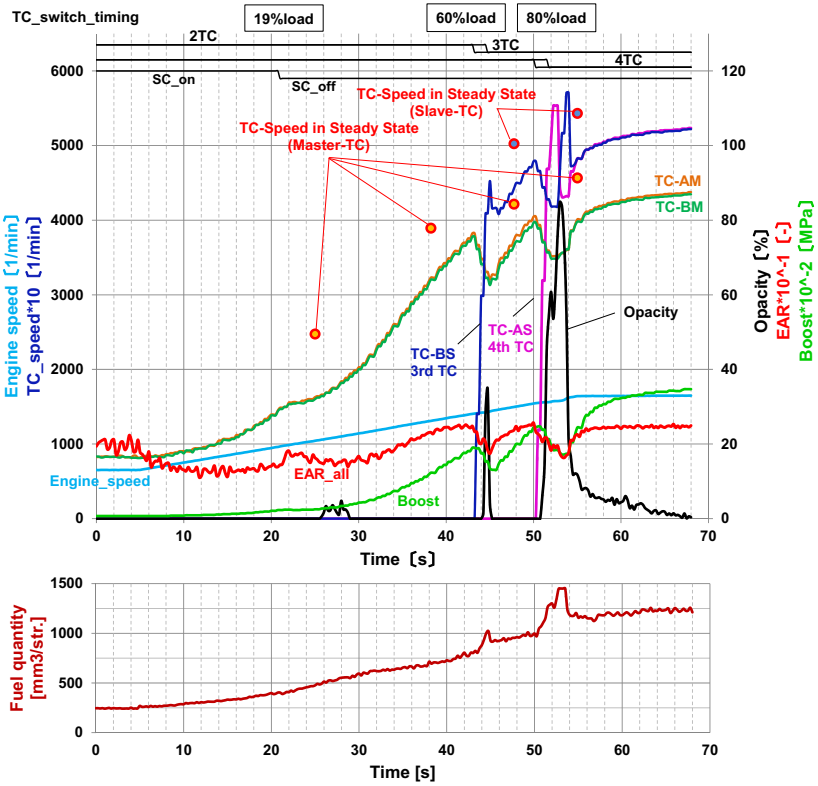

Fig.15-Test Result 1 in Transient Condition

A very slight black smoke was emitted after stopping the supercharger in this test, and then black smoke was emitted at the switching point from two to three working turbochargers. As mentioned earlier, at the same time that the third turbocharger started up, the speeds of the two turbochargers that had been in working dropped down, and with the decrease in boost pressure and the increase in fuel injection quantity, it can be seen that the drop in excess air ratio caused black smoke. This tendency is increased at the switching point from three to four working turbochargers. The fuel injection quantity reached the limit value due to the decrease in engine speed, and the decrease in the excess air ratio is also larger compared with the switching point from two to three turbochargers, so more smoke was emitted. However, the black smoke emission duration was shorter compared with the conventional switching from two to four turbochargers.

(2) Step 2: The turbocharger speed was focused in order to reduce the smoke at the switching point. As can be seen in Fig. 13, the turbocharger speed in transient condition is lower than in steady state conditions, and does not reach the upper limit value due to the delayed turbocharger response. In case of higher load, exhaust energy is much and turbine efficiency is higher compared with low load. Therefore, if the switching point is shifted to higher load, the reduction of working turbocharger speed drop down is expected. And it is expected that the added turbocharger will has good response and black smoke emission will be improved. Thereupon the switching point from two to three turbochargers was shifted from 60% load to a 70% load, and the switching point from three to four turbochargers was shifted from 80% load to 85% load in the next test. This test results are shown in Fig. 16.

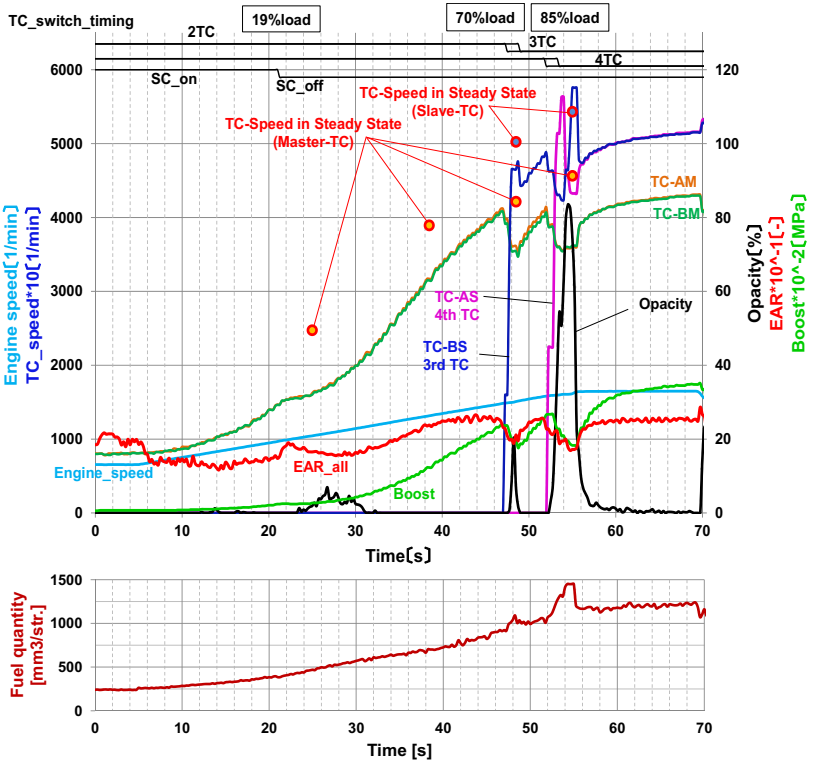

Fig.16-Test Result 2 in Transient Condition

The master turbocharger speed drop down degree was improved according to expectation at the switching point from two to three turbochargers, and the decrease level of the excess air ratio was also improved. As a result, the reduction of black smoke was verified. On the other hand, significant improvement could not be seen at the switching point from three to four turbochargers, because the switching point was shifted by only 5% from 80% load to 85% load due to the limitation of turbocharger speed.

(3) Step 3: The behavior of the third turbocharger speed was focused in order to reduce black smoke at the switching point from three to four turbochargers. Referring to Fig.15 and Fig.16, after the fourth turbocharger started up, it can be seen that the third turbocharger speed temporarily spikes. This reason is considered that this engine has common charged air chamber to all turbochargers, so the third turbocharger is exposed to fluctuations in boost pressure due to the start-up of the fourth turbocharger, and the third turbocharger is exposed to the boost blowback. In the meantime, the speed recovery of the first and second master turbocharger is also slow, and the drop level and drop duration of the excess air ratio have also increased. Therefore much black smoke was emitted.

Thereupon, air bypass system was tried to solve this issue. It aimed to control pressure fluctuations and prevent blowback by slightly lowering the pressure inside the charged air chamber with air bypass before the forth turbocharger's start up. The air bypass systems were installed in compressor outlet and turbine inlet of the two master turbochargers, and they are controlled by opening and closing the butterfly valve. The layout of the air bypass is shown in Fig.17, and the result of this test is shown in Fig.18.

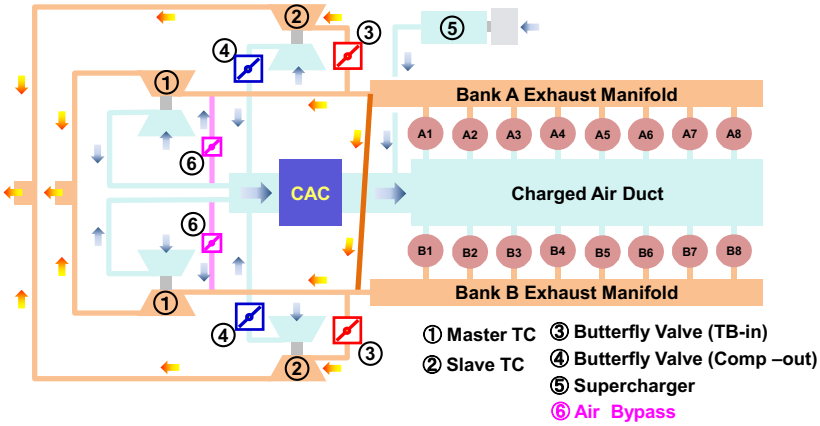

Fig.17-Air Bypass System

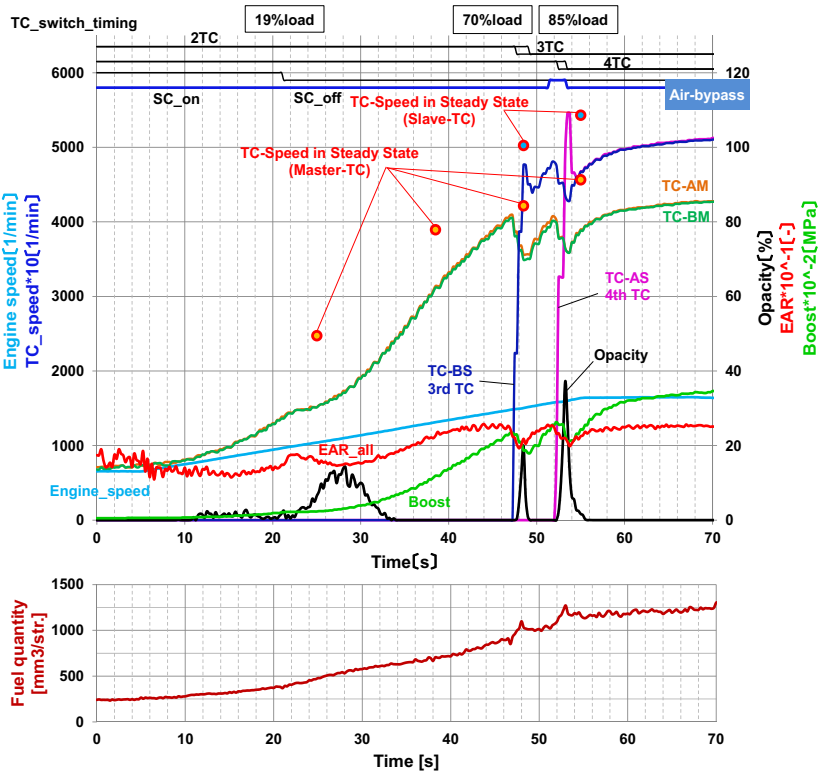

Fig.18-Test Result 3 in Transient Condition

Fig. 18 shows that the spike in the speed of the third turbocharger after start-up of the fourth turbocharger was eliminated by the air bypass. As a result, the master turbocharger speed is quickly recovered and the boost does not decrease by much, so the excess air ratio is secured and black smoke emission is successfully reduced at the switching point from three to four turbochargers.

From the above, authors proceeded the efforts to this issue that black smoke was emitted at the switching point of sequential turbocharging system during transient operation step by step. The issue was found and its cause was expected. And then the solutions were considered and verified. Finally, authors succeeded in the eliminating black smoke as non-visible level in the whole load ranges.

Although this test was conducted in winter season in Japan, as is widely known, engine performance is strongly influenced by site conditions such as atmospheric temperature and absolute humidity. In the future, the impact of site conditions shall be taken into consideration; and authors are taking consideration to address the challenge of maintaining clean exhaust gas even under adverse conditions through further improvements.

6 Summary and Conclusion

This study challenged on eliminating black smoke emitted from diesel engine and focused on the transient condition, especially the switching point of sequential turbocharging system in high speed diesel engine.

– The sequential control was changed in turbocharging system. The drop down in turbocharger speed at the switching point was reduced, and the adequate air quantity could be secured by adding three turbochargers working range, compared to before where the working turbocharger's number were switched from two to four unit.
– The common rail system was installed in fuel injection system. As a result of atomizing the fuel spray by high injection pressure and reducing the nozzle hole diameter, the target value of SMD could be achieved.
– Succeeded in eliminating black smoke to non-visible level that was short duration and low level in the opacity data by these technologies.

The reduction of black smoke from diesel engine exhaust emission including black carbon, dry soot and PM has vital significance to the improvement and preservation of grovel environment as well as human health maintenance. Authors studied on technology to eliminate black smoke emitted from high-speed diesel engines under engine load transient conditions, and obtained a clear engineering findings and practical technology with successful. In addition to the design issues related to black smoke reduction in marine engine load transient conditions, the impact on black smoke emissions of atmospheric temperatures and humidity associated with seasonal changes also needs to be addressed. Authors have a definite intention to continue working vigorously on this issue of black smoke reduction. It is clear philosophy of authors that the engineering findings which obtained via this technology development experience can be applied to other engine types and future high BMEP engines as one of core technology for black smoke reduction.

Layout of highly-stressed injection and motor components

B. A. Jochen Heizmann
is responsible for the development of new business areas at Hirschvogel Automotive Group in Denklingen (Germany).

Dr.-Ing. Hans-Willi Raedt
takes responsibility for the Advanced Engineering Department at Hirschvogel Automotive Group in Denklingen (Germany).

Dipl.-Ing. Patrice Lasne
is Senior Engineer in the Development of Transvalor S.A. in Mougins (France).

Dipl.-Ing. Helmut Dannbauer
takes responsibility for Analysis Services and Software Products of the Structural Analysis Department at Engineering Center Steyr GmbH & Co. KG in St. Valentin (Austria).

W. Siebenpfeiffer (Hrsg.), *Heavy-Duty-, On- und Off-Highway-Motoren 2017*,
Proceedings, https://doi.org/10.1007/978-3-658-21029-8_11

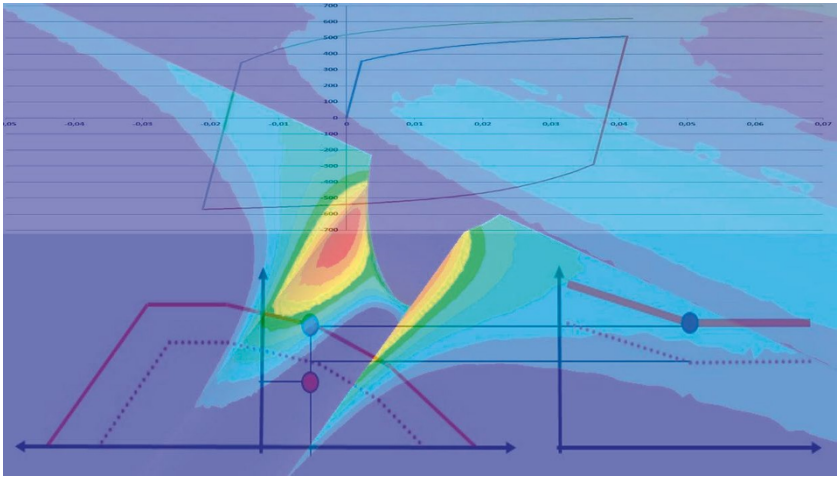

© Hirschvogel Automotive Group

Hydraulic autofrettage as a means of increasing fatigue life of components charged with internal high-pressure (for example common rails for Diesel-injection systems) is establishing itself progressively in the field of off-highway engines. During computational layout of this process step, consideration of anisotropic material behaviour is of primary importance. So far, local quite possibly directional component-strength (such as due to prior autofrettage) has not been taken into account among standards to evaluation of durability for forged components. In the context of a joint development project this gap has been closed by Hirschvogel Automotive Group, Engineering Center Steyr and Transvalor.

PRINCIPLE OF HYDRAULIC AUTOFRETTAGE

Injection pressures beyond 2000 bar contribute significantly to a more efficient exploitation of fuel in prospective engines. The so-called autofrettage method ensures, that hydraulic tubes and pipes are able to withstand ever-increasing alternating loads [1]. Autofrettage is a means of generating residual stresses in pipes, in order to improve its load-bearing capacity as well as fatigue-life [2]. In the course of hydraulic Autofrettage thick-walled metallic cylinders are subjected on the inner diameter to a high internal pressure. At present, the level has been recorded at three to four times the nominal working pressure. Thereby material at the inner diameter is expanded under tensile loading above its elastic limit, FIGURE 1, whereas deformation in outer sections still remains in the elastic area of the material. After release of the autofrettage pressure the outer zone of the cylinder will relieve elastically. Material in the area of the inner diameter, particularly at the bore-intersection will undergo plastic deformation again, this time under compressive loading. After achieving the state of equilibrium, plastically deformed sections will end up in a condition of compressive residual stresses. Later, under impact of internal working pressure this will have a positive effect, as compressive residual stresses resulting from autofrettage compensate tensile stresses: during operation reduced equivalent stresses as well as shifted local mean-stresses can lead to higher admissible amplitude stresses [3].

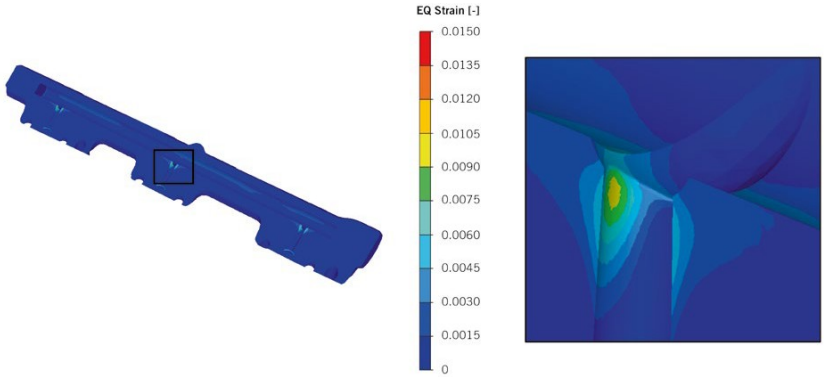

FIGURE 1 Plastic strain due to autofrettage – general view (left) and detail view (right) (© Hirschvogel Automotive Group)

OPTIMISATION OF FORGED HIGH STRENGTH COMPONENTS

Technical systems of modern times – both for automotive and off-highway applications – contain forged high-strength components, many times.

Its key role particularly can be explained by the massive load-bearing capacity, which is the crucial point whenever it comes to transmission of exalted forces, torques or pressures. Increasing requirements regarding power density necessitate more intense component optimisation, which takes painstaking tuning of material, component-geometry as well as numerous parameters along the entire development- and process-chain for granted.

In the course of full utilisation of mechanical-geometrical potentials at ideally lowest costs, vigorous application as well as continuous development of advanced design tools gains great importance. Thanks to long-standing know-how and software-tools as CAD, topology- and shape-optimisation as soon as linear-elastic FEM simulation the Hirschvogel Automotive Group is in a position to reliably design components on the basis of requirements and design-rules of customers. Furthermore, the company recently has acquired numerous further competences and refined these together with for instance industrial and academic partners (such as regarding understanding of micro-mechanical material-mechanisms). Such as application of elasto-plastic forming-simulation in combination with advanced material-models creates the possibility, to not only compute least plastic deformations precisely adjusted during autofrettage, but also to post process resulting residual stresses. Generally, whenever it comes to classical forming simulation in combination with metallic materials, isotropic hardening is assumed. In the case of minor plastic deformation and particularly in combination with cyclic material loading, as a rule kinematic hardening dominates. These will now by means of suitable models in combination with material-specific parameters be taken into consideration during FEM simulation of the autofrettage-process followed by a fatigue analysis.

PREVIOUS APPROACHES ADOPTED TO ASSESS FATIGUE LIFE OF COMMON RAILS

In cases where autofrettage does not come to fruition or whenever one chooses conservative approaches during layout of common rails, engineers are tempted to regard empirical values related to diameter ratios. If FEM software good for linear-elastic analysis of operating states (without prior autofrettage) is available, various geometry-proposals can be assessed via empirical formula which take material strength (for example YS or UTS) and

von Mises equivalent stress into account at the same time. In the event of deploying formulations of material science and fatigue, the Goodman diagram, FIGURE 2, may be applied, in order to quantify the relation of mean stress and alternating strength with respect to durability of the material. The area underneath the graph indicates, that at given stresses the material should not fail. The area above the curve represents potential failure of the material. Thereby σ_A stands for stress amplitude, σ_M for mean stress, σ_{FAT} represents fatigue limit for exclusively alternating load and σ_{TS} stands for ultimate tensile strength, respectively σ_{CS} for ultimate compressive strength of the material. The general trend, shown by the Goodman diagram for example provides decreasing sustainable stress amplitudes with increasing tensile mean stress [4].

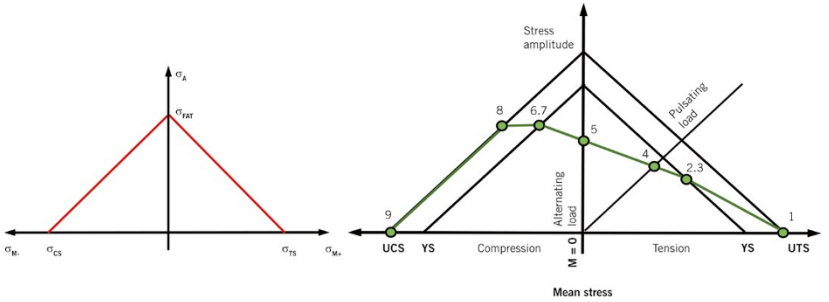

FIGURE 2 Goodman Diagram (left) and Haigh diagram (right)
(© Hirschvogel Automotive Group)

In the course of fatigue-life assessment (such as common-rails) taking autofrettage into consideration, while following advanced approaches, as a rule elasto-plastic FEM software (for example FORGE) is applicable. Simultaneously the so-called Bauschinger effect in terms of kinematic hardening models is included in the computations, so that a realistic distribution of residual stresses can be transferred from a prior autofrettage simulation to the subsequent fatigue-life analysis (for example FEMFAT). Thanks to the description of the material-characteristic by Haigh diagrams, compared to the Goodman diagram mean stress sensitivity of the material can be considered at a higher level of detail, FIGURE 2.

NEW ACCOMPLISHMENTS QUALIFIED FOR FATIGUE LIFE ASSESSMENT OF COMMON RAILS

Due to joint further development of models suitable for fatigue life assessment, in the future local strain hardening as well as softening effects related to plastic deformation can be integrated in terms of yield stress as well as ultimate tensile strength – as a result of a preceded elasto-plastic forming simulation – into the subsequent fatigue analysis, FIGURE 3. This is ensured by making a distinction between isotropic and kinematic material behaviour during transfer of local parameters to durability analysis. As a rule, for the latter behaviour directional dependency of ultimate tensile strength and yield stress due to deformation during autofrettage plays a crucial role, FIGURE 4.

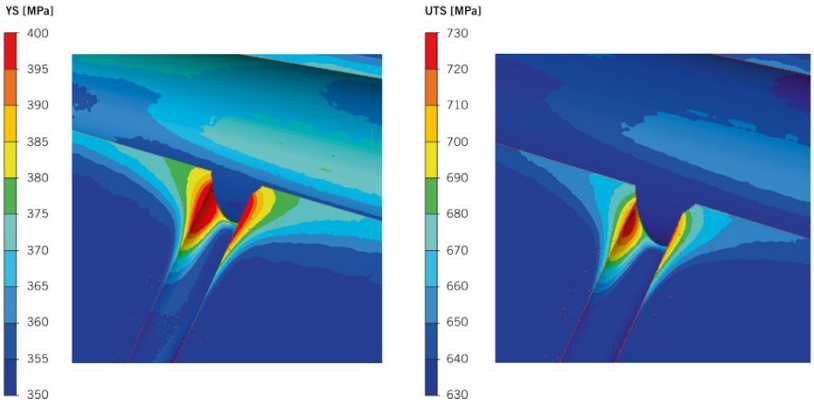

FIGURE 3 Local increase of yield stress (left) and ultimate tensile strength (right) due to autofrettage (© Hirschvogel Automotive Group)

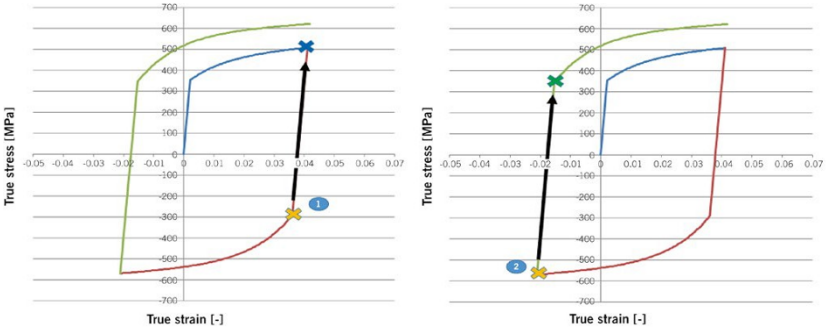

FIGURE 4 Consideration of isotropic (left) and kinematic (right) material behaviour (© Hirschvogel Automotive Group)

This in turn means that fatigue life analyses do not only operate on the basis of local Haigh diagrams, beyond that these are adapted due to present variations of strength. Whenever impacts on the material properties (such as fatigue strength) are being calculated in the FEMFAT software, the associated Haigh diagram changes. Positive impacts lead to an expansion of the diagram, whereas negative ones would entail a reduction of material properties, simultaneously the loading capacity would decrease. Any individual adaptation shall be made proportionally in accordance with existing local specifications for ultimate tensile strength. As a consequence, any node of the finite-element-mesh can carry a customised Haigh diagram and therefore also can evince a varying local s-n curve – due to dissimilar material properties and boundary conditions (temperature, notch, surface roughness etc.). Furthermore, one has not to assume homogeneous material properties anymore, because the accuracy of the material description via individual data on material strength at any finite-element-node can be transferred from forming simulation to fatigue life analysis, FIGURE 5.

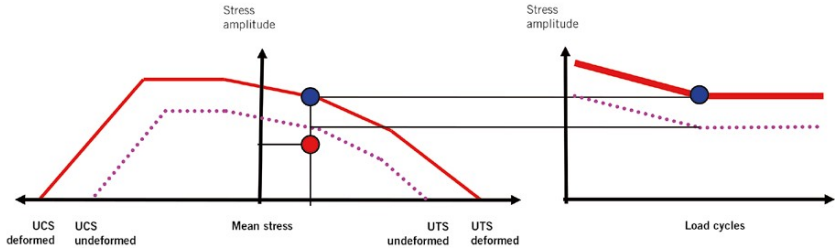

FIGURE 5 Modified Haigh diagram and S/N-curve (© Hirschvogel Automotive Group)

As a general rule, engine components are designed to have fatigue strength. As a consequence, during fatigue life analysis of common rails focus is solely placed on the two critical load cases. Considering that, the locally present safety factor will be determined – in accordance with scatter range, survival probability of the material to be investigated and the targeted survival probability. The calculated safety factor enables the development engineer to assess, whether durability can be expected for the analysed component or not. **FIGURE 6** illustrates, that the increase in ultimate tensile strength and yield stress in the critical area of the bore intersection have a significant positive impact on the respective safety factor (increase from SF_A = 1.40 to SF_A = 1.56) – hence in the present example durability can be anticipated.

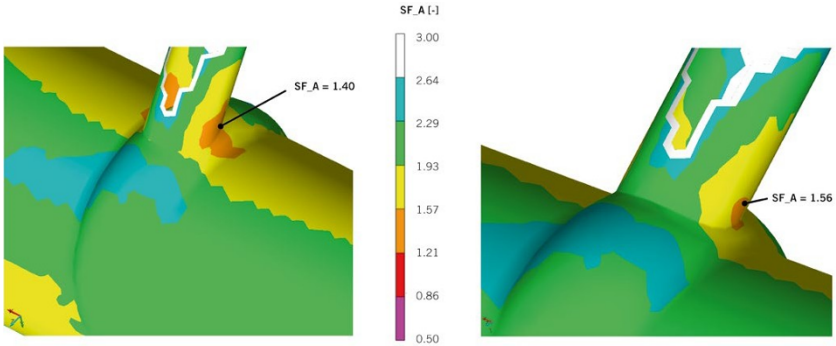

FIGURE 6 Safety factor without (left) and in (right) consideration of local parameters
(© Hirschvogel Automotive Group)

SUMMARY

Consideration of kinematic material behaviour can increase precision of the layout of components charged with internal high pressure (for example common rails for Diesel-injection systems) markedly. In case one wants to particularly assess the anticipated fatigue life of the component as well, it seems appropriate, that residual stresses computed in the course of autofrettage-simulation as well as respective local strain hardening of the material should be taken into account during a subsequent fatigue life calculation. Furthermore, new accomplishments facilitate a significant increase in the predictive quality of durability analysis. These are premised on generation and transfer of further parameters applicable for characterisation of local material strength (for the time being limited to the successful implementation of local ultimate tensile strength and local yield stress of the strain hardened component).

REFERENCES

[1] N.N.: FELSS – Shortcut Technologies. www.felss.com/verfahren-maschinen/autofrettage, access 04.06.2016

[2] Carlucci, D.; Jacobson, S.: Ballistics – Theory and Design of Guns and Ammunition. Boca Raton: Taylor & Francis Group, 2014.

[3] Narayanan, R.; Dixit, U.: Advances in Material Forming and Joining. New Delhi: Springer, 2015.

[4] N.N.: Wikipedia: Goodman Relation. https://en. wikipedia.org/wiki/Goodman_relation#cite_ref-6, access 04.06.2016

THANKS

The authors would like to thank Dipl.-Ing. Axel Werkhausen, FEMFAT-Sales- and Support-Manager, and Dr.-Ing. Christian Gaier, Team-Manager of the FFEMFAT Development Department, both at Engineering Center Steyr GmbH & Co. KG in St. Valentin (Austria), as well as Dipl.-Ing. Olivier Krafft, Sales Engineer Northern Europe at Transvalor S.A. in Mougins Cedex (France) and Dipl.-Ing. Angela Kotte, Development Engineer for Material & Technology in the Advanced Engineering Department at Hirschvogel Automotive Group in Denklingen (Germany), for their contribution during the implementation of the development project.

Changing the heat treatment process as the key to success for Hatz Diesel

Dipl.-Ing. Tobias Winter, Motorenfabrik Hatz GmbH & Co. KG, Ruhstorf a.d. Rott, Germany

Dipl.-Ing. Andreas Heitmann, MAGMA GmbH, Aachen, Germany

W. Siebenpfeiffer (Hrsg.), *Heavy-Duty-, On- und Off-Highway-Motoren 2017*, Proceedings, https://doi.org/10.1007/978-3-658-21029-8_12

Durability assessment of aluminum cylinder head finally revealed residual stresses from heat treatment as the cause for cracks

Hatz Diesel is a German manufacturer of industrial Diesel engines with 1 to 4 cylinders up to 56 kW, and also of systems based on these engines, e.g. pumps, gensets, smart-grid solutions as well as engine components for automotive and construction machinery customers, e.g. crankshafts and conrods. They produce about 60.000 engines per year with 1060 employees worldwide.

Hatz followed their clear, state-of-the-art workflow for the durability assessment of a water-cooled aluminum cylinder head.

As an input for the stress and fatigue analysis component temperature distributions have to be assessed. This happens with the use of 1D-cooling system analysis in close coupling with CFD calculations. For the stress analysis of the cylinder head and crank case – among the loads from real working process calculation and in-cylinder measurements – an accurate model of the gasket behavior is necessary. Additionally, measurements of the tensile force of cylinder head bolts are performed to ensure best possible boundary conditions for the FEA. CAT scans are performed to ensure parity between CAD data and test parts. Tensile tests are performed on several specimen from across the part to validate the static strength values (compare figure 1).

The outcome of this thoroughly performed investigation didn't reveal any critical areas, so parts were procured and the first prototypes were assembled for test bench operation.

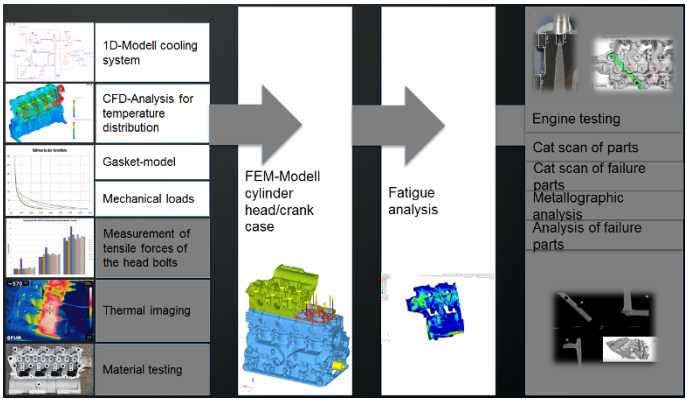

Figure 1: Simulation and testing workflow without consideration of residual stresses

After approximately 1200 hours of test bench operation a leakage of the cylinder head (water into oil) occurred in the area of the spring seat of the outlet valve. The engine was disassembled and CAT scans were performed on the defective parts. Shrink holes/voids were present in the area of the crack so for a first explanation these were blamed to be in causal connection (see figure 3). Wall thickness was according to the CAD data and within specification, so no cause could be found there either (see figure 2).

Figure 2: CAT-scan of the relevant section

During the examination of the defective parts another failure occurred after a very short test bench period of about 50 hours. Again CAT scans were performed and they showed a crack at the same location, but this time no shrink holes were present. Unfortunately the safety margin of the FEA calculation in this area was sufficient and obviously didn't reflect reality. Additional cut images of the area which were prepared in the aftermath of the CAT scans showed that the microstructure was looking good and a material analysis presented a normal composition according to the specifications (AC-45500 T6).

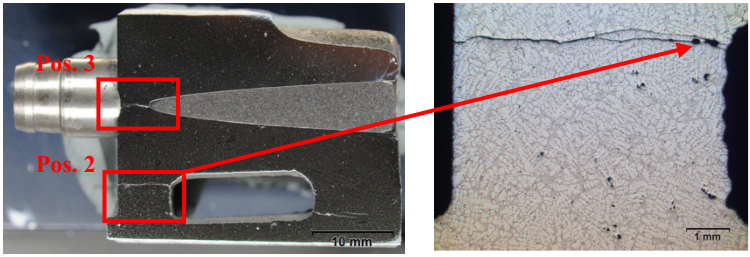

Figure 3: Polished micrograph section

With the short operation time of the second engine, a suspicion pointing to an initial defect of the cylinder head came up for the first time. As a consequence, additionally performed CAT-scans were conducted on machined parts that hadn't been mounted yet. Surprisingly, cracks were present in several parts in exactly the same location as in the defective parts.

Now it was considered that residual stresses, which had not been subject to the numerical dimensioning so far, might play a role in the phenomenon.

It was decided to make a casting process and residual stress analysis with the help of MAGMASOFT®. With MAGMASOFT®, you cannot just simulate the casting process itself, i.e. the flow pattern during the filling of the mold and the solidification of the part inside and outside the die. You can also simulate subsequent process steps such as heat treatment and machining. Furthermore, MAGMASOFT® offers the possibility to predict the residual stresses that build up in the part during this whole production process. The simulations revealed that the main cause for the buildup of the residual stresses in the cylinder head was the heat treatment process. So the focus of the simulation was put on this part of the production process (compare figure 4). The simulation revealed high residual stresses in the area of the failure (see figure 5).

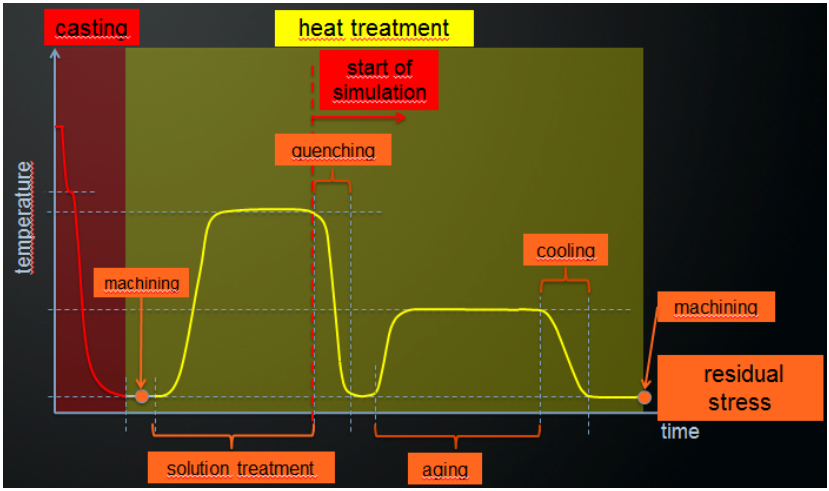

Figure 4: Heat treatment process simulation

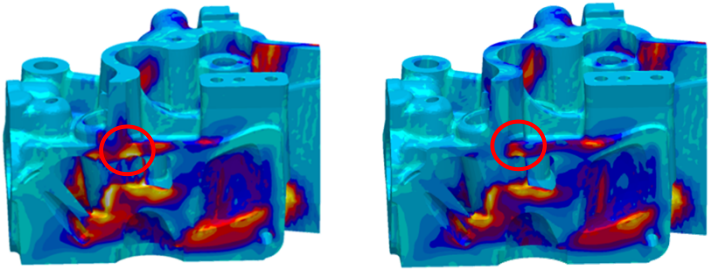

Figure 5: Residual stresses with original design (l.) and with pre-machining (r.)

Another fatigue analysis was performed, this time including the effect of the residual stresses from the T6 heat treatment in the assessment. The FEA results showed that the crack in the area of the valve guiding (Pos. 3) had been correctly predicted by the fatigue analysis. Taking into account the residual stresses, the crack at Pos. 2 also could be predicted correctly by the fatigue tools as they confirmed a safety margin S<1 in this area (compare figure 6).

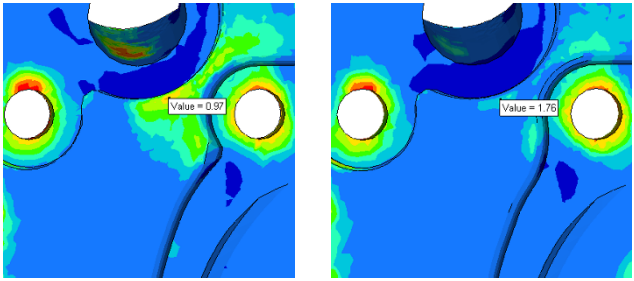

Figure 6: Results of fatigue assessment with (l.) and without (r.) consideration of residual stresses at the failure area (Pos. 2)

Now that the reason was obvious, remedies could be derived. In fact the problem was a large amount of material in the area of the valve spring seats and the injection nozzles that were adjacent to a thin wall of the oil-deck. After some simulations on variants of the heat treatment (e.g. increasing water temperature) it became clear that the problem could only be solved by removing the surplus material prior to the heat treatment. The simulation showed a significant decrease in residual stress (see figure 5) and the subsequent fatigue analysis confirmed a sufficient safety margin for the whole cylinder head. Figure 7 shows the new design process taking into account the effect of residual stresses from the production process for the fatigue assessment.

The improvements were taken over for the next sample phase and went into series production after a long testing period without any problems in this area.

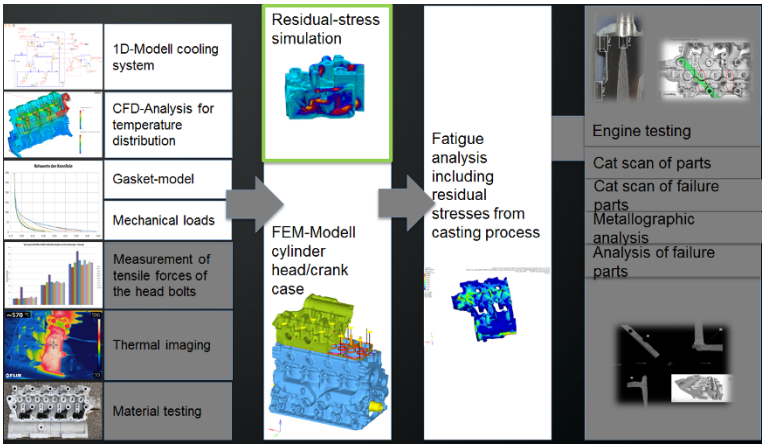

Figure 7: Simulation and testing workflow including residual stresses

Methodology for the development of variable valve drive systems from concept to series approval with focus on heavy-duty engines

Dipl.-Ing. Andreas Eichenberg

W. Siebenpfeiffer (Hrsg.), *Heavy-Duty-, On- und Off-Highway-Motoren 2017*,
Proceedings, https://doi.org/10.1007/978-3-658-21029-8_13

Abstract

The development of combustion engines is subject to the pressures of ever more stringent limits. And different limits depending on the use spectrum between trucks and construction machinery also lead to development conflicts in the engine design. Achieving great versatility in the possible uses of engines, as well as low consumption and emissions, can only be done through highly sophisticated technology. An important role in this is played by the optimized gas cycle through variable valve drives.

This article describes the methodology for the development of sliding cam systems from the concept to the series approval. This process was established at Porsche Engineering to guarantee the high flexibility and quickness according to the demand of engine development activities.

Due to the simple and modular structure in addition to the low production complexity and nearly unchangeable base valve train, the sliding cam systems are the most commonly used variable valve drives from the category of discrete switching systems. The use in many different engines leads to several boundary conditions for the application of such a system.

Depending on the desired operating strategy, the optimal valve lift curves are developed based on gas cycle simulations. The timing and length of these valve lift curves are the input data for the iterative development process of the sliding motion design. The kinematic and dynamic simulation is passed through in an iterative sequence. The result of these calculation loops is the optimal design of the dynamically simulated shift guide. In a next step, the sliding cam system is tested on the component level. This will be done in the earliest possible stage of development. The actuator and actuator pin-shift guide element are two examples of the tested elements. The main functional check of the sliding cam system is tested on a cylinder head test bench. Therefore, the dynamic displacement travel and actuator pin force is measured and analysed under realistic engine running conditions. The durability testing and series approval complete the modular development process of sliding cam systems.

Thanks to extensive expertise, the design and simulations can be carried out at a very early stage, which is amenable to ever shorter product development cycles. However, the simulation tools, compared with measurement data, also have further potential to obviate the need for loops in the testing of functions and fatigue resistance. Porsche Engineering will continue to drive the trend toward multi-level sliding cam systems both conceptually and with regard to testing.

Sliding cam systems as variable valve drive

In conventional four-stroke engines, the lift curves of the gas exchange valves are configured for a particular operating point – for example maximum engine performance. These valve lift curves represent a compromise with regard to the rest of the engine control map. With variable valve drive systems, this compromise can be resolved. This technology has been successfully used in various forms in combustion engines for years now. Fundamentally, these systems can be classed into partially and fully variable designs. The spectrum ranges from purely mechanical to purely electrical actuation of the gas exchange valves. Fully variable valve drives generate a set of possible valve lift curves. The valve lift and the width of the opening are freely adjustable. Partially variable systems generate a discrete number of valve lift curves based on defined cam contours. Series engines primarily employ switching between two valve lift curves. Sliding cam systems are the most commonly used variable valve drives from the category of discrete switching systems. The development and testing of such sliding cam systems is an area of particular expertise for Porsche Engineering, Figure 1.

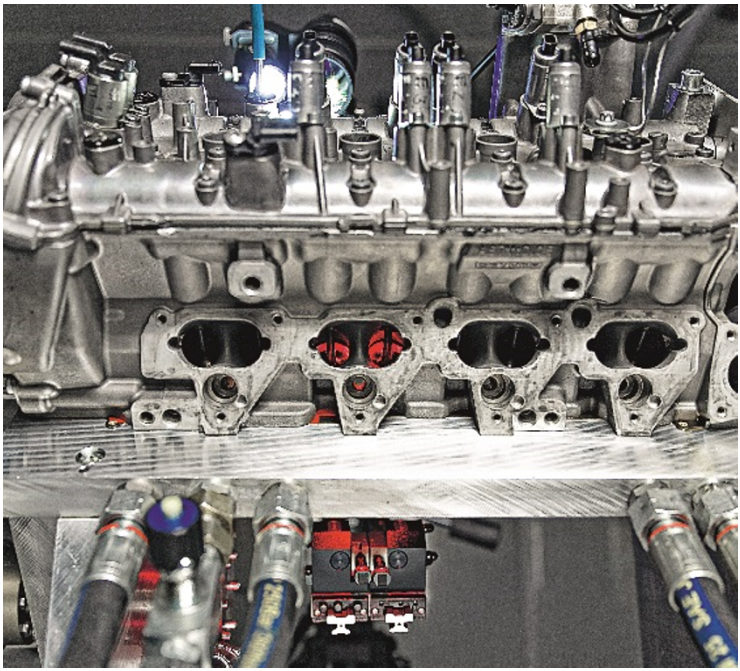

Figure 1: Valve drive dynamics in the motored cylinder head

In modern commercial vehicles, in addition to typical requirements such as robustness and reliability, the reduction of emissions and fuel consumption are important factors. This set of desired capabilities puts variable valve drives front and centre in the minds of engine developers. Sliding cam systems offer a promising starting point for the use of two independent, discrete valve lift curves. Another advantage: they do not influence the type and implementation of the proper valve actuation. This and the modular structure open up the possibility of application-specific uses in new engine generations. This also makes it possible to implement Miller cycles and functions such as cylinder deactivation and engine braking. Which operating strategy offers greatest possible potential for the customer depends on the particular use case. For example, different legal emissions thresholds apply depending on whether the vehicle is intended for on-road or off-road use. Variable valve drive systems can be used to configure the engines for the different purposes.

Modular development process and advantages of sliding cam systems

In principle, sliding cam systems are based on a sliding cam piece that controls the valve actuation using a conventional cam follower. In modern commercial vehicles, swing or rocker arms with roller actuation are primarily used for this. On the cam piece, in addition to multiple valve lift contours there are also shift guides of different shapes and designs. The cam slide piece is situated on a drive shaft with axial gear tooth structure. It transmits the rotation while simultaneously allowing the cam piece to slide axially. To change the active cam contour, a pin shift the cam piece on the shaft. The movement of the cam piece results from the desmodromic actuation of the pin in the shift guide and rotation of the cam slide piece. The pin is part of an electromagnetic actuator in the cylinder head controlled by the engine control unit on the basis of the engine control map. In some cases the cam slide pieces are also beared radially on the drive shaft. An arresting mechanism that intervenes between the drive shaft and the cam piece holds the slide piece in its respective shift position.

In addition to the simple and modular structure, as well as the low production complexity, the crucial advantage of the sliding cam system compared to other variable valve drive systems lies in the unchanged base valve train. This applies in particular to the dynamic opening and closing behavior of the gas exchange valves and the moving masses. So the system is adaptable to existing valve drives. This reduces the complexity and thus development costs.

The challenges in the development of sliding cam systems for commercial vehicle engines are only slightly different than for passenger vehicle applications. The loads on the system components and shifting time requirements are generally determined by the

maximum shift speed, the masses to be moved, the geometric area available for engagement, and the minimum shifting temperature. In commercial vehicles, the desired shifting speeds are always at a lower level than in passenger vehicles. At the same time, commercial vehicle engines have to move considerably greater masses in the cam slide piece, which means that the system loads are ultimately comparable to those of a passenger vehicle. The requisite lifetime (operational service life) as well as the maintenance and reparability of commercial vehicle systems are substantially more demanding. The goal of minimizing system costs is equally relevant. Based on experience from conventional and variable valve drive development, Porsche Engineering has established a modular development process that guarantees high flexibility and quickness.

Design and functional testing of sliding cam systems

The use spectrum of a commercial vehicle and thus the engine type define the critical framework conditions for the design of the sliding cam system. Depending on the desired operating strategy, the optimal valve lift curves of a discrete two-step valve lift adjustment are developed based on gas cycle simulations. For optimal use of the potential of a Miller cycle in a diesel engine application, the engineers first develop a 1D gas cycle model. In the process, the real parameters of the individual components from the process air path to the exhaust system are implemented in the model. If various parameters are not yet known at an early stage in the development, they are set based on the experience of Porsche Engineering. Such a calibrated gas cycle model enables reliable prediction of the possible performance figures. For the design of the maximum valve lift and the opening duration of the gas exchange valves, Design of Experiment (DoE) processes are applied and paired with the kinematics simulation.

Multi body model for dynamic simulation

At Porsche Engineering, the design of the sliding motion of the cam piece is conducted in an iterative development process. This is divided into the kinematic definition and the dynamic simulation of the displacement travel. In the process, the acceleration of the slide is adapted kinematically so as to achieve the required displacement travel within the available rotation angle range. The subsequent dynamic simulation is done using a multi body simulation model specially developed for this purpose. The multi body simulation model is compared in advance with various function measurement data and therefore generates a very good prediction in the design phase. The model represents the forces acting on the cam slide piece, including the existing component play, material stiffnesses and damping of the components, as well as the corresponding shifting speed. The dynamic displacement travel simulated in this way is evaluated in terms of the acting forces and the kinematic design reflected back iteratively. The focus here

is on minimizing the surface pressures between the pin and guide as well as the frictional forces in the actuator from the dynamic load – for example, from the contact alteration of the actuator pin. The result of these calculation loops is the optimal design of the dynamically simulated shift guide under the configured boundary conditions.

The concept design takes place in parallel with the configuration and optimization of the shift guide parameters. The definitive parameters of the sliding cam concept and an evaluation of the corresponding complexity are summarized in Figure 2. Here, the possible combination of the cam slide pieces of multiple cylinders and the positioning of the actuators are examined. The sliding cam system design is further detailed in consideration of the shift guide parameters. This refinement of the design aids in the preparation of prototype component production and encompasses the tolerance question vis-à-vis the actuator pin position, among other factors. The thus defined engagement play with regard to the shift guide must cover the minimum and maximum operating temperatures.

Parameter sliding cam system	Impact on development complexity
Characteristic sliding path contour (path / angle / type)	++
Package (cylinder distance / engine valve distance)	++
Application strategy sliding cam system	+
Sliding cam piece (bearing / weight / arresting mechanism)	+
Actuators (position / bearing)	+
Type valve actuation (cam follower)	+
Bearing drive shaft	o
Type gear tooth structure (torque transmission)	o

Legend impact: o low influence / + medium influence / ++ concept defining

Figure 2: Concept-defining parameters and their impacts

Sliding cam systems that manifest high component loads in the simulation-aided configuration are optimized from a structural-mechanical standpoint. Structure calculations using the finite-element method (FEM) aid this process. With regard to the Hertzian pressures between the actuator pin and shift guide, an analysis of the component stiffnesses, contact pattern optimization, and life cycle calculation are carried out. The special focus here is on the areas of maximum loads and minimum wall thicknesses of the shift guide. The contact conditions and the resulting material stresses are evaluated. The service life calculation in terms of fatigue and endurance strength completes the calculation analysis, Figure 3.

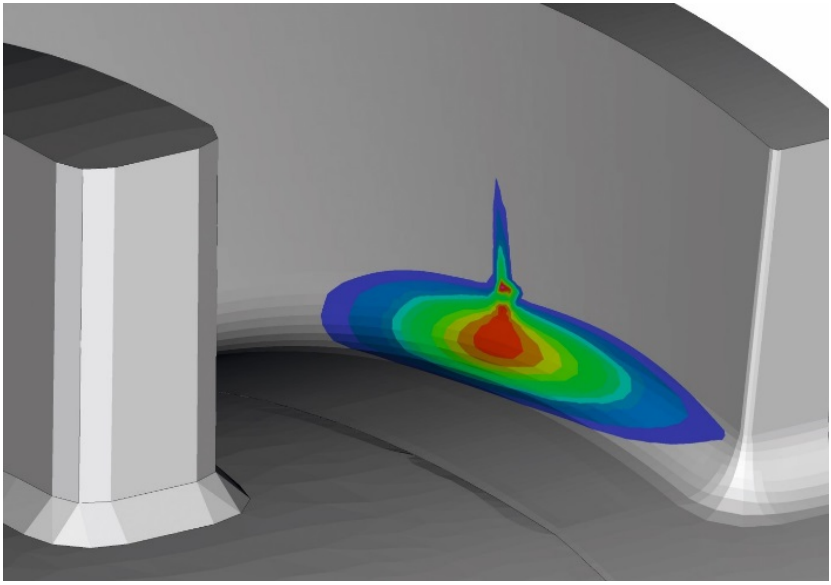

Figure 3: Result of structural calculation of shift guide parameters – life cycle

Pre-testing on tribology test bench

Before system tests on the cylinder head, the sliding cam system is tested on the component level. This is done at the earliest possible stage in the development process in order to allow the test results to flow into the product development process without extraneous development cycles. In this pre-testing, the individual components are exposed to reality-proximate loads and temperatures. The actuator pin-shift guide element is tested in two different ways. One way is a synthetic pulse test to analyze the fatigue behavior. The number of endurable shift loads in interaction with the acting forces describes the fatigue resistance of the actuator design and its mount in the cylinder head. Then there is the pre-testing on a tribology test bench specially designed for the purpose by Porsche Engineering, Figure 4. This employs an endless guide to initiate two complete displacements per revolution of the drive shaft. The loads correspond to the real, dynamically acting forces through the shift guide configuration and slide piece mass. The tribology test bench is modularly structured and is operated with changeable guides, which enable rapid changes and comparison of different parameters. This makes it possible to analyze tendency comparisons with regard to the mutual effects of various surfaces, material combinations, and coating systems in the shortest possible time, Figure 5.

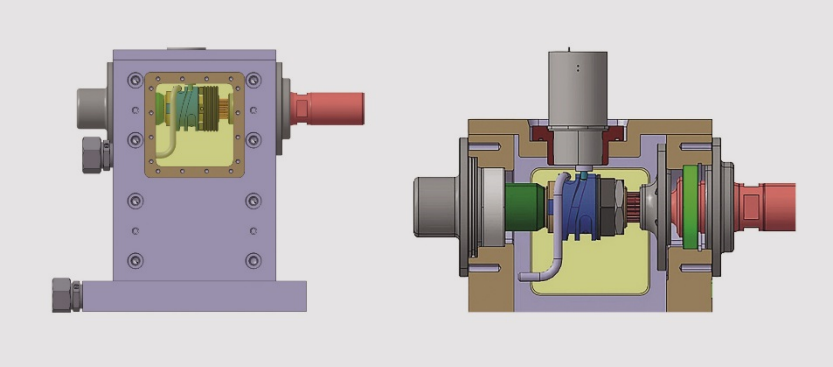

Figure 4: Set-up of the tribology test bench at Porsche Engineering

One of the most important parameters for the functioning of a sliding cam system is the shifting time (dead time and time-of-flight) of the actuators. The test analyzes the engagement of the actuator pin over a geometrically defined angle range under all functional boundary conditions. Translated by way of the drive speed, the actuators must ensure an adequate shifting time over a large component temperature and supply voltage range. For example, the influence of the component temperature on the time-of-flight and dead time is analyzed for the -30°C to 120°C range. The reproducibility of the tests plays a decisive role and is ensured by way of a defined oiling process, for example. The results of the pre-testing flow directly into the prototype design and thus into the development process.

Figure 5: Interchangeable slide piece with endless guide

Real functional evaluation on motored cylinder head test bench

The first real functional evaluation of the sliding cam system is done on the motored cylinder head test bench, on which the cylinder head is operated in its vehicle installation position. The drive force is provided by a timing drive system present in the complete engine and a powerful asynchronous motor. A torsionally stiff coupling with an integrated measurement flange records the engine speed and drive torque. The oil pressure, oil temperature, and engine speed are set to correspond with real engine operation. The focus of the function test is the validation of the displacement travel and the dynamic actuator pin forces. This is measured by special sensors in the cylinder head. The displacement travel is measured by means of magnetoresistive sensors, which can record linear movements in high resolution through a defined tooth structure. The travel of the cam piece generates sine and cosine waves that are analyzed with a precision down to 10µm. Porsche Engineering has been successfully employing this technique to measure the fired valve drive dynamics [1] since 2009. The test of the displacement travel is complemented by the optical recording of a high-speed camera. Here, the qualitative assessment of the motion of the cam slide piece is the focus rather than the quantitative measurement data. The measurement of the actuator pin force is done with a specially designed actuator. Strain gauges are applied to the electromagnetic actuator to enable measurement of the axial and radial forces for each pin, Figure 6. The strain gauges are connected to form a Wheatstone half bridge and are thus independent of the operating temperature.

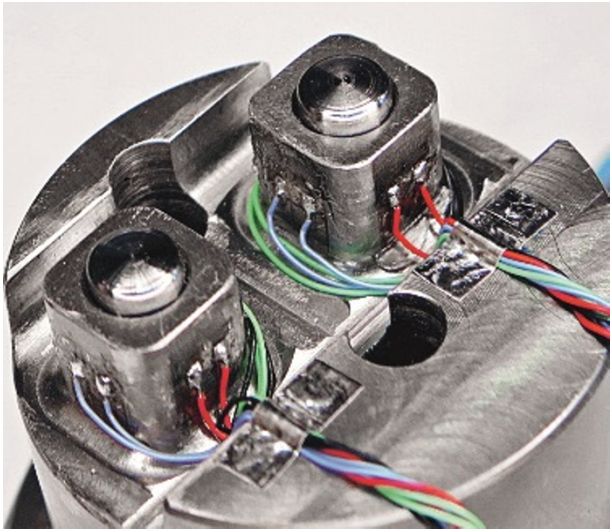

Figure 6: Strain gauge application: actuator pin force measurement

At the cylinder head test bench, the cam displacements are initiated under various boundary conditions, such as varying drive speeds, and the reaction recorded with the described measurement technology over the camshaft angle range. At the same time, a laser Doppler vibrometer optically records the reaction of the valve lift at the gas exchange valve. For the time- or angle-based actuation of the electromagnetic actuators, there are two common procedures. One option is to use a prototype control unit with speed recording by way of a rotary sensor. The other option is a control program on a real-time system in case there is not yet a control unit available at an early stage of development.

For the further development and functional approval of the sliding cam system, the recorded measurement data is used to analyse the dynamics of the motion, Figure 7. The focus here is on the dynamic response upon initial contact between the actuator pin and shift guide, as well as the change of sides in the guide from the acceleration to the deceleration flank and the engagement in the end position after a complete displacement. Functional measurement concludes with a measurement of the friction values of the sliding cam system.

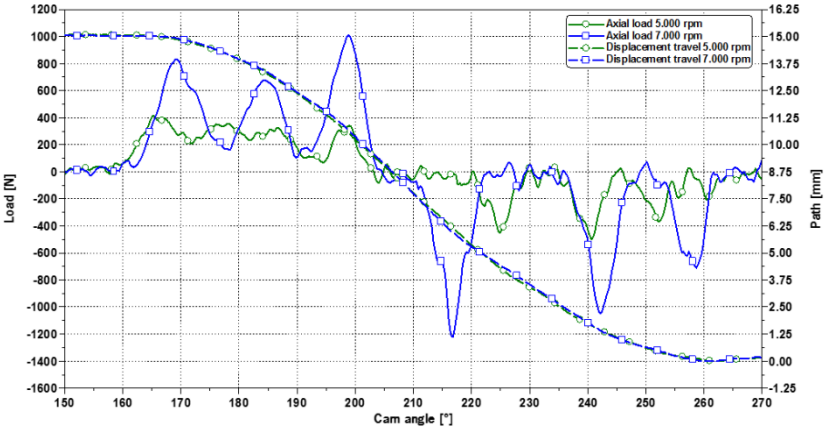

Figure 7: Measurement of the dynamic displacement travel and actuator pin force

The axial displacement of the cam pieces fundamentally influences the contact to the cam follower. Risks due to possible partial covering, edge interference, or tipping are taken into account in the design phase. Test bench measurements with rocker arms affixed with strain gauges record the acting loads. Moreover, in all test bench investigations, the inclination toward potential improper shifts is analysed.

Durability testing and series approval

The first demonstration of the durability of the sliding cam system is also conducted on the cylinder head test bench in order to ensure efficient and rapid feedback for the complete engine development process. Here, the system is subjected to an automated test of real and synthetic engine speed programs. These programs are designed to ensure that the displacements take place under realistic engine situations. The shifts are initiated by an engine control unit or the aforementioned real-time system. In addition to the variation of the shifting speed, the test also checks the functional parameters in limit sample tests of the sliding cam system. One example of such a limit sample is the maximum production tolerance for the engagement of the actuator pin in the shift guide. The endurance objective here varies depending on the respective use of the combustion engine. Thus, depending on the use profile, a load spectrum must be created for the respective engine application. Finally, after a shifting endurance test the components are dismounted and assessed.

Summary and outlook

The method described here and developed by Porsche Engineering is a flexible and efficient tool for the development of sliding cam systems and can be used in a modular fashion in accordance with the requirements of the development scope. Thanks to extensive expertise, the design and simulations can be carried out at a very early stage, which is amenable to ever shorter product development cycles. But the simulation tools, compared with measurement data, also have further potential to obviate the need for loops in the testing of functions and fatigue resistance. And Porsche Engineering accompanies the entire prototype production process from the concept to the validation of component quality. The particular focus here is on a reliable production process including the heat treatment of the cam slide piece and component measurement as a quality control measure.

Variable valve drives are subject to continuous enhancement. Porsche Engineering will continue to drive the trend toward multi-level sliding cam systems both conceptually and with regard to testing.

Reference

[1] Schwarz, D.; Bach, Dr. M.; Fuoss, K.: Valvetrain investigations on fired engines. In: MTZ worldwide 70 (2009), No. 6, pp. 36-41

Investigation of the cylinder cut-out for medium-speed dual-fuel engines

Johannes Konrad
Assoc. Prof. Dipl.-Ing. Dr. Thomas Lauer
Vienna University of Technology

Dr. Mathias Moser
Enrico Lockner
Dr. Jianguo Zhu
MAN Diesel & Turbo SE

W. Siebenpfeiffer (Hrsg.), *Heavy-Duty-, On- und Off-Highway-Motoren 2017*,
Proceedings, https://doi.org/10.1007/978-3-658-21029-8_14

Introduction

As one of the consequences of the climate change, more severe maritime emission regulations are globally in force or will become applicable during the next years. The tough competition put pressure on the maritime transport industry. Therefore, their demand for efficient and mostly environmental neutral propulsion systems – to meet the environmental legislations and reduce the cargo costs – is high.

Dual fuel engines are in accordance with these stringent requirements. They show a reduced environmental impact, compared to conventional maritime propulsion systems. This is mainly based on the chemical composition of the natural gas. The emissions of particle matter, CO_2, NO_x, and SO_x are in many cases decreased or even non-existent [1]. For this reason, it is possible to meet the requirements of IMO Tier III without additional aftertreatment systems in the NO_x emission control areas (NECA) in North America and the upcoming NECA in the Baltic & North Sea after 1st January 2021 [2, 3].

Beside maritime, dual fuel engines are also applied for stationary power applications. They are especially utilized within smaller grids with a reasonable share of electricity from volatile renewable energy sources like photovoltaics or wind turbines. Dual fuel engines can quickly adapt the power output and therefore stabilize the grid frequency by compensating the volatile supply and demand.

Another reason for the application in maritime as well as in stationary power generation are the present gas prices, which are below the liquid fuel price, especially in the U.S.A. due to the shale gas production [4]. Furthermore, both sectors often require the possibility of burning two different fuels. In maritime application, the lack of gas-infrastructure in harbours around the world generates the demand for substituting the natural gas for conventional fuel. In stationary power applications, dual fuel engines are applied to cope with disturbances in the natural gas supply. Due to the conventional fuel backup, the availability can be increased. Additionally, in stationery power applications dual fuel engines are applied to be prepared for an upcoming or sometimes already planned gas connection.

Medium speed dual fuel engines are normally optimized for operation at high loads. Consequently, the highest efficiency and the most economic operation are achieved in this load range.

In maritime transportation of goods and passengers, economical and punctual operation is the most important. To achieve planned arrival times and to avoid anchoring, part or low load operation can be necessary. Furthermore, engine operation in low and part load is typical for manoeuvring, nautical station keeping, dynamic positioning, and auxiliary energy supply. Station keeping means the operation of an offshore vessel relative to another moving object, like in a convoy. Dynamic positioning is applied to keep a fixed position, e.g., for offshore drilling, pipelay or cablelay.

Medium speed dual fuel engines typically have no throttling devices in the inlet system in order to prevent air flow losses. This leads to a very lean natural fuel gas / air mixture and, due to the increased share of pilot fuel, to a shift from a premixed to a diesel-like diffusion combustion. This results in high combustion temperatures and enhanced formation of nitrogen oxides [1].

A valuable approach to improve the efficiency and reduce the environmental impact in low and part load is represented by the cylinder cut-out. Hereby one or more cylinders are not fired and the applied load is distributed to the remaining working cylinders. Thus, the operation of the individual cylinders is shifted towards higher mean effective pressures, which results in elevated efficiencies, increased combustion stability and reduced methane slip [5, 6, 7, 8].

This paper will discuss the benefit of cylinder cut-out for dual fuel medium speed engines based on numerical investigations.

Description of the Thermodynamic and Fluid Mechanic Engine Model

A 1D engine model is set up in the commercial simulation environment GT-Power 7.5. In Fig. 1, a schematic overview of the modelled MAN 7-cylinder in-line dual fuel engine is illustrated.

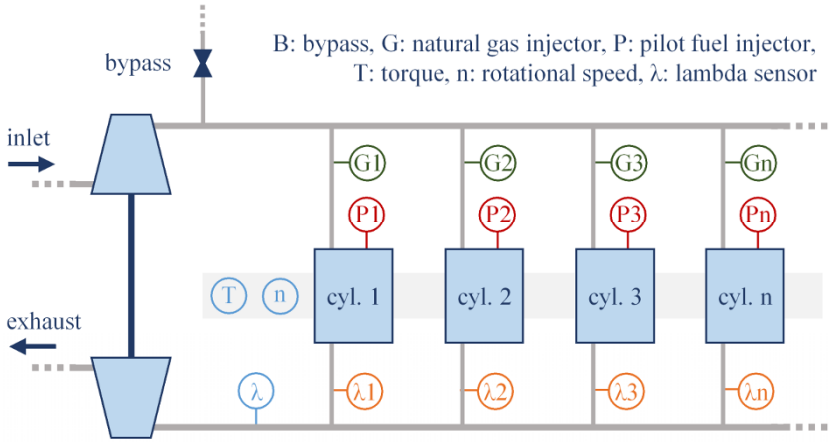

Figure 1: Schematic MAN 7-cylinder in-line dual fuel engine model.

The natural gas is admitted upstream of each cylinder in the inlet manifold, where it is mixed with compressed and cooled charge air. The pilot fuel is injected in the cylinder and provides the ignition energy for the premixed main charge. In order to keep a constant relative air/fuel ratio, the oxygen partial pressure is permanently detected by a lambda sensor upstream of the turbine and utilized for the natural gas admission control. A load control, at a constant relative air/fuel ratio, is realized with a compressor bypass.

The so called electronic cylinder cut-out is carried out by the deactivation of the natural gas admission of the respective cylinder. If cylinders are cut-out, the relative air/fuel ratio upstream of the turbine differs from the ratio downstream of the fired cylinders due to the scavenged air. In order to maintain the operation of the fired cylinders at a defined relative air/fuel ratio, only the ratios downstream of these fired cylinders are employed for engine control, see Fig. 1.

Adjustment of the Combustion- and NO-Models

During a previous project, dual fuel combustion- and NO-models were developed for high and medium speed diesel-gas dual fuel engines. The dual fuel combustion model predicts the ignition delay and the burn rate. To consider the characteristics of the dual fuel combustion, the model must include the diesel spray as an ignition source and the following premixed combustion of the lean fuel gas mixture [9, 10]. The diesel injection spray is characterized by a package spray model that was first proposed by Hiroyasu et al. and extended by Stiesch [11, 12]. The premixed combustion is described by the entrainment model, originally proposed by Tabaczynski [13]. Furthermore, models for the ignition delay, as well as turbulence and flame propagation are included [9, 10]. The reaction kinetic NO-model by Pattas and Häfner was applied, which considers the NO formation based on N and N_2O [14].

The implemented submodels have variable input parameters. Typically, the spray- and turbulence-models are parameterized with measured spray data and CFD-simulation results. In this case, this data was unavailable and, therefore, all parameters of the submodels had to be adjusted simultaneously based on measured low and high pressure indications and raw emissions from a multi- and single-cylinder engine. The numerical optimization Software Optimus 10.18 from Noesis Solutions was used for this task.

Optimization of the Dual Fuel Combustion- and NO-Models

Start of combustion, position of 2% and 50% burned mass fraction, and fraction of burned fuel were compared to the experimental results and their deviation was minimized during the optimization process. To that purpose the Covariance Matrix Adaption – Evolution Strategy algorithm, a derandomized evolutionary optimization algorithm was applied [15]. This was carried out for 17 measured engine operating points with different loads,

injection timings, and relative air/fuel ratios. Fig. 2 illustrates the deviation between simulation and experiment with the optimized set of parameters. The numerical model generally represents the engine combustion process with good accuracy.

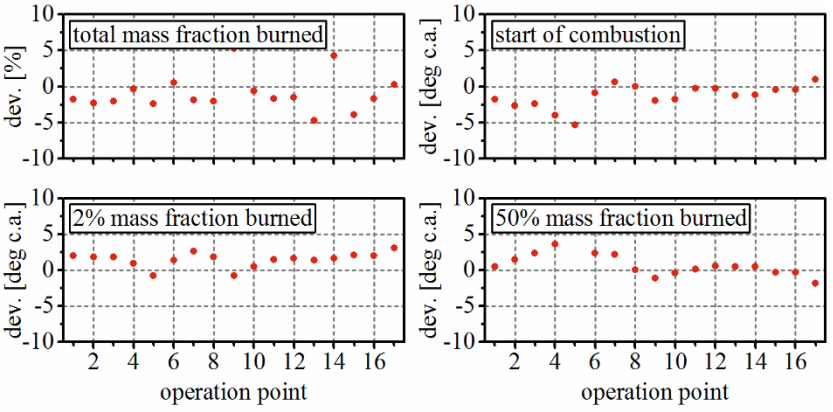

Figure 2: Deviation (simulation – measurement) of significant combustion parameters.

In Fig. 3, burn rates from the simulation are compared to measurement data. They correlate generally well and represent the variation of load, start of injection, and relative air/fuel ratio with good accuracy. The focus of the optimization was on low and part load that was of particular interest for the analyzed cylinder cut-out.

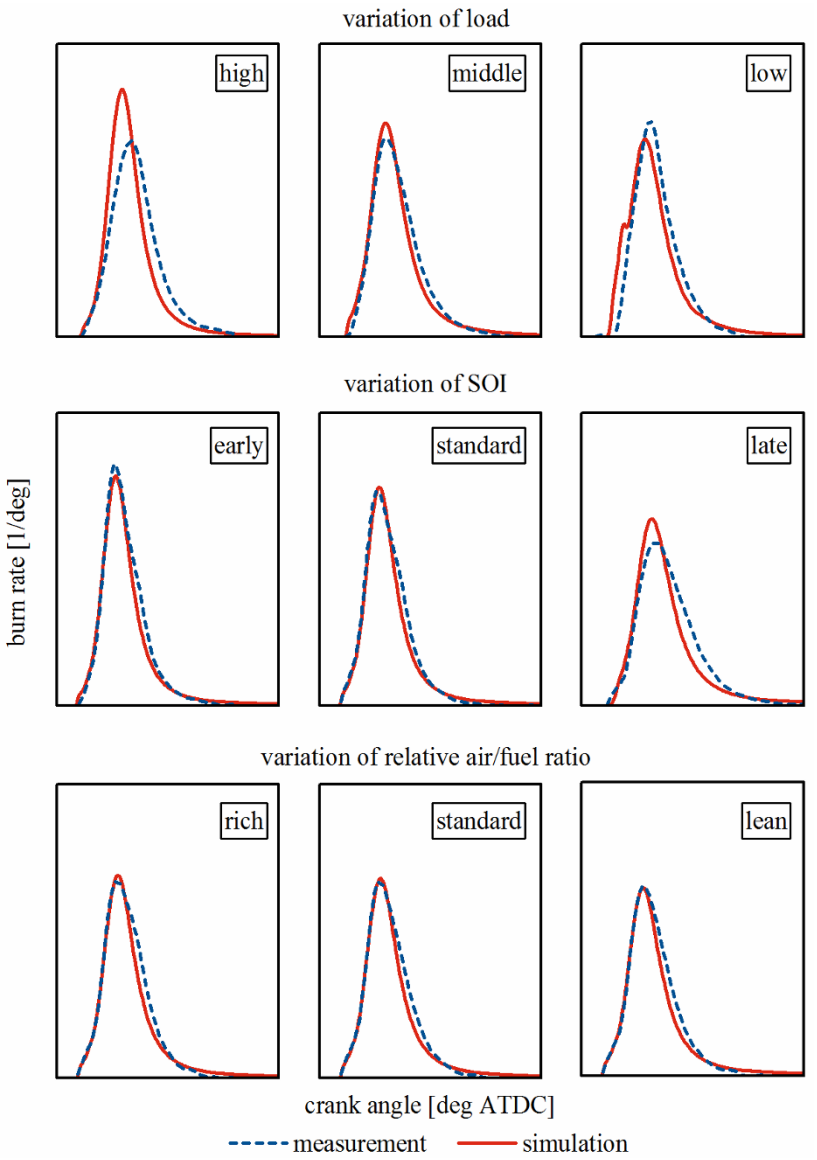

Figure 3: Comparison of simulated and measured burn rates for variation of load, injection timings, and relative air/fuel ratio.

The predicted NO emissions are related to the peak temperature that strongly depends on the fraction of diesel fuel and ignition delay. In Fig. 4, the normalized measured and simulated NO emissions are plotted for the considered engine operation points. Generally, the prediction of NO emissions was achieved with good accuracy.

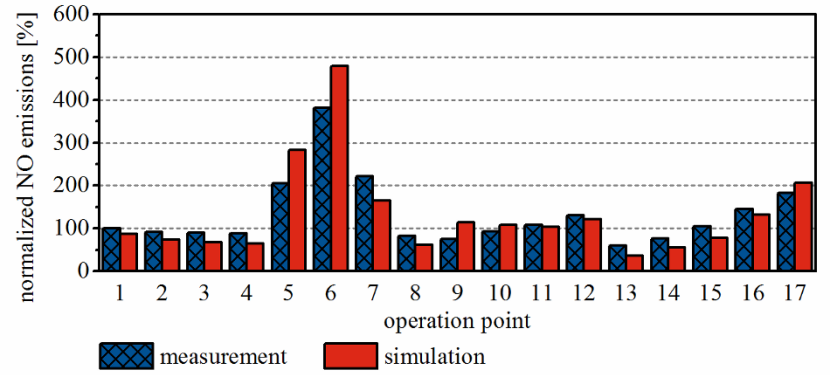

Figure 4: Normalized measured and simulated NO emissions.

The optimized dual fuel combustion model was implemented in the multi-cylinder engine model. A comparison of the measured and simulated pressure signals up- and downstream of two engine cylinders and upstream of the turbine are illustrated in Fig. 5 for a representative engine operation point. Good correlations, in particular with the data from the low and high pressure indication, were accomplished.

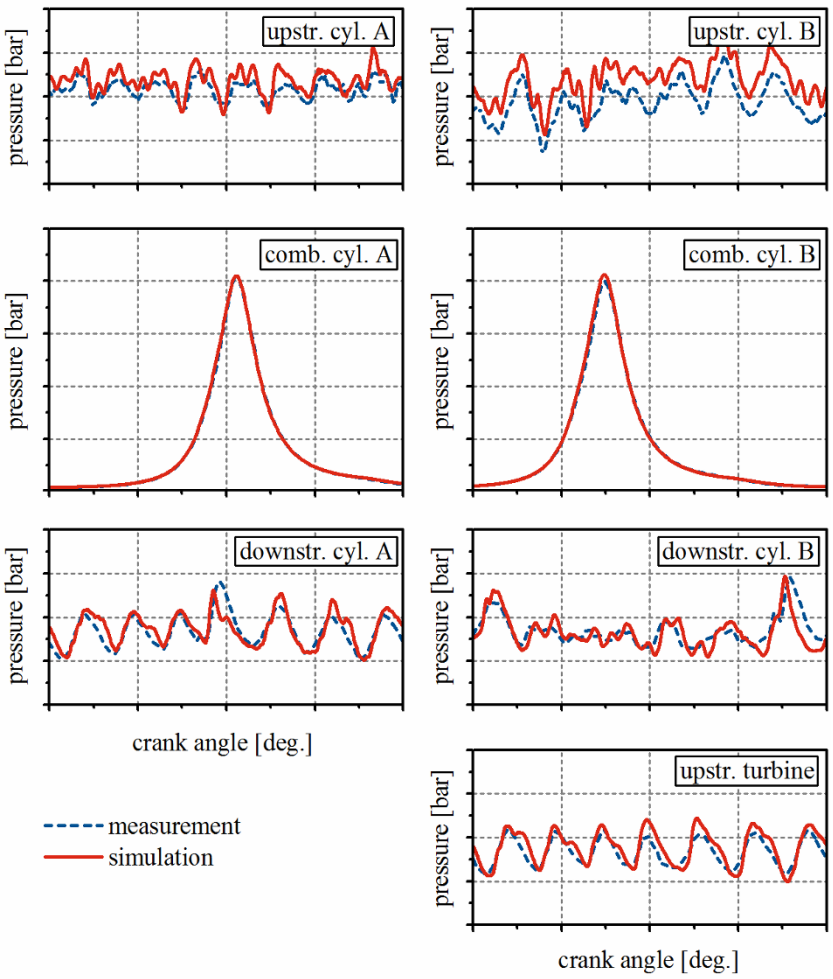

Figure 5: High and low pressure indication of a representative engine operation point.

Results of Engine Operation with Cylinder Cut-Out

The cylinder deactivation is analyzed for the static cylinder cut-out of one to three cylinders in parallel. Static cut-out means the permanent deactivation of cylinders. Thereby, the focus of the analysis is on fuel efficiency, NO emissions, and methane slip.

Load Range and Load Depending Results

The static cut-out is simulated for one to three cut-out cylinders at a constant relative air/fuel ratio. The resulting brake efficiency, NO emissions, and fraction of burned fuel are compared to the engine operation with all cylinders fired and are illustrated in Fig. 6.

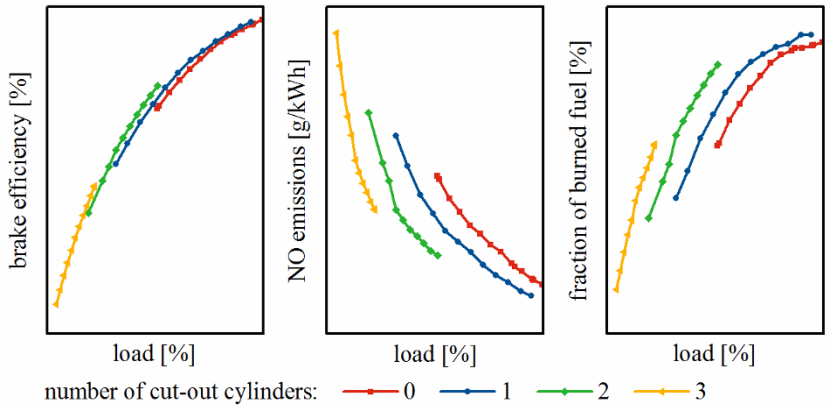

Figure 6: Brake efficiency, NO emissions, and fraction of burned fuel for load depending static cut-out of one to three cylinders at constant relative air/fuel ratio.

The graphs show that the load range where the cylinder cut-out can be applied is limited. Cylinders can be cut-out in low and part load. The lower margin depends on the flow area of the compressor bypass that restricts the air mass flow, see Fig. 1. The complete opening of the bypass defines the minimum air mass flow and, as a result, the lower load margin. The upper limit depends on the turbocharger that determines the maximum air mass flow. Both margins additionally depend on the relative air/fuel ratio. To expand the load range up- or downwards, a richer or leaner ratio has to be applied. Furthermore, the simulation results show the low load restriction of the complete fired engine. This consequently depends on the prescribed relative air/fuel ratio and the compressor bypass.

With the cut-out of one to three cylinders, the brake efficiency rises. Additionally, the cylinder cut-out leads to decreased NO emissions and an increased fraction of burned fuel, which can be linked to a reduced methane slip. These effects grow with the number of cylinders cut-out. An analysis of the underlying mechanisms is presented for a selected engine operation point.

Results of a Selected Engine Operation Point

Due to the cylinder cut-out, the load is shifted to the remaining fired cylinders. This is depicted in Fig. 7 for static cut-out, constant load, and relative air/fuel ratio. The peak pressure of the fired cylinders is increased by approx. 25% for two cylinders cut-out. The peak pressure of the cut-out cylinders equals the compression pressure and is therefore noticeably reduced compared to the fired cylinders. Both, the pressure of fired and deactivated cylinders increases with the number of cut-out cylinders. This is based on the distribution of load to a reduced number of fired cylinders that have to provide an increased load share. Consequently, the elevated charge air pressure leads to raised compression pressures of the cut-out cylinders.

The indicated mean effective pressure (IMEP) of the fired cylinders is increased by approx. 45% for two cylinders cut-out. The deactivated cylinders show a negative IMEP as a consequence of their pumping work.

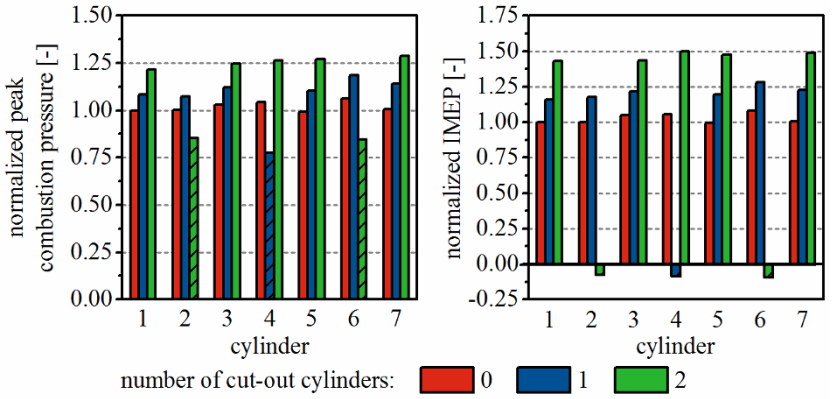

Figure 7: Normalized peak pressure and IMEP for static cut-out cylinders, constant load, and relative air/fuel ratio.

The effects on efficiency, NO emissions, and the fraction of burned fuel are illustrated in Fig. 8. Here, the engine operation is performed with constant load and relative air/fuel ratio. Due to the static cut-out of two cylinders, the brake efficiency is increased by more than 4%. Further, the NO emissions are reduced by 50% and the fraction of burned fuel is raised by more than 3%.

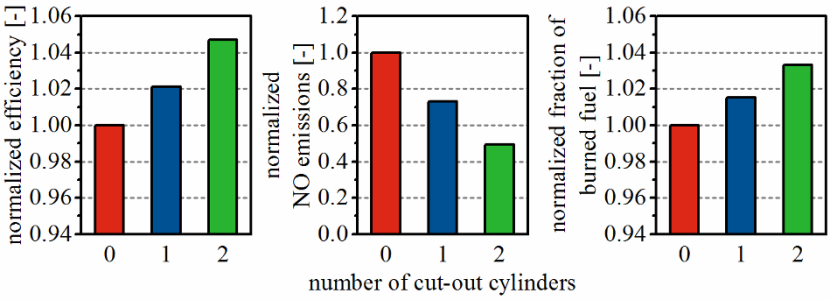

Figure 8: Efficiency, NO emissions, and fraction of fuel burned for static cut-out at constant load and relative air/fuel ratio.

The increased efficiency and reduced methane slip are based on several effects that are depicted for static cut-out in Fig. 9.

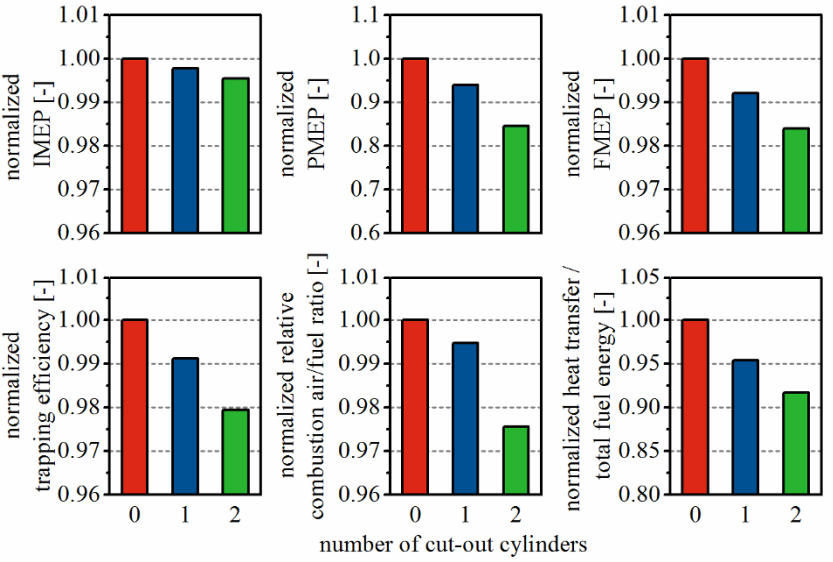

Figure 9: IMEP, PMEP, FMEP, trapping efficiency, relative combustion air/fuel ratio, and heat transfer / total fuel energy for static cut-out at constant load and relative air/fuel ratio.

The cylinder cut-out leads to less friction loss (friction mean effective pressure, FMEP) and ultimately to a reduced IMEP at a constant brake mean effective pressure (BMEP). Furthermore, the pumping mean effective pressure (PMEP) is lowered due to the elevated charge air pressure and scavenging gradient. The reduced trapping efficiency demonstrates the increased scavenging gradient.

The oxygen partial pressure of the resulting increased fraction of scavenging air and of the scavenged exhaust gas are detected by the lambda sensors downstream of the fired cylinders and applied for gas admission control. Consequently, to compensate the increased scavenging air mass and thereby maintain the operation of the fired cylinders at a defined relative air/fuel ratio, the combustion is shifted to rich, see Fig. 9. The rich combustion contributes, together with the elevated cylinder individual IMEP, to the increased fraction of burned fuel.

Furthermore, the cylinder cut-out results in a lowered fraction of wall heat loss. This is based on the reduced total wall surface of the fired cylinders.

Due to the cylinder cut-out, reduced NO emissions are achieved. At low load, the relative amount of the diesel pilot is enhanced to ensure a stable combustion. This causes higher peak temperatures due to the instantaneous combustion of the evaporated diesel fuel after the ignition delay. The increased IMEP of the remaining fired cylinders enables a reduced fraction of diesel pilot. Thus, the combustion is shifted from a partial diesel combustion towards a largely premixed combustion, which results in reduced peak temperatures and NO emissions. The corresponding burn rates of a selected cylinder for zero to two cylinders static cut-out, constant load, and relative air/fuel ratio are depicted in Fig. 10. Additionally, the average peak temperatures of the fired cylinders are illustrated.

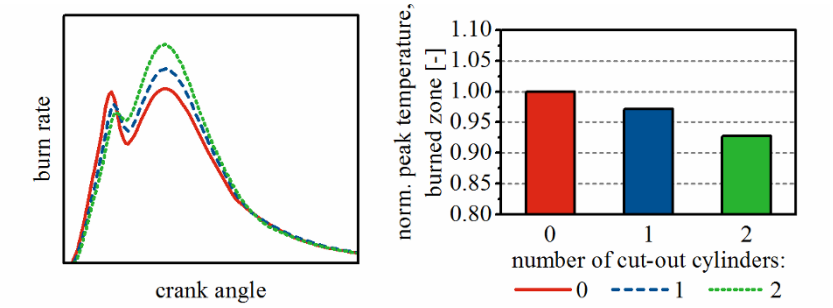

Figure 10: Burn rates and peak temperature for static cylinder cut-out, constant load, and relative air/fuel ratio.

The cylinder cut-out leads to increased air mass flow and charge air pressure. Thus, the exhaust gas enthalpy is elevated and the turbocharger's rotational speed as well as the pressure ratio increase. The compressor operation is shifted to distinctive higher efficiencies, as depicted in Fig. 11 for the static cut-out of zero to two cylinders. Due to the reduced flow area of the bypass valve that restricts the air mass flow, the flow through the compressor is reduced, but its share directed to the cylinders is increased. The shift of the compressor and turbine operation point results in a raised turbocharger efficiency by approx. 35% for the static cut-out of two cylinders. This leads to an increased scavenging gradient, a reduced PMEP, and contributes to the raised engine efficiency.

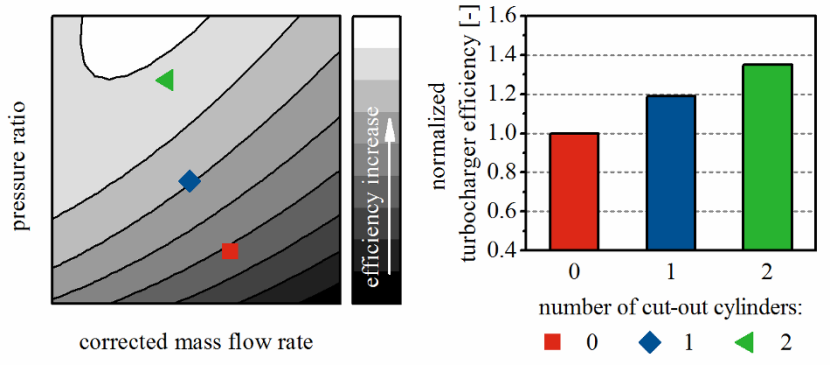

Figure 11: Compressor map and turbocharger efficiency for static cylinder cut-out, constant load, and relative air/fuel ratio.

Summary

The maritime industry has an increasing demand for efficient and mostly environmentally neutral propulsion systems to meet the strict environmental legislations and reduce the cargo costs.

Medium speed dual fuel engines are in accordance with the severe maritime emissions legislation IMO Tier III. They do not require any exhaust gas aftertreatment, show economic benefit due to the reduced fuel expenses, and allow fuel flexibility. Hence, they are a good solution to fulfil the demands of the maritime industry.

This paper addressed the problem of improving the engine efficiency and additionally reducing the NO and methane emissions by static cylinder cut-out in low and part load operation.

A predictive thermodynamic and fluid mechanic engine model that is able to perform the cut-out of selected cylinders is developed. The included combustion and NO-models predict crank angle depending burn rates and NO emissions. The models are optimized according to given engine operation points. A good correlation of the combustion rates and NO emissions with measured data is achieved.

The simulation model predicts a general increase of brake efficiency and a decrease of NO emissions as well as methane slip with cylinder cut-out. At a specific operation point, the efficiency is increased by more than 4%, NO emissions are decreased by 50%, and the fraction of burned fuel is raised by more than 3%. The efficiency increase depends on the increased turbocharger efficiency, reduced pumping work, less friction loss, reduced wall heat loss, richer combustion, and the increased fraction of burned fuel. Thus, an improved combustion and engine efficiency are achieved. The methane slip can be reduced due to an increased fraction of burned fuel. The decrease in NO emissions is mainly caused by the shift from partial diesel combustion towards a largely premixed combustion with lowered peak temperatures due to the reduced fraction of diesel pilot. These effects rise with the number of cylinders that are cut-out.

Outlook

The discussed work provided a detailed insight in the static cylinder cut-out, the effects on engine and combustion efficiency, NO emissions, and methane slip. The further work will concentrate on skip-firing, a dynamic cylinder cut-out method. Moreover, the relative air/fuel ratio will be adjusted to optimize the engine efficiency, considering NO emissions and knock limits.

Acknowledgements

This project has received funding from the European Union’s Horizon 2020 research and innovation programme under grant agreement No 634135.

References

[1] Karim, G.A.: Dual-fuel diesel engines. CRC Pres, 2015.

[2] International Maritime Organization: MARPOL Annex VI. Regulations for the prevention of air pollution from ships and the NOx Technical Code, 2008.

[3] International Maritime Organization: Resolution MEPC.286(71) – amendments to Marpol Annex VI, MEPC 71, 2017, London.

[4] US Department of Energy: Annual Energy Outlook 2017 with projections to 2050, https://www.eia.gov/outlooks/aeo, accessed Aug. 2017.

[5] Younkins, A.; Serrano. J.; Fuerst, J.; Schiffgens, H.-J.; Kirwan. J.; Fedor, W.: Dynamic Skip Fire: The Ultimate Cylinder Deactivation Strategy, 38. Internationales Wiener Motorensymposium 2017, 2017, Wien.

[6] Middendorf, H.; Theobald, J.; Lang, L.; Hartel, K.: The 1.4-L TSI Gasoline Engine with Cylinder Deactivation, Springer, Motortechnische Zeitschrift, Volume 73, 3/2012.

[7] Klimstra, J.; Hatter, C.; Nylund, I.; Sillanpää, H.: The Technology and Benefits of Skip-Firing for Large Reciprocating Engines, ASME Internal Combustion Engine Division, 2005 Spring Technical Converence, 2005, Chicago.

[8] Lilijenfeldt, N.: Active cylinder technology in Wärtsilä engines, 28th CIMAC World Congress 2016, 2016, Helsinki.

[9] LEC GmbH: EU Project Hercules-C internal: Zusammenarbeit LEC/TU Graz – MAN D&T. Abschlussmeeting, December 2014.

[10] Krenn, M.; Redtenbacher, C.; Pirker, G.; Wimmer, A.: A new approch for combustion modeling of large dual-fuel engines, 10. Internationale MTZ-Fachtagung: Heavy-Duty-, On- und Off-Highway-Motoren, 2015, Speyer.

[11] Hiroyasu, H.; Kadota T.; Arai M.: Development and Use of a Spray Combustion Model to Predict Diesel Engine Efficiency and Pollutant Emissions, Bulletin of the JSME, Vol. 26, No. 214, 1983.

[12] Stiesch, G.; Merker, G.P.: A Phenomenological Model for Accurate and Time Efficient Prediction of Heat Release and Exhaust Emissions in Direct-Injection Diesel Engines, SAE Paper 1999-01-1535, 1999.

[13] Tabaczynski, R.; Ferguson, C.; Radhakrishnan, K.: A Turbulent Entrainment Model for Spark-Ignition Engine Combustion, SAE Paper 770647, 1977.

[14] Pattas, K.; Häfner, G.: Stickoxidbildung bei der ottomotorischen Verbrennung, Springer, Motortechnische Zeitschrift, Volume 34, 12/1973.

[15] Hansen, N.; Müller, S.; Koumoutsakos, P.: Reducing the Time Complexity of the Derandomized Evolution Strategy with Covariance Matrix Adaptation (CMA-ES), Evolutionary Computation 2003 Volume 11 Issue 1 Pages 1-18, MIT Press Cambridge MA USA, 2003.

Upgrading EU Stage III B engines to achieve EU Stage IV

Dominik Lamotte

Klaus Schrewe

Ingo Zirkwa

W. Siebenpfeiffer (Hrsg.), *Heavy-Duty-, On- und Off-Highway-Motoren 2017*,
Proceedings, https://doi.org/10.1007/978-3-658-21029-8_15

Introduction

Despite the current public debate, there will be no substitute for all diesel applications within the coming decades. Energy density, availability and storage property of the diesel fuel are only some reasons for this. On the other hand, immission limits are often exceeded in metropolitan areas. To achieve improved air quality a reduction of emission for all types of diesel engines is required by several regulations[1].

In the Off-Highway segment the main challenge in the last years was the implementation of the emission regulations EU Stage III B and EU Stage IV in 2012 and 2014, respectively. The introduction of two emission stages in such a short period forced the manufactures of engines and mobile machines to use a large share of their development capacities to secure the fulfilment of the latest emission legislation.

While EU Stage III A often was achieved by internal engines measures, from 2012 on complex aftertreatment systems (ATS) had to be introduced for EU Stage III B applications. At this point, mainly two different strategies were possible:

1. Optimizing the engine regarding NO_x emission and introduction of an ATS for particle reduction like Diesel Oxidation Catalyst (DOC) and / or Diesel Particulate Filter (DPF)
2. Optimizing the engine regarding particulate emission and introduction of an ATS for NO_x reduction like Selective Catalytic Reduction (SCR)

With regulation EU Stage IV NO_x emission limits were reduced drastically[2], which implied the need of NO_x aftertreatment systems. Meeting the EU Stage IV emission limits seemed to be an enormous technical challenge for many engine manufactures, especially for those who decided for particulate filter strategy for EU Stage III B because they had to manage a technology transition within less than 3 years' time. For that reason, the EU Non-Road Directive 97/68/EC included a flexibility scheme[3], to give the engine and machinery constructors additional time they needed to execute this switchover. With this scheme the OEMs were allowed to place applications complying EU Stage III B with, for example, engines between 75 kW and 130 kW, on the mobile machinery market until 2017.

1 Reg EC No: 595/2009 and implementing regulations (EU) No 582/2011 and 64/2012) Schmid, J.: Baumaschinentechnik im Aufbruch. Fachtagung Baumaschinentechnik 2012, TU Dresden

2 11 / 2011, VDMA-Broschüre "Abgasgesetzgebung Diesel- und Gasmotoren"

3 N. N.: Merkblatt zum Flexibilitätssystem der Richtlinie 97/68/EHG (MFLEXI). KBA, Flensburg, Dezember 2010

Many manufacturers used this possibility by stockpiling what were known as pre-built engines. The quantity of required pre-built engine was estimated based on their calculations on the statutory restrictions on the permissible number of units and their own production figures from previous years. In 2014 the number of new registrations of tractors in Germany dropped by 4 % compared to the average over the previous three years. This deficit rose up to 20.5 % in 2016[4]. Due to these market data many OEMs must have a huge surplus of pre-built engines in their warehouses.

In light of the situation of pre-built engines this paper describes an upgrade of the existing EU Stage III B system (incl. engine and ATS) by replacing the originally installed ATS with a more sophisticated one. As part of this replacement the control unit of the ATS was exchanged as well. With both measures an upgrade of the system in compliance to EU Stage IV regulation was achieved.

Emission Limits

The emission limits were continuously reduced from Stage EU III A to EU Stage IV (Table 1). While the requirements to achieve EU Stage III A were mostly fulfilled by internal engine measures the introduction of complex aftertreatment systems was mandatory to achieve EU Stage III B limits. Complying with EU Stage IV NO_x emissions for engines in a power category from 56 kW to 130 kW were further reduced by approx. 88 %.

Table 1: European emissions limits for EU Stage III A to EU Stage IV

Engine performance [kW]	EU Stage III A				EU Stage III B				EU Stage IV			
	NO_x [g/kWh]	HC [g/kWh]	CO [g/kWh]	PM [g/kWh]	NO_x [g/kWh]	HC [g/kWh]	CO [g/kWh]	PM [g/kWh]	NO_x [g/kWh]	HC [g/kWh]	CO [g/kWh]	PM [g/kWh]
19–37	7.5		5.5	0.6	7.5		5.5	0.6	7.5		5.5	0.6
37–56	4.7		5	0.4	4.7		5	0.025	4.7		5	0.025
56–75	4.7		5	0.4	3.3	0.19	5	0.025	0.4	0.19	5	0.025
75–130	4		5	0.3	3.3	0.19	5	0.025	0.4	0.19	5	0.025
130–560	4		3.5	0.2	2	0.19	3.5	0.025	0.4	0.19	3.5	0.025

Original Stage III B Application

The original Stage III B application, in this case a tractor application, was established for five different power ratings (81 kW, 89 kW, 96 kW, 110 kW, 129 kW) in two different chassis variants. As the base engine was identical for all variants, only the two

4 Knechtges, H.; Renius, K. Th.: Gesamtentwicklung Traktoren. In: Jahrbuch Agrartechnik (2016), pp. 1-10

highest power ratings were installed in the vehicle with the bigger chassis. As a consequence of different track widths of the tractors there are two different connection pipes to satisfy chassis variants.

The Stage III B aftertreatment system consists of:

– SCR-System
– AdBlue® dosing and supply module
– Connection pipe
– Temperature & NO_x sensors
– Dosing control module (DCM)

The DCM is responsible for the sensors and the AdBlue® dosing and supply module. The DCM reads in the sensor values for temperature and NO_x and sends them to the engine control module (ECM) via CAN-Bus. Based on these values and additional internal information the ECM calculates the AdBlue® dosing amount and sends it back to the DCM. The DCM triggers the AdBlue® dosing and supply module to inject the correct amount of AdBlue® into the exhaust system.

In case of any disfunction or misuse the ECM detects this failure and starts the warning system (visualisation in display) and triggers based on the strategy the inducement. The detection could appear by sending a malfunction of sensors, e.g. NO_x sensor, from the DCM to the ECM or by comparing the expected NO_x emission with the NO_x sensor value by the ECM itself. The inducement system is split – based on the NO_x Control Regulations (NCD) requirements – into low level (max. 75 % torque) and severe inducement (max. 50 % torque and 60 % remaining rpm).

EU Stage IV Aftertreatment Solution

System Integration and Signal Communication

To achieve the requirements for EU Stage IV a higher NO_x conversion rate is necessary. Due to missing access to the ECM it is not possible to modify this parameter. In addition, further sensors are required to achieve the NO_x conversion rate (e.g. NO_x sensor upstream SCR) (Figure 1). For these reasons the HJS aftertreatment control unit (ACU) is used for the application. The ACU takes over all functions for the control of the ATS, in particular the AdBlue® dosing strategy.

For the former EU Stage III B ATS the ECM expected a feedback of operation status and specific values, like current dosing amount, from the DCM. For the Stage IV ATS the ACU controls the dosing system with different specific values, e.g. higher dosing amount. Therefore, the ACU has not only the task to control the complete system. Furthermore, it generates an expected feedback to the ECM. In case of malfunction or

misuse a signal is sent, which forces the ECM to execute the correct warning and inducement system as requested for EU Stage IV.

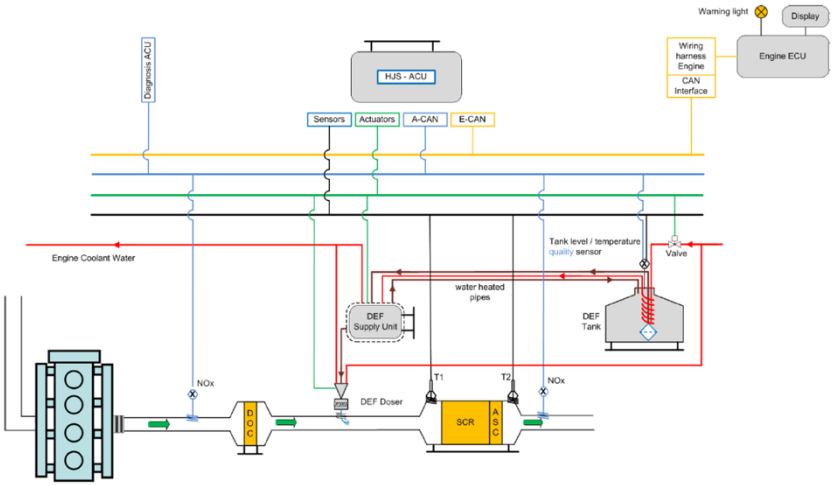

Figure 1: Communication concept for EU Stage IV aftertreatment system

New Exhaust Aftertreatment Design

To achieve the ambitious requirements for EU Stage IV following changes in the hardware of the ATS were done:

– Integration of a close coupled Diesel Oxidation Catalyst (DOC)
– Substitution of the current SCR catalysts with an advanced SCR technology

The new ATS had to substitute the existing SCR-System without significant dimensional modifications of the packaging environment. The DOC was integrated under the hood of the tractor. The outer geometry of the previous SCR catalyst was kept and substrates with an advanced SCR technology were integrated (Figure 2). With the new hardware configuration and the changed control system, the engineering target was set by an NO_x emission reduction of 90 %.

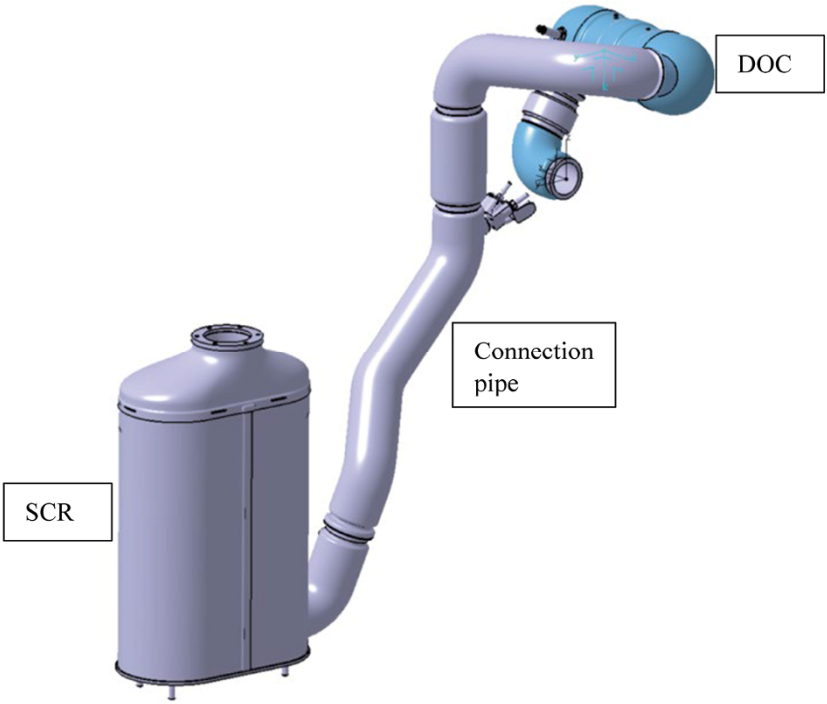

Figure 2: Aftertreatment system including DOC, connection pipe and SCR

The two different connection pipes from chassis variants have been redesigned and are identical for the important section of the injection zone of AdBlue® (Figure 3).

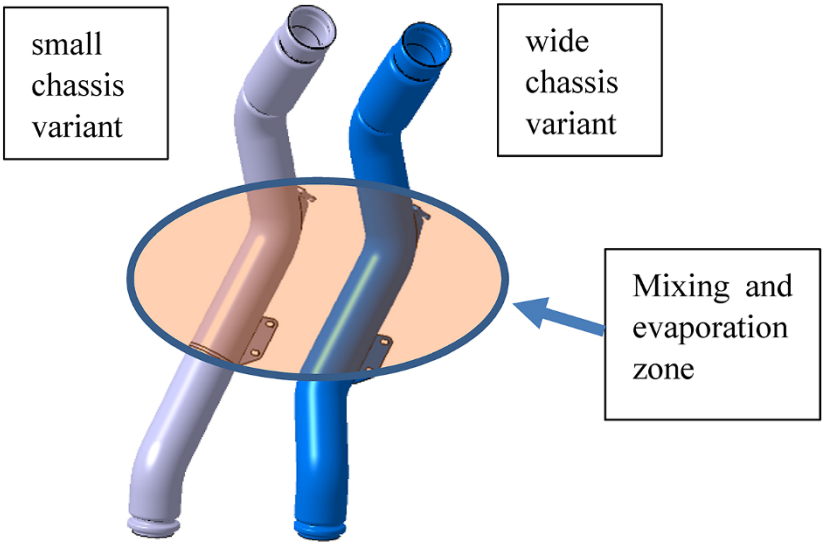

Figure 3: Variant in connection pipe, depending on tractor configuration

As an example, the simulation results for flow und ammonia distribution at the inlet of the SCR system are given for one connection pipe variant. Figure 4 shows the simulation for two representative engine load points, full load and partial load. All results demonstrate an excellent uniformity index to allow high NO_x conversion rates. The simulation was done for the other downpipe variant as well and the results were comparable. Based on these results, the above marked area is the important zone to achieve high quality in mixing and evaporation.

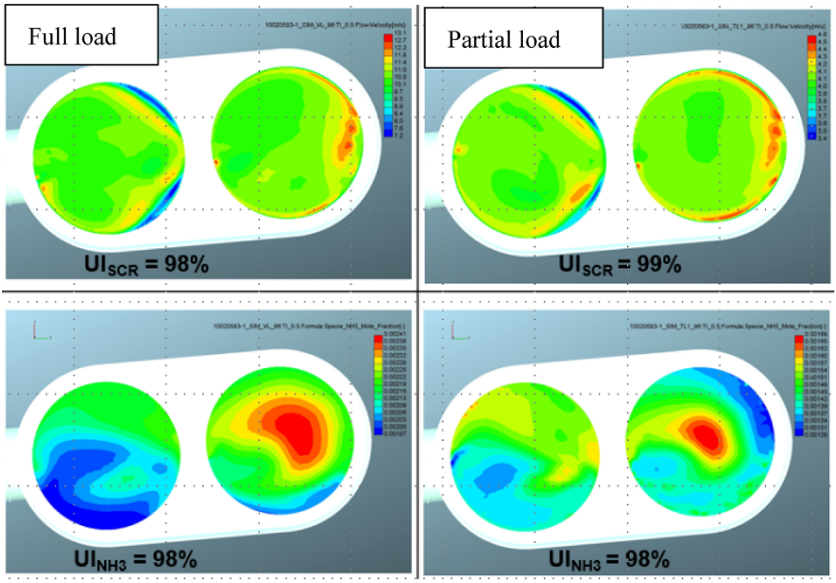

Figure 4: Uniformity of flow and NH_3 for different engine load points

Certification

Emissions

To comply with the EU Stage IV regulation (0.4 g/kWh NO_x in NRSC and NRTC) a high conversion rate of approx. 97 % in NO_x emission is needed. For choosing the right combination of DOC and SCR the following characteristics of the SCR system are from major importance:

– Ammonia storage capacity
– NO_x conversion rates as a function of temperature, ammonia storage level, NO_2 concentration
– Mechanical robustness for agriculture conditions.

Based on these parameters and the raw emissions data recorded on the engine test bench (Figure 5) suitable catalyst technologies were chosen. The characteristics of the catalyst measured on the model gas test bench were used as input data for the parameter set of the ACU at the engine test bench. Owing to the high temperature levels at rated power output in the NRSC cycle (Figure 5) the usage of Fe zeolite SCR technology was

initially considered, but discarded after measuring the enhanced low-temperature activity of high temperature stabilised vanadia-based (V_2O_5) SCR catalysts.

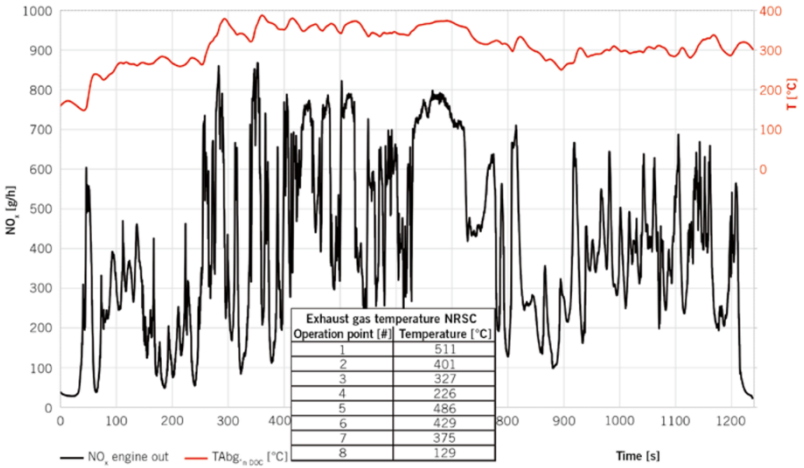

Exhaust gas temperature NRSC	
Operation point [#]	Temperature [°C]
1	511
2	401
3	327
4	226
5	486
6	429
7	375
8	129

Figure 5: Exhaust gas temperatures and NO_x raw emissions for NRTC warm
Table: Exhaust gas temperatures for NRSC

During the engine test bench investigation, the parameters of the ACU were optimised based on the dynamical behaviour of the ATS, like NO_2 conversion, heating up and cooling down behaviour as well as ammonia storage level. With this adjusted set of parameters, the emission limits for NRSC and NRTC were achieved. After 300 s in the NRTC warm (Figure 6) the conversion rate of NO_x was close to 99 %. Based on this configuration the NO_x emission in the combined NRTC the engineering target was achieved.

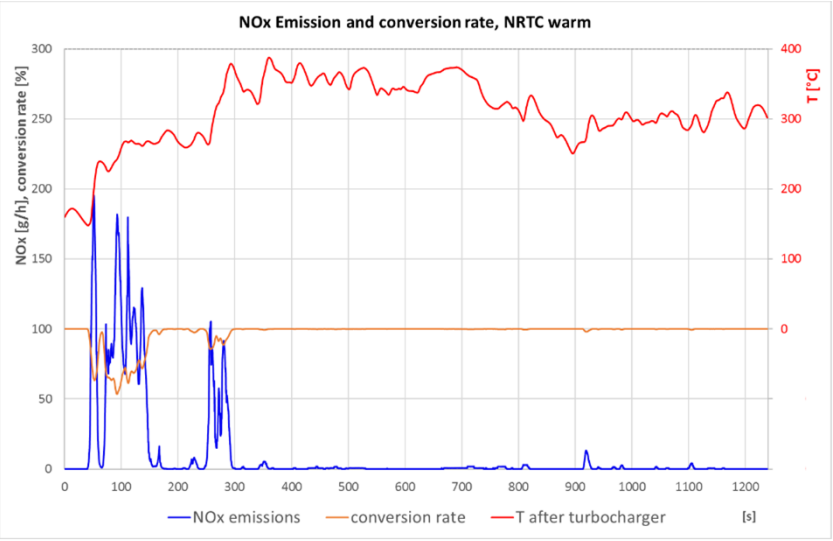

Figure 6: NO_x conversion rate in NRTC warm

NO_x Control Diagnostic (NCD)

EU Stage IV requires a warning and inducement system of the engine in case of any malfunction or mis-usage relating to NO_x emission. Required inducements are still executed by the engine control unit Does any malfunction occur, which is detected by the ACU, the ECU will receive the appropriate signal to start inducement. As an example, the temperature sensor downstream SCR system was dismounted. The ACU detected the missing sensor and set the signal to “malfunction” as an operating status to the ECM. Based on this information the ECM started the warning and inducement system which ends in derating the engine power.

Defreezing Test

To achieve a EU Stage IV certification, it is mandatory to set-up a heating concept in case of impossible injection of AdBlue® due to frozen AdBlue®. For this situation the regulation demands a defrosting of the complete system. After a duration of maximum 70 min the system has to be able to inject AdBlue®. In this application the cooling system of the engine is connected to the heating system of the AdBlue® tank by a three-way valve. This valve is controlled by the ACU. For certification the complete tractor was frozen at a test bench for 70 h at -18 °C. Complying to the regulation the engine

was idling for 20 min after starting, then 40 % load of the lowest engine power variant (81 kW) was used. Sufficient AdBlue® was defrosted after approx. 50 min and the complete system was ready for injection.

AdBlue® Quality

An additional requirement for EU Stage IV is the detection of too low urea concentration in AdBlue® which is specified to 32.5 %[5]. With reduced urea concentration the NO_x conversion will also be reduced. Therefore, the EU Stage IV regulation requires the declaration of a minimum concentration (CDmin). The NO_x emission in NRTC warm must not exceed 0.9 g/kWh when operating the system with CDmin. AdBlue® concentrations below CDmin have to be detected by the diagnostic system.

To ensure a correct concentration of AdBlue® tolerances have to be considered, in this case for production of AdBlue® and for the used AdBlue® quality sensor. To ensure a stable and robust set of parameters in the ACU the value for CDmin is set with enough gap to the value from tolerance consideration. With this CDmin the NRTC was conducted and passed the limits of 0.9 g/kWh.

After passing all certification tests, the tractor manufacturer becomes formally the engine manufacturer in front of the KBA with all the responsibilities like ‘Conformity of Production’ evidence.

5 12 / 2012: COMMISSION DIRECTIVE 2012/46/EU: amending Directive 97/68/EC of the European Parliament and of the Council on the approximation of the laws of the Member States relating to measures against the emission of gaseous and particulate pollutants from internal combustion engines to be installed in non-road mobile machinery

Summary

The existing Stage EU III B SCR system of two tractor platforms was replaced in order to recertify the engines for EU Stage IV. To achieve this, it was necessary to add a diesel oxidation catalyst (DOC) and to install an SCR catalyst with the latest SCR coating technology. Over that a new emissions treatment control unit (HJS ACU) with a sophisticated AdBlue® dosing strategy was implemented. With these measures, HJS succeeded in upgrading an engine that had originally been approved for EU Stage III B without changing the engine control module (ECM). With a NO_x conversion rate of higher than 97 % in NRTC and NRSC the required NO_x emission limits were achieved. After the achievement of the other parts of the certification: NCD, defreezing test and AdBlue® the tractor manufacturer becomes formally the engine manufacturer in front of the federal certification authority (like KBA) with all the responsibilities like 'Conformity of Production' evidence.

Oil system optimization of HD diesel engines

Dr. Simon Schneider
MAHLE International GmbH

Holger Conrad
MAHLE Filtersysteme GmbH

Geno Marinov
MAHLE Powertrain GmbH

W. Siebenpfeiffer (Hrsg.), *Heavy-Duty-, On- und Off-Highway-Motoren 2017*,
Proceedings, https://doi.org/10.1007/978-3-658-21029-8_16

1 Introduction and state of the art

At the present time, there is no legal regulation in Europe for the fuel consumption or CO_2 emissions of diesel engines in heavy-duty commercial vehicles, unlike as for passenger cars. The European Union is now monitoring current truck CO_2 emissions using the VECTO[1] tool, however, so that data will be available as a basis for future regulations. Fuel consumption is also one of the most important features of a truck, as it largely determines the operating costs.

The oil circuit in a combustion engine affects measures for fuel savings through two mechanisms: firstly, the power for driving the oil pump forms part of the friction of engine auxiliaries, and secondly, the oil supply to engine components influences the friction of those components, due, for example, to the temperature and mass flow of oil at the point of consumption, but also to any splashing losses when the oil supply is very high.

The oil pump in a commercial vehicle engine is currently directly coupled to the engine and cannot be controlled, although variable systems are in use in the passenger car sector. The temperature of the oil is often influenced by means of a thermostat, which controls whether a heat exchanger is engaged between the oil and engine coolant. In most cases, oil is provided to all consumers at the same temperature and pressure level.

The objective of the following investigation is to identify and quantify the potential of variable components in the oil circuit of a commercial vehicle engine with respect to fuel savings and oil change intervals. This will be used to define the most promising alternative topologies for the oil circuit.

1.1 Current structure of the HD diesel oil circuit

The oil circuit serves two major purposes in a combustion engine:

- Lubrication of moving components, in order to keep friction low and avoid wear (Affenzeller 1996)
- Heat dissipation from engine components (friction heat or other heat inputs to the components)

The engine oil can also be used as a hydraulic fluid, for example, for cam phasers in the valve train, switchable rockers, or hydraulic valve lash compensation. In a typical commercial vehicle engine (13 L displacement, 6-cylinder diesel engine, Euro 6), the main consumers in the oil circuit are piston cooling, lubrication of plain bearings in the crank train and valve train, and supply to auxiliary consumers (turbocharger, gear drive, and

1 Vehicle Energy Consumption Calculation Tool

possibly others)—see Figure 1. This engine is also the research engine for all other investigations shown in this publication.

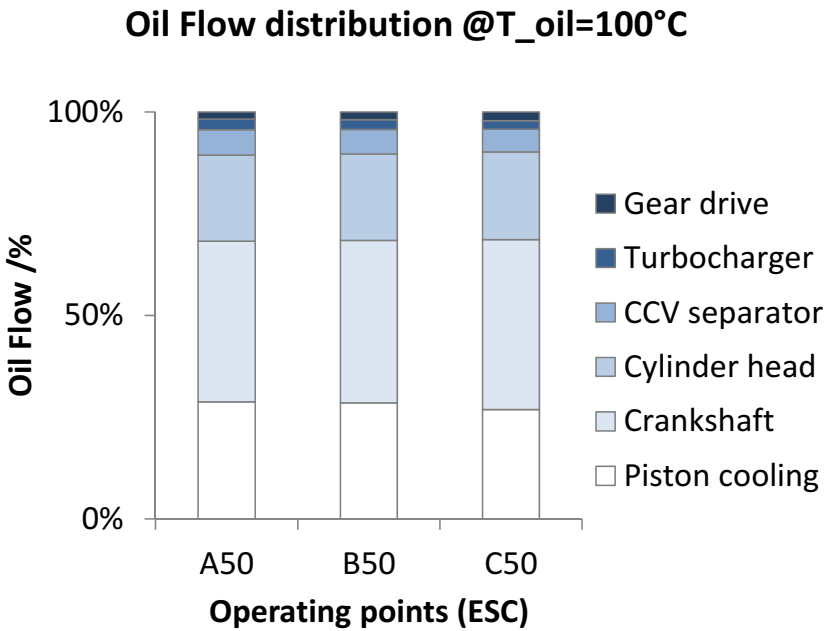

Figure 1: Main consumers in the oil circuit for 50% load points at A, B, and C speeds of the ESC cycle in a commercial vehicle engine.

1.2 Fuel savings potential through variability

The consumers have a characteristic flow rate behavior in the engine operating map. Together with the characteristic curve of the oil pump, this results in a system working point for each engine operating point, characterized by a pressure and a volumetric flow rate. For a positive displacement pump, this results in an oil pressure operating map, for example, as is shown in the top left of Figure 2. As the pump speed increases, it supplies higher oil pressure with only a slight increase in volumetric flow rates. At various load points for an engine speed, the oil pressure is virtually constant. For the consumer "piston cooling", an oil mass flow with a defined relationship to the engine power output is desirable. This is perfectly achieved under full load, but for partial loads this consumer is oversupplied. The current state is not optimal for fuel consumption (Figure 2, top right). In order to achieve optimal supply for this consumer, very different oil pressures

at the same speed, depending on the load, would be sensible (Figure 2, bottom left). This would allow the optimal requirements for this consumer to be fulfilled over a large portion of the operating map (Figure 2, bottom right).

In order to operate the entire oil circuit optimally, the operating limits of all consumers must be known. Consideration of these limits results in the least possible permissible oil delivery rate.

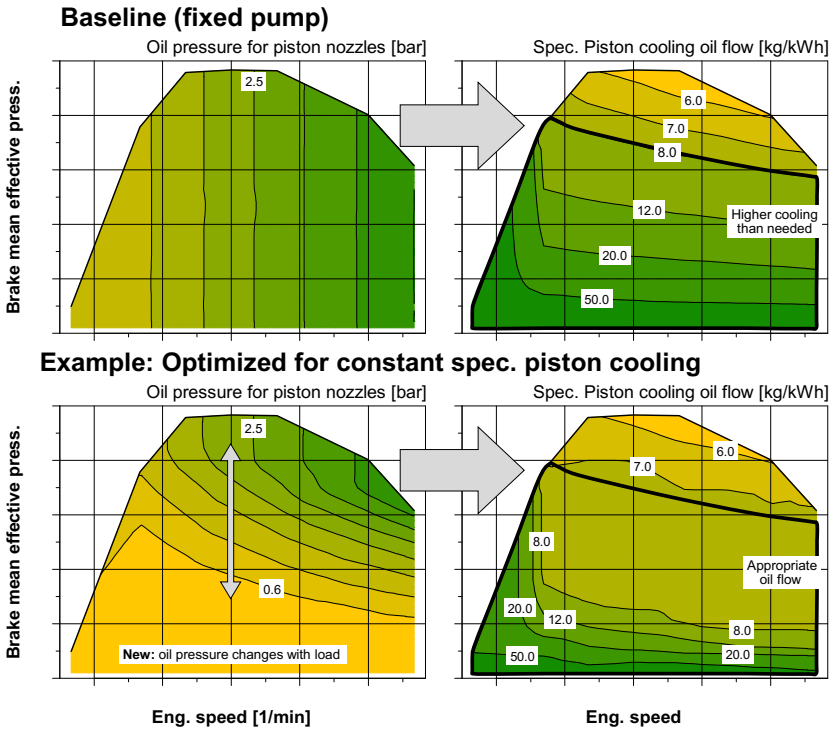

Figure 2: Optimization example—optimal oil volume for piston cooling

1.3 Investigation approach of the oil circuit at MAHLE

The MAHLE product range includes many components throughout the oil circuit. This offers excellent conditions for the assessment of the system as a whole using expertise in individual components. As part of this initiative, activities were undertaken in various fields to examine the oil system by means of simulations and testing (Figure 3). This

includes simulation of individual components in 1D flow simulation and EHD calculations, investigation of assemblies on component test stands, testing of the entire engine, and modeling the overall system as a 1D model.

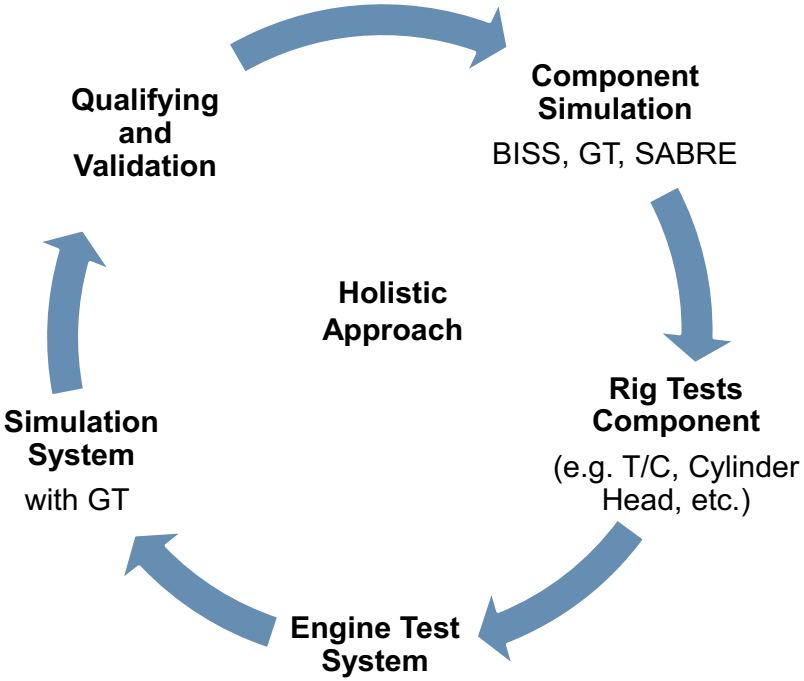

Figure 3: Holistic investigation of the oil system at MAHLE

1.4 Determining the overall power requirements for the oil circuit with direct measurement

MAHLE has investigated the power requirements for the oil system in its current form using a test engine. In order to freely set optimal pressures, several configurations were used (Figure 4). The engine was operated with the series production pump, a variable MAHLE pump, and an external variable oil supply.

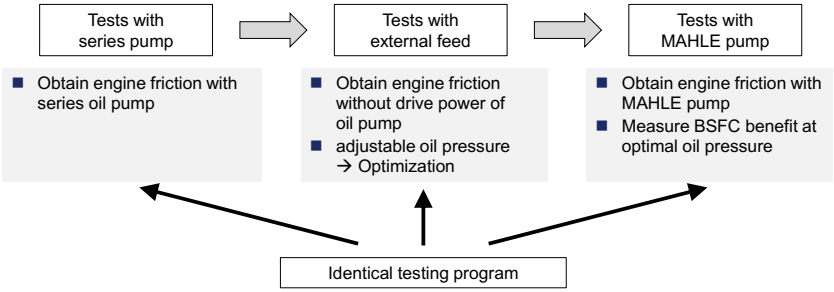

Figure 4: Configurations of the test engine

The comparison of the externally supplied engine with the series configuration provided the power consumption for operating the oil circuit. This can be influenced by optimizing the oil flow rates for all consumers and differs from engine to engine, depending on the initial state.

In the case of the HD diesel engine studied here (Figure 5), the total effort of the oil supply under medium loads ranges from 1% to 1.5% of fuel consumption. Near full load it is somewhat less. Because the effort is constant across the engine load, the relative effort increases significantly in near-idle range, so that in the range below 5 bar indicated brake mean effective pressure, the effort rises above 6% BSFC.

The tests were performed using a standard engine oil of 5W30 viscosity.

While the oil pump power to be provided in the near-full-load range is absolutely necessary for the engine to function, part of this effort can be saved in the partial- and low-load ranges.

The goal is to reduce the drive power to the oil pump without inducing any negative consequences (e.g., increased wear, premature oil aging, increased engine friction, impermissible component temperatures).

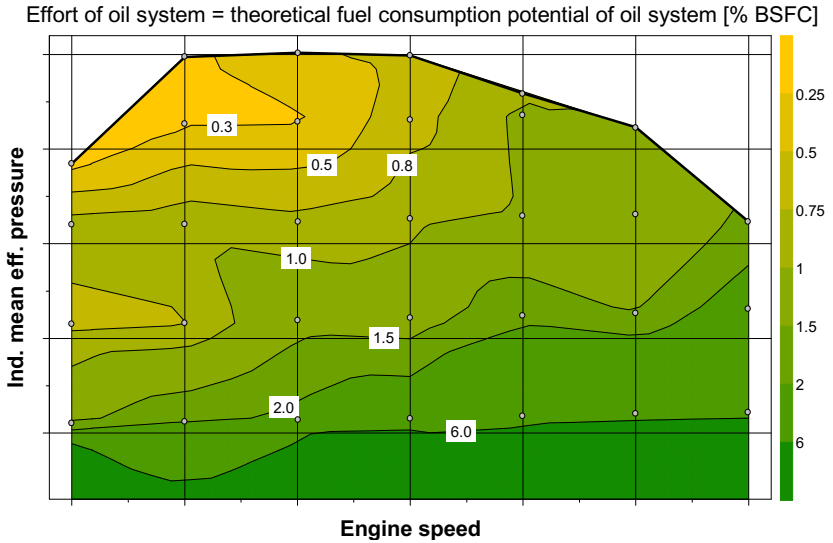

Figure 5: Total effort for operating the oil system

2 Minimum demand for engine oil mass flow

A prognosis of the minimum requirement for demand-based oil supply to engine components was developed across the engine operating map using numerical calculations.

2.1 Determining the minimum oil demand using simulations

For the study, the entire lubrication system was first modeled as a one-dimensional model using GT-SUITE. The computation model consists of resistances, lines, filters, throttles and nozzles, cross-sectional diameters, and characteristics of pump, consumers design, and lubrication parameters. The calculated volumetric oil flow rates from the series design were successfully correlated to test results at different oil temperatures and pressures and used as the basis for subsequent testing. The kinematic model for cylinder head and crank train was developed in particular detail in order to define as accurately as possible the minimum oil film thicknesses and pressures at the bearings under consideration of gas loads, inertia, and spring forces. The critical components were determined during this process.

These include the rocker arm bearing at the outlet in the valve train, for example, as well as the roller pins and all other contact points where maximum contact pressure

occurs in conjunction with minimum lubricating film thickness. For the oil volume flow simulation, the plain bearings in the crank train and valve train were given special attention, because they require between 60% and 65% of the total volumetric flow rate, depending on the engine speed and oil pressure (Figure 1).

For the main and conrod bearings, SABRE-TEHL software (**T**hermal-**E**lasto-**H**ydrodynamic **L**ubrication) was also used. This numerical computation is used for designing the bearing and includes conrod, crank pin, and engine block stiffness effects, conrod distributed mass inertia effects, and crank journal misalignment. The dynamic bearing clearance was thereby determined by the ancillary program SABRE-FIT as °CA for each bearing (Merrit, Mian 2013; Merrit, Haxha 2013; Kalogiannis 2017).

To evaluate the change in friction regime in the bearing after variation in pressure, the parameters such as minimum lubricating film thickness and pressure, contact pressure (solid-to-solid and asperity), bearing temperature, frictional losses (hydro and asperity), and film intensity x sliding velocity were used for the calculation. The objective was to predict the minimum oil feed pressure required to keep the bearing severity parameters within acceptable levels with respect to fatigue, seizing, and wear (cf. Knoll 2006).

In this context, special attention is required for pressure conditions in the crank drilling because the pressure increases parabolically from the inlet near the main bearing to the outlet at the crankshaft pin. With a CFD analysis for calculating the required oil pressure in the main engine gallery based on the minimum requirements at the bearing points and to prevent cavitation in the crank drilling to the conrod bearing (Eulerian multiphase model), the following reduction in oil pressure is recommended (Figure 6).

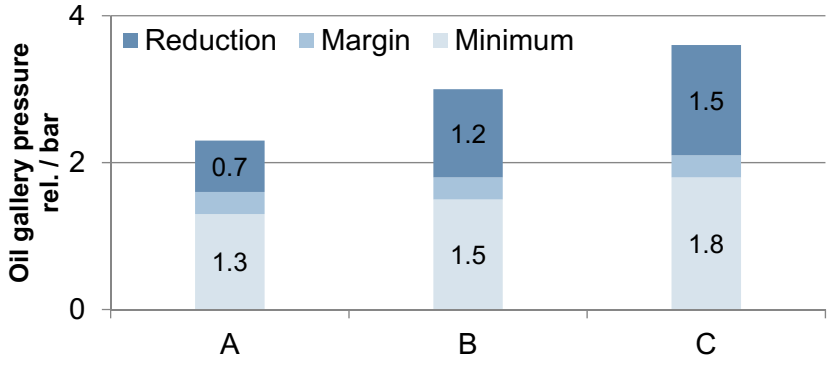

Figure 6: Recommended reduction in pressure for A, B, and C engine speeds in ESC cycle

As an example, Figure 7 shows the A speed of the ESC cycle, where, assuming 14% oil aeration, the first gas bubble formation is seen to occur at a critical reduction of the oil pressure by 1.6 to 0.8 bar. This results in a collapse in pressure in the feed bore to the conrod bearing.

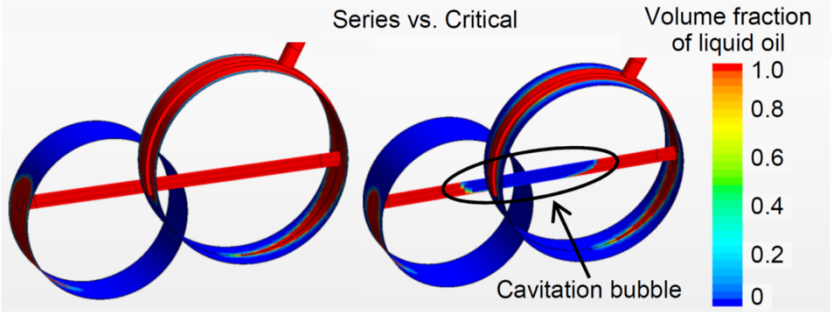

Figure 7: Pressure collapse in the feed bore to the conrod bearing at A speed with critical oil pressure of 0.8 bar

The critical components in the crank train are the lower bearing shell of the main bearing and the upper bearing shell of the conrod bearing. For example, the loads on the conrod bearing consist of forces of up to 300 kN. Typical critical points on the conrod bearing are the edges of the top bearing shell and the point of the infeed bore, wherein the maximum contact pressure (MPa) and minimum oil film thickness (µm) were computed (Figure 8).

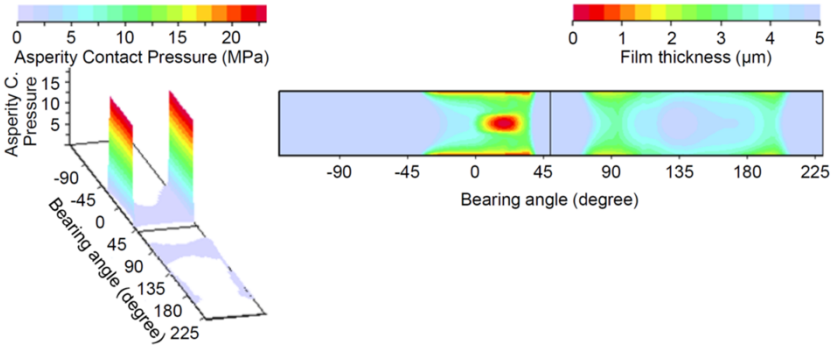

Figure 8: Critical zones of the conrod bearing at A speed and 160 bar PCP (left: contact pressure, right: minimum oil film thickness)

The advantage of a simulation model is that it gives the opportunity to vary parameters of the oil and the component design, as well as operating condition parameters (pressure and temperature, load, and speed) and to obtain an initial result for the behavior of the system. The prerequisite for this is good correlation of the basis to the test data.

2.2 Engine measurement at minimum demand, proof of potential limit

After the minimum demand was studied in the simulation, it was also tested in the engine as part of a functional test. Using an external oil feed, two partial circuits were provided with freely adjustable oil volumes: the piston cooling and the rest of the engine circuit. The turbocharger was fed with a constant supply in a separate circuit and was not considered in this variation. The oil supply was varied at selected operating points and the effects tested using suitable measurement parameters.

2.3 Minimum requirement for piston cooling

The oil required for piston cooling is well-known at MAHLE. As a measure of the effect of reduced oil supply, relevant piston temperatures and overall engine friction were evaluated because the friction in the piston group can change when piston cooling is very low. For example, thermal expansion of the piston can reduce clearances.

In comparison with the tight limits for the base engine, the oil supply for piston cooling can presumably be lowered significantly. Therefore, a conservative criterion was deliberately selected for the optimal oil pressure. The temperature rise in the piston during variation was limited to a maximum of 20 K. In testing, the base engine circuit was supplied with a constant oil pressure in accordance with the baseline parameters. Under this boundary condition, the operating point ESC A50 has an optimal oil pressure of just 0.5 bar for piston cooling, for example. A savings effect (relative to the partial oil volume for the piston) of about 400 W of oil pump drive power is thereby achieved. The piston temperature that arises at optimal oil pressure is much lower at all tested operating points than the respective component temperature under full load.

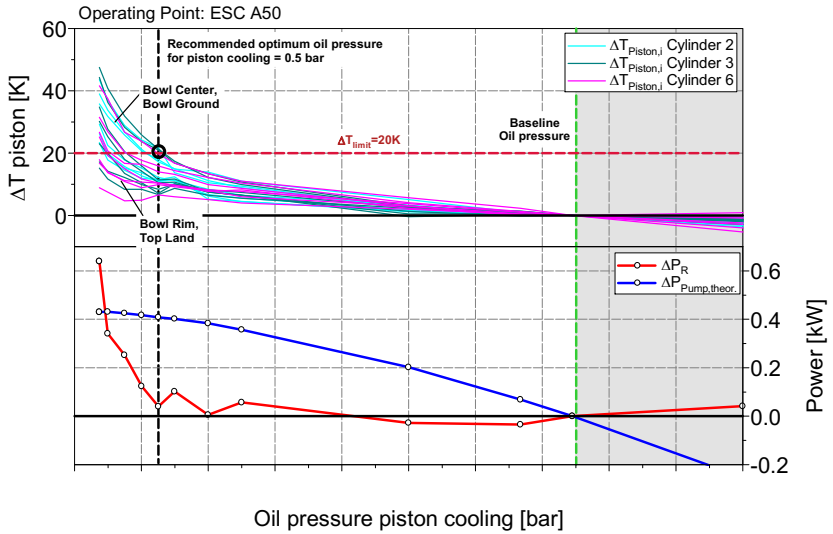

Figure 9: Optimum oil pressure for piston cooling for operating point A50

Looking at the energy balance, a shift in the quantity of heat of about 4 kW from engine oil to coolant is evident for extremely low piston cooling, where primarily the heat flow across the piston skirt and rings to the cylinder increases. The influence of the reduced piston cooling on the aging of the oil was not considered in these experiments. The influence on the combustion process is minor; for example, the emissions and exhaust gas temperature remain virtually constant. A more significant effect on the combustion process would only occur with very large changes in piston temperature, such as if the piston cooling were shut off. But this is not permissible for steel pistons.

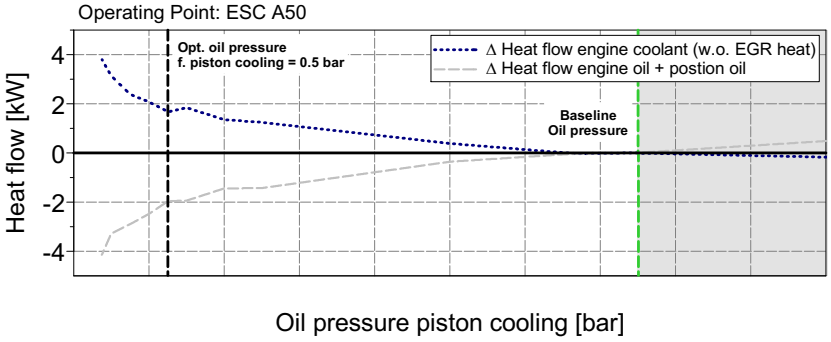

Figure 10: Shift in the energy balance from engine oil to engine coolant when piston cooling is reduced

When determining the optimum oil pressure for the piston group for various partial-load operating points, the greatest possible pressure drop is found for each case; the optimum pressure is between 0.3 and 1.5 bar, depending on the operation point.

2.4 Minimum requirement for the base engine

Determining the minimum requirement for the engine cooling partial circuit is more complex than for piston cooling due to the large number of oil consumers. In case of doubt, the demand of the critical consumer is definitive for the permissible minimum. Therefore, the results of the numerical calculation plus a safety factor were taken as the operating limit for the base engine. The bearing temperature in the main bearing was captured as an indicator of the load on the consumers. Acoustic sensors on the crankcase were also used to diagnose any mixed friction that may have started. The results of the bearing simulation were that the supply to the conrod bearing becomes critical first. A direct measurement of the conrod bearing was not technically feasible.

The results of the minimum pressure test for the crank mechanism are shown in Figure 11. For all tested points, a minimum pressure from the simulation results plus a 300 mbar safety factor was approached. This is to take account for consumers far from the main oil gallery that are supplied at a lower pressure due to flow losses. The temperatures at the main bearings increase by 1–2 K as the oil pressure drops from the series design to the minimum pressure, and the effect is reversible. This can be explained by the fact that the lower volume of oil must dissipate the same amount of heat from the bearing. The measurement points were installed 1 mm below the surface of the bearing shell at the center of the bearing. A second measurement point on each bearing was offset 60° circumferentially. The comparison between these two measurement points also showed no critical effects as a result of

lowering the oil pressure. In no case was a critical value detected at the acoustic sensors or the temperatures. A conclusion about durability at the optimum setting can be drawn only with a future endurance test.

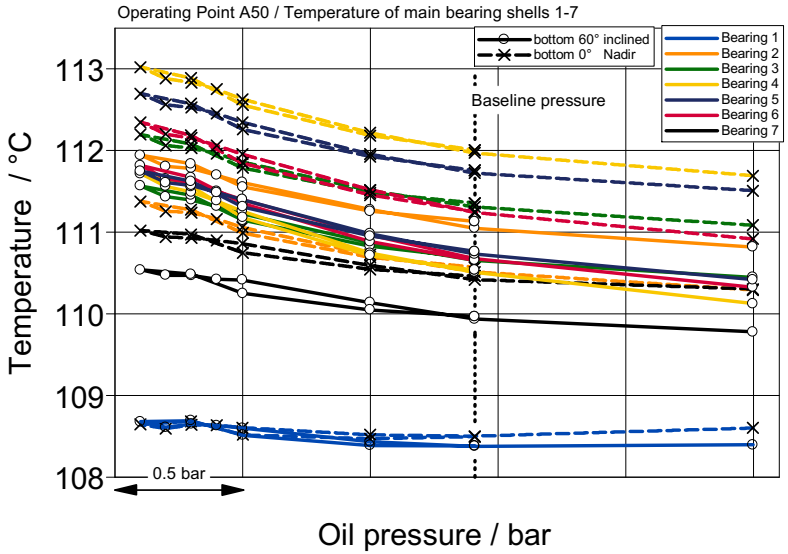

Figure 11: Temperature influence of supply to the base engine at the main bearings. Inflow to engine with oil temperature of 105°C.

2.5 Minimum pressures and expected potential

After determining the optimal pressures for selected operating points, it was found that the optimal pressure for the base engine at near-idle speed was 1.0 bar gage and for the range from 1200 to 1800 rpm was between 1.5 and 2.1 bar gage. The optimal pressures for piston cooling were lower in comparison, as discussed in section 2.3. The optimum pressures in this publication were developed exemplarily for one specific engine by MAHLE. They are dependent on the application.

In the event that an oil pump can provide one freely selectable pressure level, the base engine circuit is always determinative of the optimal pressure in the case considered here. For the selected operating points, fuel consumption savings of 0.6% to 2.0% were measured resp. calculated from this measurement. Therefore, the engine test without the oil pump, with external supply, was analyzed and the drive power for the oil pump was added back (Figure 15).

3 MAHLE variable oil pump

The preceding sections showed the potential limit for fuel savings in the given oil system. The following explores how much of this can be realized by using an oil pump with variable volume flow. MAHLE operated a variable oil pump for commercial vehicles on the test engine for this purpose. With the pump, the realization of the optimum oil pressures and the resulting fuel consumption benefits were demonstrated in the full engine. In MAHLE's view, the pendulum-slider pump design is very well suited for use in commercial vehicles (see also Hannibal 2015).

3.1 Construction of the MAHLE pendulum-slider oil pump for commercial vehicle applications

In a pendulum-slider pump, several pendulums are supported on an eccentric external rotor and guided by the inner rotor (Figure 12). A feeding cell that is intrinsically very well sealed is formed between each set of two pendulums. The seal is largely independent of the component tolerances and therefore of a broad range of wear conditions. The pendulum rolls in the groove of the rotor, similar to how an involute gear tooth makes rolling contact. This results in high volumetric efficiency, low friction, and thus higher overall efficiency.

Pressure buildup in the pressure regulating chamber changes the eccentricity of the external and inner rotors and thus influences the volumetric flow rate.

The construction as described provides the pendulum-slider pump with the decisive advantages of robustness and wear resistance in comparison with other controlled pumps, specifically for use in commercial vehicles. It is not sensitive to contaminants and abrasive particles. The pendulums are protected against excessive wear by the external rotor. This means that it maintains its high efficiency over its entire service life (Jensen 2010).

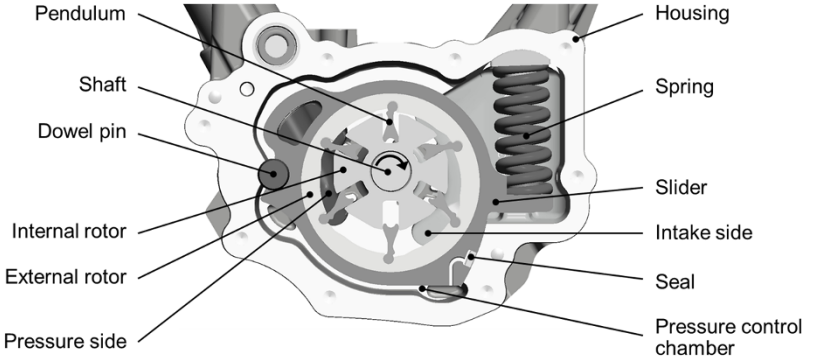

Figure 12: Construction of the MAHLE pendulum-slider oil pump for commercial vehicle applications

3.2 Measurements on the component test bench

Extensive tests on the component test bench were used to determine the characteristic data of the oil pump. The main question was the overall efficiency that could be achieved (and the necessary drive power) for various operating points (Figure 13).

Reducing the pump output pressure and therefore the volumetric flow rate tends to lead to a reduction in the efficiency of the pump, due to the resulting drop in hydraulic work under similar tribological conditions within the pump.

The ultimate goal was to demonstrate that the benefit in oil pump power consumption from reducing the pump output pressure (that is, turning down the pump) is not outmatched by a reduction in the efficiency of the pump in the partial-load range.

The measurements showed that the change in eccentricity (to adapt the volumetric flow rate to the current engine requirements) across a wide range did not have a significantly detrimental effect on efficiency. Increasing the PWM rate of the solenoid valve (and thus reducing the pump output pressure) leads to a decrease in efficiency of 2% to 10% when running on the engine (Figure 14). The fuel efficiency evaluation is shown in the engine testing below.

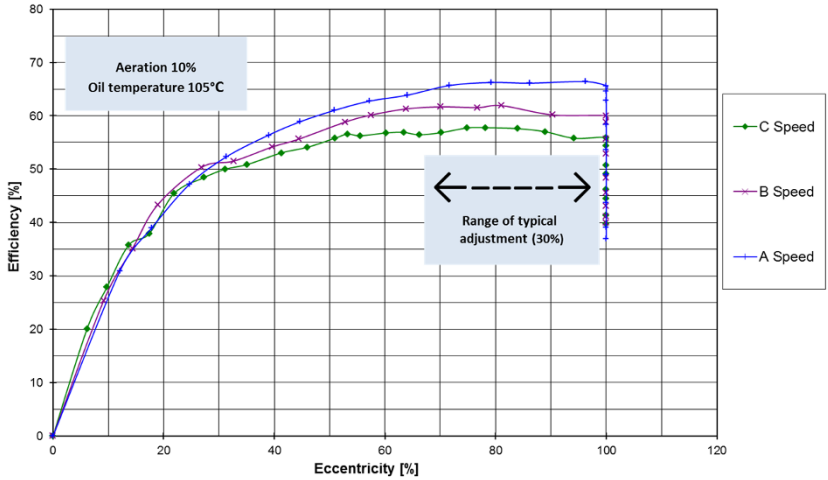

Figure 13: Dependency of the pump efficiency on eccentricity

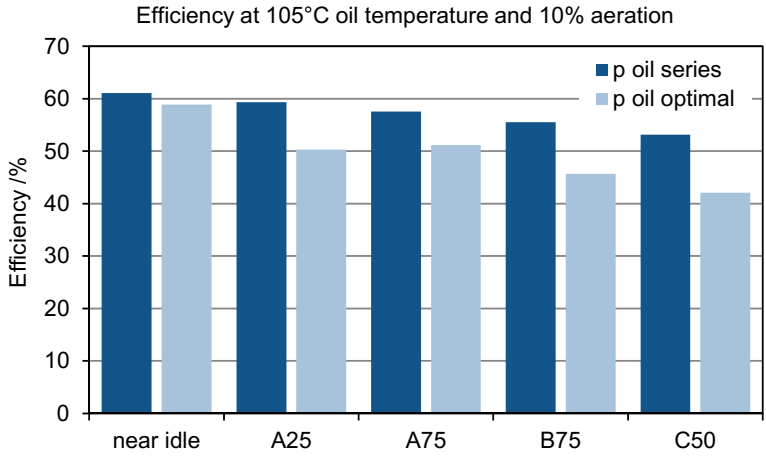

Figure 14: Pump efficiency of the MAHLE pendulum-slider oil pump from component testing for series and optimum oil pressures

3.3 Testing the variable volume flow oil pump on the engine

The MAHLE pendulum-slider oil pump was adapted to the test engine and actuated by the engine control unit, so that it could be measured directly against the potential determined in the preceding setup with external supply. The pump was installed in the location for the series pump, and the oil circuit and boundary conditions were identical to the test with external supply. The advantage of this setup is that the series and optimal pressure can be run and measured in succession with very good accuracy and repeatability. The result includes driving the pump and all effects on the engine (oil mass flow, temperature changes, etc.).

3.4 Demonstration of realized fuel consumption potential

The result of the pump measurements on the engine was in good agreement with the expected consumption values from the measurement with the external supply (Figure 15). For the operating point ESC A50, consumption savings were just under 0.5%, for example. This measurement also demonstrates (in good agreement with the results of the component test) that the efficiency of the oil pump at lower oil pressure is very close to the original efficiency, so the expected fuel consumption results are barely affected.

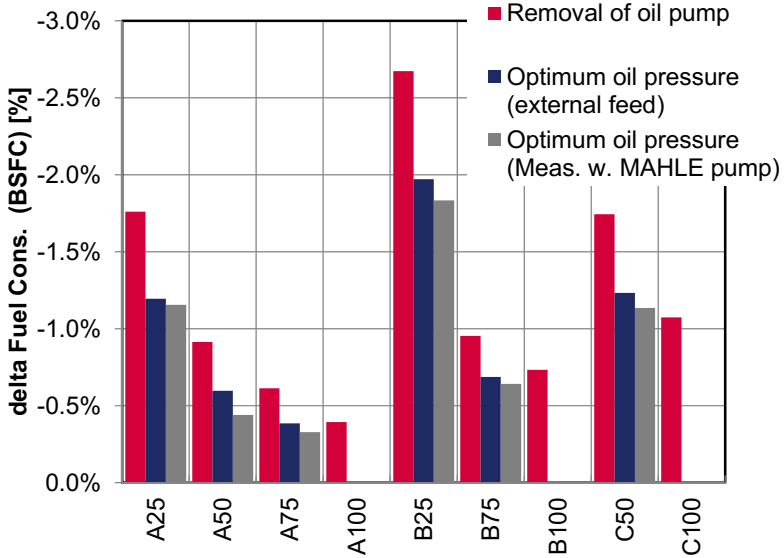

Figure 15: Total power required for the oil system, fuel consumption potential at optimal oil pressure (setup with external feed) and in direct measurement with the MAHLE oil pump

When the consumption levels thus determined are evaluated in a driving cycle simulation, fuel savings of 0.6% are seen in the VECTO long haul cycle with reference loading (Figure 16).

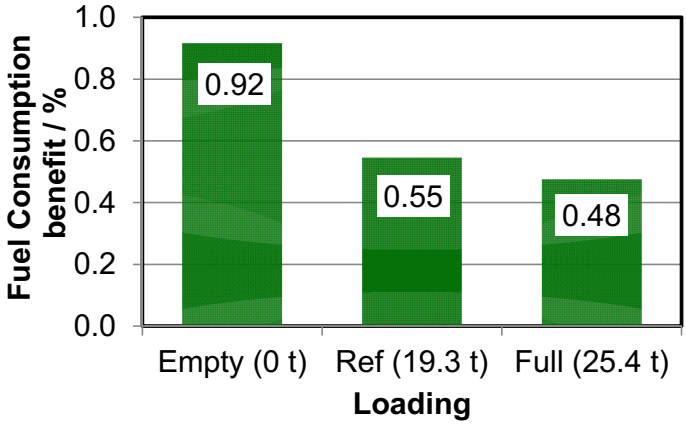

Figure 16: Improved fuel consumption with controlled MAHLE pendulum-slider oil pump at optimal oil pressure (driving cycle simulation)

4 Fuel consumption saving potential with other oil system topologies

4.1 Provision of additional pressure levels

The most obvious topology from the tests shown so far is the use of the MAHLE pendulum-slider oil pump without any further changes in topology. Nevertheless, other configurations were tested for potential effects. For example, the piston spray nozzles could be supplied at a second, freely selectable pressure, theoretically using an additional freely controlled pump for this partial flow. The case where the pressure for the piston spray nozzles is reduced to the optimum oil pressure is considered. The extent of this reduction in pressure is very great (Figure 17, left). The consideration of the hydraulic power requirements of the oil circuit, however, reveals that the impact in terms of power is comparably small (Figure 17, right). From the engine tests with external supply, the additional consumption benefit for the concept with a second pressure level for piston cooling is a maximum of 0.2% at operating point A25 (with about 0.1% at operating point A50). This is very little in comparison with the introduction of the first freely selectable pressure level and is also associated with a high level of effort on the engine side.

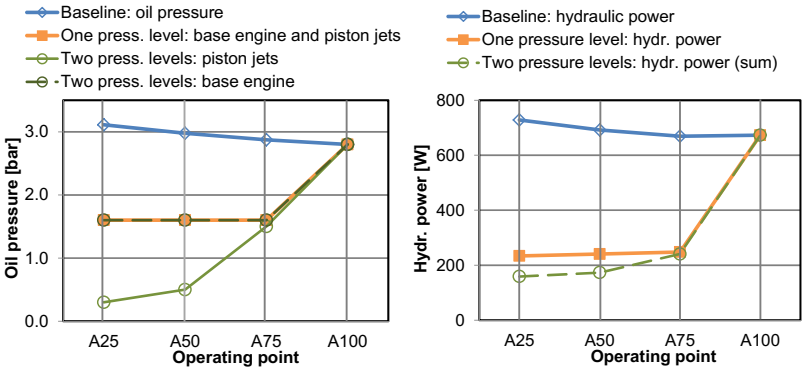

Figure 17: Potential fuel consumption savings from the provision of a second, independent pressure level for piston cooling

4.2 Implementing two temperature levels as a measure for optimizing oil service life

Oxidation is one of the most important criteria for an oil quality change caused by thermo-chemical reactions. Oxidation greatly contributes to the formation of organic acids, typically carbonic acid and sludge, leading to resins and varnishes, which in turn leave carbonaceous deposits on systems components. Oxidation is temperature dependent and can be described empirically as a chemical reaction using the Arrhenius equation. The calculation indicates doubling to tripling of the reaction kinetics for every 10 K temperature increase in the medium (Totten 2006). The amount of air in the oil (oil aeration) also contributes to increased oxidation rates, because a greater amount of air (oxygen) is transported through the crank train and mixed into the oil.

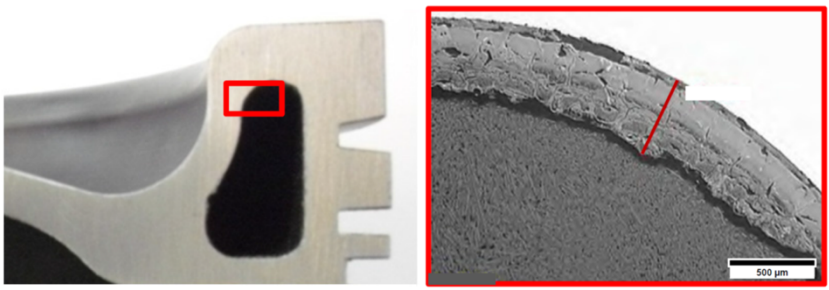

Figure 18: Examples of carbon deposits in the cooling channel of a steel piston

The high oil temperatures also cause the hydrocarbons to degrade thermally into smaller molecules (cracking), or they are functionalized with carbonyl groups in particular, and after polycondensation they tend to form varnishes that can capture and deposit additional carbonaceous particles.

These carbon deposits are primarily found in the piston ring zone, in the piston cooling channel (Figure 18), in the bearing housing of the turbocharger, and on the valve guides. In general, they form wherever the engine oil makes contact with very hot material surfaces.

In order to reduce the oil temperature in the cooling channel of a steel piston, MAHLE performed preliminary tests with low-temperature oil piston cooling. The piston cooling was fed externally and conditioned. The base engine continued to operate at series oil pressure and temperature. At a relevant design point for the engine oil cooler, but also at the critical point for piston cooling power C100 (ESC), two temperature levels were compared as examples: the baseline engine oil temperature (T = 105°C, continuous line) and a low temperature (LT = 60°C, dashed line).

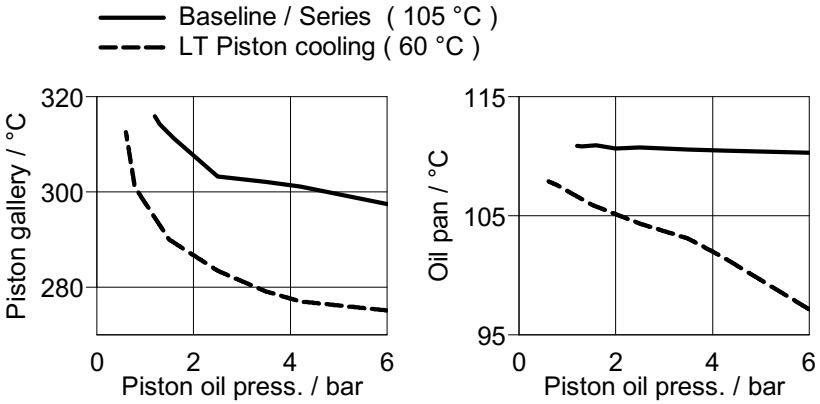

Figure 19: Piston cooling pressure variation at 105°C compared with 60°C oil temperature in the piston circuit for C100 (ESC). Base engine oil temperature: 105°C (both cases).

The higher the oil injection pressure, the greater the cooling effect in the piston cooling gallery (Figure 19, left) and the cooling of the oil sump as a side effect (Figure 19, right). This can be used as a means for improving the operational reliability of the lubricant. In long-term operation, the lubricating oil should not exceed the temperature of 130 °C in the oil sump. Oil aging accelerates rapidly at temperatures above 125 °C. The heat dissipated from the oil for engines with piston cooling gallery corresponds to

4.5%–7.0% of the effective engine output. At the same time, reducing the oil temperatures also increases lubricating film thickness, and therefore improves the operational reliability of the plain bearing by reducing the intensity of mixed friction. On the other hand, reducing the oil feed temperature has a negative effect of increasing frictional losses with fluid friction. It must be considered that in the highly loaded plain bearings, operating conditions arise in which very small lubricating film thicknesses <1 µm prevail, and the fluid friction is accompanied by mixed friction. The proportion of mixed friction ranges should never be increased.

Reducing the oil temperature for piston cooling by 20 K leads to a reduction in material surface temperature in the piston cooling gallery by about 10 K. In addition to the now cooler return flow of the hot oil from the piston cooling gallery, the overall temperature level in the oil sump is reduced by about 5 K. Relative to the slower reaction kinetics (Arrhenius) and reduction in high temperature peaks, low-temperature piston cooling shows good potential for increasing oil change intervals and improving piston robustness, especially in at-risk applications.

5 Summary and outlook

MAHLE has performed intensive activities with the oil system and presents an overview of its competences in the fields of component and systems simulation, design of oil circuit components, and testing (component and systems testing).

The oil circuit still has potential for improvement, particularly due to the high level of interest in fuel savings in the HD diesel engine. These, however, depend greatly on the particular initial state and therefore differ from engine to engine. For the test engine, it was 0.5%–0.9% in the driving cycle, depending on loading.

MAHLE performed tests on a mass-production commercial vehicle engine and determined the appropriate reduction in oil pressure for various partial-load demands in an optimal variant. A functional test demonstrated that this strategy can be implemented in an otherwise unchanged oil circuit with the MAHLE pendulum-slider oil pump. Perfect functionality with very good efficiency, even at lowered pressures, was demonstrated.

The MAHLE pendulum-slider oil pump can be applied easily in HD and MD diesel engines.

MAHLE has tested another variant with an oil circuit split by pressure and temperature. The advantage of two pressure levels is very application specific and is rather limited on the test engine. One oil circuit with two temperature levels can be very interesting with respect to increasing oil service life and component robustness.

As a further step, the optimal pressure strategy is being tested at MAHLE in an endurance test for oil aging and deposit formation in the piston cooling chamber and to confirm the target values for sliding bearing wear.

6 Literature

1. Affenzeller, J., and Gläser, H. *Lagerung und Schmierung von Verbrennungsmotoren*. Springer-Verlag Wien, 1996.
2. Merrit, R., and Mian, O. *The use of Abaqus in an engine bearing design environment*. SIMULIA Community Conference, Vienna/Austria, 2013.
3. Merrit, R., Haxha, V., Mian, O., and Ferreyra, S. *Crankshaft Bearings Oil Flow Prediction Tools including CFD*. 13th Stuttgart Int. Symposium, 2013.
4. Kalogiannis, K., Merritt, R., and Mian, O. *Contact and wear thermo-elastohydrodynamic model validation for engine bearings,* Proc. Inst. Mech. Eng. J: J. Eng. Tribol. 231, no. 9 (2017).
5. Knoll, G., Backhaus, K., Berg, M., Schultheiß, H., and Ludwig, F. *Ölbedarf von Grund- und Pleuellagern Simulationstechniken und experimentelle Validierung*, MTZ 67, no. 9 (2006): 672–679.
6. Hannibal, W., Schütte, S., and Holzer, A. *Systematischer Vergleich von Ölpumpenkonzepten an Verbrennungsmotoren: Simulation und Prüfstandsuntersuchungen*. 2nd International Engine Congress, Baden-Baden/Germany, 2015.
7. Jensen, H., Janssen, M., Beez, G., and Cooper, A. *Kraftstoffeinsparpotenzial der geregelten Pendelschieberpumpe,* MTZ 71, no. 2 (2010): 104–109.
8. George E. Totten. *Handbook of Lubrication and Tribology*, vol. 1, 2006.

Rankine cycle – from thermodynamic equation to road test

Thibault Fouquet
System architect group leader, Faurecia

W. Siebenpfeiffer (Hrsg.), *Heavy-Duty-, On- und Off-Highway-Motoren 2017*,
Proceedings, https://doi.org/10.1007/978-3-658-21029-8_17

Introduction

The Rankine cycle is currently one of the most promising solutions when it comes to the fuel consumption reduction for long haul trucks or the improvement of Brake Thermal Efficiency (BTE) to more than 50%. Several publications already show proof of its fuel saving abilities, by discussing simulation or test bench results. This paper however is going to present the experimentation done by Faurecia, in collaboration with Renault Trucks (Volvo group) and Exoes, to give a first-hand impression on reachable fuel saving levels.

The testing was conducted by assembling already available components on an 11 l Engine Euro 6 truck, under consideration of packaging constraints.

This paper is going to present the full scope of the undergoing, from creating the simulation model, to the methodology of component sizing, followed by an overview of the testing setup and the control strategy, which enables to automatically run the system. Subsequently, after an overview of the integration of the system into the truck, the reader will find the final results and an overview of future perspectives. The conclusion will finally highlight what are the key elements to improve the fuel saving, on the Rankine system or truck itself to further contributes to the Rankine performance, taking into consideration this experience on an 11 l. EuroVI engine.

Technology presentation

The Rankine cycle and its usages

The first theoretical description of the Rankine cycle was given by William John Macquorn Rankine during the 19th century. The principle defines how to transform heat power into mechanical power by using the phase change of a fluid with four major components. A heat source first vaporizes the fluid under high pressure in the boiler. Then, this vapour is expanded into a so-called expander (this can be either a turbine or a volumetric machine) to generate mechanical power. The residual heat power in the fluid, which often reaches values of more than 80% in the herein discussed application, is removed by a condenser. The close loop flow is created by a pump. A TS diagram, as shown below, is the most common way to illustrate the cycle.

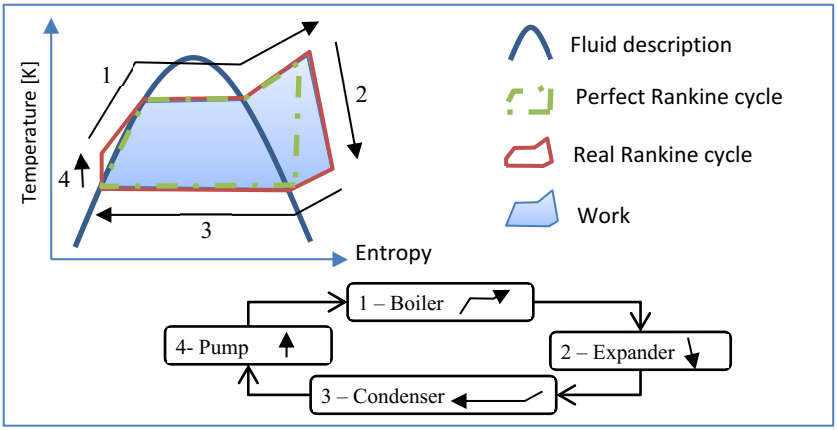

Figure 1: Rankine cycle and main components

While in the beginning, water was used as the working fluid, nowadays there is a wide variety of liquids to be used, depending on the usage conditions, most importantly the temperature of the heat and cold source

The main area of interest for this is the boiling and condensing pressure driven by the two temperatures sources in which the cycle operates (i.e. hot and cold). The work provided by the cycle is illustrated in blue. This area directly depends on the temperature difference between the two sources: the larger the difference between the temperatures, the higher the efficiency of the cycle.

The Rankine cycle was first used for powering steam engines for applications such as trains and is now implemented across various industries to generate power or limit heat waste. Primary utilizations for waste heat recovery are industrial processes, (e.g. steel mills, glass mills, furnaces), “small scale” power generation (biogas, diesel, gas engines), biomass plants, solar power or cogeneration for gas turbines.

All of these employments work in a static environment with often quasi static working conditions. Those two factors significantly differ in case of ground vehicles.

Challenges of on-road applications

This study focuses on heavy duty applications, especially in long haul trucks. From static to dynamic application, the long haul truck is the most promising, due to its long working periods and the expected steady state operation on highway. Even though, working points can vary largely depending on the slope of the roads:

Table 1: Influence of slope or vehicle speed on the engine power demand

Speed [km/h]	Slope [%]	Typical engine power output [kW]
90	0	100
90	1	180
90	-1	20
80	0	80

As shown in the above table, value of power output can vary by more than 100% depending on the slope. Whereas the working point of long haul trucks could be imagined stable, the range of variation makes sizing the system difficult.

Another major challenge regarding the implementation of the Rankine cycle into a vehicle is the necessary available space. While this issue is more prevalent for an implementation in light vehicles, it can also arise in heavy duty vehicles when one needs to load an additional 200 kg of material. Several companies attempted to deal with this difficulty, most recently done by Cummins and IVECO / AVL. The target of Faurecia to this end was to challenge the state-of-the art, and to prove the readiness of the technology regarding vehicle integration.

Project context

Faurecia background on Rankine and system

Faurecia has a profound experience in the development and manufacturing of mechanical components for exhaust systems. The portfolio is comprised of customized products that improve air quality and acoustic performance. An Exhaust Heat Recovery System is already available and serially developed. The Rankine premises in Faurecia started several years ago, first with purely experimental approach and building laboratory proof of concepts. During this starting phase, several expanders were tested to elaborate our knowledge. After deciding to further investigate the Rankine system, the theoretical approach and the modelling were introduced.

The system approach was also an important part of this innovation. It was a transition from pure mechanic product to mechatronics system and from drawings to requirement management approach. Within this scope, the support of an OEM is welcome to gain time regarding mechanical and electrical integration.

OEM partner for the demotruck

Renault trucks (Volvo group) puts a lot of efforts into the investigation of fuel economies. Besides other technologies, they have built up a Rankine-related expertise, on simulation, testing, but also on truck integration. One result of these activities is the truck optifuel lab 2, which incorporates various different fuel economy solutions, including Rankine. While Faurecia was responsible for the development and integration of the entire system, Renault Trucks delivered the vehicle, simulation input data and their expertise with regards to the system integration.

Starting position

Faurecia baseline expertise

As stated before, Faurecia already experimented the Rankine cycle using an engine bench for light vehicle applications. The take-off of the heavy duty project marked the beginning of laying the necessary theoretical foundation. As a base, we first addressed the Rankine cycle with all the thermodynamic equations to build our own 0D tool and understand the cycle in steady state.

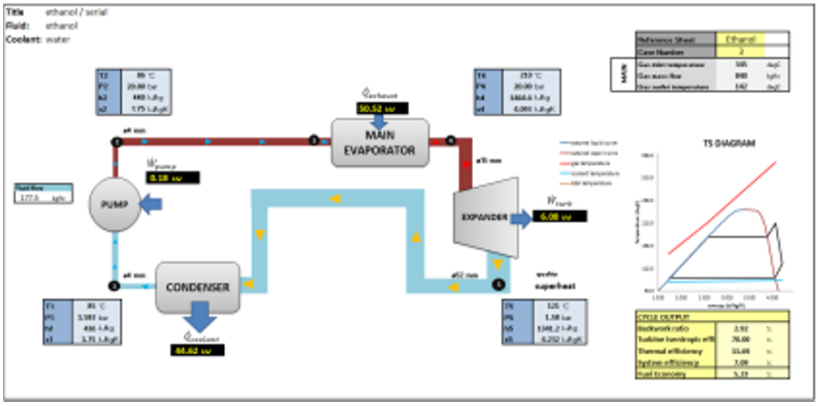

Figure 2: Internal Excel 0D tool

This study enabled us to gain a broad understanding of the main parameters and how they influence the cycle output. However, it does not sufficiently explain the full complexity of the cycle. “On the field”-Experience helped to offset the lack of an available simulation tool at the beginning of the project

Truck description

The truck in use during the project is a T460 equipped with an 11 l. diesel turbocharged engine, which was chosen and delivered by Renault Trucks (Volvo group). It is equipped neither with Exhaust Gas Recirculation (EGR) nor with a turbo-compound. Output temperature is rather hot, which is favourable for the Rankine cycle. The typical nominal point 1200 rpm / 800 N.m is 340 °C at exhaust gas after-treatment outlet. This temperature is expected to drop to between 250 and 300 in the coming years with the development of new generation engines.

Therefore, one must bear in mind, that on this application, the hot source side is favourable to Rankine. On the other hand, with the most powerful 11 liters of Renault Trucks engine range within the small cabin, the cold source is limited and this situation is not the best for the system.

Simulation

Preliminary Architecture choice

The truck has only one hot source at high temperature and to limit the integration modification, the use of the engine coolant as a cold source is preferred. At this point it is necessary to define the internal architecture of our Rankine system. In fact the temperature of the available sources strongly influences the selection of the fluid, as it impacts the pressure in the different sections of the circuit.

Basic demands are:

- Keep fluid below critical temperature when boiling
- Keep pressure in the circuit above 1 bar, as under pressure relative to atmosphere is difficult to manage with dynamic sealing.
- Get the maximum pressure ratio between expander inlet and outlet

Several fluids were studied and classified based on performance and constraint mentioned before:

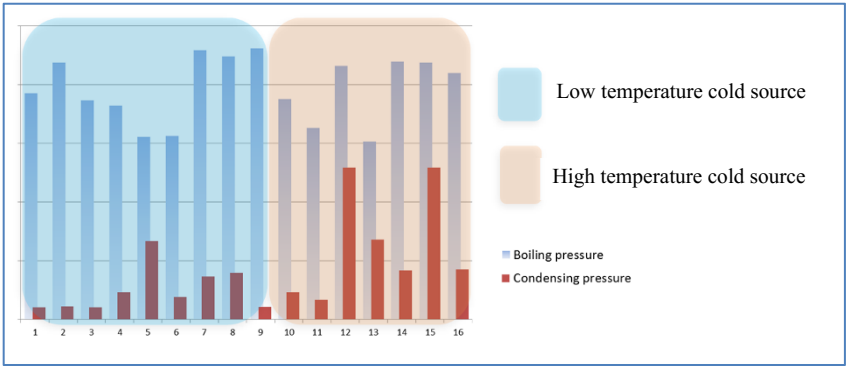

Figure 3: Fluid classification (internal source)

The Rankine set up and its efficiency themselves depend on the temperature of the hot source. However, it must be also considered that the cold source has a huge influence on its temperature but also on its capability to extract from the fluid the power that cannot be transformed to mechanical power by the expander. Considering the truck architecture it was decided to focus on the available cold source (~90°C), despite the loss of efficiency compared to a cold source at ambient air temperature (<40°C).

Mechanical connexion will ensure better efficiency and therefore promote volumetric expander with lower rotation speed.

Expander partner for the demotruck

Exoes was identified as a potential partner for this project as their expander perfectly fits the given technical requirements. They own an 8 year-long experience on Rankine cycles, starting with light vehicle applications and currently having expanders dedicated to truck application.

Besides the product development, Exoes also provides Tier Ones, OEMs and universities with Rankine test benches and simulation codes that allow waste heat recovery benefits estimation or system architecture comparison and selection.

Expander definition

The expander supplied by Exoes is called EVE® (Energy via Exhaust) T1.It is a piston expander with 6 reciprocating pistons, compatible with a water-ethanol mixture.

Table 2: Exoes' EVE® expander features

Architecture	6 pistons, swashplate double acting	
Filling control	Inlet poppet valve, outlet ports	
Lubrification	Embedded oil pump and separation device for low oil circulation rate	
Nominal shaft power range	<15kW	
Nominal speed range	1,000 – 4,250 rpm	
Capacity	300cm3, can be set lower	

Before integration on truck, this prototype was preliminarily tested on test bench. This first evaluation test confirmed the total efficiency around 55% on the targeted working point.

Dynamic truck model

In order to define the last open point for architecture and the components size required, a dynamic model was built. This was used to assess the expected performance on several working points on steady state but also on the reference cycle proposed by Renault Truck.

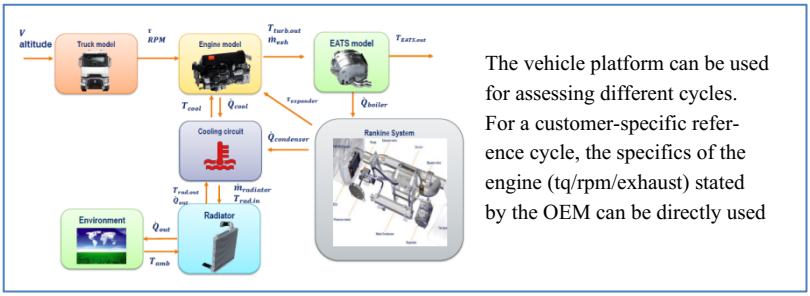

Figure 4: GT truck model

This platform was also used to validate the compatibility of a mechanical Rankine system with the cycle (i.e., the phase of available heat power vs cold source capacity and the required mechanical power). Concerning the heat source, the graph below shows up to 20% of heat is available when not needed. This is due to the specific inertia of the Exhaust After Treatment System (EATS).

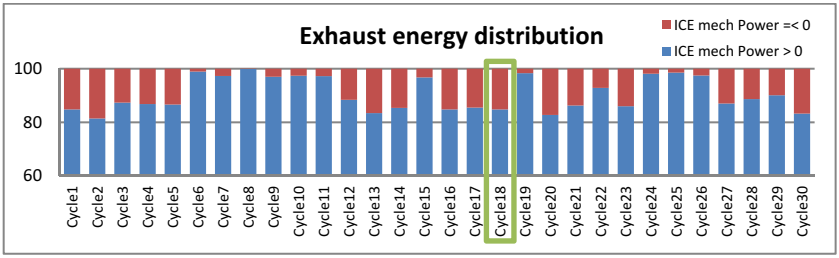

Figure 5 – Cycle potential

This study showed the baseline cycle proposed by Renault Trucks (circle in green on fig 5) didn't offer the best potential for Rankine, as more than 15% of exhaust heat energy is available when there is no need of mechanical power. However, the mechanical connection was maintained (vs electric), as there was not enough electricity consumption on the truck to absorb the Rankine production.

Dynamic of the Rankine model

Also based on GT, we built our cycle connected to engine boundary conditions.

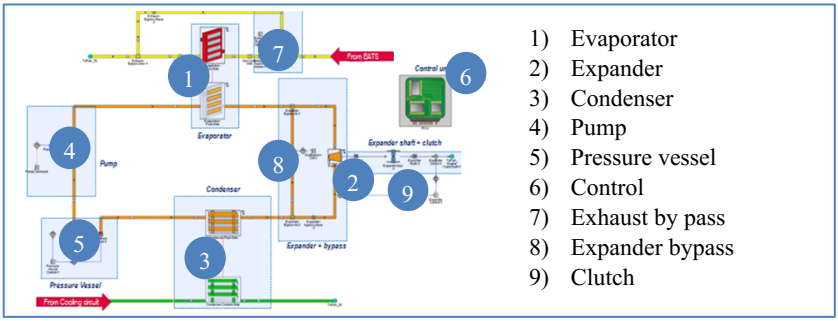

Figure 6 – GT, Suite Rankine model

The full set of actuators was included from the beginning with a basic control. The overall system is linked to the engine speed but there is no power feedback from the Rankine system to the powertrain. This choice was made to have an open loop organisation between the engine and the Rankine on powertrain side, taking the hypothesis the Rankine will supply less than 10% of the total mechanical power. The overall platform runs slightly faster than real time.

This model allows running variation of component sizing and evaluating how it affects the performance of the system. It also helps to have a first view of dynamic, such as the 15 min starting time due to exhaust after treatment and fluid thermal inertia.

Architecture choice and sizing

Based on the previous model and considering the integration, component availability and safety, we finally chose

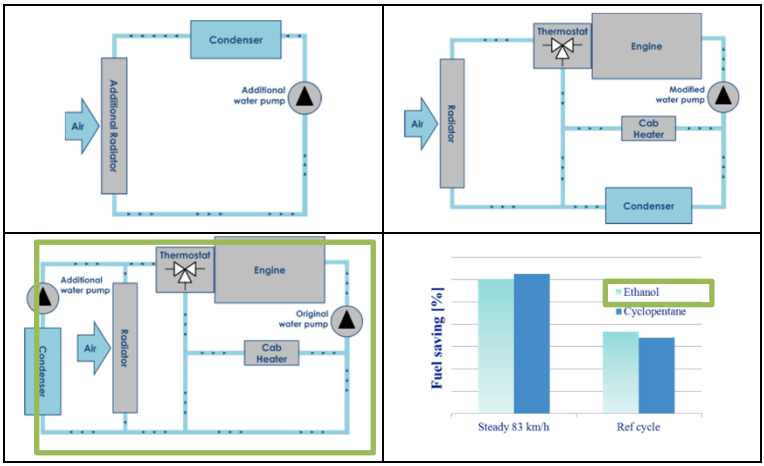

Figure 7: Cooling architectures and working fluids comparison

It can be noticed that the choice was oriented toward ethanol whereas cyclopentane could be a better choice for steady point. The safety aspect as well as lubricant compatibility played an important role to validate the final choice. The target of this short term project is to bring fuel saving with a picture of available component. Therefore new material compatibility tests are out of the scope, especially when the gain is limited.

From simulation to real-life testing

Bench assembly

Changing a simulation into a reality always represents a challenge and discovery. Despite preparation with thermodynamic simulation, the behaviour of the system can be surprisingly different due to one important factor: gravity. To limit the degree of surprise during

the integration on the truck, we targeted from the beginning to respect the vertical arrangement, starting with our first test on the engine bench. At first, the only interaction with the engine was the exhaust flow. The expander was connected to a small generator and the coolant temperature through condenser controlled independently.

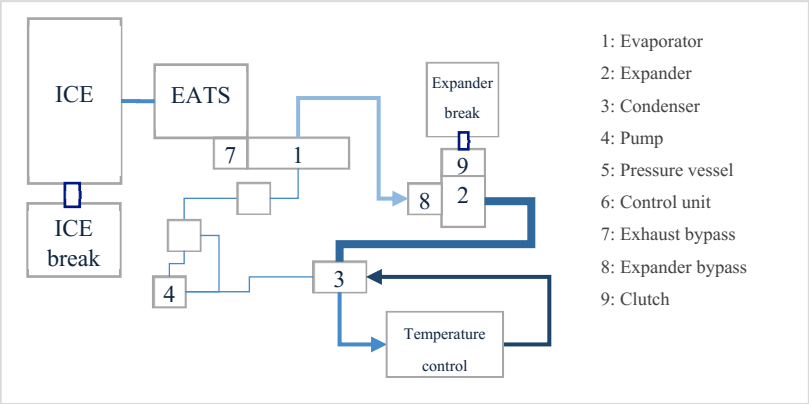

Figure 8: Bench setup, phase 1

Running manual and control law setup

The first test running on steady state had several objectives: To ensure that the simulation model didn't differ too much from reality, and then perform the calibration of our control. The control is based on model included in the control supported by PID regulator. The model are simplified enough to be compatible with standard ECU. In order to reduce the calibration time and not loose time in design we followed different architecture for the control with the goal to limit the modifications:

Table 3: System simulation sequence

Control	System model	Steps
GT	GT	First assessment of performance. No co-simulation to reduce computation time
Simulink	GT	Preparation of the command to be used in rapid prototyping. Clear split between the model and the control
Simulink	Bench	Same Simulink than the one used in simulation

It ended with a Simulink having a standard architecture for embedded control, including diagnosis. Those were integrated since the beginning as active parts for safety, towards material and test team.

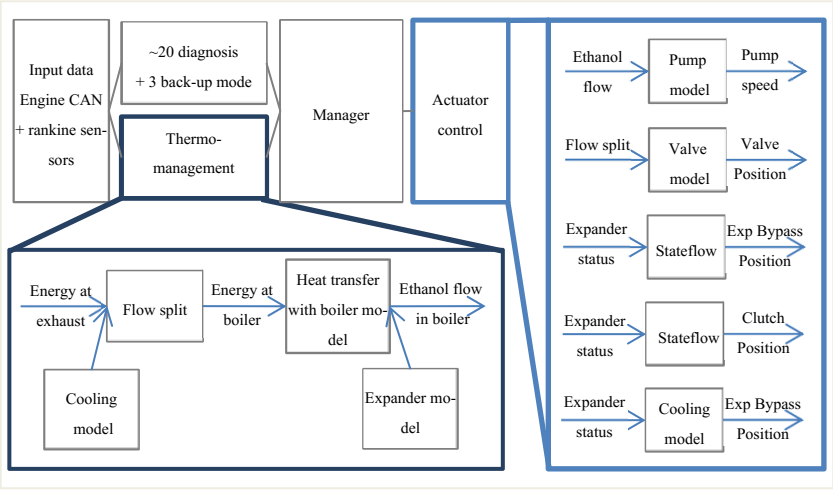

Figure 9: Control law architecture

The calibration process on bench mostly consisted in adapting dynamic behaviour: static performances were available from suppliers but transient performance was more an evaluation based on components' mass. Therefore, the system reaction time had to be adapted, but also the control which comes with it. This adjustment was done before going on step 2.

Expander mechanical connexion

As the expander had never been connected to an engine before, it was safer to connect it first on the bench to prevent any mechanical failure on the truck and also check if the behaviour of the system could be affected by vibrations. The bench setup was changed to the following configuration.

The control laws were slightly modified and calibrations were improved before running through fully automated tests on baseline driving profile. No failure occurred except for the instrumentation because of engine vibrations.

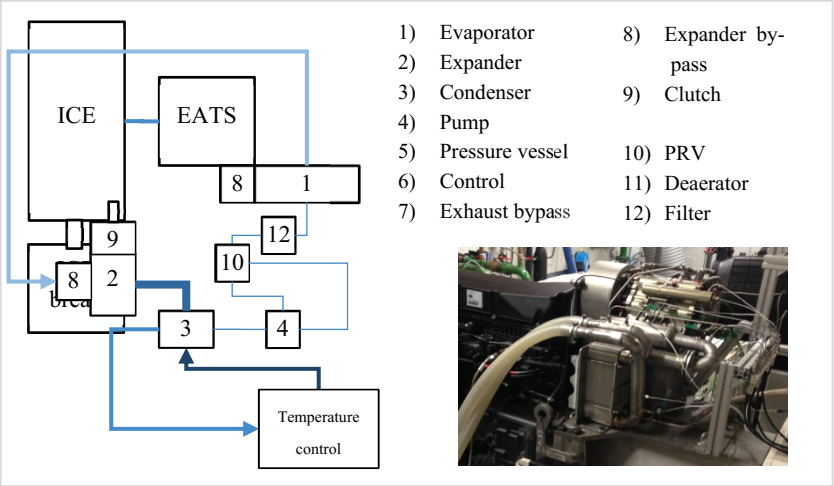

Figure 10: Bench setup, phase 2

Test cycle results

The first automatic test over Renault Trucks reference cycle was successful with the overheating controlled at the 40 K target

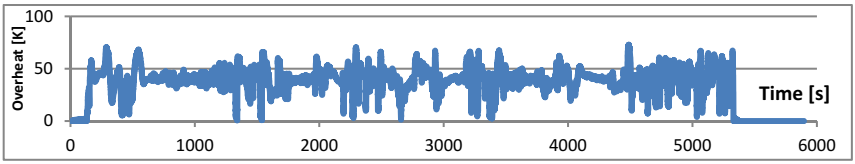

Figure 11: Super heating control

The two tests showed 1,6% of fuel saving with 60°C cooling and 0,9% with 80°C respectively. Those figures are not raw measurement but take into account the ethanol pump consumption. Indeed, electrical supply didn't come from the engine in our setup.

Integration

3D integration and truck modification

The volume and weight of the full Rankine system complicated the integration. We chosed to prepare all connections, including pipes setup, in 3D before continuing with real tools thanks to the support of Exoes and Renault Trucks. The overall system weights 300 kg, including all parts (brackets, support). Some rooms were available on the side, but our internal target was to not modify the truck performances, including autonomy. Installing the Rankine on the add blue or diesel tank was a choice we didn't want to make.

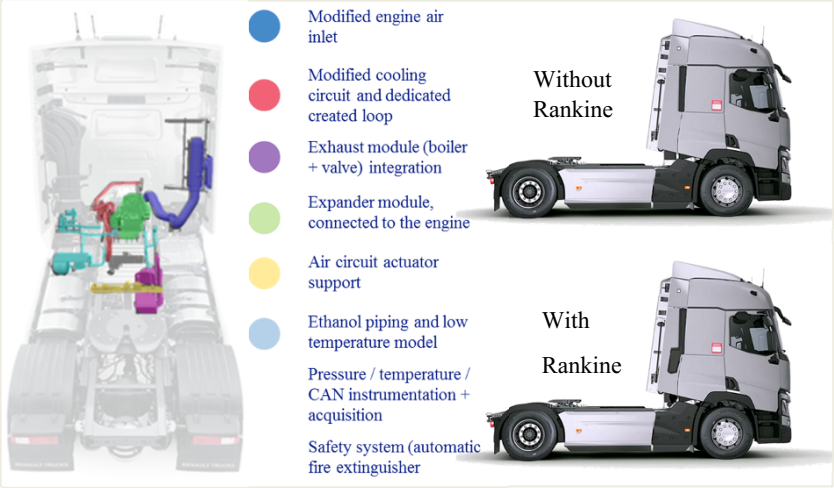

Figure 12: Truck integration

The integration of all the parts was done internally while the visual difference before / after is barely noticeable for non-experts.

The first objective of the project was achieved, but we had then to demonstrate the operability and the fuel saving.

Demotruck prototypes

Roller bench test

The system was tested on the engine bench, where the performance was assessed using the fuel consumption coming from the Engine Control Unit. For a finalized result, the target was to have :

1) Measurement on truck
2) An external mean of measurement.

For repeatability purposes, the only solution in this case was a truck roller bench equipped with instantaneous flowmeter. This device allowed to officially validate the fuel saving capacity and also the internal simulation tool, that was developed to assess the performance of our system on the road.

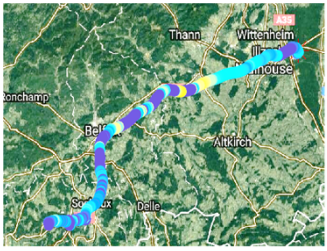

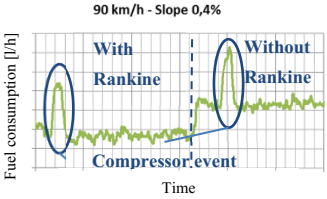

Top left : Picture of the truck in the roller bench

Top right : Fuel consumption with and without Rankine

Bottom left : Fuel saving estimation along road rest (colour scale)

Figure 13: Truck data and analysis

Indeed, before going on the bench, the truck was tested on more than 3000 km. To support the analysis of this large amount of collected data, an internal tool was developed (see fig 19)

Performance and forecast

Results from this tests program show a level of ~2% fuel saving taking into account a 20°C ambient air reference temperature. To make sure that the difference in the fuel consumption resulted from an implementation of Rankine, initial conditions were checked, as well as instantaneous parameters of the bench. Furthermore, points with too much variation were excluded. These results were obtained with the components available at that time and the goal was then to predict the potential of Rankine technologies for long haul trucks. After model correlation, extrapolation was done to see how to increase the fuel savings.

Table 4: Performance optimisation

Topic	Impact	Comment
Boiler next generation	+0,4	Considering realistic packaging
Expander next generation	+0,5	
Improvement on control	+0,1	Less margin on temperature and pressure
External cooling	+0,3	

This leads to fuel saving between 3,3% (on baseline cycle) and 3,9% for this application. This computation, together with the cost improvement of the components, enables to yield positive returns on investment after less than 2 years.

Conclusion

Planning and system approach

All the technical content, which has just been described, was a challenge, but the greatest challenge was the total duration of the project. Here are the main milestones of the project:

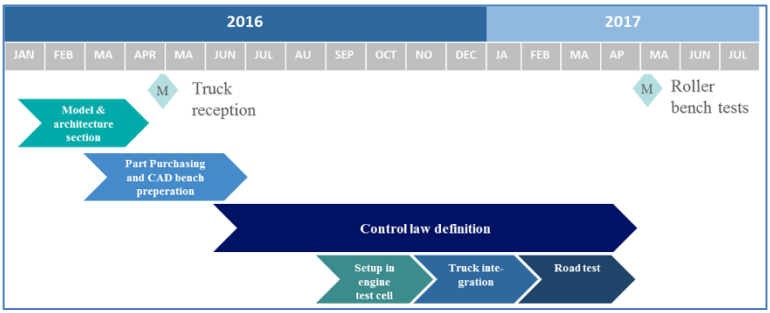

Figure 14: Demotruck project planning

This tight schedule was possible thanks to the introduction of system engineering and requirement management. Clear specifications with all information added in the documents were released in order to make sure the interfaces between parts would be compatible. Starting with pure mechanical experience and with Exoes support, we have proven Faurecia's capability to handle system project.

Rankine future

This common project proves the technical feasibility and the performance potential of a Rankine system in a heavy duty application. The resulting performance could be further enhanced by using a EGR heat source and over-perform 4% of fuel economy on cycle. While the system seems complex on the first sight, we have proven the possibility of integration into a serial truck without impacting its architecture. Beyond its complexity, the cost of the system needs to be consistent with the Total Cost of Ownership (TCO) target. It is achievable as the components are improving and will allow simpler, cheaper installation. One example for the expander:

Table 5: Expander content optimisation

EVE:Truck 1	EVE:Truck 2	EVE: Truck 3
Swashplate – Double acting 6 pistons – 300cm^3 Max Eff. Is. Efficiency: 60% Size D215xL350mm Weight 21 kg External bypass valve and oil management	Swashplate – Single acting 3 pistons – 240cm^3 Max Eff. Is. Efficiency: 70% Size D200xL200mm Weight 15kg Internal bypass valve and oil management	Scroll technology Vol. ratio 4.3 – 134cm^3 Max Eff. Is. Efficiency: 80% Size D216xL150mm Weight 18kg Internal bypass valve and oil management
		

Beyond the engineering challenges, the profitability of the system is highly linked to fuel costs, setting boundaries for the price of the system and therefore, the future of such technologies.

Tagungsbericht

Andreas Fuchs

W. Siebenpfeiffer (Hrsg.), *Heavy-Duty-, On- und Off-Highway-Motoren 2017*,
Proceedings, https://doi.org/10.1007/978-3-658-21029-8_18

12. Internationale MTZ-Fachtagung Heavy-Duty-, On- und Off-Highway-Motoren

Der Wirkungsgrad sowie die gesetzlichen Anforderungen bezüglich Abgasemissionen sind nach wie vor die Treiber in der Heavy-Duty-Motorenindustrie. Das Motto "Effizienz und Emissionen" der 12. Internationalen MTZ-Fachtagung Heavy-Duty-, On- und Off-Highway-Motoren, die am 28. und 29. November 2017 in Augsburg stattfindet, spiegelt diese Herausforderungen wider.
Daneben gibt es weitere branchenspezifische Treiber. So zeigte Dr. Christian Poensgen von MAN Diesel & Turbo SE in seinem Keynote-Vortrag unter anderem die Herausforderungen für die Hersteller von stationären Motoren für den Bereich Power Generation und Schiffsmotoren auf. So unterliegt die Motorenentwicklung bei MAN in diesem Jahrzehnt einer Zeit des starken Strukturwandels bei den Kunden und der Regularien. Dadurch waren die letzten Jahre geprägt von der Umstellung und Neuentwicklung von Motoren auf Gas und Dual-Fuel-Fähigkeiten.
Das Produkt-Portfolio von MAN wurde hierfür im unteren Bereich (1- bis 4-MW-Klasse) um einen 5-l-Highspeed-Motor erweitert. Gleichzeitig erfolgte die Umstellung aller Motoren auf die NO_x-Vorgaben der IMO von Tier II auf Tier III. Hierfür wurden SCR-Lösungen entwickelt, welche sowohl hinter dem Motor als auch zwischen den Turbinen bei einer 2-stufigen Aufladung oder vor der Turbine der Turbolader bei 2-Takt-Motoren eingesetzt werden können.

HYBRIDISIERUNG ALS KOMMENDE HERAUSFORDERUNG

Die parallel erfolgte Umstellung von PLD-Einspritzsystemen zu CR-Systemen erlaubte es, Motoren wesentlich effizienter zu gestalten, die Regeneration der Abgasnachbehandlung zu unterstützen und durch Systemintegration des konventionellen Antriebsstranges wesentliche Kraftstoffverbrauchsvorteile zu erzielen. Auch für die Zukunft prognostizierte Dr. Poensgen weitere Herausforderungen für die Motorenhersteller, wie zum Beispiel durch die Hybridisierung der Antriebstränge, die unbemannte Schifffahrt sowie Kraftstoffumstellungen im Rahmen der IMO-Schwefelgrenzwerte.
Dr. Udo Schlemmer-Kelling von FEV Europe GmbH ging im anschließenden ersten Tagungsblock "Mittelschnellläufer" in seinem Vortrag "Agenda 2030 – Mega Trends in the Large Bore Marine Engine Business" ebenfalls auf die Herausforderungen im Schiffsbereich ein. Waren bis zum Jahr 2000 im Marinegeschäft die wesentlichen Treiber bei der Entwicklung von Großmotoren die Zuverlässigkeit der Anlage, die Anschaffungs- und Betriebskosten sowie die Wartungsfreundlichkeit, kam ab dem neuen Jahrtausend ein weiterer Schwerpunkt hinzu: die Emissionsminderung, die schrittweise verschärft wird.

IMMER SCHÄRFERE EMISSIONSGRENZWERTE

So sind seit 2016 NO_x-Grenzwerte von 2 g/kWh vorgeschrieben. Und auch die SO_x-Emission wird 2020 auf 5000 ppm begrenzt. Für CO_2 wird ein EEDI-Index für die Gesamtanlage aus dem Kraftstoffverbrauch berechnet. Er ist für die verschiedenen Schiffstypen unterschiedlich und wird alle 5 Jahre um 10 % gesenkt. Durch diese Maßnahmen sind seit 2015 die Grenzwerte für einige Komponenten so niedrig, dass sie motorintern nicht mehr erfüllbar sind und für Dieselmotoren ein Abgasnachbehandlungssystem notwendig wurde. Als Folge steigen Anschaffungs- und Betriebskosten. "Auf Grund des immensen Kostendrucks werden die meisten Betreiber daher immer die kostengünstigste Lösung bevorzugen, die die momentan gültigen Gesetze gerade eben erfüllen", sagte Dr. Schlemmer-Kelling. Das scheint aus heutiger Sicht ein Kraftstoff auf Mineralölbasis zu sein. "Es gibt zwar einige Bereiche, in denen gasförmige Kraftstoffe eine sinnvolle Alternative darstellen. Sie werden aber vermutlich nicht zum Mainstream werden", so das Fazit von Dr. Schlemmer-Kelling.
Der zweite Tagungsblock widmete sich dann in drei Vorträgen neuen Heavy-Duty-Motoren für die Kraftstoffarten Diesel, LNG und Wasserstoff. Falko Arnold von MAN Truck & Bus stellte einen auf dem D3876 basierenden neuen Offroad-Motor vor. Gerade im Offroad-Bereich mit der geringen Anzahl von Maschinen ist eine kosteneffiziente Entwicklung unerlässlich. Aus diesem Grund werden Lösungen aus dem Straßenverkehr oftmals auf mobile Maschinen übertragen. Mit dem D3876 hat MAN einen Reihensechszylinder für schwere Nutzfahrzeuge, landwirtschaftliche Anwendungen und Baumaschinen entwickelt. Während der grundlegende Antriebsstrang und die Einspritzung für On- und Offroad-Versionen identisch sind, unterscheiden sich die Turboaufladung, Verbrennung und Elektronik sowie Abgasnachbehandlung je nach Applikation, wie Falko Arnold in seinem Vortrag aufzeigte. Der neue Motor wird im Leistungsbereich von 415 kW bis 485 kW (564 bis 660 PS) angeboten, bietet ein Drehmoment von bis zu 3100 Nm und erfüllt EU Stage IV und US Tier 4 final.

[Quelle: ATZelektronik 12 (2017), Nr. 4, S. 8ff]